Subordinated Fields and Random Elliptic Partial Differential Equations

Von der Fakultät Mathematik und Physik sowie dem Stuttgarter Zentrum für Simulationswissenschaften der Universität Stuttgart
zur Erlangung der Würde eines
Doktors der Naturwissenschaften (Dr. rer. nat.)
genehmigte Abhandlung

vorgelegt von

Robin Merkle

aus Stuttgart

Hauptberichterin:	Prof. Dr. Andrea Barth
Mitberichter:	Prof. Dr. Hanno Gottschalk
	Jun.-Prof. Dr. Marco Oesting
Tag der mündlichen Prüfung:	07.12.2022

Institut für Angewandte Analysis und Numerische Simulation

Universität Stuttgart

2022

Für Katja.

Danksagung

An erster Stelle bedanke ich mich bei Prof. Dr. Andrea Barth für die Betreuung meiner Arbeit in den letzten dreieinhalb Jahren. Die exzellente fachliche Unterstützung in Kombination mit ihrer außergewöhnlich positiven Art haben mich aus vielen (vermeintlichen) Sackgassen geleitet - und mir gezeigt, dass es eigentlich keine echten Sackgassen gibt. Ihre Fröhlichkeit und Positivität sind bewundernswert und ich könnte mir eine angenehmere Zusammenarbeit kaum vorstellen.

Außerdem bedanke ich mich bei Prof. Dr. Hanno Gottschalk und Jun.-Prof. Dr. Marco Oesting für die Begutachtung meiner Dissertation sowie bei Dr. rer. nat. habil. Jürgen Dippon, dass er sich bereiterklärt hat, bei meinem Promotionsverfahren als Prüfer mitzuwirken. Ich bedanke mich ebenfalls bei Prof. Dr. Dominik Göddeke und Elke Gangl für die Unterstützung bei der Finalisierung dieser Arbeit.

Darüber hinaus bedanke ich mich bei Dr. Andreas Stein, Cedric Beschle, Fabio Musco, Lukas Brencher und Oliver König für viel fachliche (und viel nicht-fachliche) Unterstützung, anregende Diskussionen und die angenehme Teamatmosphäre.

Mein besonderer Dank gilt hierbei Cedric, meinem Büronachbarn sowie Fabio, meinem langjährigen Freund. Cedric und Fabio haben viele Momente während meiner Promotion unvergesslich gemacht, meine Arbeit in schwierigeren Zeiten erheblich erleichtert und diesen Abschnitt meines Lebens in vielerlei Hinsicht bereichert.

Meiner Familie gilt mein unendlich großer Dank für die Unterstützung und den Rückhalt in den letzten Jahren und in meinem gesamten Leben. Ihr habe ich so viel zu verdanken - zu viel für diese Danksagung. Ohne meine Familie wäre ich nicht, wer ich bin. Danke. Für alles.

Zuletzt bedanke ich mich bei einem ganz besonderen Menschen: bei meiner Freundin Katja Nau, der diese Arbeit gewidmet ist. Ich bedanke mich für die bedingungslose Unterstützung,

Liebe und Kraft, die sie mir gegeben und die Ausdauer, die sie selbst in Bezug auf meine - für sie nicht immer einfache - Promotionszeit gezeigt hat. Katja hat mir immer den Rücken freigehalten um mich zu entlasten, mich in schlechten Zeiten aufgeheitert wie niemand sonst es könnte und war einfach immer da, wenn ich sie gebraucht habe - nicht nur als meine Partnerin, sondern auch als meine beste Freundin. Du, Katja, bist mir unendlich wichtig. Danke aus tiefstem Herzen. Du bist die Beste.

Contents

Abstract

Partial differential equations (PDEs) are used to describe phenomena in a variety of fields, such as physics, engineering, biology or finance. Due to unavoidable measurement errors or data sparsity, the determination of accurate model parameters is often difficult and subject to uncertainty in practical PDE applications. In order to take these uncertainties into account, it is common to consider stochastic/random PDE models, where some of the model components are described as random objects. In many situations, Gaussian random fields or processes are used to model uncertain parameters in a PDE. Gaussian random fields provide a rich theory and are comparatively easy to simulate, which makes them attractive for applications. However, in some situations, the standard Gaussian model is not flexible enough since pointwise distributions of Gaussian random fields are always Gaussian and, therefore, (semi-)heavy tailed distributions cannot be displayed. Further, the paths of commonly used Gaussian random fields are spatially continuous, which is unnatural in some applications, for example, when mathematical models for subsurface/groundwater flow in fractured porous media are considered.

In order to overcome these restrictions of the standard Gaussian model, this thesis presents distributionally flexible random fields with discontinuous realizations and explores their application in the diffusion coefficient of an elliptic PDE.

The subordinated Gaussian random field is constructed by the composition of a Gaussian random field on a higher-dimensional parameter space with independent Lévy subordinators. This thesis investigates theoretical properties of these fields, including results on pointwise distributions, covariance functions and the existence of pointwise moments, all of which are important for practical applications.

Besides the theoretical investigations, the subordinated Gaussian random field is considered in the diffusion coefficient of an elliptic PDE as an extension of the standard Gaussian model.

The existence of a unique solution is proven and possible spatial discretization techniques are discussed. Further, an approximation theory for the considered diffusion coefficient is provided and the resulting error propagation to the PDE solution is investigated.

In many applications of Uncertainty Quantification, one is interested in moments of (functionals of) the solution to a random PDE. Therefore, problem specific multilevel Monte Carlo estimators are constructed to approximate the mean of a random elliptic PDE, where the discontinuous subordinated Gaussian random field occurs in the diffusion coefficient. General a-priori error bounds are derived for these estimators and various numerical experiments complete their investigation.

In addition to the subordinated Gaussian random field, the so called Gaussian subordinated Lévy field is studied, which is constructed by the composition of a general Lévy process with a positive transformation of a Gaussian random field. The resulting fields are discontinuous and display great flexibility in the jump geometries. Besides theoretical investigations regarding the pointwise distributions and the covariance formulas, these fields are considered in the diffusion coefficient of an elliptic PDE.

Zusammenfassung

Partielle Differentialgleichungen (PDGs) werden zur Beschreibung von Phänomenen in einer Vielzahl verschiedener Bereiche, wie beispielsweise der Physik, dem Ingenieurwesen, der Biologie oder dem Finanzwesen verwendet. Aufgrund von Messfehlern oder fehlerbehafteten Daten ist die genaue Bestimmung von Modellparametern in praktischen PDG-Anwendungen oft erschwert und Unsicherheiten ausgesetzt. Um diese Unsicherheiten zu berücksichtigen ist es üblich stochastische/zufällige PDG-Modelle zu betrachten, bei denen einige der Modellparameter als Zufallsobjekte modelliert werden. Oft werden Gaußsche Zufallsfelder/Prozesse verwendet, um unsichere Parameter in einer PDG zu modellieren. Gaußsche Zufallsfelder bieten eine umfassende Theorie und sind vergleichsweise einfach zu simulieren, weswegen sie für Anwendungen attraktiv sind. In einigen Situationen ist das klassische Gauß-Modell jedoch nicht hinreichend flexibel, da punktweise Verteilungen von Gaußschen Zufallsfeldern immer einer Normalverteilung folgen und daher Verteilungen mit schweren Rändern, sogenannte Heavy-tailed-Verteilungen, nicht abgebildet werden können. Außerdem sind die Pfade in der Praxis gängiger Gaußscher Zufallsfelder im Raum stetig, was in einigen Anwendungen unnatürlich ist, zum Beispiel bei der mathematischen Modellierung von unterirdischen Strömungen oder dem Grundwasserfluss in geklüfteten porösen Medien.

Um diese Einschränkungen des Gaußschen Standardmodells zu überwinden, werden in dieser Arbeit Zufallsfelder mit unstetigen Realisierungen und flexiblen Verteilungseigenschaften vorgestellt und deren Anwendung im Diffusionskoeffizienten einer elliptischen PDG untersucht.

Das subordinierte Gaußsche Zufallsfeld wird durch die Komposition eines Gaußschen Zufallsfeldes auf einem höherdimensionalen Parameterraum mit unabhängigen Lévy-Subordinatoren konstruiert. Diese Arbeit untersucht theoretische Eigenschaften dieser Felder. Dies beinhaltet Resultate zu punktweisen Verteilungen, Kovarianzfunktionen und der Existenz punktweiser

Momente, welche für praktische Anwendungen von großer Bedeutung sind.

Neben diesen theoretischen Untersuchungen wird das subordinierte Gaußsche Zufallsfeld als Erweiterung des klassischen Gaußschen Modells im Diffusionskoeffizienten einer elliptischen PDG betrachtet. Die Existenz einer eindeutigen Lösung des Problems wird bewiesen und mögliche räumliche Diskretisierungstechniken werden diskutiert. Darüber hinaus liefert diese Arbeit eine Approximationstheorie für den betrachteten Diffusionskoeffizienten und untersucht, wie sich der resultierende Fehler auf die PDG-Lösung fortpflanzt.

In vielen Anwendungen der Unsicherheitsquantifizierung (Uncertainty Quantification) sind Momente (von Funktionalen) der Lösung einer zufälligen PDG von Interesse. Daher werden problemspezifische multilevel Monte-Carlo-Schätzer zur Approximation des Erwartungswerts einer zufälligen elliptischen PDG konstruiert, in welcher das unstetige subordinierte Gaußsche Zufallsfeld im Diffusionskoeffizienten auftritt. Es werden allgemeine a-priori-Fehlerschranken für diese Schätzer bewiesen und verschiedene numerische Experimente vervollständigen deren Untersuchung.

Als Alternative zum subordinierten Gaußschen Zufallsfeld wird das sogenannte Gaußsch' subordinierte Lévy-Feld untersucht, das als Komposition eines allgemeinen Lévyprozesses mit einer positiven Transformation eines Gaußschen Zufallsfeldes definiert ist. Die resultierenden Zufallsfelder sind unstetig und weisen große Flexibilität bezüglich der Sprunggeometrien auf. Neben theoretischen Untersuchungen der punktweisen Verteilungen sowie der Herleitung von Formeln für die Kovarianzfunktion werden diese Felder im Diffusionskoeffizienten einer elliptischen PDG betrachtet.

I

Introduction

Introduction and contribution of this thesis

1

1.1 Introduction and motivation

Various real-world phenomena may be described by partial differential equations (PDEs). Application areas of PDEs include, but are not limited to, electro- and thermodynamics, quantum and fluid mechanics, heat propagation or flow problems. A popular PDE model, which is of particular interest in this thesis, is described by the equation

$$-\nabla \cdot (a \nabla u) = f \text{ on a domain } \mathcal{D} \subset \mathbb{R}^d, \text{ with dimension } d \in \mathbb{N}, \tag{1.1}$$

equipped with some appropriate boundary conditions. Here, f is some source function, a is the diffusion coefficient, which may be space-dependent and u denotes the solution to the problem. In the following, this PDE is also referred to as *elliptic model problem*. Such a problem arises, for example, in the context of subsurface/groundwater flow modeling in heterogeneous/porous/fractured media or in other hydrology applications, where the diffusion coefficient models the permeability of the considered material (see [14, 16, 36, 98, 101][1] and the references therein).

In many applications of PDE models, information about input parameters is incomplete or the available data suffer from measurement errors. In order to take this uncertainty into account, one often considers randomized PDE models instead of their deterministic counterparts. This opens the door to an immense research field which is known as *Uncertainty Quantification*. Randomization of a PDE can be done in very different ways. For example, one might consider

[1] The references for the introduction and all following chapters can be found in the unified bibliography at the end of this thesis after Chapter 8

random boundary conditions, random domains, random differential operators or random initial conditions for a time-dependent problem. Either way, a randomization of a PDE model naturally yields a stochastic (i.e. random) solution. Since the exact probability distribution of such a solution is usually not accessible, it is a classical goal in Uncertainty Quantification to approximate moments (of functionals) of this solution. In the elliptic model problem (1.1), the diffusion field a is often the candidate for a randomization, which is then considered to be a random field on the domain $\mathcal{D}$ (see [1, 14, 16, 29, 30, 32, 55, 63, 81, 83, 101, 111, 112]). In the majority of the cited articles, Gaussian random fields (GRFs) are used in the diffusion coefficient a. GRFs are stochastically very well understood and provide a rich theory (see, for instance, [3]). Further, they are attractive for any numerical application since they are comparatively easy to simulate in most cases. However, GRFs also have limitations. The underlying distributions are restricted to the Gaussian family and, therefore, lack flexibility since one cannot model, for example, pointwise distributions with (semi-)heavy tails. Furthermore, realizations of commonly used GRFs, like Matérn fields, are continuous in space. This is unnatural in some situations, for instance, in the context of flow modeling in porous or fractured media, where the values of the permeability a might change abruptly over the domain. Hence, diffusion coefficients based on GRFs are not flexible enough for some applications of the elliptic model problem (cf. [16, 49, 87, 119]) and there is a need for random field models which display a high distributional flexibility and allow for discontinuities in space. On the other side, such a random field model should also provide a sound theory and sample path generation should be computationally cheap to make it well suited for practical applications. In this sense, a reasonable tradeoff has to be found to construct highly flexible models which are numerically and theoretically attractive.

There have been approaches to define more general random field models for the diffusion coefficient a in the elliptic PDE (1.1) in the literature (cf. [94, 96]). For example, the authors of [49] define the diffusion coefficient a as a transformation of a smoothed Lévy noise field. This results in a coefficient with continuous realizations and high distributional flexibility. The references [87] and [119] consider a jump-diffusion coefficient a in problem (1.1) to model two-phase random media. In these references, the coefficient a is discontinuous along an interface, which divides the solution domain into two subdomains. Jump-diffusion coefficients in the elliptic model problem are also frequently used in Bayesian approaches for the corresponding inverse problem. In this situation, level-set priors based on GRFs often serve as a model for the coefficient a which allow for jump modeling since they are spatially discontinuous (see e.g. [46, 76]). However, the distributional flexibility is again limited since the stochasticity of the model is governed by the underlying GRF. In the recent article [16], the authors propose a general jump-diffusion coefficient for the elliptic model problem which has great flexibility in jump

geometries and distributional properties. However, in its general form, it is not straightforward to investigate theoretical properties of the random field model, which is important for practical applications.

1.2 Contribution of this thesis

As explained in Section 1.1, the standard Gaussian model has too many limitations for some applications of the elliptic model problem (1.1). The construction and theoretical investigation of flexible, discontinuous random field models, which are easy to handle numerically, combined with a theoretical and numerical consideration of their application in the diffusion coefficient of the elliptic model problem is, in a nutshell, the topic and the contribution of this thesis. Motivated by the subordinated Brownian motion, random fields on higher-dimensional parameter spaces are constructed combining GRFs with standard Lévy processes: the *subordinated Gaussian random field* and the *Gaussian subordinated Lévy field*. Similar constructions of random fields based on a subordination approach have received only little attention in the recent literature: in the article [42] on generalized random fields, subordinated fields are described in terms of multiple Itô-integrals. Deterministic transformations of GRFs and their excursion sets are considered in [91] and the authors of [85] investigate the (asymptotic) Rosenblatt-type distribution of (subordinated) fields. In [13], the concept of subordination is extended to multivariate Lévy processes and self-decomposibility of the resulting processes, which are defined on a one-dimensional parameter space, is investigated. The subordinated GRF considered in this thesis is constructed by the composition of a GRF on a higher-dimensional parameter space with several independent Lévy subordinators. This definition yields a random field with discontinuous paths and high distributional flexibility (see Chapter 5, which is a reproduction of the article [95]). A main contribution of this thesis is the theoretical investigation of the subordinated GRF in Chapter 5. The results include formulas for the pointwise characteristic function, the spatial covariance function of the fields and a proof on the existence of pointwise absolute moments of the subordinated GRF. These theoretical results are valuable for practical applications, for example, when the subordinated GRF has to image certain statistical properties of given real-world data.

The application of the subordinated GRF in the diffusion coefficient a of the elliptic model problem (1.1) is the main contribution of Chapter 6, which is a reproduction of the article [96]. The diffusion coefficient a is often modeled as log-normal random field, which is not flexible enough for some applications, like flow problems in fractured/porous media. In Chapter 6, the coefficient a consists of a deterministic part, a transformation of a GRF and a transformation

of the subordinated GRF. This significantly extends the flexibility of the standard model with regard to the distributional properties and the ability for jump modeling. While the existence of the resulting random weak solution is straightforward and proven by a pathwise application of the Lax-Milgram lemma, its numerical approximation is more involved and essentialy splits into two steps. The first step is the approximation of the diffusion coefficient itself since GRFs and Lévy processes may in general not be simulated exactly on continuous domains. In Chapter 6, the coefficient a is approximated by the combination of approximations of the GRFs and the Lévy processes. An error bound is proven and, further, it is investigated how this approximation error propagates to the random PDE solution, which is important to control the overall error. The second step consists in the spatial discretization of the elliptic model problem for a given sample of the diffusion coefficient. Chapter 6 considers pathwise finite element methods to approximate paths of the solution. Combining both steps, Chapter 6 describes how to obtain approximate samples of the random solution to the elliptic model problem, where the diffusion coefficient incorporates the subordinated GRF. These solution samples may be used, for example, to estimate (functionals of) moments of the solution, which is of great interest in applications of *Uncertainty Quantification*. The main contribution of Chapter 7, which is a reproduction of the article [93], is the theoretical and practical investigation of multilevel Monte Carlo methods for the elliptic model problem considered in Chapter 6, where the subordinated GRF occurs in the diffusion coefficient. Based on the results of Chapter 6, an a-priori error bound is derived for a multilevel Monte Carlo estimator for the approximation of the expectation of the random solution. By construction, the number of jumps in samples of the diffusion coefficient is defined by the jumps of the underlying Lévy subordinators in the subordinated GRF. Using Lévy subordinators with high jump-activity results in a large number of jump discontinuities in the diffusion coefficient. In order to improve the performance of the multilevel Monte Carlo estimator in this regime, Chapter 7 also considers an extension of the standard multilevel Monte Carlo estimator by the application of a variance reduction technique, which is motivated by the recent paper [101].

Although the subordinated GRF allows to model spatial discontinuities and displays great flexibility with regard to the pointwise distributions, it also has to be mentioned that the jump geometries of the fields are naturally restricted as they always have a rectangular shape, which might be unnatural in some applications. Therefore, the main contribution of Chapter 8, which is a reproduction of the article [94], is to present another construction of a discontinuous random field model by a subordination approach: the Gaussian subordinated Lévy field, which essentially consists of a Lévy process evaluated at a positive transformation of a GRF. The resulting random fields display high distributional flexibility and allow for jump modeling with complex jump geometries. Chapter 8 presents valuable theoretical results on the random

fields including pointwise characteristic functions, covariance functions and their numerical approximation. A further contribution of Chapter 8 consists in the theoretical and numerical investigation of the elliptic model problem (1.1), where the diffusion coefficient incorporates the Gaussian subordinated Lévy field, resulting in a high flexibility with regard to the pointwise distributions and the jump geometries.

1.3 Overall structure of the work

The rest of this thesis is structured as follows: Chapter 2 provides the theoretical and methodological background for this thesis. Sections 2.1 and 2.2 introduce Lévy processes and Gaussian random fields and collect some theoretical results. The elliptic model problem is addressed in Section 2.3 and Section 2.4 is devoted to Monte Carlo methods. Thereafter, Chapter 3 presents the main results of this work in more detail, followed by a summary and a discussion of possible future research directions. Finally, as the main part of this thesis, the cumulative part consists of Chapters 5, 6, 7 and 8, which are reproductions of the four articles [95], [96], [93] and [94], respectively. The unified bibliography can be found at the end of this thesis after Chapter 8.

Theoretical and methodological background

2

The following chapter aims to introduce basic theoretical and methodological concepts that are essential for the rest of this work. In Section 2.1 and 2.2, Lévy processes and GRFs are introduced, which play an important role in this thesis. Section 2.3 takes a closer look into the elliptic model problem (1.1) and Section 2.4 introduces Monte Carlo methods. For the remainder of this work, the triplet $(\Omega, \mathcal{F}, \mathbb{P})$ always denotes a complete probability space.

2.1 Lévy processes

Lévy processes have an extensive theory, great distributional flexibility and allow for discontinuity modeling. They play a crucial role in the construction of discontinuous random fields in Chapters 5 and 8 and, therefore, we introduce them in the following section, highlighting some of their fundamental properties. For a more detailed introduction to Lévy processes we refer to [8] and [108]. The section is structured as follows: we start with the definition of a Lévy process and some basic examples in Subsection 2.1.1. The rest of this subsection will be devoted to the well-known Lévy-Khinchin formula and some other basic properties of Lévy processes. In Subsection 2.1.2, we introduce the concept of time-changing with non-negative Lévy processes, which strongly motivates the construction of discontinuous random fields in Chapters 5 and 8.

2.1.1 Definition and basic properties

Let $\mathcal{T} \subseteq \mathbb{R}_+ := [0, +\infty)$ be a Borel-measurable index set. A (real-valued) stochastic process $X = (X(t),\ t \in \mathcal{T})$ is a family of random variables on $(\Omega, \mathcal{F}, \mathbb{P})$ with values in $\mathbb{R}$. That is, for each $t \in \mathcal{T}$, the mapping $X(t) : \Omega \to \mathbb{R}$ is $\mathcal{F} - \mathcal{B}(\mathbb{R})$-measurable, where $\mathcal{B}(\mathbb{R})$ denotes the Borel σ-algebra, which is the smallest σ-algebra over $\mathbb{R}$ which contains all open subsets (see e.g. [79, Definition 1.21 and Definition 9.1]). We say that a stochastic process $X = (X(t),\ t \in \mathcal{T})$ is a *modification* or a *version* of the stochastic process $Y = (Y(t),\ t \in \mathcal{T})$ if, for any $t \in \mathcal{T}$, it holds $X(t) = Y(t)$ $\mathbb{P}$-almost surely. For a fixed $\omega \in \Omega$, the mapping $t \mapsto X(t, \omega)$ is called a *path* of the stochastic process. We say that the stochastic process X has càdlàg (continue à droite, limite à gauche) paths if there exists $\Omega_0 \in \mathcal{F}$ with $\mathbb{P}(\Omega_0) = 1$ such that for any $\omega \in \Omega_0$ the path $t \mapsto X(t, \omega)$ is right-continuous with left limits, i.e. for all $t \in \mathcal{T}$ it holds

$$\lim_{s \searrow t} X(\omega, s) = X(\omega, t) \text{ and } \lim_{s \nearrow t} X(\omega, s) \text{ exists,}$$

(see [106, Chapter 1, Section 1]). Lévy processes build an extensive class of stochastic processes which are attractive for many applications due to their flexibility and their theoretical properties (see for example [109] for some applications in finance). They are formally defined as follows (see e.g. [8, Section 1.3]).

Definition 2.1.1.
A stochastic process $l = (l(t),\ t \in \mathbb{R}_+)$ is said to be a Lévy process if

i $l(0) = 0$ $\mathbb{P}$*-a.s.,*

ii l *has independent increments, i.e. for each $0 \leq t_1 \leq t_2 \leq \cdots \leq t_{n+1} < +\infty$ the random variables $(l(t_{j+1}) - l(t_j),\ 1 \leq j \leq n)$ are mutually independent,*

iii l *has stationary increments, i.e. for each $0 \leq t_1 \leq t_2 \leq \cdots \leq t_{n+1} < +\infty$ it holds*

$$l(t_{j+1}) - l(t_j) \stackrel{\mathcal{D}}{=} l(t_{j+1} - t_j) - l(0) \stackrel{\mathcal{D}}{=} l(t_{j+1} - t_j),$$

iv l *is stochastically continuous, i.e. for all $a > 0$ and $s \geq 0$, it holds*

$$\lim_{t \to s} \mathbb{P}(|l(t) - l(s)| > a) = 0.$$

◆

In Definiton 2.1.1, we denote by $\stackrel{\mathcal{D}}{=}$ equivalence in distribution. In general, the paths of a Lévy process allow jumps and, hence, are discontinuous. It is well-known that any Lévy process admits a càdlàg modification, which is also a Lévy process (see [106, Chapter 1, Theorem 30]). In the following, we always consider the càdlàg version of a Lévy process. We continue with four examples of Lévy processes that will reappear repeatedly in this thesis.

Example 2.1.2. *A very popular Lévy process is given by the Brownian motion, which is a Lévy process $B = (B(t),\ t \geq 0)$ with $\mathbb{P}$-a.s. continuous paths and $B(t) \sim \mathcal{N}(0,t)$ (see [79, Definition 21.8]). A Poisson, Gamma or Normal Inverse Gaussian (NIG) process is a Lévy process whose increments follow a Poisson, Gamma or NIG distribution, respectively. (see [109, Sections 5.3.1, 5.3.3 and 5.3.8]). Figure 2.1 shows samples of different Lévy processes.* ◆

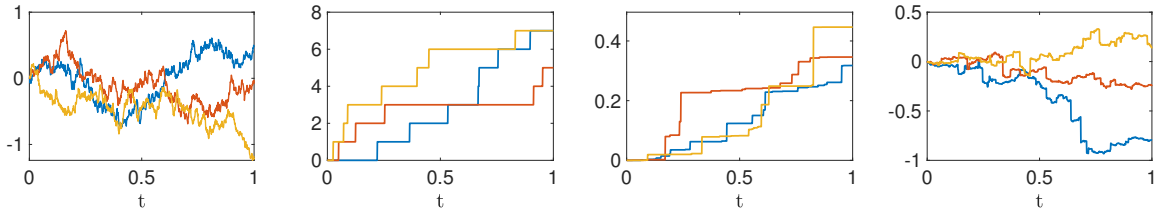

Figure 2.1: Three sample paths of a Brownian motion (left), a Poisson(5) process (second from left), a Gamma(4,10) process (second from right) and a NIG(5,-1,1) process (right).

The class of Lévy processes may be parametrized by the so called *Lévy triplet*: Any Lévy process is uniquely determined by a triplet (b, σ_N^2, ν), which consists of constants $b,\ \sigma_N^2 \in \mathbb{R}$ and a measure ν on $(\mathbb{R}, \mathcal{B}(\mathbb{R}))$. This connection is formalized in the popular *Lévy-Khinchin formula*, which gives an explicit representation of the pointwise characteristic function of any Lévy process in terms of its Lévy triplet. A proof can be found, for example, in [8, Th. 1.3.3 and p. 45] and [108, Theorem 8.1]. As usual, we denote by $\mathbb{E}(X) = \int_\Omega X\, d\mathbb{P}$ the *expectation* of a real-valued random variable X.

Theorem 2.1.3 (Lévy-Khinchin formula)**.**
Let l be a real-valued Lévy process on $\mathbb{R}_+$. There exist parameters $b \in \mathbb{R}$, $\sigma_N^2 \in \mathbb{R}_+$ and a measure ν on $(\mathbb{R}, \mathcal{B}(\mathbb{R}))$ such that the characteristic function $\phi_{l(t)}$ of the Lévy process l admits the representation

$$\phi_{l(t)}(\xi) := \mathbb{E}(\exp(i\xi l(t))) = \exp(t\psi(\xi)),\ \xi \in \mathbb{R},$$

for $t \in \mathbb{R}_+$. Here, ψ denotes the characteristic exponent of l, which is given by

$$\psi(\xi) := ib\xi - \frac{\sigma_N^2}{2}\xi^2 + \int_{\mathbb{R}\setminus\{0\}} e^{i\xi y} - 1 - i\xi y \mathbb{1}_{\{|y|\leq 1\}}(y)\, \nu(dy).$$

The measure ν satisfies

$$\nu(\{0\}) = 0 \text{ and } \int_{\mathbb{R}} \min(y^2, 1)\, \nu(dy) < \infty, \tag{2.1}$$

and a measure with this property is called Lévy measure. Further, (b, σ_N^2, ν) is called Lévy triplet of l. ◆

We proceed with a remark on the connection between the Lévy-Khinchin formula, infinitely divisible distributions and Lévy processes.

Remark 2.1.4. *In its most general formulation, the Lévy-Khinchin formula gives a representation for the characteristic function of any infinitely divisible distribution and, conversely, any distribution whose characteristic function admits a Lévy-Khinchin form is infinitely divisible (see [108, Theorem 8.1]) . Further, there is a one-to-one correspondence between infinitely divisible distributions and Lévy processes: if l is a Lévy process, then the random variable $l(t)$ is infinitely divisible for any $t \in \mathbb{R}_+$ (see [8, Proposition 1.3.1]) and, conversely, for any infinitely divisible distribution μ there exists a Lévy process l with $l(1) \stackrel{\mathcal{D}}{=} \mu$ (see [108, Theorem 7.10]).* ◆

The existence of moments plays a fundamental role in probability theory. For example, even the well-known strong law of large numbers requires finiteness of the first absolute moment of the considered distribution. In the purely Gaussian case, this is not a real problem since the Gaussian distribution admits a finite n-th absolute moment for any $n \in \mathbb{N}$. However, when general Lévy processes are considered, this is not the case anymore. The Lévy-Khinchin formula demonstrates that the pointwise distribution of any Lévy process l is determined by the pointwise distribution of the real-valued random variable $l(1)$. This suggests that the existence of moments of a Lévy process at time t does not depend on the time parameter. In fact, one can show that for any Lévy process l and any $n \in \mathbb{N}$, it holds

$$\mathbb{E}(|l(t)|^n) < +\infty \text{ for all } t \geq 0 \Leftrightarrow \int_{|x|\geq 1} |x|^n\, \nu(dx) < +\infty,$$

where ν denotes the Lévy measure of l (see [8, Theorem 2.5.2]). Further, it is possible to prove an even stronger property: in [23] the authors prove an explicit polynomial expansion of the

$2n$-th absolute moment of a Lévy process in the time parameter, provided that the moment exists. This property is needed in Chapter 8 and we formulate it in the following lemma. For a proof we refer to [23, Proposition 2.3].

Lemma 2.1.5.
Let $n \in \mathbb{N}$ and l be a Lévy process with $\mathbb{E}(|l(1)|^{2n}) < +\infty$. There exists real numbers $m_1, \dots, m_{2n}$, which are independent of t, such that

$$\mathbb{E}(|l(t)|^{2n}) = m_1 t + m_2 t^2 + \cdots + m_{2n} t^{2n},$$

for all $t \geq 0$. ◆

2.1.2 Subordinators and subordinated processes

Subordination in the context of Lévy processes means a time-change of a Lévy process with respect to another non-negative Lévy process. It turns out that the resulting process is again a Lévy process and this approach strongly motivates the construction of the discontinuous random fields in Chapters 5 and 8.

A *Lévy subordinator* $S = (S(t),\ t \geq 0)$ is a Lévy process with $\mathbb{P}$-almost surely non-decreasing paths and, hence, any subordinator satisfies $S(t) \geq 0$ $\mathbb{P}$-a.s. for all $t \geq 0$ (see [8, Section 1.3.2]). For any $t \in \mathbb{R}_+$, the pointwise characteristic function of a Lévy subordinator S admits the following form (see [8, Theorem 1.3.15])

$$\phi_{S(t)}(\xi) = \mathbb{E}(\exp(i\xi S(t))) = \exp\Big(t\big(i\gamma\xi + \int_0^\infty e^{i\xi y} - 1\,\nu(dy)\big)\Big), \quad \text{for } \xi \in \mathbb{R}, \tag{2.2}$$

where, ν is the Lévy measure of S and γ is called drift parameter. The Lévy measure ν of a Lévy subordinator satisfies the condition

$$\nu(-\infty, 0) = 0 \text{ and } \int_0^\infty \min(y, 1)\,\nu(dy) < \infty.$$

Note that this condition is stronger than (2.1), which holds for any Lévy process. Since a Lévy subordinator S is by definition a Lévy process, the Lévy-Khinchin formula holds and we obtain $\sigma_N^2 = 0$ and $b = \gamma + \int_0^1 y\,\nu(dy)$ in Theorem 2.1.3 for the subordinator S. In the following, we always mean the triplet $(\gamma, 0, \nu)$ corresponding to representation (2.2) if we refer to the characteristic triplet of a Lévy subordinator.

Since Lévy subordinators are non-negative, they may be used as a time-change process. This

leads to the construction of the subordinated Lévy process: if l is a Lévy process and S a Lévy subordinator independent of l, then the process

$$t \mapsto l(S(t))$$

is called subordinated Lévy process and it is again a Lévy process (see [8, Theorem 1.3.25]). In this construction, l is often chosen as Brownian motion which yields the well-known subordinated Brownian motion. Many Lévy processes admit a representation by a subordinated Brownian motion. For examlple, the NIG process from Example 2.1.2 may be represented by a (drifted) Brownian motion time-changed by an Inverse Gaussian process (see [109, Section 5.3.8]). Further, the extensive class of Generalized hyperbolic (GH) Lévy processes admit a similar representation (see e.g. [15, Section 4]). We emphasize that this combination of a continuous and a discontinuous stochastic process via the subordination approach motivates the constructions of discontinuous random fields in Chapters 5 and 8.

2.2 (Gaussian) random fields

In Section 2.1 we introduced Lévy processes as a specific class of stochastic processes depending on a one-dimensional parameter. The generalization of a stochastic process to higher-dimensional parameters is called *random field* and is used to model spatially dependent functions in a stochastic setting. For example, random fields are often used to randomize spatially dependent coefficients in PDEs, see e.g. [1, 14, 16, 30, 55, 101, 112] and the references therein for elliptic problems. In this section we introduce random fields in general and the GRF, which builds a very important subclass. We refer to [3] for a more detailed introduction. GRFs provide a rich and well-understood theory and are comparatively easy to simulate. After their definition in Subsection 2.2.1, we introduce the covariance operator and derive the Karhunen-Loève expansion in Subsection 2.2.2, which yields a natural way to simulate GRFs. We close this section with a brief motivation of the circulant embedding method to draw samples of a GRF on a discrete grid following [64].

2.2.1 Definition of (Gaussian) random fields

In Subsection 2.1.1 we introduced a stochastic process as family of random variables parametrized by a one-dimensional parameter. A random field is the natural extension to higher-dimensional

parameter spaces: let $\mathcal{D} \subset \mathbb{R}^d$ be a Borel set with $d \in \mathbb{N}$. A random field $R = (R(\underline{x}),\ \underline{x} \in \mathcal{D})$ is a family of real-valued random variables on $(\Omega, \mathcal{F}, \mathbb{P})$ parametrized by $\underline{x} \in \mathcal{D}$ (see e.g. [8, Subsection 1.1.8]). The GRFs build one of the most popular classes of random fields. We start with the definition of the multivariate Gaussian distribution: a vector-valued random variable $Z : \Omega \to \mathbb{R}^n$, $n \in \mathbb{N}$, follows a multivariate Gaussian distribution if, for any $\alpha \in \mathbb{R}^n$, the real-valued random variable

$$\alpha^T Z : \Omega \to \mathbb{R}$$

follows a (one-dimensional) Gaussian distribution (see [3, Section 1.2]). In this case, we write $Z \sim \mathcal{N}_n(\mu, \Sigma)$, where $\mu = (\mathbb{E}(Z_1), \dots, \mathbb{E}(Z_n))^T$ is the mean vector and Σ is the covariance matrix with entries $\Sigma_{i,j} = \mathrm{Cov}(Z_i, Z_j) := \mathbb{E}((Z_i - \mathbb{E}(Z_i))(Z_j - \mathbb{E}(Z_j)))$ for $i, j = 1, \dots, n$. A random field $W = (W(\underline{x}),\ \underline{x} \in \mathcal{D})$ is a GRF if, for any $n \in \mathbb{N}$ and any $\underline{x}_1, \dots, \underline{x}_n \in \mathcal{D}$ the n-dimensional random vector

$$(W(\underline{x}_1), \dots, W(\underline{x}_n)) : \Omega \to \mathbb{R}^n$$

is multivariate Gaussian distributed (see e.g. [3, Section 1.2]). For a GRF W, we define the mean $\mu_W : \mathcal{D} \to \mathbb{R}$ and covariance function $q_W : \mathcal{D} \times \mathcal{D} \to \mathbb{R}$ by

$$\begin{aligned} \mu_W(\underline{x}) &:= \mathbb{E}(W(\underline{x})), \\ q_W(\underline{x}, \underline{x}') &:= \mathrm{Cov}(W(\underline{x}), W(\underline{x}')) = \mathbb{E}\big((W(\underline{x}) - \mathbb{E}(W(\underline{x})))(W(\underline{x}') - \mathbb{E}(W(\underline{x}')))\big), \end{aligned}$$

for $\underline{x},\ \underline{x}' \in \mathcal{D}$. We say that the GRF W is *centered* if $\mu_W \equiv 0$. Further, W is *stationary* or *isotropic* if the mean μ_W is constant and there exists a function $\tilde{q}_W$ such that the covariance function q_W can be written in the form $q_W(\underline{x}, \underline{x}') = \tilde{q}_W(\underline{x} - \underline{x}')$, resp. $q_W(\underline{x}, \underline{x}') = \tilde{q}_W(|\underline{x} - \underline{x}'|_2)$ for $\underline{x},\ \underline{x}' \in \mathcal{D}$, where $|\underline{x}|_2 := (x_1^2 + \dots + x_d^2)^{1/2}$ denotes the Euclidean norm of $\underline{x} = (x_1, \dots, x_d) \in \mathbb{R}^d$ (see e.g. [3, Section 5]). The GRFs considered in the following are always assumed to be mean-square continuous, which is a common assumption in the context of GRFs (cf. [3, Chapter 1]).

It follows by the Kolmogorov existence theorem (see [79, Satz 14.36] and [44, 12.1.2 Theorem]) that all distributional properties of a random field are determined by its finite dimensional distributions (cf. [4, Section 2.1]). Therefore, by definition, a GRF is uniquely determined by its mean and covariance function. Further, we point out that there is a one-to-one correspondence between GRFs and their mean and covariance functions: it is clear that for any GRF W there exists the mean and a covariance function, which is always non-negative definite. On the other hand, for a given function $\mu_W : \mathcal{D} \to \mathbb{R}$ and a non-negative definite function $q_W : \mathcal{D} \times \mathcal{D} \to \mathbb{R}$

there always exists a GRF W with mean function μ_W and covariance function q_W (see [44, 12.1.3 Theorem]).

GRFs allow for a detailed investigation of the path regularity. We refer to [3, Section 1.3] for more details and a general investigation of path continuity of GRFs. It turns out that under quite mild assumptions a GRF has (or can be assumed to have) almost surely continuous realizations. For specific GRFs, continuity of realizations is often proven by the Kolmogorov continuity theorem, which we state for completeness in the following (see [8, Theorem 1.1.18]).

Theorem 2.2.1 (Kolmogorov continuity theorem)**.**
Let $W = (W(\underline{x}),\ \underline{x} \in \mathcal{D})$ be a random field on the Borel set $\mathcal{D} \subset \mathbb{R}^d$ with some $d \in \mathbb{N}$ and suppose that there exist strictly positive constants $\gamma_W,\ C_W$ and ε such that

$$\mathbb{E}(|W(\underline{x}) - W(\underline{x}')|^{\gamma_W}) \leq C_W |\underline{x} - \underline{x}'|_2^{d+\varepsilon},$$

for all $\underline{x},\ \underline{x}' \in \mathcal{D}$. Then, there exists a modification of W with almost surely continuous paths. ◆

We emphasize that two random fields $W_1 = (W_1(\underline{x}),\ \underline{x} \in \mathcal{D})$ and $W_2 = (W_2(\underline{x}),\ \underline{x} \in \mathcal{D})$ which are modifications of one another, have the same finite dimensional distributions (cf. [28, Section 7]) and, hence, they have the same distributional properties by the Kolmogorov existence theorem. In this sense, a GRF satisfying the assumptions of the Kolmogorov continuity theorem can always be assumed to have almost surely continuous realizations in the sense that one can always consider the almost surely continuous modification, which is also a GRF and has the same distributional properties.

2.2.2 Covariance operator and Karhunen-Loève expansion

In this subsection, we derive the well-known Karhunen-Loève expansion, which is a series representation of a GRF with respect to the eigenbasis of its covariance operator. In order to do so, we need to introduce the (Lebesgue-)Bochner spaces for Banach-space-valued random variables. Therefore, let B be a Banach space and denote by B' its dual. A mapping $Z : \Omega \to B$ is said to be *separably valued* if there exists a closed, separable subspace $B_0 \subseteq B$ with $Z(\Omega) \subseteq B_0$ and Z is called *weakly measurable* if for any $b' \in B'$ the mapping

$$\omega \mapsto b'(Z(\omega)),\ \omega \in \Omega,$$

is $\mathcal{F} - \mathcal{B}(\mathbb{R})$-measurable (see [74, Section 1.1]). Further, we say that $Z : \Omega \to B$ is *strongly measurable*, if Z is separably valued and weakly measurable (see [74, Theorem 1.1.6]) and $Z : \Omega \to B$ is strongly $\mathbb{P}$-measurable if there exists a strongly measurable mapping $\hat{Z} : \Omega \to B$ with $\mathbb{P}(Z = \hat{Z}) = 1$ (see [74, Proposition 1.1.16]). We can now define the (Lebesgue-)Bochner spaces $L^p(\Omega; B)$ as the natural extension of the Lebesgue L^p spaces (see e.g. [74, Definition 1.2.15]).

Definition 2.2.2.
For $p \in [1, +\infty]$, we define $L^p(\Omega; B)$ to be the space of all (equivalence classes of) strongly $\mathbb{P}$-measurable mappings $Z : \Omega \to B$ with $\|Z\|_{L^p(\Omega;B)} < +\infty$, where the norm is defined by

$$\|Z\|_{L^p(\Omega;B)} = \begin{cases} \mathbb{E}(\|Z\|_B^p)^{\frac{1}{p}} & , \text{ if } 1 \leq p < +\infty, \\ \operatorname{ess\,sup}_{\omega \in \Omega} \|Z\|_B & , \text{ if } p = +\infty. \end{cases}$$

◆

Consider a centered GRF $W = (W(\underline{x}),\ \underline{x} \in \mathcal{D})$ on a compact set $\mathcal{D} \subset \mathbb{R}^d$ with paths in $L^2(\mathcal{D})$, where we denote by $L^p(\mathcal{D})$ the usual Lebesgue space, for $p \in [1, +\infty]$ (see e.g. [2, Chapter 2]). Further, we assume that $W : \Omega \to L^2(\mathcal{D})$ is strongly measurable which is equivalent to weak measurability in this case since $L^2(\mathcal{D})$ is separable (see [22, Theorem 4.13]). We define the *covariance operator* of the GRF W:

$$Q_W : L^2(\mathcal{D}) \to L^2(\mathcal{D}),\ \psi \mapsto \int_{\mathcal{D}} q_W(\cdot, \underline{y}) \psi(\underline{y})\, d\underline{y}.$$

This operator is linear and well defined since for any $\psi \in L^2(\mathcal{D})$ it holds by Hölder's inequality

$$\begin{aligned} \|Q_W \psi\|_{L^2(\mathcal{D})}^2 &= \int_{\mathcal{D}} \Big(\int_{\mathcal{D}} q_W(\underline{x}, \underline{y}) \psi(\underline{y}) d\underline{y} \Big)^2 d\underline{x} \\ &= \int_{\mathcal{D}} \Big(\int_{\mathcal{D}} \mathbb{E}(W(\underline{x}) W(\underline{y})) \psi(\underline{y}) d\underline{y} \Big)^2 d\underline{x} \\ &\leq \int_{\mathcal{D}} \mathbb{E}(W(\underline{x})^2) d\underline{x} \Big(\int_{\mathcal{D}} \mathbb{E}(W(\underline{y})^2)^{1/2} |\psi(\underline{y})| d\underline{y} \Big)^2 \\ &\leq \|W\|_{L^2(\Omega; L^2(\mathcal{D}))}^4 \|\psi\|_{L^2(\mathcal{D})}^2 < +\infty. \end{aligned}$$

For the rest of this subsection, we assume that W has continuous paths and $\sup_{\underline{x} \in \mathcal{D}} \mathbb{E}(W(\underline{x})^2)) < +\infty$. In this case, $W : \Omega \to L^2(\mathcal{D})$ is strongly measurable (see [79, Theorem 14.16], [6, Lemma 4.51]) and the covariance function is continuous: For $(\underline{x}^{(n)},\ n \in \mathbb{N}),\ (\underline{y}^{(n)},\ n \in \mathbb{N}) \subset \mathcal{D}$ with

$\underline{x}^{(n)} \to \underline{x},\ \underline{y}^{(n)} \to \underline{y}$, for $n \to \infty$ it holds

$$\lim_{n\to\infty} \mathbb{E}(W(\underline{x}^{(n)})W(\underline{y}^{(n)})) = \mathbb{E}(\lim_{n\to\infty} W(\underline{x}^{(n)})W(\underline{y}^{(n)})) = \mathbb{E}(W(\underline{x})W(\underline{y})),$$

where the exchange of limit and expectation is justified by the dominated convergence theorem together with the Borell-TIS inequality (see [3, Theorem 2.1.1]). It follows now by the spectral theorem that there exists a decreasing, non-negative sequence of real eigenvalues $(\lambda_i,\ i \in \mathbb{N})$ and eigenfunctions $(e_i,\ i \in \mathbb{N}) \subset L^2(\mathcal{D})$ of the covariance operator Q_W such that $(e_i,\ i \in \mathbb{N})$ is an orthonormal basis of $L^2(\mathcal{D})$ (see [115, Theorem VI.3.2]). Further, Mercer's theorem states that the covariance function can be expanded in terms of this eigenbasis. In fact, it holds

$$q_W(\underline{x}, \underline{y}) = \sum_{i=1}^{\infty} \lambda_i e_i(\underline{x}) e_i(\underline{y}),$$

where the series converges absolutely and uniformly on $\mathcal{D}$ (see [3, Theorem 3.2.1]). Further, the GRF W itself admits a representation in terms of the eigenbasis of Q_W, which is known as the *Karhunen-Loève expansion* (see [3, Theorem 3.1.1, Theorem 3.1.2 and Lemma 3.2.2]). In fact, it holds

$$W(\underline{x}) = \sum_{i=1}^{\infty} \sqrt{\lambda_i} e_i(\underline{x}) Z_i,$$

where $(Z_i,\ i \in \mathbb{N})$ are i.i.d. $\mathcal{N}(0,1)$-distributed random variables and the series converges in $L^2(\Omega)$ and uniformly on $\mathcal{D}$. This expansion is often used in applications when realizations of a GRF have to be simulated: If the eigenbasis of a GRF W is known, the Karhunen-Loève expansion motivates the numerical approximation of paths of W by an evaluation of the truncated series

$$W^N(\underline{x}) := \sum_{i=1}^{N} \sqrt{\lambda_i} e_i(\underline{x}) Z_i \approx \sum_{i=1}^{\infty} \sqrt{\lambda_i} e_i(\underline{x}) Z_i = W(\underline{x}),$$

with some cut-off index $N \in \mathbb{N}$. This simulation approach is widely used in numerical simulations (see, for example, [1, 14, 16, 30, 55, 101, 112] and Chapter 8).

2.2.3 Sampling a Gaussian random field on a discrete grid: the circulant embedding method

In Subsection 2.2.2, we introduced the Karhunen-Loève expansion, which is often used in practical simulations since it yields a direct approach to produce (approximate) samples of a GRF W by truncating the series at a finite threshold $N \in \mathbb{N}$. If the eigenvalues and eigenfunctions are available, the resulting approximation is naturally defined on the continuous parameter domain. A conceptually different approach to simulate paths of a GRF is to produce samples on a discrete grid on $\mathcal{D}$.

We explain this in more detail for the case $\mathcal{D} = [0, 1]$ for simplicity. Consider a centered GRF W on $\mathcal{D}$ with covariance function q_W and let $N \in \mathbb{N}$ be given. We aim to simulate the GRF W evaluated on the discrete grid $(x_i,\ i = 0, \dots, N)$ with grid points $x_i := i/N$. In other words, we aim to draw a sample from the random vector $(W(x_0), \dots, W(x_N))^T : \Omega \to \mathbb{R}^{N+1}$, which follows a zero-mean multivariate Gaussian distribution with covariance matrix $\Sigma_N = (q_W(x_i, x_j))_{i,j=0}^N \in \mathbb{R}^{(N+1)\times(N+1)}$. Assume that the covariance matrix admits a decomposition of the form

$$\Sigma_N = CC^T, \tag{2.3}$$

where $C \in \mathbb{R}^{(N+1)\times k}$ is a matrix with entries $C_{i,j}$, for $i = 1, \dots, N+1$ and $j = 1, \dots, k$ for some $k \geq N + 1$. If $Z = (Z_1, \dots, Z_k)^T$ is vector with independent standard normal random variables, then the product CZ follows the same distribution as $(W(x_0), \dots, W(x_N))^T$. In fact, CZ is a centered and multivariate Gaussian distributed random vector with covariances

$$\mathrm{Cov}((CZ)_i, (CZ)_j) = \sum_{l,m=1}^{k} C_{i,l} C_{j,m} \mathbb{E}(Z_l Z_m) = \sum_{l=1}^{k} C_{i,l} C_{l,j}^T = (CC^T)_{i,j},$$

for $i, j = 1, \dots, N+1$, and, hence, the covariance matrix of CZ equals Σ_N. Therefore, if a decomposition of type (2.3) is available, sampling of the GRF W on the discrete grid reduces to the generation of i.i.d. standard normal random variables and a transformation according to the matrix C. We emphasize that the same approach can be applied on higher-dimensional parameter spaces under appropriate ordering of the discrete points in the multidimensional grid.

Obviously, the key of this sampling approach is the computation of the factorization (2.3). Such a decomposition may for example be obtained by the Cholesky factorization which, however, becomes extremely expensive when the resolution of the grid and, hence, the size of the

covariance matrix Σ_N grows. The circulant embedding (CE) method provides a computationally efficient way to compute a decomposition of type (2.3) for stationary GRFs on a regular grid using the specific structure of the resulting covariance matrix: under lexicographical ordering of the grid points, the covariance matrix is a nested block Toeplitz matrix and, further, it can be embedded in a larger nested block circulant matrix, whose spectral decomposition can be efficiently computed using the d-dimensional fast Fourier transform (FFT) (see e.g. [64]). In this sense, the CE method can be seen as a computationally efficient alternative to the Cholesky decomposition to compute the factorization of the covariance matrix Σ_N and, hence, to draw a sample of a GRF on the discrete grid. We refer to [64] for more details.

In contrast to the approximation of a GRF with a truncated Karhunen-Loève expansion, the CE method does not require the truncation of a series and yields an exact simulation of the field on the grid points. On the other hand, this simulation techniques is restricted to the case of stationary fields and it requires the grid to be regular and evaluations of the GRF outside this grid require an additional interpolation (cf. [65]).

We close this section with the definition of a very important class of stationary GRFs with continuous paths: the Matérn fields. For a smoothness parameter $\nu > 1/2$, correlation length $r > 0$ and variance $\sigma^2 > 0$, the Matérn-ν covariance function is given by $q_M(\underline{x}, \underline{y}) = \rho_M(\|\underline{x} - \underline{y}\|_2)$, for $(\underline{x}, \underline{y}) \in \mathbb{R}^d_+ \times \mathbb{R}^d_+$, with

$$\rho_M(s) = \sigma^2 \frac{2^{1-\nu}}{\Gamma(\nu)} \Big(\frac{2s\sqrt{\nu}}{r}\Big)^{\nu} K_\nu\Big(\frac{2s\sqrt{\nu}}{r}\Big), \text{ for } s \geq 0,$$

where $\Gamma(\cdot)$ is the Gamma function and $K_\nu(\cdot)$ is the modified Bessel function of the second kind (see [63, Section 2.2] and Chapter 5). A Matérn-ν GRF is a centered GRF with covariance function q_M.

2.3 The elliptic model problem and the finite element method

In this section, we introduce the elliptic partial differential equation (PDE) which plays an important role in this thesis (see Chapters 6 - 8). This type of equation may be used, for example, as a simplified model for general subsurface flow problems or groundwater flow models in heterogeneous/porous media (cf. [14, 16, 101]). For simplicity and ease of notation, we consider the deterministic version of the problem in this section. In Subsection 2.3.2, we derive the weak solution followed by a brief introduction to the finite element method in Subsections 2.3.3 and 2.3.4. For a more general introduction to elliptic PDEs and the finite element method

we refer to [67] and [21]. We close the section with a discussion of a randomized version of the considered PDE, which is considered in more detail in Chapters 6 - 8 of this thesis.

2.3.1 The deterministic elliptic model problem

Let $\mathcal{D} \subset \mathbb{R}^d$ be a bounded, connected Lipschitz domain with $d \in \mathbb{N}$. Further let $a : \mathcal{D} \to \mathbb{R}_+$ and $f : \mathcal{D} \to \mathbb{R}$ be measurable functions. We are interested in the solution $u : \mathcal{D} \to \mathbb{R}$ of the PDE

$$-\nabla \cdot (a(\underline{x})\nabla u(\underline{x})) = f(\underline{x}) \text{ on } \mathcal{D}, \tag{2.4}$$

where we focus on the homogeneous Dirichlet boundary conditions

$$u(\underline{x}) = 0 \text{ on } \partial\mathcal{D}, \tag{2.5}$$

in this section to keep notation simple. Note that the extension to more general boundary conditions is straightforward (see e.g. [67, 50] and Chapters 6 - 8). We denote by $C^k(\overline{\mathcal{D}})$ the space of k-times continuously differentiable functions on the closure $\overline{\mathcal{D}}$, for $k \in \mathbb{N}_0$. For a diffusion coefficient $a \in C^1(\overline{\mathcal{D}})$ we say that $u \in C^2(\overline{\mathcal{D}})$ is a *classical solution* if it satisfies Equations (2.4) and (2.5) in the classical sense. This solution concept, however, imposes restrictive regularity assumptions on a and u which are not fulfilled, for example, for a discontinuous diffusion coefficient. Therefore, it is convenient to consider the so called *weak solution*, which we introduce in the following subsection. We refer to [21, 50, 67] for more details.

2.3.2 The weak solution

We denote by $H^k(\mathcal{D}) := W^{k,2}(\mathcal{D})$ the Sobolev spaces which consist of all measurable, k-times weakly differentiable and square integrable functions on $\mathcal{D}$ with $k \in \mathbb{N}_0$ (see [2, Chapter 3]). Further, we denote by $H_0^1(\mathcal{D}) := \{v \in H^1(\mathcal{D}) \mid Tv = 0\}$ the space of weakly differentiable, square integrable functions which vanish on the boundary in a weak sense. Here, $T : H^1(\mathcal{D}) \to H^{1/2}(\partial\mathcal{D})$ denotes the *trace operator*, which is linear and continuous with $Tv = v|_{\partial D}$ for $v \in C^\infty(\overline{D})$ (see [41]). We multiply (2.4) by a test function $v \in V := H_0^1(\mathcal{D})$

and integrate by parts (see e.g. [113, Section 6.3]) to obtain

$$\int_{\mathcal{D}} a(\underline{x})\nabla u(\underline{x}) \cdot \nabla v(\underline{x}) d\underline{x} = \int_{\mathcal{D}} f(\underline{x}) v(\underline{x}) d\underline{x},$$

for any $v \in V$. This motivates the weak formulation of the problem: For a measurable function $a \in L^\infty(\mathcal{D})$ and a linear, continuous functional $F \in V'$, find $u \in V$ such that

$$B_a(u, v) = F(v), \text{ for all } v \in V, \tag{2.6}$$

where the bilinear form B_a is defined by

$$\begin{aligned} B_a : V \times V &\to \mathbb{R} \\ (u, v) &\mapsto \int_{\mathcal{D}} a(\underline{x})\nabla u(\underline{x}) \cdot \nabla v(\underline{x}) d\underline{x}. \end{aligned}$$

If we assume that the diffusion coefficient a is bounded away from zero, we obtain the following theorem by the Lax-Milgram lemma. Although this is a standard result, we give a proof for completeness.

Theorem 2.3.1.
Let $a \in L^\infty(\mathcal{D})$ with $a(\underline{x}) \geq a_- > 0$ almost everywhere on $\underline{x} \in \mathcal{D}$ and $F \in V'$. There exists a unique weak solution $u \in V$ satisfying (2.6) *. Further, it holds*

$$\|u\|_V \leq C(a_-, \mathcal{D}, d)\|F\|_{V'},$$

where $C(a_-, \mathcal{D}, d)$ is a constant depending only on the indicated parameters. ◆

Proof. We use Hölder's inequality and the assumption $a \in L^\infty(\mathcal{D})$ to obtain the continuity of the bilinear form B_a:

$$|B_a(u, v)| \leq \|a\|_{L^\infty(\mathcal{D})}\|\nabla u\|_{L^2(\mathcal{D})}\|\nabla v\|_{L^2(\mathcal{D})} \leq \|a\|_{L^\infty(\mathcal{D})}\|u\|_V\|v\|_V, \text{ for } u, v \in V.$$

Further, we obtain by the Poincaré inequality (see e.g. [22, Corollary 9.19])

$$\begin{aligned} B_a(u,u) &\geq a_- \int_{\mathcal{D}} |\nabla u(\underline{x})|_2^2 d\underline{x} \\ &= a_-/2(\|\nabla u\|^2_{L^2(\mathcal{D})} + \|\nabla u\|^2_{L^2(\mathcal{D})}) \\ &\geq a_-/2(\|\nabla u\|^2_{L^2(\mathcal{D})} + 1/C(\mathcal{D},d)^2 \|u\|^2_{L^2(\mathcal{D})}) \\ &\geq a_-/2 \ \min\left(1, 1/C(\mathcal{D},d)^2\right) \|u\|_V^2, \end{aligned}$$

where $C(\mathcal{D},d)$ denotes the Poincaré constant. The assertion now follows by the Lax-Milgram lemma (see [21, 2.7.7 Theorem and 2.7.11 Remark]). □

2.3.3 The finite element method

In Subsection 2.3.2, we introduced the weak solution as the unique element $u \in V$ which satisfies the variational formulation (2.6) of the problem. In order to be able to compute a numerical approximation of the solution, one has to discretize the (in general) infinite dimensional solution space V. One approach to do so is the finite element (FE) method: assume V_h denotes a finite-dimensional subspace of V with $\dim(V_h) = d_h \in \mathbb{N}$. Here, h usually denotes some accuracy parameter as explained below in more detail. Since V_h is a finite-dimensional subspace of V it is closed and, hence, again a Hilbert space. We define the solution approximation $u_h \approx u$ on V_h by the relation

$$B_a(u_h, v_h) = F(v_h), \text{ for all } v_h \in V_h. \tag{2.7}$$

As in Theorem 2.3.1, we obtain the unique existence of $u_h \in V_h$ satisfying (2.7). If we denote by $\{v_h^{(1)}, \ldots, v_h^{(d_h)}\}$ a basis of V_h, Equation (2.7) becomes equivalent to

$$B_a(u_h, v_h^{(i)}) = F(v_h^{(i)}), \text{ for } i = 1, \ldots, d_h. \tag{2.8}$$

The approximation u_h of the weak PDE solution may be expanded in the basis of V_h. That is, we may write $u_h = \sum_{j=1}^{d_h} c_j v_h^{(j)}$, where $\mathbf{c} = (c_1, \ldots, c_{d_h})^T \in \mathbb{R}^{d_h}$ is defined by the system of linear equations

$$\mathbf{B}\mathbf{c} = \mathbf{f}, \tag{2.9}$$

with the so called *stiffness matrix* $\mathbf{B} = (B_a(v_h^{(j)}, v_h^{(i)}),\ i,j = 1, \ldots, d_h) \in \mathbb{R}^{d_h \times d_h}$ and *load vector* $\mathbf{f} = (F(v_h^{(1)}), \ldots, F(v_h^{(d_h)}))^T \in \mathbb{R}^{d_h}$. Therefore, the computation of the solution

approximation $u_h \approx u$ in V_h reduces to the determination of the solution to the system of linear equations (2.9). We refer to [21, 67] for a more detailed introduction to FE methods.

2.3.4 Finite element spaces and approximation error

In this Subsection we consider the case $d = 2$ in more detail. Given a finite dimensional subspace $V_h \subset V$, Subsection 2.3.3 demonstrates how a numerical approximation u_h to the weak PDE solution u of (2.4) - (2.5) may be computed by solving a system of linear equations. In the following, we describe one possible choice of V_h in more detail and discuss the quality of the resulting approximation. We denote by $\mathcal{K}$ an admissible triangulation of the domain $\mathcal{D}$. That is, $\mathcal{K}$ consists of open, disjoint triangles $\mathcal{T} \subset \mathcal{D}$ with $\dot{\bigcup}_{\mathcal{T}\in\mathcal{K}} \overline{\mathcal{T}} = \overline{\mathcal{D}}$ and, for any pair of triangles $\mathcal{T},\ \mathcal{T}' \in \mathcal{K}$ with $\mathcal{T} \neq \mathcal{T}'$, the intersection $\overline{\mathcal{T}} \cap \overline{\mathcal{T}'}$ is either empty, or a common vertice, or a common edge of the triangles $\mathcal{T}, \mathcal{T}'$ (see [67, Section 8.4]). We denote the maximum diameter, i.e. the longest side-length of all triangles in $\mathcal{K}$ by

$$h := \max_{K\in\mathcal{K}} \operatorname{diam}(K),$$

and indicate this accuracy parameter by the notation $\mathcal{K}_h = \mathcal{K}$ (see [67, Section 8.5]). The parameter h is called *finite element discretization parameter* and is crucial for the error analysis of the FE method, since it determines the resolution of the triangulation of the domain. We define the finite dimensional subspace $V_h \subset V$ by

$$V_h := \{v \in V \mid v|_K \in \mathcal{P}_1,\ K \in \mathcal{K}_h\}. \tag{2.10}$$

Here, $\mathcal{P}_1$ denotes all polynomials of degree one in two variables which have the form $p(x, y) = p_0 + p_1 x + p_2 y$ with some coefficients $p_0,\ p_1,\ p_2 \in \mathbb{R}$. This definition leads to the FE method with *linear* elements. Other FE spaces may, for example, be defined by partitioning the domain $\mathcal{D}$ into rectangles or replacing $\mathcal{P}_1$ by polynomials of higher degree. The latter in general leads to an improved accuracy of the approximation, provided the solution is smooth enough. We refer to [21, Chapter 3], [67, Section 8.4] and [107, Section 6.2] for more details.

The regularity of the weak solution $u \in V$ dictates the convergence rate of the FE approximation. In fact, if $\mathcal{K}_h$ is an admissible triangulation, u_h the corresponding FE approximation on V_h defined in (2.10) and $u \in V \cap H^s(\mathcal{D})$ for some real value $s \geq 1$, it holds (see [67, Section 8.5 and Theorem 8.62])

$$\|u - u_h\|_V \leq C h^{\min(s-1,1)} \|u\|_{H^s(\mathcal{D})}, \tag{2.11}$$

where C is a constant independent of h and $\|\cdot\|_s$ denotes the fractional Sobolev norm (see [39]). The exponent $\min(s-1,1)$ of the discretization parameter h is bounded by one due to the choice of polynomials of degree one in (2.10).

The existence result in Theorem 2.3.1 already implies $u \in H^1(\mathcal{D})$. Further, it turns out that it suffices to assume $f \in L^2(\mathcal{D})$ and $a \in C^1(\overline{\mathcal{D}})$ to obtain $u \in H^2(\mathcal{D})$, which is enough to ensure full order convergence in the case of $\mathcal{P}_1$ basis functions (see e.g. [50, 112]). However, we point out that the assumption $a \in C^1(\overline{\mathcal{D}})$ is quite restrictive: in many applications (e.g. flow models in fractured media) it is natural to consider discontinuous diffusion coefficients. In general, lower regularity of the diffusion coefficient leads to lower regularity of the solution and, hence, slower convergence of the FE method. For discontinuous diffusion coefficients a we cannot expect full order convergence of the FE method for standard triangulations of the domain and in general we obtain $s \in (1, 3/2)$ in Equation (2.11) (cf. [10], [105] and [112]). The article [105] presents explicit worst case regularity results for the weak solution of the considered elliptic PDE with discontinuous, piecewise constant diffusion coefficient, where the regularity depends on global bounds of the coefficient.

There are different approaches to improve the convergence of the FE method in the situation of discontinuous diffusion coefficients. For example, the use of adapted meshes, where the discontinuities lie on edges of the elements, improves the performance of the FE method significantly (cf. [16] and Chapter 6). The construction of adapted triangulations is, however, only possible if the jump locations are known a-priori. Another approach is the adaptive FE method, in which the triangulation of the domain is refined specifically in regions with high contribution to the approximation error (see [5, 66] and Chapter 8). In this approach, no explicit knowledge on the jump locations is necessary. We refer to Chapters 6 and 8 where we investigate these approaches in the context the discontinuous random fields presented in this thesis.

We close this subsection with a comment on alternative methods to approximate the weak PDE solution u. In most situations, the FE method is the method of choice for the considered elliptic model equation (2.4) - (2.5). Of course, there are other numerical techniques to solve this type of PDE. For example, one could also use finite difference or collocation methods (see e.g. [11, 86, 102, 107]). However, in the case of discontinuous diffusion coefficients, these methods are in general less suitable than the FE method, since they perform poorly in low-regularity regimes or severely restrict the possible choices of domain triangulations.

2.3.5 Random elliptic partial differential equations

In many applications, the coefficient a in (2.4) is modeled randomly in order to take into account measurement errors or insufficient knowledge about the input data (cf. Section 1.1 and [16, 30, 101]). In this case, the diffusion coefficient is not only varying over the domain but depends on an additional parameter $\omega \in \Omega$ which reflects the randomness. Formally, we may then consider the coefficient as a mapping

$$a : \Omega \times \mathcal{D} \to \mathbb{R}_+.$$

The corresponding PDE is called *random* elliptic PDE. If we fix $\omega \in \Omega$ and assume that the realizations $a(\omega, \cdot) : \mathcal{D} \to \mathbb{R}_+$ are measurable mappings bounded from above and away from zero, Theorem 2.3.1 yields the existence of a pathwise solution $u(\omega) \in V$ depending naturally on $\omega \in \Omega$. In Chapters 6 - 8 we use the (discontinuous) random fields investigated in Chapters 5 and 8 in the construction of the diffusion coefficient.

In the context of random PDEs one is often interested in expectations of (functionals of) the random solution (see e.g. [14, 16, 101]). In general, we cannot draw exact samples $u(\omega)$ of the solution to the random elliptic PDE. However, given a realization $a(\omega)$ of the random diffusion coefficient, the corresponding pathwise weak solution $u(\omega)$ may be approximated by the FE method introduced in the previous subsections. The approximations $u_h(\omega) \approx u(\omega)$ on the FE subspace $V_h \subset V$ may then be used to approximate the expectation of (functionals of) the solution by Monte Carlo methods, which are introduced in the following section.

2.4 Monte Carlo methods

In many applications of stochastic modeling, one is interested in estimations of moments of some quantity of interest, for example the expected payoff of a financial derivative (see, for example, [109] and [62]) or the expectation of solutions to random PDEs. In this section, we introduce the (multilevel) Monte Carlo method to approximate the mean of some random variable X (see e.g. [59]). This plays an important role in this thesis, especially in Chapter 7, where we construct estimators for the expectation of the mean of the solution to a random elliptic PDE. We start with the singlelevel Monte Carlo estimator which is motivated by the strong law of large numbers, followed by the biased singlelevel Monte Carlo esimation for situations in which it is not possible to draw exact samples of the quantity of interest. The construction of its multilevel variant is presented in Subsection 2.4.3 and we close the section

with some comments on extensions and alternatives to Monte Carlo methods. For notational simplicity, we consider mainly real-valued random variables in this section and emphasize that the presented methods easily extend to Banach space-valued random variables (see, e.g., Chapter 7 and the references therein).

2.4.1 The standard Monte Carlo method

We consider a real-valued, square integrable random variable $X \in L^2(\Omega)$ and aim to estimate the expectation $\mathbb{E}(X)$. The (standard) Monte Carlo (MC) method is motivated by the strong law of large numbers: assume $(X^{(i)},\ i \in \mathbb{N})$ is a sequence of i.i.d. random variables following the same distribution as X. For a natural number $M \in \mathbb{N}$, we define the MC estimator $E_M : \Omega \to \mathbb{R}$ by

$$E_M(X) := \frac{1}{M} \sum_{i=1}^{M} X^{(i)} \approx \mathbb{E}(X).$$

It is obvious that this construction yields an unbiased estimator for $\mathbb{E}(X)$ and, further, we immediately obtain by the Bienaymé-formula (see [79, Satz 5.7]) for the mean squared error (MSE):

$$\|\mathbb{E}(X) - E_M(X)\|^2_{L^2(\mathcal{D})} = \Big\| \frac{1}{M} \sum_{i=1}^{M} \mathbb{E}(X) - X^{(i)} \Big\|^2_{L^2(\Omega)} = \frac{\mathrm{Var}(X)}{M}. \tag{2.12}$$

Therefore, for a growing number of samples, the MC estimator converges in $L^2(\Omega)$ to $\mathbb{E}(X)$ and the convergence of the root mean square error (RMSE) $\|\mathbb{E}(X) - E_M(X)\|_{L^2(\mathcal{D})}$ is of order $\mathcal{O}(1/\sqrt{M})$.

In many situations it is not possible to draw exact samples from the random variable X. In this case, one has to use samples of an approximation $\tilde{X} \approx X$ to estimate the expected value of X by the MC method. For example, one could imagine the situation $X = Q(u)$ with a measurable transformation $Q : H^1(\mathcal{D}) \to \mathbb{R}$, where $u : \Omega \to H^1(\mathcal{D})$ is the (pathwise weak) solution of some random elliptic PDE on a domain $\mathcal{D}$ as described in Section 2.3 and $\tilde{X} = \Phi(\tilde{u})$ where $\tilde{u} \approx u$ is some (pathwise) FE approximation. This results in a biased version of the MC estimator which is discussed in more detail in the following subsection.

2.4.2 Biased singlelevel Monte Carlo estimation

As in the previous subsection, we aim to approximate the expected value $\mathbb{E}(X)$ for a random variable $X \in L^2(\Omega)$. Further, we assume that we cannot draw samples from the X directly but have to use approximations instead. In fact, we assume $(X_\ell,\ \ell \in \mathbb{N}) \subset L^2(\Omega)$ is a sequence of random variables which approximate X, that is $X_\ell \to X$, for $\ell \to \infty$ in some sense, e.g. in $L^2(\Omega)$. If we choose $L \in \mathbb{N}$ and a sample number $M \in \mathbb{N}$, we may approximate the quantity of interest by a MC estimator of X_L, that is

$$\mathbb{E}(X) \approx E_M(X_L) = \frac{1}{M} \sum_{i=1}^{M} X_L^{(i)},$$

where $(X_L^{(i)},\ i \in \mathbb{N})$ are i.i.d. copies of X_L. The estimator is $E_M(X_L)$ is also called singlelevel Monte Carlo (SLMC) estimator since it is based on a single approximation level L. The approximation error of the SLMC estimator may be split into the *bias* and the *statistical error*:

$$\begin{aligned} \|\mathbb{E}(X) - E_M(X_L)\|_{L^2(\Omega)} &\leq \|X - X_L\|_{L^2(\Omega)} + \|\mathbb{E}(X_L) - E_M(X_L)\|_{L^2(\Omega)} \\ &= \|X - X_L\|_{L^2(\Omega)} + \Big(\frac{\mathrm{Var}(X_L)}{M}\Big)^{1/2}. \end{aligned} \tag{2.13}$$

Therefore, in order to obtain an approximation of $\mathbb{E}(X)$ of a certain accuracy, one has to choose the *approximation level* L high enough to achieve a small bias and the *sample number* M large enough to avoid a large statistical error. We emphasize that the costs to draw a sample from the distribution of X_ℓ in general grows if ℓ becomes larger, since this index usually corresponds to some accuracy parameter of a certain numerical method, as described in the end of Subsection 2.4.1.

2.4.3 The multilevel Monte Carlo method

The popular multilevel Monte Carlo (MLMC) estimator uses multigrid ideas to improve the efficiency the SLMC estimator (cf. [57]). In its current form, the MLMC method has first been presented by Heinrich in [70] who introduced it to compute high dimensional parametric integrals. The ideas originated in his related work [69]. In the popular paper [57], Giles used the MLMC algorithm to estimate an expected value arising from a stochastic differential equation. Since then, it has been applied to various applications: see for example, [7, 27, 58] for finance related applications to stochastic differential equations (SDEs) governed by Brownian motions,

the references [61, 117] for Lévy-driven SDEs and the references [1, 14, 16, 30, 93, 101, 112] for applications to random elliptic PDEs. We emphasize that these lists are by far not exhaustive. We sketch the idea behind MLMC briefly in the following. As in the previous subsection, we aim to estimate the expected value of a random variable X using samples of random variables $(X_\ell,\ \ell \in \mathbb{N})$ approximating X (see Subsection 2.4.2).

Consider a fixed number $L \in \mathbb{N}$ as above. We define $X_{-1} := 0$ and obtain the following telescopic expansion for the expected value of $X_L \approx X$.

$$\mathbb{E}(X_L) = \sum_{\ell=0}^{L} \mathbb{E}(X_\ell - X_{\ell-1}). \tag{2.14}$$

The idea behind the MLMC estimator is to estimate the left hand side of (2.14) by the sum of independent SLMC estimators of the differences $X_\ell - X_{\ell-1}$ on the right hand side of (2.14). To be more specific, for level-dependent sample numbers $M_\ell \in \mathbb{N}$, with $\ell = 0, \dots, L$, the MLMC estimator $E^L(X_L)$ is defined by

$$E^L(X_L) := \sum_{\ell=0}^{L} E_{M_\ell}(X_\ell - X_{\ell-1}) = \sum_{\ell=0}^{L} \frac{1}{M_\ell} \sum_{i=1}^{M_\ell} X_\ell^{(i,\ell)} - X_{\ell-1}^{(i,\ell)},$$

where, for each $\ell = 0, \dots, L$, the random variables $(X_\ell^{(i,\ell)} - X_{\ell-1}^{(i,\ell)},\ i = 1 \dots, M_\ell)$ are i.i.d. following the distribution of the difference $X_\ell - X_{\ell-1}$. It is obvious that $E^L(X_L)$ is unbiased for the estimation of $\mathbb{E}(X_L)$ and the variance may be computed by the Bienaymé-formula :

$$\begin{aligned}
\mathrm{Var}(E^L(X_L)) &= \|\mathbb{E}(X_L) - E^L(X_L)\|^2_{L^2(\Omega)} \\
&= \Big\| \sum_{\ell=0}^{L} \mathbb{E}(X_\ell - X_{\ell-1}) - E_{M_\ell}(X_\ell - X_{\ell-1}) \Big\|^2_{L^2(\Omega)} \\
&= \sum_{\ell=0}^{L} \|\mathbb{E}(X_\ell - X_{\ell-1}) - E_{M_\ell}(X_\ell - X_{\ell-1})\|^2_{L^2(\Omega)} \\
&= \sum_{\ell=0}^{L} \frac{\mathrm{Var}(X_\ell - X_{\ell-1})}{M_\ell},
\end{aligned}$$

where we used (2.12) in the last step. Similar to the SLMC-error in (2.13), we split the error of the overall approximation $E^L(X_L) \approx \mathbb{E}(X)$ into the bias and the statistical error:

$$\|\mathbb{E}(X) - E^L(X_L)\|_{L^2(\Omega)} \le \|X - X_L\|_{L^2(\Omega)} + \Big(\sum_{\ell=0}^{L} \frac{\mathrm{Var}(X_\ell - X_{\ell-1})}{M_\ell} \Big)^{1/2}. \tag{2.15}$$

Choosing L and the sample numbers M_ℓ, for $\ell = 0, \dots, L$, large enough ensures that the bias and the statistical error are small enough. The main difference and advantage of the MLMC estimator consists in the composition of the statistical error.

In order to obtain a certain statistical error, one should choose the sample numbers M_ℓ such that the statistical error is evenly distributed on the levels $\ell = 0, \dots, L$. Further, it is reasonable to assume that the variances $\mathrm{Var}(X_\ell - X_{\ell-1})$ decay with growing level ℓ, since

$$\mathrm{Var}(X_\ell - X_{\ell-1})^{1/2} \leq \|X_\ell - X_{\ell-1}\|_{L^2(\Omega)} \leq \|X_\ell - X\|_{L^2(\Omega)} + \|X - X_{\ell-1}\|_{L^2(\Omega)} \to 0,$$

for $\ell \to \infty$. Therefore, in order to equilibrate the contributions of the statistical error over all levels in (2.15), the sample numbers M_ℓ should also decrease with growing ℓ. In other words, in contrast to the SLMC estimator, which requires the (computationally expensive) generation of M samples on the highest accuracy level L in (2.13), the MLMC estimator requires many samples to be drawn on the lower accuracy levels and a significantly smaller number of samples with high accuracy, which in general leads to a significant reduction of the computational costs. We refer to [57] and [59] for more details.

2.4.4 Extensions and multilevel Monte Carlo for random PDEs

There are various extensions and modifications of the (multilevel) Monte Carlo approach. For example, the Multi-index Monte Carlo method was first presented in [68] and uses multi-dimensional levels $\underline{\ell}$ instead of a scalar level parameter ℓ. Another modification is the (multilevel) quasi-Monte Carlo approach where samples are not random but chosen carefully in a deterministic way (cf. [59, 40, 60]). We do not go into further details and refer to [59] for a more detailed overview.

MLMC is often applied in the context of random PDEs where one is interested in moments of functionals of the solution: consider the general elliptic PDE introduced in Section 2.3. Modeling the diffusion coefficient a as a random field $a : \Omega \times \mathcal{D} \to \mathbb{R}_+$ naturally leads to a randomized version of the problem with random PDE solution $u : \Omega \to V$, where V denotes the solution space of the considered PDE (see Subsection 2.3.5). The MLMC method may then be used to approximate (functionals of) moments of the random elliptic PDE solutions, which has been further investigated in the literature in the last decade. We refer to the the articles [1, 14, 16, 30, 32, 81, 83, 93, 101, 111, 112] and the references therein for more details. In Chapter 7, we consider the subordinated GRF (see Chapter 5) in the diffusion coefficient of the elliptic model problem. Samples of the random solution $u(\omega)$ cannot be produced exactly but have to be approximated. In order to estimate the expectation $\mathbb{E}(u)$ by MLMC, we use

the FE method to produce pathwise approximations $X_\ell(\omega) = u_{h_\ell}(\omega)$ to the random PDE solution $X(\omega) = u(\omega)$, where we adapted the notation from the previous subsection and h_ℓ is a decreasing sequence of FE mesh refinement parameters. The corresponding MLMC estimator is analyzed theoretically and numerically in Chapter 7.

2.4.5 Stochastic Galerkin and stochastic collocation

The (ML)MC method is one approach to approximate moments of functionals of random PDE solutions. In addition, there exist approaches which are not sampling-based, where stochastic Galerkin and stochastic collocation methods are particularly worth mentioning. The idea behind these approaches is to rewrite the random PDE as a deterministic problem on a higher-dimensional parameter space and discretize it in both, the stochastic space and the spatial domain, by common deterministic methods. The deterministic reformulation of the problem may be obtained by interpreting the driving random variables of the input field as additional parameters besides the spatial parameter $\underline{x} \in \mathcal{D} \subset \mathbb{R}^d$, $d \in \mathbb{N}$.

We sketch the idea for the elliptic PDE with random diffusion coefficient $a : \Omega \times \mathcal{D} \to \mathbb{R}_+$ from Subsection 2.3.5. Assume the coefficient a admits an expansion of the form

$$a(\omega, \underline{x}) = \sum_{i=1}^{\infty} e_i(\underline{x})\xi_i(\omega), \tag{2.16}$$

$\mathbb{P}$-almost surely for $\underline{x} \in \mathcal{D}$, with some deterministic functions $e_i : \mathcal{D} \to \mathbb{R}$ and independent random variables $\xi_i : \Omega \to \Gamma \subseteq \mathbb{R}$, for $i \in \mathbb{N}$. For example, the ξ_i could be uniformly distributed on $[-1, 1] = \Gamma$. Under admissible assumptions, the random field a may be associated with the deterministic operator

$$\begin{aligned} A : \Gamma^{\mathbb{N}} \times \mathcal{D} &\to \mathbb{R} \\ (\underline{y}, \underline{x}) &\mapsto \sum_{i=1}^{\infty} e_i(\underline{x}) y_i, \end{aligned}$$

where we use the notation $\underline{y} = (y_1, y_2, \dots) \in \Gamma^{\mathbb{N}} := \bigtimes_{i=1}^{\infty} \Gamma$ and we obtain the representation

$$a(\omega, \underline{x}) = A(\underline{\xi}(\omega), \underline{x}),$$

$\mathbb{P}$-almost surely for the random vector $\underline{\xi} = (\xi_1, \xi_2, \dots)$ from (2.16) and $\underline{x} \in \mathcal{D}$. This relation may be used to reformulate the random elliptic PDE as deterministic PDE on an *infinite*-dimensional parameter space. If $\|e_i\|_{L^\infty(\mathcal{D})}$ decays fast, the coefficient is essentially determined

by the first summands in (2.16) and, hence, the operator A may be approximated by

$$\begin{aligned} A^N : \Gamma^N \times \mathcal{D} &\to R \\ (\underline{y}^N, \underline{x}) &\mapsto \sum_{i=1}^{N} e_i(\underline{x}) y_i, \end{aligned}$$

for some $N \in \mathbb{N}$ large enough. In this sense, the diffusion coefficient a may be associated with a deterministic operator A on an infinite-dimensional parameter space, which is approximated by the operator A^N on a parameter space with dimension $N + d < +\infty$. Moments of the random PDE solution may then be approximated by the solution to a deterministic PDE related to the operator A^N on a higher-dimensional parameter space (see e.g. [12]).

Stochastic Galerkin (SG) and stochastic collocation (SC) differ in the numerical methods used to discretize the deterministic PDE associated to the operator A^N. The former uses a Galerkin approach and the latter applies a collocation method. SG and SC have been successfully applied to random elliptic PDEs in various situations (see [11, 12, 33, 48, 100] and the references therein). The weak point of both approaches are high stochastic dimensions of the problem: both approaches perform well if the contributions $\|e_i\|_{L^\infty(\mathcal{D})}$ of the deterministic functions decay fast. However, for problems with high stochastic dimension, where $\|e_i\|_{L^\infty(\mathcal{D})}$ decays slowly, SG and SC are not feasible since the dimension of the corresponding deterministic PDE grows rapidly as the stochastic dimension increases (cf. [11, 32]). The random elliptic PDEs considered in this thesis incorporate random fields with complex discontinuities and random jump location, which results in a very high stochastic dimension and, hence, SG and SC approaches are out of reach.

3 Main results and outlook

3.1 Main results

This section aims to summarize and describe the most important results of this thesis, whose main part consists of the following four articles:

1. Robin Merkle and Andrea Barth, *On some distributional properties of subordinated Gaussian random fields*, published in Methodology and Computing in Applied Probability (2022), [95], link: `https://doi.org/10.1007/s11009-022-09958-x`
   Chapter 5 of this thesis is a reproduction of this article.

2. Robin Merkle and Andrea Barth, *Subordinated Gaussian random fields in elliptic partial differential equations*, published in Stochastics and Partial Differential Equations: Analysis and Computations (2022),
   [96], link: `https://doi.org/10.1007/s40072-022-00246-w`
   Chapter 6 of this thesis is a reproduction of this article.

3. Robin Merkle and Andrea Barth, *Multilevel Monte Carlo estimators for elliptic PDEs with Lévy-type diffusion coefficient*, published in BIT Numerical Mathematics (2022),
   [93], link: `https://doi.org/10.1007/s10543-022-00912-4`
   Chapter 7 of this thesis is a reproduction of this article.

4. Robin Merkle and Andrea Barth, *On properties and applications of Gaussian subordinated Lévy fields*, submitted to Methodology and Computing in Applied Probability, preprint available on arxiv: `https://arxiv.org/pdf/2208.01278.pdf`, [94]
   Chapter 8 of this thesis is a reproduction of this article.

The statement on the contributions of the author of this thesis to these articles can be found in Chapter 4.

In the rest of this section, these articles will also be referred to as *Article 1 - 4*. After a brief overview of the articles, their main results are going to be presented in more detail. Article 1, 2 and 3 are naturally connected since they all consider the subordinated GRF, highlighting different aspects of it. The subordinated GRF is a discontinuous random field constructed by the composition of a general GRF with independent Lévy subordinators (see Sections 2.1 and 2.2). Article 1 (reproduced in Chapter 5) investigates theoretical properties of the subordinated GRFs and Article 2 (reproduced in Chapter 6) considers the fields in the diffusion coefficient of an elliptic PDE (see Section 2.3). Advanced multilevel Monte Carlo methods (see Subsection 2.4.3) for an efficient approximation of the expectation of the corresponding random elliptic PDE are presented in Article 3 (reproduced in Chapter 7). In order to overcome some of the restrictions of the subordinated GRF regarding the jump geometry, Article 4 (reproduced in Chapter 8) presents another approach to construct discontinuous random fields: the Gaussian subordinated Lévy field (GSLF). These fields are constructed by the composition of a Lévy process with a positive transformation of a general GRF. Article 4 consists of theoretical investigations of the GSLF and considers an elliptic PDE, where the fields occur in the diffusion coefficient.

Section 1.1 already emphasized the restrictions of GRF models in the elliptic model problem regarding the distributional flexibility and the ability to model spatial discontinuities. In order to overcome these restrictions, Article 1 proposes a subordination approach to generate discontinuous random fields on higher-dimensional parameter spaces. Being more precise, the subordinated GRF is constructed by changing the spatial variables of a GRF on a higher-dimensional parameter space with respect to several Lévy subordinators (see Sections 2.1 and 2.2). One of the reasons why GRFs are commonly used in stochastic modeling is their rich and well understood theory. This raises the question whether the subordinated GRF also allows for a detailed investigation of some of its theoretical properties, which is the main topic of Article 1. It turns out that the profound theory of real-valued Lévy processes and GRFs allows to derive important theoretical results for the subordinated GRF. For instance, the Lévy-Khinchin formula for Lévy processes (see Theorem 2.1.3) together with the distributional properties of a GRF allow to prove a Lévy-Khinchin-type formula for an explicit representation of the pointwise distribution of the subordinated GRF (see Corollary 5.4.3 and Theorem 5.4.6). This is valuable for example for practical applications where pointwise distributions have to be fitted to real-world data. Technically, the most important theoretical instrument used in the derivation of this result is a lemma on the computation of the expectation of functionals of the subordinated GRF. It allows the expectations with respect to the GRF and the Lévy processes to be taken iteratively (see Lemma 5.4.1). Besides pointwise distributional properties, the covariance function of a

random field plays an important role in practical applications. Often, one aims to tailor a stochastic model in order to mimic a specific correlation structure determined by real-world data. In Article 1, a semi-explicit formula for the covariance function of the subordinated GRF is presented, which may be used for this purpose (see Section 5.5). The distributional flexibility of the subordinated GRF raises the question up to which order pointwise moments of the field exist. This is relevant for many statistical methods since the existence of moments up to a certain order is often required. In case of a GRF, pointwise distributions follow a Gaussian distribution and, therefore, absolute moments of any order exist. However, when a general subordinated GRF is considered, it is a-priori not clear under which assumptions pointwise moments exist. This question is answered in Article 1 (see Section 5.6), where conditions on the tails of the distributions of the GRF and the corresponding Lévy processes are derived which ensure the existence of pointwise absolute moments up to a specific order.

The results presented in Article 1 provide useful instruments for theoretical and practical applications of the subordinated GRF. One of these applications is to consider the field in the diffusion coefficient of an elliptic PDE (see also Section 2.3 and Subsection 2.3.5). Such a problem might, for example, be interesting for subsurface/groundwater flow modeling in fractured or porous media. The resulting random PDE is investigated theoretically in Article 2. In order to achieve a high flexibility of the model, the diffusion coefficient of the considered PDE is defined as the sum of a deterministic part, a transformation of a GRF and a transformation of the subordinated GRF. The existence of a random weak solution to the corresponding PDE is shown by a pathwise application of the Lax-Milgram lemma (cf. Subsection 2.3.2). However, accessing this solution is a different matter and mainly consists of two steps: drawing samples of the diffusion coefficient and, given such a sample, approximating the pathwise weak solution by some numerical method. Regarding the first step, the main issue is that samples of the constructed diffusion coefficient a may in general not be simulated exactly, since this includes the simulation of paths of GRFs and Lévy subordinators, which is in general only possible in an approximative way. For example, one may use a truncated Karhunen-Loève expansion or the circulant embedding method to produce approximate realizations of the GRFs (see Subsections 2.2.2 and 2.2.3) and piecewise constant approximations of the Lévy processes obtained from simulated values on a discrete grid (see Article 2 and [15]). Combining approximations of the GRFs and the Lévy subordinators leads to an approximate version of the diffusion coefficient, which naturally induces a perturbation in the considered PDE. In order to investigate the corresponding approximation error of the PDE solution, one has to quantify the error for the approximation of the diffusion coefficient itself. While it is well-investigated how approximation errors for GRFs may be quantified, it is a non-trivial question how a combined approximation of the GRF and the Lévy subordinators affects the approximation of the subordinated GRF.

However, in Article 2 it is shown that, under moderate assumptions, one may quantify the overall error for the approximation of the diffusion coefficient in an $L^s(\Omega; L^t(\mathcal{D}))$-sense for admissible $1 \leq t \leq s < +\infty$ (see Section 6.4). It has to be pointed out that it is in general not possible to obtain a bound in an $L^s(\Omega; L^\infty(\mathcal{D}))$-norm as it is the case in purely Gaussian models (see e.g. Lemma 6.4.4). Note that this is to be expected since the L^∞-norm is not natural for the approximation of the diffusion coefficient due to the discontinuities with random location. Having quantified the approximation error of the diffusion coefficient it remains to investigate how this approximation affects the PDE solution. The classical theory for perturbed diffusion coefficients in the considered elliptic PDE gives an upper bound on the approximation error of the solution in terms of the approximation error of the diffusion coefficient measured in the L^∞-norm on the spatial domain (see [84]). Since this is too sharp for the diffusion coefficient with the subordinated GRF, another approach had to be used in Article 2. Hölder's inequality allows for the derivation of a bound on the approximation error of the random solution by the approximation error of the diffusion coefficient in an $L^s(\Omega; L^t(\mathcal{D}))$-norm instead of the stronger $L^s(\Omega; L^\infty(\mathcal{D}))$-norm under certain integrability assumptions, which completes the investigation of the error induced by the approximation of the diffusion coefficient (see Theorem 6.5.11). Being able to produce approximate samples of the diffusion coefficient with sufficient accuracy, it remains to discretize the PDE in space in order to approximate the corresponding pathwise PDE solution. Finite element (FE) methods with standard triangulations perform poorly due to the low regularity of the problem caused by the jumps of the diffusion coefficient (see also Subsection 2.3.4). Therefore, besides standard meshes, sample-adapted triangulations are used for the spatial discretization, where the edges of the elements align with the jump discontinuities of the coefficient. This improves the performance of the FE method as numerical examples on the strong error estimation confirm (see Section 6.7).

In practical applications one is often interested in the estimation of (functionals of) moments of a random PDE solution (see, for example, the references mentioned in Subsection 2.4.4). Article 3 considers the random elliptic PDE from Article 2 with the goal to approximate the expectation of the random solution. Due to the high stochastic dimension of the problem, sampling-based approaches are used since stochastic Galerkin or stochastic collocation approaches are out of reach (cf. Subsection 2.4.5). A multilevel Monte Carlo (MLMC) estimator for the mean of the random PDE solution is constructed, where a FE method with linear elements is used to obtain pathwise approximations of the weak PDE solution (see Subsections 2.4.3 and 2.4.4). Naturally, the approximation error of the MLMC estimator may be split into the bias and the statistical error (see Subsection 2.4.3). Both error components depend on the FE approximation error and the approximation of the diffusion coefficient, as it has been considered in Article 2. An a-priori error bound is derived on the approximation error of the MLMC estimator in

terms of the sample numbers, the FE approximation parameters and the parameters for the approximation of the diffusion coefficient (see Theorem 7.6.3). In order to equilibrate all error contributions, this a-priori bound is used to derive rules for the choice of the parameters of the MLMC estimator: the level-dependent sample numbers, the FE approximation parameters and parameters for the approximation of the Lévy subordinators and the GRFs (see Corollary 7.6.4). As in Article 2, the MLMC estimator is used in combination with a FE method with standard meshes and with sample-adapted triangulations. The latter improve the performance of the MLMC estimator (see Subsection 7.8.2). However, this approach is only applicable for Lévy processes with low jump intensity, since otherwise the computation of adapted meshes becomes computationally unfeasible. Article 3 proposes an approach to improve the MLMC estimation for coefficients with high jump intensity by a variance reduction technique (see Section 7.7). In fact, the presented MLMC estimator is combined with a control variate (CV) approach, which is highly motivated by the recent article [101]. Being precise, a (Gaussian kernel-)smoothed version of the diffusion coefficient is used to construct a control variate (see Article 3 and [62, Section 4]) in order to reduce the variance of the MLMC estimator. It turns out that the approximation error for the smoothed diffusion coefficient in terms of the approximation of the GRFs and the Lévy subordinators is bounded by the corresponding approximation error for the unsmoothed coefficient (see Lemma 7.7.3). This is used to prove a bound on the error of the constructed MLMC-CV estimator in terms of the level-dependent sample numbers, the FE approximation parameters and the approximation parameters for the GRFs and the Lévy subordinators (see Theorem 7.7.5) and to derive rules for the choice of these approximation parameters in order to equilibrate all error contributions (see Corollary 7.7.6). Numerical examples demonstrate the improved performance of the constructed estimator (see Section 7.8.3).

One restriction of the subordinated GRF is its jump geometry: by construction, the jump-domains of the subordinated GRF are always rectangular and therefore not rotationally invariant. Article 4 proposes another approach to construct discontinuous random fields on higher parameter dimensions. The GSLF is the composition of a general one-dimensional Lévy process with a positive transformation of a GRF. This results in a generalization of the level-set approach for GRFs (see Section 8.3) and the corresponding random fields are discontinuous in space. Further, the discontinuities display a high geometrical flexibility and complexity. Similar to the situation of the subordinated GRF in Article 1, the key for the theoretical investigation of the GSLF in Article 4 is a lemma which allows to compute expectations of functionals of the GSLF by the computation of expectations with respect to the Lévy process and the GRF iteratively (see Lemma 8.4.1). This allows access to the pointwise distribution of the GSLF (see Corollary 8.4.3). The mentioned lemma is also applied to derive a formula for the covariance function of

the GSLF (see Section 8.6). As already pointed out in the context of the subordinated GRF, it is in general impossible to simulate exact realizations of GRFs and Lévy processes on continuous domains. Therefore, one has to use approximations of the GRF and the Lévy process to produce (approximate) realizations of the GSLF. In Article 4, a corresponding error bound is derived in an $L^p(\Omega; L^p(\mathcal{D}))$-norm for admissible $1 \leq p < +\infty$ and the pointwise distribution of the approximated random fields are investigated (see Section 8.5). Articles 2 and 3 consider the subordinated GRF in the diffusion coefficient of an elliptic PDE. This application is also of interest in the context of the GSLF. Therefore, Article 4 presents some theoretical investigations on the random elliptic model problem where the GSLF occurs in the diffusion coefficient (see Section 8.8). This leads again to a discontinuous diffusion coefficient and, therefore, one cannot expect full order convergence in the FE method for the pathwise approximation of the random weak solution. In the context of the subordinated GRF, sample-adapted meshes lead to a significant improvement of the FE method, provided that the jump intensity of the underlying Lévy subordinators is small enough (cf. Articles 2 and 3). In the context of the GSLF, a direct alignment of the FE meshes according to the jump discontinuities is impossible, since the jump interfaces are given implicitly. Further, their complex geometrical properties will in general not allow for an exact alignment. Therefore, in Article 4, an adaptive FE method is applied to improve the accuracy of the FE method compared to standard triangulations (see Section 8.8), which is confirmed in numerical examples (see Subection 8.8.3).

3.2 Summary and outlook

In order to overcome the restrictions of the standard Gaussian model in random elliptic PDEs regarding its distributional flexibility and path continuity, this thesis uses subordination approaches to construct random fields with discontinuous paths which are distributionally flexible and investigates their application in the diffusion coefficient of an elliptic problem. This represents an important step in order to generalize the standard Gaussian model towards flexible, discontinuous random field diffusion models with accessible distributional properties.

The subordinated GRF is constructed by the composition of a GRF on a higher-dimensional parameter space with independent Lévy subordinators and the Gaussian subordinated Lévy field is constructed by the composition of a general Lévy process with some positive transformation of a GRF. Both approaches yield random field models which display great pointwise distributional flexibility and allow for discontinuity modeling in the spatial domain. The various theoretical investigations of the random fields presented in this thesis include, among others, pointwise characteristic functions and formulas for the covariance functions. These results

are valuable for practical applications since they may be used to fit the random fields to given real-world data. The application of the proposed random fields in the diffusion coefficient of a random elliptic model problem significantly increases the variability compared to the standard Gaussian model in terms of distributional flexibility and the ability to model jump discontinuities. This is important for some applications, for example, when subsurface/groundwater flow in fractured/porous media is considered. Besides crucial theoretical results on the corresponding random elliptic PDE and insightful numerical experiments on the estimation of the strong error, this thesis presents problem specific MLMC estimators for the random elliptic PDE, where the subordinated GRF occurs in the diffusion coefficient. The estimators are of great importance for applications since they are comparatively easy to implement and allow for an efficient approximation of the mean of the solution to the considered random PDE. Apart from a theoretical analysis of the MLMC estimators, various numerical experiments complete their investigation.

This thesis may serve as starting point for various directions of further research and open research questions. Regarding the random field models and their construction, it would be interesting to investigate other subordination-based constructions of random field models. Further, it has to be emphasized that the constructions presented in this thesis are not restricted to Gaussian random fields and Lévy processes and one could consider other classes of fields/processes in these constructions. Besides this general research direction, it would be of great interest to develop problem specific methods to fit the subordinated GRF or the GSLF to real-world data in order to obtain models which display certain pointwise distributional properties and covariance structures. Here, the presented formulas for the subordinated GRF and the GSLF will be useful (see Chapters 5 and 8 and especially Subsection 5.5.3).

Concerning the application of the subordinated GRF and the GSLF in the elliptic model problem, one possible starting point for future research could be the spatial discretization technique. Besides FE methods with standard triangulations, this thesis investigates discontinuity-adapted triangulations and residual-based adaptive FE methods to discretize the considered random elliptic interface problem (see Chapters 6 - 8). In addition to these approaches, there are other extensions of the standard FE method which could be applied in the context of the subordinated GRF and the GSLF. Here, the immersed FE (IFE) method has to be mentioned explicitly. Instead of sample-dependent triangulations, the IFE method uses domain triangulations that do not depend on the diffusion coefficient. On the other hand, information about the location of the jump discontinuities in the diffusion coefficient is directly incorporated in the FE basis functions (see [88]). In [119], this approach has successfully been applied to two-dimensional random elliptic interface problems with a single, deterministic jump interface.

Besides the spatial discretization, it would also be interesting to use the subordinated GRF

and the GSLF in other PDEs. For example, the recent articles [17] and [110] consider a discontinuous random field as the coefficient in a time-dependent advection-diffusion equation. In these papers, the diffusion coefficient is modeled in the same way as in [16] and one could also consider the subordinated GRF or the GSLF as coefficient in such an equation.

Regarding the discretization of the stochastic domain, the current thesis presents problem specific MLMC estimators to approximate the mean of the random elliptic PDE, where the subordinated GRF occurs in the diffusion coefficient. Here, sample-wise approximations of the PDE solution are computed by a FE method. In the recent literature various (Deep) Neural Network approaches have been applied to learn the solution operator to PDEs and these methods often outperform classical PDE solvers in terms of computational efficiency (see, for example, [80] and [89]). Using (Deep) Neural Networks as a surrogate model to generate approximate samples of PDE solutions efficiently in combination with multilevel approaches could improve the computational performance of the estimator. Besides Monte Carlo approaches, there are also conceptionally different discretization techniques in Uncertainty Quantification. Stochastic Galerkin and stochastic collocation methods are currently out of reach for the random PDE problems considered in this thesis due to the high stochastic dimension of the diffusion coefficient with random jump discontinuities (see also Subsection 2.4.5). Quasi-Monte Carlo (QMC) methods have been successfully applied to random elliptic problems in the recent literature (see, for example, [82, 81, 47, 63] and the references therein). In contrast to Monte Carlo approaches, QMC methods are based on carefully chosen deterministic samples with low discrepancy instead of (pseudo-)random numbers. In some situations this approach allows for the construction of highly efficient estimators (see [59] and [40]). The application of problem specific QMC methods in the context of the random elliptic PDE considered in this thesis would be of great interest, but also poses major challenges due to the high stochastic dimension of the diffusion coefficient. In addition to QMC approaches, the recently developed continuous level Monte Carlo (CLMC) method also has to be mentioned (see [38]). The CLMC algorithm may be considered as a generalization of MLMC where the level parameter ℓ is not discrete but continuous. Sample-wise FE approximations of a random elliptic PDE are computed with adaptive mesh refinement techniques using goal-oriented FE error estimators. The CLMC method has been successfully applied to log-normal coefficients and a similar approach could be applied to the discontinuous random elliptic PDEs considered in this thesis.

II

Cumulative part

Declaration to the cumulative part

4

The cumulative part of this thesis consists of four research articles (Chapters 5 - 8). Their title and current publication status is:

1. Robin Merkle and Andrea Barth, *On some distributional properties of subordinated Gaussian random fields*, published in Methodology and Computing in Applied Probability (2022), [95], link: `https://doi.org/10.1007/s11009-022-09958-x`
   Chapter 5 of this thesis is a reproduction of this article.

2. Robin Merkle and Andrea Barth, *Subordinated Gaussian random fields in elliptic partial differential equations*, published in Stochastics and Partial Differential Equations: Analysis and Computations (2022),
   [96], link: `https://doi.org/10.1007/s40072-022-00246-w`
   Chapter 6 of this thesis is a reproduction of this article.

3. Robin Merkle and Andrea Barth, *Multilevel Monte Carlo estimators for elliptic PDEs with Lévy-type diffusion coefficient*, published in BIT Numerical Mathematics (2022),
   [93], link: `https://doi.org/10.1007/s10543-022-00912-4`
   Chapter 7 of this thesis is a reproduction of this article.

4. Robin Merkle and Andrea Barth, *On properties and applications of Gaussian subordinated Lévy fields*, submitted to Methodology and Computing in Applied Probability, preprint available on arxiv: `https://arxiv.org/pdf/2208.01278.pdf`, [94]
   Chapter 8 of this thesis is a reproduction of this article.

I, *Robin Merkle*, hereby declare that the co-author lists are complete and that I have not

reproduced, without acknowledgement, the work of another. I declare that I majorly contributed to these articles, including in particular the phase of problem selection, literature research, the derivation of theoretical and numerical results as well as the writing process. This applies to all four articles listed above.

Chapters 5 - 8 represent the original articles except for the following changes that have been made:

- slight changes for the purpose of homogenization of notation.
- the articles have been reformatted in the style of this thesis.
- some typing errors and grammatical errors have been corrected.
- in some figures the font size/line width has been adjusted to improve readability.
- the bibliography for the introduction part and all four articles has been unified and can be found at the end of this thesis.

Except for these changes, Chapters 5 - 8, are reproductions of the corresponding published / submitted papers listed above.

Robin Merkle Stuttgart, December 2022

On some distributional properties of subordinated Gaussian random fields

5

Robin Merkle[1] and Andrea Barth[1]

Published in Methodology and Computing in Applied Probability (2022)
Reproduced with permission from Springer Nature
Reference: [95], Link: https://doi.org/10.1007/s11009-022-09958-x

Abstract: *Motivated by the subordinated Brownian motion, we define a new class of (in general discontinuous) random fields on higher-dimensional parameter domains: the subordinated Gaussian random field. We investigate the pointwise marginal distribution of the constructed random fields, derive a Lévy-Khinchin-type formula and semi-explicit formulas for the covariance function. Further, we study the pointwise stochastic regularity and present various numerical examples.*

5.1 Introduction

In many applications of stochastic modeling, it is meaningful to consider random fields which are discontinous in space (e.g. in fractured porous media modeling). In the situation of a one-dimensional parameter space, like financial modeling, Lévy processes turned out to be a very powerful class of (in general) discontinuous stochastic processes, combined with useful properties, see for example [109], [8], [108].

Whereas the extension of $\mathbb{R}$-valued Lévy processes with one-dimensional parameter space to Hilbert space $\mathcal{H}$-valued Lévy processes is straight forward (see for example [15]), the extension of Lévy processes to higher-dimensional *parameter spaces* is more challenging. The reason can

[1]IANS/SimTech, University of Stuttgart, Stuttgart, Germany

be found at the very starting point of the definition of Lévy processes where time increments are considered: In fact, the definition of Lévy processes makes explicitly use of the total ordered structure underlying the considered time interval. The absence of such a structure on a higher-dimensional parameter space makes it difficult to extend the definition of a standard Lévy process to higher-dimensional parameter spaces.

Subordinated fields did receive only little attention in the recent literature. In some classical papers on generalized random fields, of which [42] is an important representative (see also the references therein), subordinated fields are defined in terms of iterated Itô-integrals. In the recent article [91], the authors investigate deterministic transformations of Gaussian random fields, so called Gaussian subordinated fields, and study excursion sets. The Rosenblatt distributions and long-range dependence of (subordinated) fields are looked into in [85]. The article [13] presents an extension of the concept of subordination to multivariate Lévy processes and investigates self-decomposibility of the resulting processes defined on a one-dimensional parameter domain. In the recent paper [25], the authors define the so called weak subordination of multivariate Lévy processes as a generalization of the classical subordination. The resulting multivariate processes depend on a one-dimensional time parameter and the authors prove that weak subordination is an extension of the classical (strong) subordination. In [24] and [26], the authors consider multivaritate Brownian motions (weakly) subordinated by multivariate Thorin subordinators, investigate self-decomposibility as well as the existence of moments of the resulting distributions and present some applications in mathematical finance. The considered subordinated multivariate processes are defined on a one-dimensional parameter domain.

In contrast, the main contribution of our work is to prove properties of the (discontinuous) subordinated random fields on higher-dimensional parameter domains and of their pointwise distributions, which are important in applications (see for example [118], [18] and [16]).

We present an approach for an extension of a subclass of Lévy processes to more general parameter spaces: Motivated by the subordinated Brownian motion, we employ a higher-dimensional subordination approach using a Gaussian random field together with Lévy subordinators.

Figure 5.1 illustrates the approach with samples of a Gaussian random field (GRF) on $[0, 1]^2$ with Matérn-1.5 covariance function and the corresponding subordinated field, where we used Poisson and Gamma processes on $[0, 1]$ to subordinate the GRF. These examples illustrate how the jumps of the Lévy subordinators produce jumps in the two-dimensional subordinated GRF. The flexibility of the resulting random fields make them attractive for a variety of applications. In the recent article [96], the authors consider a randomized elliptic partial differential equation, where the subordinated GRF occur in the diffusion coefficient, to name just one possible

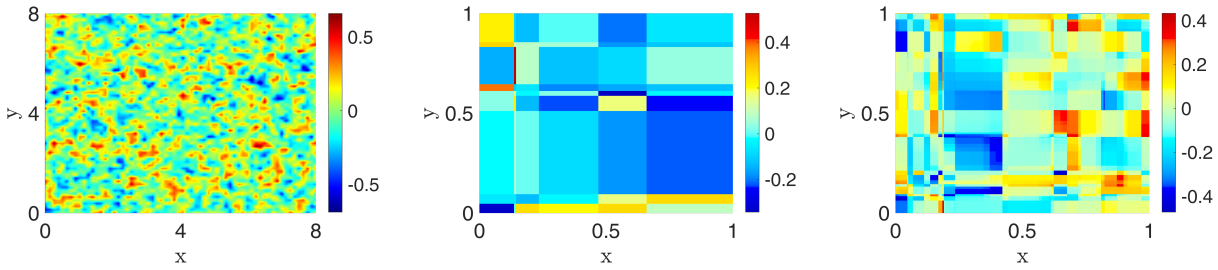

Figure 5.1: Sample of Matérn-1.5-GRF (left), Poisson-subordinated GRF (middle) and Gamma-subordinated GRF (right).

application.

The question arises whether it is possible to transfer some theoretical results of one–dimensional Lévy processes to these random fields on higher-dimensional parameter spaces. In particular, a Lévy-Khinchin-type formula to access the pointwise distribution of the constructed random field is of great interest (see Section 5.4). In Section 5.5 we investigate the covariance structure of the subordinated fields and show how it is influenced by the choice of subordinators. The stochastic regularity of the subordinated fields is studied in Section 5.6. There, we derive conditions which ensure the existence of pointwise moments. In the last section we present some numerical experiments on the theoretical results presented in this paper intended to help fitting random fields to data.

5.2 Preliminaries

In this section we give a short introduction to Lévy processes and Gaussian random fields as basis for the construction of subordinated Gaussian random fields. Throughout the paper, let $(\Omega, \mathcal{F}, \mathbb{P})$ be a complete probability space.

5.2.1 Lévy processes

Let $\mathcal{T} \subseteq \mathbb{R}_+ := [0, +\infty)$ be an arbitrary time domain. A stochastic process $X = (X(t),\ t \in \mathcal{T})$ on $\mathcal{T}$ is a family of random variables on the probability space $(\Omega, \mathcal{F}, \mathbb{P})$. A stochastic process l on $\mathcal{T} = [0, +\infty)$ is said to be a *Lévy process* if $l(0) = 0$ $\mathbb{P}$-a.s., l has independent and stationary increments and l is stochastically continuous. A very important characterization property of Lévy processes is given by the so called *Lévy-Khinchin formula* (see, for example, [8, Th. 1.3.3 and p. 29]).

Theorem 5.2.1 (Lévy-Khinchin formula)**.**
Let l be a real-valued Lévy process on $\mathcal{T} = \mathbb{R}_+ := [0, +\infty)$. There exist parameters $b \in \mathbb{R}$, $\sigma_N^2 \in \mathbb{R}_+$ and a measure ν on $(\mathbb{R}, \mathcal{B}(\mathbb{R}))$ such that the pointwise characteristic function $\phi_{l(t)}$, for $t \in \mathcal{T}$, admits the representation

$$\begin{aligned}\phi_{l(t)}(\xi) &:= \mathbb{E}(\exp(i\xi l(t))) \\ &= \exp\Big(t\big(ib\xi - \frac{\sigma_N^2}{2}\xi^2 + \int_{\mathbb{R}\setminus\{0\}} e^{i\xi y} - 1 - i\xi y \mathbb{1}_{\{|y|\leq 1\}}(y)\, \nu(dy)\big)\Big),\end{aligned}$$

for $\xi \in \mathbb{R}$. The measure ν on $(\mathbb{R}, \mathcal{B}(\mathbb{R}))$ satisfies

$$\int_{\mathbb{R}} \min(y^2, 1)\, \nu(dy) < \infty,$$

and a measure with this property is called Lévy measure. ◆

It follows from the Lévy-Khinchin formula that every Lévy process is fully characterized by the so called Lévy triplet (b, σ_N^2, ν).

Within the class of Lévy processes there exists a subclass which is given by the so called subordinators: A *Lévy subordinator* on $\mathcal{T}$ is a Lévy process that is non-decreasing $\mathbb{P}$-almost surely. The pointwise characteristic function of a Lévy subordinator $l(t)$, for $t \in \mathcal{T}$, admits the form

$$\phi_{l(t)}(\xi) = \mathbb{E}(\exp(i\xi l(t))) = \exp\Big(t\big(i\gamma\xi + \int_0^\infty e^{i\xi y} - 1\, \nu(dy)\big)\Big), \quad \text{for } \xi \in \mathbb{R}, \tag{5.1}$$

(see [8, Theorem 1.3.15]). Here, ν is the Lévy measure and γ is called drift parameter of l. The Lévy measure ν on $(\mathbb{R}, \mathcal{B}(\mathbb{R}))$ of a Lévy subordinator satisfies

$$\nu(-\infty, 0) = 0 \text{ and } \int_0^\infty \min(y, 1)\, \nu(dy) < \infty.$$

Since any Lévy subordinator l is a Lévy process, the Lévy-Khinchin formula holds and we obtain $\sigma_N^2 = 0$ and $b = \gamma + \int_0^1 y\, \nu(dy)$ in Theorem 5.2.1 for the subordinator l. In the following, we always mean the triplet $(\gamma, 0, \nu)$ corresponding to representation (5.1) if we refer to the characteristic triplet of a Lévy subordinator.

5.2.2 Gaussian random fields

Let $\mathcal{D} \subset \mathbb{R}^d$ be a spatial domain. A random field $R = (R(\underline{x}),\ \underline{x} \in \mathcal{D})$ is a family of random variables on the probability space $(\Omega, \mathcal{F}, \mathbb{P})$. In our approach to extend Lévy processes on higher-dimensional parameter domains, one important component is given by the Gaussian random field (see [3, Sc. 1.2]):

Definition 5.2.2.
A random field $W : \Omega \times \mathcal{D} \to \mathbb{R}$ on a d-dimensional domain $\mathcal{D} \subset \mathbb{R}^d$ is said to be a Gaussian random field (GRF) if, for any $\underline{x}^{(1)}, \dots, \underline{x}^{(n)} \in \mathcal{D}$ with $n \in \mathbb{N}$, the n-dimensional random variable $(W(\underline{x}^{(1)}), \dots, W(\underline{x}^{(n)}))$ is multivariate Gaussian distributed. For a GRF W and arbitrary points $\underline{x}^{(1)},\ \underline{x}^{(2)} \in \mathcal{D}$, we define the mean function by $\mu_W(\underline{x}^{(1)}) := \mathbb{E}(W(\underline{x}^{(1)}))$ and the covariance function by

$$q_W(\underline{x}^{(1)}, \underline{x}^{(2)}) := \mathbb{E}\big((W(\underline{x}^{(1)}) - \mu_W(\underline{x}^{(1)}))(W(\underline{x}^{(2)}) - \mu_W(\underline{x}^{(2)}))\big).$$

The GRF W is called centered, if $\mu_W(\underline{x}^{(1)}) = 0$ for all $\underline{x}^{(1)} \in \mathcal{D}$. ◆

Note that every Gaussian random field is determined uniquely by its mean and covariance function. We denote by $Q : L^2(\mathcal{D}) \to L^2(\mathcal{D})$ the *covariance operator* of W which is, for $\psi \in L^2(\mathcal{D})$, defined by

$$Q(\psi)(\underline{x}) = \int_{\mathcal{D}} q_W(\underline{x}, \underline{y})\psi(\underline{y})d\underline{y}, \text{ for } \underline{x} \in \mathcal{D}.$$

Here, $L^2(\mathcal{D})$ denotes the set of all square integrable functions over $\mathcal{D}$. Further, if $\mathcal{D}$ is compact, there exists a decreasing sequence $(\lambda_i,\ i \in \mathbb{N})$ of real eigenvalues of Q with corresponding eigenfunctions $(e_i,\ i \in \mathbb{N}) \subset L^2(\mathcal{D})$ which form an orthonormal basis of $L^2(\mathcal{D})$ (see [3, Section 3.2] and [115, Theorem VI.3.2 and Chapter II.3]). The GRF W is called *stationary* if the mean function μ_W is constant and the covariance function $q_W(\underline{x}^{(1)}, \underline{x}^{(2)})$ only depends on the difference $\underline{x}^{(1)} - \underline{x}^{(2)}$ of the values $\underline{x}^{(1)},\ \underline{x}^{(2)} \in \mathcal{D}$. Further, the stationary GRF W is called *isotropic* if the covariance function $q_W(\underline{x}^{(1)}, \underline{x}^{(2)})$ only depends on the Euclidean length $|\underline{x}^{(1)} - \underline{x}^{(2)}|_2$ of the difference of the values $\underline{x}^{(1)},\ \underline{x}^{(2)} \in \mathcal{D}$ (see [3], p. 102 and p. 115).

5.3 The subordinated Gaussian random field

Throughout the rest of this paper, let $d \in \mathbb{N}$ be a natural number with $d \geq 2$ and $T_1, \ldots, T_d > 0$ be positive values. We define the horizon vector $\mathbb{T} := (T_1, \ldots, T_d)$ and consider the spatial domain $[0, \mathbb{T}]_d := [0, T_1] \times \cdots \times [0, T_d] \subset \mathbb{R}^d$. In the following, we will also use the notation $(0, \mathbb{T}]_d := (0, T_1] \times \cdots \times (0, T_d]$. After a short motivation we define next the subordinated field and show that it is indeed measurable.

5.3.1 Motivation: the subordinated Brownian motion

In order to motivate the novel subordination approach for the extension of Lévy processes, we shortly repeat the main ideas of the *subordinated Brownian motion* which is defined as a Lévy-time-changed Brownian motion: Let $B = (B(t),\ t \in \mathbb{R}_+)$ be a Brownian motion and $l = (l(t),\ t \in \mathbb{R}_+)$ be a subordinator. The subordinated Brownian motion is then defined to be the process

$$L(t) := B(l(t)),\ t \in \mathbb{R}_+.$$

It follows from [8, Theorem 1.3.25] that the process L is again a Lévy process. Note that the class of subordinated Brownian motions is a rich class of processes with great distributional flexibility. For example, the well known Generalized Hyperbolic Lévy process can be represented as a NIG-subordinated Brownian motion (see [15] and especially Lemma 4.1 therein).

5.3.2 The definition of the subordinated Gaussian random field

Let $W = (W(\underline{x}),\ \underline{x} = (x_1, \ldots, x_d) \in \mathbb{R}^d_+)$ be a GRF such that W is $\mathcal{F} \otimes \mathcal{B}(\mathbb{R}^d_+) - \mathcal{B}(\mathbb{R})$-measurable. We denote by $\mu_W : \mathbb{R}^d_+ \to \mathbb{R}$ the mean function and by $q_W : \mathbb{R}^d_+ \times \mathbb{R}^d_+ \to \mathbb{R}$ the covariance function of W. Let $l_k = (l_k(x),\ x \in [0, T_k])$ be independent Lévy subordinators with triplets $(\gamma_k, 0, \nu_k)$, for $k \in \{1, \ldots, d\}$, corresponding to representation (5.1). Further, we assume that the Lévy subordinators are stochastically independent of the GRF W. We consider the random field

$$L : \Omega \times [0, \mathbb{T}]_d \to \mathbb{R} \text{ with } L(x_1, \ldots, x_d) := W(l_1(x_1), \ldots, l_d(x_d)),$$

for $(x_1, \ldots, x_d) \in [0, \mathbb{T}]_d$ and call it *subordinated Gaussian random field (subordinated GRF)*.

Remark 5.3.1. *Note that assuming that W has continuous paths is sufficient to ensure that W is a jointly measurable function since W is a Carathéodory function in this case (see [6, Lemma 4.51]). A sufficient condition for the pathwise continuity of GRFs is given, for example, in [3, Theorem 1.4.1] (see also the discussion in [3, Section 1.3, p. 13]). A specific example for a class of GRFs with at least continuous samples is given by the Matérn GRFs: for a given smoothness parameter $\nu > \frac{1}{2}$, a correlation parameter $r > 0$ and a variance parameter $\sigma^2 > 0$ the Matérn-ν covariance function on $\mathbb{R}^d_+ \times \mathbb{R}^d_+$ is given by $q^M_W(\underline{x}, \underline{y}) = \rho_M(|\underline{x} - \underline{y}|_2)$ with*

$$\rho_M(s) = \sigma^2 \frac{2^{1-\nu}}{\Gamma(\nu)} \Big(\frac{2s\sqrt{\nu}}{r}\Big)^{\nu} K_\nu\Big(\frac{2s\sqrt{\nu}}{r}\Big), \text{ for } s \geq 0,$$

where $\Gamma(\cdot)$ is the Gamma function and $K_\nu(\cdot)$ is the modified Bessel function of the second kind (see [63, Section 2.2 and Proposition 1]). Here, $|\cdot|_2$ denotes the Euclidean norm on $\mathbb{R}^d$. A Matérn-ν GRF is a centered GRF with covariance function q^M_W. ◆

The subordinated GRF constructed above is one possible way to extend the concept of the subordinated Brownian motion to higher-dimensional parameter domains. However, construction of a random field by subordination in each spatial variable is not confined to this approach. For example, the construction itself is not limited to the case that W is a GRF and l is a Lévy subordinator. One could consider more general random fields $(R(\underline{x}),\ \underline{x} \in \mathbb{R}^d_+)$ subordinated by d positive valued stochastic processes. However, in general it might be difficult or impossible to investigate theoretical properties of the resulting random field. In contrast, the subordinated GRFs inherits several properties from the GRF and the Lévy subordinators investigated in the following sections.

5.3.3 Measurability

In Subsection 5.3.2 we introduced the subordinated GRF L as a *random field*. Strictly speaking, we therefore have to verify that point evaluations of the field L are random variables, meaning that we have to ensure measurability of these objects. Note that this is not trivial, since - due to the construction of L - the Lévy subordinators induce an additional ω-dependence in the spatial direction of the GRF W. The following lemma proves joint measurability of L.

Lemma 5.3.2.
Let L be a subordinated GRF on the spatial domain $[0, \mathbb{T}]_d$ as constructed in Subsection 5.3.2,

where we use the notation $\underline{x} = (x_1, \dots, x_d) \in [0, \mathbb{T}]_d$. *The mapping*

$$L : \Omega \times [0, \mathbb{T}]_d \to \mathbb{R}, \quad (\omega, \underline{x}) \mapsto W(\omega, l_1(\omega, x_1) \dots, l_d(\omega, x_d)),$$

is $\mathcal{F} \otimes \mathcal{B}([0, \mathbb{T}]_d) - \mathcal{B}(\mathbb{R})$*-measurable.* ◆

Proof. For any $k \in \{1, \dots, d\}$, the Lévy process l_k has càdlàg paths and, hence, the mapping $l_k : \Omega \times [0, T_k] \to \mathbb{R}_+$, is $\mathcal{F} \otimes \mathcal{B}([0, T_k]) - \mathcal{B}(\mathbb{R}_+)$-measurable (see [106, Chapter 1, Theorem 30] and [108, Section 30]). We consider domain-extended versions of the processes: for any $k \in \{1 \dots, d\}$, we define the mapping $\tilde{l}_k(\omega, \underline{x}) := l_k(\omega, x_k)$, for $(\omega, \underline{x}) \in \Omega \times [0, \mathbb{T}]_d$, which is $\mathcal{F} \otimes \mathcal{B}([0, \mathbb{T}]_d) - \mathcal{B}(\mathbb{R}_+)$ measurable by [6, Lemma 4.51]. An application of [6, Lemma 4.49] yields the $\mathcal{F} \otimes \mathcal{B}([0, \mathbb{T}_d]) - \mathcal{B}(\mathbb{R}^d_+)$-measurability of the mapping

$$\Omega \times [0, \mathbb{T}]_d \to \mathbb{R}^d_+, \quad (\omega, \underline{x}) \mapsto (\tilde{l}_1(\omega, \underline{x}), \dots, \tilde{l}_d(\omega, \underline{x})) = (l_1(\omega, x_1), \dots, l_d(\omega, x_d)).$$

Further, the mapping $(\omega, \underline{x}) \mapsto \omega$ is $\mathcal{F} \otimes \mathcal{B}([0, \mathbb{T}]_d) - \mathcal{F}$-measurable and, hence, [6, Lemma 4.49] yields that the mapping

$$\begin{aligned} &\Omega \times [0, \mathbb{T}]_d \to \Omega \times \mathbb{R}^d_+, \\ &\quad (\omega, \underline{x}) \mapsto (\omega, (\tilde{l}_1(\omega, \underline{x}), \dots, \tilde{l}_d(\omega, \underline{x}))) = (\omega, (l_1(\omega, x_1), \dots, l_d(\omega, x_d))), \end{aligned}$$

is $\mathcal{F} \otimes \mathcal{B}([0, \mathbb{T}_d]) - \mathcal{F} \otimes \mathcal{B}(\mathbb{R}^d_+)$-measurable. By assumption, the GRF W is $\mathcal{F} \otimes \mathcal{B}(\mathbb{R}^d_+) - \mathcal{B}(\mathbb{R})$-measurable and, therefore, the mapping

$$L : \Omega \times [0, \mathbb{T}]_d \to \mathbb{R}, \quad (\omega, \underline{x}) \mapsto W(\omega, (l_1(\omega, x_1) \dots, l_d(\omega, x_d))),$$

is $\mathcal{F} \otimes \mathcal{B}([0, \mathbb{T}_d]) - \mathcal{B}(\mathbb{R})$-measurable as composition of measurable functions. □

5.4 The pointwise distribution of the subordinated GRF and the Lévy-Khinchin formula

In this section we prove a Lévy-Khinchin-type formula for the subordinated GRF in order to have access to the pointwise distribution. This is important, for example, in view of statistical fitting and other applications. In order to be able to do so we need the following technical lemma about the expectation of the composition of independent random variables, which is a

generalization of the corresponding assertion given in the proof of [108, Theorem 30.1].

Lemma 5.4.1.
Let $W : \Omega \times \mathbb{R}^d_+ \to \mathbb{R}$ be a $\mathbb{P}$-a.s. continuous random field and let $Z : \Omega \to \mathbb{R}^d_+$ be a $\mathbb{R}^d_+$-valued random variable which is independent of the random field W. Further, let $g : \mathbb{R} \to \mathbb{R}$ be a deterministic, continuous function. It holds

$$\mathbb{E}(g(W(Z)) = \mathbb{E}(m(Z)),$$

where $m(z) := \mathbb{E}(g(W(z))$ for deterministic $z \in \mathbb{R}^d_+$. ◆

Proof. *Step 1:* Assume that g is globally bounded. We denote by $C_b(\mathbb{R}^d_+)$ the space of continuous, bounded functions on $\mathbb{R}^d_+$ equipped with the usual supremum norm. We define the function

$$F : C_b(\mathbb{R}^d_+) \times \mathbb{R}^d_+ \to \mathbb{R},\ (f, \underline{x}) \mapsto g(f(\underline{x})),$$

which is continuous and, hence, Borel-measurable. For a fixed threshold $A > 0$, we define the cut function $\chi_A(x) := \min(x, A)$, for $x \in \mathbb{R}$ and consider the random field $W_A(\omega, \underline{x}) := W(\omega, \chi_A(x_1), \ldots, \chi_A(x_d))$, for $\omega \in \Omega$ and $\underline{x} = (x_1, \ldots, x_d) \in \mathbb{R}^d_+$. Since W has continuous paths and $[0, A]^d$ is compact, W_A has paths in $C_b(\mathbb{R}^d_+)$ and we have the pathwise identity $g(W_A(Z)) = F(W_A, Z)$. Using the independence of W and Z together with [35, Proposition 1.12] yields

$$\mathbb{E}(g(W_A(Z)) = \mathbb{E}(F(W_A, Z)) = \mathbb{E}(\mathbb{E}(F(W_A, Z) \,|\, \sigma(Z))) = \mathbb{E}(m_A(Z)),$$

where $m_A(z) := \mathbb{E}(g(W_A(z)))$ for $z \in \mathbb{R}^d_+$. Further, since g is continuous and bounded and W has continuous paths, we obtain the pathwise convergence $g(W_A(Z)) \to g(W(Z))$ and $m_A(Z) \to m(Z)$, for $A \to \infty$. Using again the boundedness of g and the dominated convergence theorem, we obtain $\mathbb{E}(g(W(Z))) = \mathbb{E}(m(Z))$.

Step 2: In this step we assume that $g(x) \geq 0$ on $\mathbb{R}$ but g does not necessarily have to be bounded. It follows that m is also non-negative on $\mathbb{R}^d_+$. Since g and m are non-negative we obtain the $\mathbb{P}$-a.s. monotone convergence of $\chi_A(g(W(Z)))) \to g(W(Z)))$ for $A \to +\infty$. We define $m_A(z) := \mathbb{E}(\chi_A(g(W(z)))$, for $z \in \mathbb{R}^d_+$, and obtain by the monotone convergence theorem

$$m_A(Z) \to m(Z)\ \mathbb{P}\text{-a.s. for } A \to +\infty.$$

Using Step 1 and the monotone convergence theorem we obtain:

$$\mathbb{E}(g(W(Z))) = \lim_{A\to+\infty} \mathbb{E}(\chi_A(g(W(Z)))) = \lim_{A\to+\infty} \mathbb{E}(m_A(Z)) = \mathbb{E}(m(Z)).$$

Step 3: Finally, we consider an arbitrary continuous function $g : \mathbb{R} \to \mathbb{R}$. We write $g^+ = \max\{0, g\},\ g^- = -\min\{0, g\}$ as well as

$$\tilde{m}^+(z) = \mathbb{E}(g^+(W(z))),\ \tilde{m}^-(z) = \mathbb{E}(g^-(W(z))),$$

for $z \in \mathbb{R}^d_+$ and obtain the additive decomposition $g(x) = g^+(x) - g^-(x)$ for $x \in \mathbb{R}$ and $m(z) = \tilde{m}^+(z) - \tilde{m}^-(z)$ for $z \in \mathbb{R}^d_+$ by the additivity of the integral with respect to the integration domain. We apply Step 2 to optain

$$\begin{aligned}\mathbb{E}(g(W(Z))) &= \mathbb{E}(g^+(W(Z))) - \mathbb{E}(g^-(W(Z)))\\ &= \mathbb{E}(\tilde{m}^+(Z)) - \mathbb{E}(\tilde{m}^-(Z))\\ &= \mathbb{E}(m(Z)),\end{aligned}$$

which proves the assertion. □

Remark 5.4.2. *We emphasize that the assumptions on the random field W and the random variable Z in Lemma 5.4.1 are very mild. In particular, we do not assume the existence of continuous densities of the random field W or the random vector Z. Further, we mention that the assertion obviously may be extended to deterministic, bounded and continuous functions $g : \mathbb{R} \to \mathbb{C}$ which are complex-valued.* ◆

A GRF W is pointwise normally distributed with parameters specified by the mean μ_W and covariance function q_W. Using this together with Lemma 5.4.1 and Remark 5.4.2 we obtain the following semi-explicit formula for the pointwise characteristic function of a subordinated GRF.

Corollary 5.4.3.
Let W be a $\mathbb{P}$-a.s. continuous GRF on $\mathbb{R}^d_+$ with mean function $\mu_W : \mathbb{R}^d_+ \to \mathbb{R}$ and covariance function $q_W : \mathbb{R}^d_+ \times \mathbb{R}^d_+ \to \mathbb{R}$. Further, let $l_k = (l_k(t),\ t \in [0, T_k])$, for $k = 1, \dots, d$, be independent Lévy subordinators which are independent of W. The pointwise characteristic function of the subordinated GRF defined by $L(\underline{x}) := W(l_1(x_1), \dots, l_d(x_d))$, for $\underline{x} = (x_1, \dots, x_d) \in$

$[0, \mathbb{T}]_d$, *admits the formula*

$$\begin{aligned}\mathbb{E}(\exp(i\xi L(\underline{x}))) &= \mathbb{E}(\exp(i\xi W(l_1(x_1), \dots, l_d(x_d)))) \\ &= \mathbb{E}\Big(\exp\big(i\mu_W(l_1(x_1), \dots, l_d(x_d)) - \frac{1}{2}\xi^2\sigma_W^2(l_1(x_1), \dots, l_d(x_d))\big)\Big),\end{aligned}$$

for $\xi \in \mathbb{R}$ *and any fixed point* $\underline{x} = (x_1, \dots, x_d) \in [0, \mathbb{T}]_d$. *Here, the variance function* $\sigma_W^2 : \mathbb{R}_+^d \to \mathbb{R}_+$ *is given by* $\sigma_W^2(\underline{x}) := q_W(\underline{x}, \underline{x})$ *for* $\underline{x} \in \mathbb{R}_+^d$. ◆

In the one-dimensional case, the Lévy-Khinchin formula gives an explicit representation of the pointwise characteristic function of a Lévy process. This representation also applies to the subordinated Brownian motion, since it is itself a Lévy process (see Subsection 5.3.1). Note that in the construction of the subordinated Brownian motion one cannot replace the Brownian motion by a general one-parameter GRF on $\mathbb{R}_+$ without losing the validity of the Lévy-Khinchin formula. Hence, in the case of a subordinated GRF on a higher-dimensional parameter space, it is natural that we have to restrict the class of admissible GRFs in order to obtain a Lévy-Khinchin-type formula which is the d-dimensional analogon of Theorem 5.2.1. We recap that the pointwise characteristic function of a standard Brownian motion B is given by

$$\phi_{B(t)}(\xi) = \mathbb{E}(\exp(i\xi B(t))) = \exp\big(-\frac{1}{2}t\xi^2\big), \text{ for } \xi \in \mathbb{R},$$

for $t \geq 0$. Note that the Brownian motion ist not characterized by this property, i.e. not every zero-mean GRF on $\mathbb{R}_+$ with the above pointwise characteristic function is a Brownian motion, since this specific characteristic function can be attained by different covariance functions, whereas the covariance function of the Browian motion is given uniquely by $q_{BM}(s,t) = \mathrm{Cov}(B(s), B(t)) = \min\{s,t\}$ for $s, t \geq 0$ (see for example [109, Section 3.2.2]). Motivated by this, we impose the following assumptions on the GRF on $\mathbb{R}_+^d$.

Assumption 5.4.4.
Let $W = (W(\underline{x}),\ \underline{x} \in \mathbb{R}_+^d)$ *be a zero-mean continuous GRF. We assume that there exists a constant* $\sigma > 0$ *such that the pointwise characteristic function of* W *is given by*

$$\phi_{W(\underline{x})}(\xi) = \mathbb{E}(\exp(i\xi W(\underline{x}))) = \exp\big(-\frac{1}{2}\sigma^2\xi^2(x_1 + \dots + x_d)\big),$$

for $\xi \in \mathbb{R}$ *and every* $\underline{x} = (x_1, \dots, x_d) \in \mathbb{R}_+^d$. ◆

Remark 5.4.5. *Note that for a zero-mean, continuous and stationary GRF* $\tilde{W} = (\tilde{W}(\underline{x}),\ \underline{x} \in \mathbb{R}^d_+)$*, the GRF* W *defined by*

$$W(\underline{x}) := \sqrt{x_1 + \cdots + x_d}\tilde{W}(\underline{x}),\ \textit{for}\ \underline{x} = (x_1, \ldots, x_d) \in \mathbb{R}^d_+,$$

satisfies Assumption 5.4.4. ◆

We are now able to derive the Lévy-Khinchin-type formula for the subordinated GRF.

Theorem 5.4.6 (Lévy-Khinchin-type formula)**.**
Let Assumption 5.4.4 hold. We assume independent Lévy subordinators $l_k = (l_k(x),\ x \in [0, T_k])$*, with Lévy triplets* $(\gamma_k, 0, \nu_k)$*, for* $k = 1, \ldots, d$*, are given corresponding to representation* (5.1)*. Further, we assume that these processes are independent of the GRF* W*. We consider the subordinated GRF defined by* $L : \Omega \times [0, \mathbb{T}]_d \to \mathbb{R}$ *with* $L(\underline{x}) := W(l_1(x_1), \ldots, l_d(x_d))$ *for* $\underline{x} = (x_1, \ldots, x_d) \in [0, \mathbb{T}]_d$*. The pointwise characteristic function of the random field* L *is, for any* $\underline{x} = (x_1, \ldots, x_d) \in [0, \mathbb{T}]_d$*, given by*

$$\begin{aligned}\phi_{L(\underline{x})}(\xi) &= \mathbb{E}(\exp(i\xi W(l_1(x_1), \ldots, l_d(x_d))))\\ &= \exp\Big(-(x_1, \ldots, x_d) \cdot (\frac{\sigma^2\xi^2}{2}(\gamma_1, \ldots, \gamma_d)^t + \int_{\mathbb{R}\setminus\{0\}} 1 - e^{i\xi z} + i\xi z \mathbb{1}_{\{|z|\leq 1\}}(z)\nu_{ext}(dz))\Big),\end{aligned}$$

for $\xi \in \mathbb{R}$*. Here, the jump measure* ν_{ext} *is defined through*

$$\nu_{ext}([a,b]) := \begin{pmatrix} \nu_1^{\#}([a,b]) \\ \vdots \\ \nu_d^{\#}([a,b]) \end{pmatrix},$$

for $a, b \in \mathbb{R}$ *where the Lévy measure* $\nu_k^{\#}$*, for* $k = 1, \ldots, d$ *and* $a, b \in \mathbb{R}$*, is given by*

$$\nu_k^{\#}([a,b]) := \int_0^\infty \int_a^b \frac{1}{\sqrt{2\pi\sigma^2 t}} \exp\left(-\frac{x^2}{2\sigma^2 t}\right) dx\, \nu_k(dt).$$

◆

Proof. It follows by [108, Theorem 30.1 and Lemma 30.3] that the measures $\nu_k^{\#}$ are Lévy measures for $k = 1, ..., d$. For notational simplicity we prove the assertion for $d = 2$. For general $d \in \mathbb{N}$ the assertion follows by the same arguments.

Claim 1: For a Lévy measure ν on $(\mathbb{R}_+, \mathcal{B}(\mathbb{R}_+))$ it holds for every $\xi \in \mathbb{R}$:

$$\int_0^\infty \exp(-\frac{\xi^2}{2}y) - 1\nu(dy) = \int_{\mathbb{R}\setminus\{0\}} \exp(i\xi x) - 1 - i\xi x \mathbb{1}_{\{|x|\leq 1\}}(x)\nu^\sharp(dx),$$

where the measure $\nu^\sharp$ is defined by $\nu^\sharp(\mathcal{I}) = \int_0^\infty \int_a^b \frac{1}{\sqrt{2\pi t}} \exp(-\frac{x^2}{2t})dx\nu(dt)$, for $\mathcal{I} = [a, b]$ with $a, b \in \mathbb{R}$. We use the notation $f_s(x) := \frac{1}{\sqrt{2\pi s}} \exp(-\frac{x^2}{2s})$ for $s > 0$ and $x \in \mathbb{R}$ and derive this equation by a direct calculation using the definition of the measure $\nu^\sharp$:

$$\begin{aligned}
&\int_{\mathbb{R}\setminus\{0\}} \exp(i\xi x) - 1 - i\xi x \mathbb{1}_{\{|x|\leq 1\}}(x)\nu^\sharp(dx) \\
&\qquad = \int_{\mathbb{R}\setminus\{0\}} (\exp(i\xi x) - 1 - i\xi x \mathbb{1}_{\{|x|\leq 1\}}(x)) \int_0^\infty f_s(x)\nu(ds)dx \\
&\qquad = \int_0^\infty \Big(\int_{\mathbb{R}\setminus\{0\}} \exp(i\xi x) f_s(x)dx - 1 - i\xi \int_{-1}^1 x f_s(x)dx \Big)\nu(ds) \\
&\qquad = \int_0^\infty \exp(-\frac{s\xi^2}{2}) - 1\nu(ds).
\end{aligned}$$

In the last step we used that the characteristic function of a $\mathcal{N}(0, s)$-distributed random variable is given by $\phi(\xi) = \exp(-\frac{s\xi^2}{2})$ for $\xi \in \mathbb{R}$ and $s > 0$. Further, we used the fact that $f_s'(x) = -x/s f_s(x)$ to see that

$$\int_{-1}^1 x f_s(x) = -s(f_s(1) - f_s(-1)) = 0.$$

Claim 2: (See [8, p. 53]) For a Lévy subordinator l with triplet $(\gamma, 0, \nu)$ it holds

$$\mathbb{E}(\exp(-\xi l(t))) = \exp(-t(\gamma\xi + \int_0^\infty (1 - \exp(-\xi y))\nu(dy))),$$

for $t \geq 0$ and $\xi > 0$.

With these two assertions at hand we can now prove the Lévy-Khinchin-type formula. The case $\xi = 0$ is trivial since both sides equal 1 in this case. Let $(x, y) \in [0, \mathbb{T}]_2$ and $0 \neq \xi \in \mathbb{R}$ be fixed. Using Lemma 5.4.1 and Remark 5.4.2 with $g(\cdot) = \exp(i\xi\cdot)$ and $Z = (l_1(x), l_2(y))$ we calculate

$$\mathbb{E}(\exp(i\xi W(l_1(x), l_2(y)))) = \mathbb{E}(m(l_1(x), l_2(y)))$$

where

$$m(x',y') := \mathbb{E}(\exp(i\xi W(x',y'))) = \exp(-\frac{1}{2}\sigma^2\xi^2(x'+y')) \text{ for } (x',y') \in \mathbb{R}^2_+,$$

where we used Assumption 5.4.4. Therefore, using the independence of the processes l_1 and l_2 together with Claim 2 we obtain

$$\begin{aligned}\phi_{L(x,y)}(\xi) &= \mathbb{E}(\exp(-\frac{1}{2}\sigma^2\xi^2 l_1(x)))\,\mathbb{E}(\exp(-\frac{1}{2}\sigma^2\xi^2 l_2(x))) \\ &= \exp(-x(\gamma_1\frac{\sigma^2\xi^2}{2} + \int_0^\infty (1-\exp(-\frac{\xi^2}{2}y))\hat{\nu}_1(dy))) \\ &\quad \cdot \exp(-y(\gamma_2\frac{\sigma^2\xi^2}{2} + \int_0^\infty (1-\exp(-\frac{\xi^2}{2}y))\hat{\nu}_2(dy))),\end{aligned}$$

where we define the (Lévy-)measures $\hat{\nu}_1$ and $\hat{\nu}_2$ by $\hat{\nu}_k([a,b]) = \nu_k([a/\sigma^2, b/\sigma^2])$ for $a,\ b \in \mathbb{R}_+$ and $k = 1, 2$. Now, using Claim 1 we calculate

$$\begin{aligned}\phi_{L(x,y)}(\xi) = \exp\big(&- x(\gamma_1\frac{\sigma^2\xi^2}{2} - \int_{\mathbb{R}\setminus\{0\}} \exp(i\xi x) - 1 - i\xi x \mathbb{1}_{\{|x|\le 1\}}(x)\hat{\nu}_1^\sharp(dx))) \\ &- y(\gamma_2\frac{\sigma^2\xi^2}{2} - \int_{\mathbb{R}\setminus\{0\}} \exp(i\xi x) - 1 - i\xi x \mathbb{1}_{\{|x|\le 1\}}(x)\hat{\nu}_2^\sharp(dx))),\end{aligned}$$

where the measures $\hat{\nu}_k^\sharp$ for $k = 1, 2$ are given by:

$$\begin{aligned}\hat{\nu}_k^\sharp([a,b]) &= \int_0^\infty \int_a^b \frac{1}{\sqrt{2\pi t}} \exp(-\frac{x^2}{2t}) dx \hat{\nu}_k(dt) \\ &= \int_0^\infty \int_a^b \frac{1}{\sqrt{2\pi\sigma^2 t}} \exp(-\frac{x^2}{2\sigma^2 t}) dx \nu_k(dt),\end{aligned}$$

for $a, b \in \mathbb{R}$. This finishes the proof. □

Using Theorem 5.4.6 together with the convolution theorem (see for example [79, Lemma 15.11 (iv)]) we immediately obtain the following corollary.

Corollary 5.4.7.
Let Assumption 5.4.4 hold. We assume d independent Lévy subordinators $l_k = (l_k(x),\ x \in [0, T_k])$ are given for $k = 1, \dots, d$, which are independent of W and the corresponding Lévy triplets are given by $(\gamma_k, 0, \nu_k)$ for $k = 1, \dots, d$. We consider the subordinated GRF $L : \Omega \times [0, \mathbb{T}]_d \to \mathbb{R}$ defined by $L(\underline{x}) := W(l_1(x_1), \dots, l_k(x_d))$, for $\underline{x} = (x_1, \dots, x_d) \in [0, \mathbb{T}]_d$. Further, we assume that independent Lévy processes $\tilde{l}_k$ on $[0, T_k]$ are given with triplets $(0, \sigma^2\gamma_k, \nu_k^\#)$

for $k = 1, \dots, d$ in the sense of the one-dimensional Lévy-Khinchin formula, see Theorem 5.2.1. Here, the Lévy measure $\nu_k^{\#}$ is defined by

$$\nu_k^{\#}([a,b]) := \int_0^\infty \int_a^b \frac{1}{\sqrt{2\pi\sigma^2 t}} \exp\left(-\frac{x^2}{2\sigma^2 t}\right) dx\, \nu_k(dt),$$

for $k = 1, \dots, d$ and $a, b \in \mathbb{R}$. The pointwise marginal distribution of the subordinated GRF satisfies

$$L(\underline{x}) \stackrel{\mathcal{D}}{=} \tilde{l}_1(x_1) + \cdots + \tilde{l}_d(x_d),$$

for every $\underline{x} = (x_1, \dots, x_d) \in [0, \mathbb{T}]_d$. ◆

We point out that the case of stationary GRFs is excluded by Assumption 5.4.4. Therefore, we consider this situation in the following remark where we again assume $d = 2$ for notational simplicity.

Remark 5.4.8. *Let W be a stationary, centered GRF with covariance function $q_W((x,y),(x',y')) = \tilde{q}_W((x-x', y-y'))$, for $(x,y),\ (x',y') \in \mathbb{R}_+^2$, and pointwise variance $\sigma^2 := \tilde{q}_W((0,0)) > 0$. Let l_1 and l_2 be independent Lévy subordinators, which are also independent of W. We obtain by Lemma 5.4.1 the following representation for the pointwise characteristic function of the subordinated random field defined by $L(x,y) := W(l_1(x), l_2(y))$, for $(x,y) \in [0,\mathbb{T}]_2$:*

$$\phi_{L(x,y)}(\xi) = \mathbb{E}(\exp(i\xi W(l_1(x), l_2(y))) = \mathbb{E}(m(l_1(x), l_2(y))),$$

where

$$m(x',y') = \mathbb{E}(\exp(i\xi W(x',y'))) = \exp\big(-\frac{1}{2}\sigma^2\xi^2\big),$$

which is a constant function in (x', y'). Therefore we obtain

$$\phi_{L(x,y)}(\xi) = \exp\big(-\frac{1}{2}\sigma^2\xi^2\big),$$

for $(x,y) \in [0,\mathbb{T}]_2$. Hence, in case of a stationary GRF, the subordinated GRF is pointwise normally distributed with variance σ^2. ◆

We conclude this subsection with a remark on the given Lévy-Khinchin formula.

Remark 5.4.9. *With the approach of subordinating GRFs on a higher-dimensional domain, we obtain a discontinuous Lévy-type random field and a Lévy-Khinchin formula which allows access to the pointwise distribution of the random field. Further we obtain a similar parametrization of the class of subordinated random fields, as it is the case for Lévy processes on a one-dimensional parameter space: Under the assumptions of Theorem 5.4.6, every subordinated GRF can be characterized by the tuple* $(\sigma^2, \gamma_1, \ldots, \gamma_d, \nu_{ext}, q_W)$*, where* $q_W : \mathbb{R}_+^d \times \mathbb{R}_+^d \to \mathbb{R}$ *is the covariance function of the GRF. Further, the class of subordinated GRFs is linear in the sense that for the sum of two independent subordinated GRFs one can construct a single subordinated GRF with the same pointwise characteristic function.* ◆

5.5 Covariance function

One advantage of the subordinated GRF is that the correlation between spatial points is accessible. The correlation structure is hereby determined by the covariance function of the underlying GRF and the specific choice of the subordinators. For statistical applications it is often important to image or enforce a specific correlation structure in view of fitting random fields to physical phenomena. In this context the question arises whether one can find analytically explicit formulas for the covariance function of a subordinated Gaussian random field. This will be explored in the following section.

For notational simplicity we restrict the dimension to be $d = 2$ in this section but we point out that analogous results apply for dimensions $d \geq 3$. A direct application of Lemma 5.4.1 yields the following corollary.

Corollary 5.5.1.
Let W *be a continuous, zero-mean GRF on* $\mathbb{R}_+^2$*. Further, let* l_1 *and* l_2 *be two independent Lévy subordinators which are independent of* W*. Then the subordinated GRF* L *defined by* $L(x, y) := W(l_1(x), l_2(y))$*, for* $(x, y) \in \mathbb{R}_+^2$*, is zero-mean with covariance function*

$$q_L((x, y), (x', y')) := \mathbb{E}(L(x, y)L(x', y')) = \mathbb{E}\big(q_W((l_1(x), l_2(y)), (l_1(x'), l_2(y')))\big),$$

for $(x, y),\ (x', y') \in \mathbb{R}_+^2$*, where* $q_W : \mathbb{R}_+^2 \times \mathbb{R}_+^2 \to \mathbb{R}$ *denotes the covariance function of the GRF* W*.* ◆

Proof. For $(x, y) \in [0, \mathbb{T}]_2$, we use Lemma 5.4.1 and the fact that the GRF W is centered to deduce $\mathbb{E}(L(x, y)) = \mathbb{E}(W(l_1(x), l_2(y))) = 0$. Let $(x, y),\ (x', y') \in [0, \mathbb{T}]_2$ be

fixed. Another application of Lemma 5.4.1 with $\tilde{W}(x_1, y_1, x_2, y_2) := W(x_1, y_1) \cdot W(x_2, y_2)$, $g = \mathrm{id}_{\mathbb{R}}$ and $Z := (l_1(x), l_2(y), l_1(x'), l_2(y'))$ yields the desired formula. □

5.5.1 The isotropic case

We use Corollary 5.5.1 to derive a semi-explicit formula for the covariance function of the subordinated GRF, where the underlying GRF is isotropic.

Lemma 5.5.2.
Let $W : \Omega \times \mathbb{R}^2_+ \to \mathbb{R}$ be a zero-mean, continuous and isotropic GRF with covariance function $q_W((x, y), (x', y')) = \tilde{q}_W(|x - x'|, |y - y'|)$. Further, suppose that l_1 and l_2 are independent Lévy subordinators on $[0, T_1]$ (resp. $[0, T_2]$) with density functions f_1 and f_2, i.e. $f_1^x(\cdot)$ (resp. $l_2^y(\cdot)$) is the density function of $l_1(x)$ (resp. $l_2(y)$) for $(x, y) \in (0, \mathbb{T}]_2$. The covariance function of the subordinated GRF L with $L(x, y) := W(l_1(x), l_2(y))$, for $(x, y) \in [0, \mathbb{T}]_2$, admits the representation

$$q_L((x, y), (x', y')) = \int_{\mathbb{R}_+} \int_{\mathbb{R}_+} \tilde{q}_W(s, t) f_1^{|x-x'|}(s) f_2^{|y-y'|}(t) ds dt,$$

for $(x, y),\ (x', y') \in [0, \mathbb{T}]_2$ with $x \neq x'$ and $y \neq y'$. ◆

For $x = x'$ and $y \neq y'$ it holds

$$q_L((x, y), (x, y')) = \int_{\mathbb{R}_+} \tilde{q}_W(0, t) f_2^{|y-y'|}(t) dt,$$

for $x \neq x'$ and $y = y'$ one obtains

$$q_L((x, y), (x', y)) = \int_{\mathbb{R}_+} \tilde{q}_W(s, 0) f_1^{|x-x'|}(s) ds,$$

and for $(x, y) = (x', y')$ the pointwise variance is given by

$$\mathrm{Var}(L(x, y)) = q_L((x, y), (x, y)) = \tilde{q}_W(0, 0).$$

Proof. The assertion follows immediately by Corollary 5.5.1 together with the independence of the processes l_1 and l_2 and the fact that $|l_k(x) - l_k(x')| \overset{\mathcal{D}}{=} l_k(|x - x'|)$ for $x,\ x' \in [0, T_k]$ and $k = 1, 2$ by the definition of a Lévy process. □

5.5.2 The non-isotropic case

In this subsection, we derive a formula for the covariance function of the subordinated GRF for the case that the underlying GRF is not isotropic. In the following, we use the notation $x \wedge y := \min(x, y)$ and $x \vee y := \max(x, y)$ for real numbers $x, y \in \mathbb{R}$. The next lemma will be useful in the proof of the covariance representation.

Lemma 5.5.3.
Let $l = (l(x),\ x \in [0, T])$ be a general Lévy process with density function $f : (0, T] \times \mathbb{R} \to \mathbb{R}$, i.e. the probability density function of the random variable $l(x)$ is given by $f^x(\cdot)$, for $x \in (0, T]$. In this case, the joint probability density function of the random vector $Z := (l(x \wedge x'), l(x \vee x'))$, with $x \neq\ x' \in (0, T]$, is given by $f_Z(s, t) = f^{\min(x,x')}(s) \cdot f^{|x'-x|}(t - s)$ for $t, s \in \mathbb{R}$. ◆

Proof. Let $x,\ x' \in (0, T]$ with $x < x'$ and $x_1, x_2 \in \mathbb{R}$ be fixed. The increment $l(x') - l(x)$ is stochastically independent of the random variable $l(x)$, which yields

$$\begin{aligned}
\mathbb{P}(l(x) \leq x_1 \wedge l(x') \leq x_2) &= \mathbb{E}(\mathbb{1}_{\{l(x)\leq x_1\}}\mathbb{1}_{\{l(x')\leq x_2\}}) \\
&= \mathbb{E}(\mathbb{1}_{\{l(x)\leq x_1\}}\mathbb{1}_{\{l(x')-l(x)\leq x_2-l(x)\}}) \\
&= \int_{\mathbb{R}}\int_{\mathbb{R}} \mathbb{1}_{\{s\leq x_1\}}\mathbb{1}_{\{t\leq x_2-s\}} f^x(s) f^{x'-x}(t) dtds \\
&= \int_{-\infty}^{x_1}\int_{-\infty}^{x_2-s} f^x(s) f^{x'-x}(t) dtds \\
&= \int_{-\infty}^{x_1}\int_{-\infty}^{x_2} f^x(s) f^{x'-x}(t-s) dtds.
\end{aligned}$$

For the case that $x' < x$ the same argument yields

$$\mathbb{P}(l(x) \leq x_1 \wedge l(x') \leq x_2) = \int_{-\infty}^{x_1}\int_{-\infty}^{x_2} f^{x'}(s) f^{x-x'}(t-s) dsdt,$$

which finishes the proof. □

Remark 5.5.4. *Note that Lemma 5.5.3 immediately implies that the joint density $f_Z(s, t)$ of the two-dimensional random vector $Z = (l(x \wedge x'), l(x \vee x'))$ for a Lévy subordinator l with $x \neq x' \in (0, T]$ is given by*

$$f_Z(s, t) = f^{\min(x,x')}(s) \cdot f^{|x'-x|}(t - s),\ \text{for } s, t \in \mathbb{R}_+.$$

◆

With this lemma at hand we are able to derive a formula for the covariance function of the subordinated (non-isotropic) GRF. Without loss of generality we consider points $(x, y),\ (x', y')$ with $x \leq x'$ and $y \leq y'$ in the following lemma. Formulas for the other cases follow by the same arguments with Lemma 5.5.3 and Remark 5.5.4.

Lemma 5.5.5.
Let $W : \Omega \times \mathbb{R}_+^2 \to \mathbb{R}$ be a zero-mean, continuous and non-isotropic GRF with covariance function q_W. Further, suppose that l_1 and l_2 are independent Lévy subordinators on $[0, T_1]$ (resp. $[0, T_2]$) with density functions f_1 and f_2, i.e. $f_1^x(\cdot)$ (resp. $l_2^y(\cdot)$) is the density function of $l_1(x)$ (resp. $l_2(y)$) for $(x, y) \in (0, \mathbb{T}]_2$. The covariance function of the subordinared GRF L with $L(x, y) := W(l_1(x), l_2(y))$, for $(x, y) \in [0, \mathbb{T}]_2$, admits the representation

$$q_L((x, y), (x', y')) = \int_{\mathbb{R}_+}\int_{\mathbb{R}_+}\int_{\mathbb{R}_+}\int_{\mathbb{R}_+} q_W((x_1, x_2), (x_3, x_4)) f_1^x(x_1) f_2^y(x_2) \times f_1^{x'-x}(x_3 - x_1) f_2^{y'-y}(x_4 - x_2) dx_1\, dx_2\, dx_3\, dx_4,$$

for $(x, y),\ (x', y') \in (0, \mathbb{T}]_2$ with $x < x'$ and $y < y'$.

For $x = x'$ and $y < y'$, it holds

$$q_L((x, y), (x, y')) = \int_{\mathbb{R}_+}\int_{\mathbb{R}_+}\int_{\mathbb{R}_+} q_W((x_1, x_2), (x_1, x_4)) f_1^x(x_1) f_2^y(x_2) \times f_2^{y'-y}(x_4 - x_2) dx_1\, dx_2\, dx_4,$$

and for $x < x'$ and $y = y'$ it holds

$$q_L((x, y), (x', y)) = \int_{\mathbb{R}_+}\int_{\mathbb{R}_+}\int_{\mathbb{R}_+} q_W((x_1, x_2), (x_3, x_2)) f_1^x(x_1) f_2^y(x_2) \times f_1^{x'-x}(x_3 - x_1) dx_1\, dx_2\, dx_3.$$

For $(x, y) = (x', y')$ one obtains for the pointwise variance of the field

$$\mathrm{Var}(L(x, y)) = q_L((x, y), (x, y)) = \int_{\mathbb{R}_+}\int_{\mathbb{R}_+} q_W(x_1, x_2, x_1, x_2) f_1^x(x_1) f_2^y(x_2) dx_1 dx_2.$$

◆

Proof. Using Corollary 5.5.1, the independence of the processes l_1 and l_2, Lemma 5.5.3

and Remark 5.5.4 we calculate for $(x,y),\ (x',y') \in (0,\mathbb{T}]_2$ with $x < x'$ and $y < y'$:

$$\begin{aligned} q_L((x,y),(x',y')) &= \int_{\mathbb{R}_+^4} q_W((x_1,x_2),(x_3,x_4)) d\mathbb{P}_{(l_1(x),l_2(y),l_1(x'),l_2(y'))}(x_1,x_2,x_3,x_4) \\ &= \int_{\mathbb{R}_+}\int_{\mathbb{R}_+}\int_{\mathbb{R}_+}\int_{\mathbb{R}_+} q_W((x_1,x_2),(x_3,x_4)) f_1^x(x_1) f_2^y(x_2) \\ &\qquad \times f_1^{x'-x}(x_3-x_1) f_2^{y'-y}(x_4-x_2) dx_1\, dx_2\, dx_3\, dx_4. \end{aligned}$$

The remaining cases follow by the same argument. □

5.5.3 Statistical fitting of the covariance function

The parametrization property of the subordinated GRF (see Remark 5.4.9) motivates a direct approach of covariance fitting: For a natural number $N \in \mathbb{N}$, we assume that discrete points $\{(x_i,y_i),\ i=1,\dots,N\}$ are given with corresponding empirical covariance function data $C^{emp} = \{C^{emp}_{i,j},\ i,j=1,\dots,N\}$, where $C^{emp}_{i,j}$ represents the empirical covariance of the field evaluated at the points (x_i,y_i) and (x_j,y_j). We search for the solution to the problem

$$\arg\min \left\{ \|\tilde{q}_L - C^{emp}\|_* \;\middle|\; \text{admissible tuples } (\sigma^2,\gamma_1,\gamma_2,\nu_{ext},q_W) \right\}$$

where we use the notation $\tilde{q}_L := \{q_L(x_i,y_i),\ i,j=1,\dots,N\}$ and $\|\cdot\|_*$ is an appropriate norm on $\mathbb{R}^N$, e.g. the Euclidian norm. In order to solve this type of problem, the formulas for the covariance function given by Lemma 5.5.2 and Lemma 5.5.5 can be used, but still accessing the solution will be challenging due to the complexity of the set of admissible parameters.

5.6 Stochastic regularity - pointwise moments

In this section we consider pointwise moments of a subordinated GRF L. In particular, we derive conditions which ensure the existence of pointwise p-th moments of the subordinated GRF L defined by $L(\underline{x}) := W(l_1(x_1),\dots,l_d(x_d))$, for $\underline{x} = (x_1,\dots,x_d) \in [0,\mathbb{T}]_d$.

Obviously, in order to guarantee the existence of moments of the random variable $L(\underline{x})$, we have to impose conditions on the GRF W *and* the subordinators $l_1,\dots,l_d$. The following theorem gives a better insight into the interaction between the underlying GRF and the stochastic regularity of the subordinators and presents coupled regularity conditions on the tail behaviour of both components of the random field.

Theorem 5.6.1.
We assume that W is a centered and continuous GRF on $\mathbb{R}^d_+$ with covariance function $q_W : \mathbb{R}^d_+ \times \mathbb{R}^d_+ \to \mathbb{R}$. Further, we assume that there exist a positive number $N \in \mathbb{N}$, coefficients $\{c_j,\ j = 1, \dots, N\} \subset [0, +\infty)$ and d-dimensional exponents $\{\underline{\alpha}^{(j)},\ j = 1, \dots, N\} \subset \mathbb{R}^d_+$ such that the pointwise variance function σ^2_W of W satisfies

$$\sigma_W(\underline{z}) = q_W(\underline{z}, \underline{z})^{1/2} \leq \sum_{j=1}^{N} c_j \underline{z}^{\underline{\alpha}^{(j)}},\ \text{for } z_1, \dots, z_d \geq 0. \tag{5.2}$$

Here, we use the notation $\underline{z}^{\underline{\alpha}} = z_1^{\alpha_1} \cdot \dots \cdot z_d^{\alpha_d}$ for $\underline{z} = (z_1, \dots, z_d) \in \mathbb{R}^d_+$ and $\underline{\alpha} = (\alpha_1, \dots, \alpha_d) \in \mathbb{R}^d_+$. We consider a fixed point $\underline{x} \in [0, \mathbb{T}]_d$ and assume that the densities $f_1^{x_1}, \dots, f_d^{x_d}$ of the evaluated processes $l_1(x_1), \dots, l_d(x_d)$ fulfill

$$f_i^{x_i}(z) \leq C|z|^{-\eta_i},\ \text{for } z \geq K \text{ and } i = 1, \dots, d, \tag{5.3}$$

with positive decay rates $\{\eta_i,\ i = 1, \dots, d\}$. Here, the constants C and K are independent of z but may depend on the evaluation point $\underline{x} = (x_1, \dots, x_d)$ and η_i may depend on x_i, for $i = 1, \dots, d$. We define the number

$$a := \min\{(\eta_i - 1)/\alpha_i^{(j)} \mid i = 1, \dots, d,\ j = 1, \dots, N,\ \alpha_i^{(j)} \neq 0\}.$$

Then, the random variable $L(\underline{x})$ admits a p-th moment for $p \in [1, a)$, i.e. $L(\underline{x}) \in L^p(\Omega; \mathbb{R})$ for $p \in [1, a)$. ◆

Proof. Let $Z \sim \mathcal{N}(0, \sigma^2)$ be a real-valued, centered, normally distributed random variable with variance $\sigma^2 > 0$. It follows by Equation (18) in [116] that the p-th absolute moment of Z admits the form $\mathbb{E}(|Z|^p) = C_p \sigma^p$, for all $p > -1$, with a constant C_p depending on p. Let $p \geq 1$ be a fixed number. We use Lemma 5.4.1 to calculate

$$\mathbb{E}(|L(\underline{x})|^p) = \mathbb{E}(|W(l_1(x_1), \dots, l_d(x_d))|^p) = \mathbb{E}(m(l_1(x_1), \dots, l_d(x_d))),$$

with

$$m(x'_1, \dots, x'_d) := \mathbb{E}(|W(x'_1, \dots, x'_d)|^p) = C_p \sigma_W^p(x'_1, \dots, x'_d),$$

for $(x_1', \dots, x_d') \in \mathbb{R}_+^d$. Hence, we obtain

$$\mathbb{E}(|L(\underline{x})|^p) = C_p \mathbb{E}\big(\sigma_W^p(l_1(x_1), \dots, l_d(x_d))\big).$$

Next, we use the tail estmations (5.2) and (5.3), Hölder's inequality and the independence of the subordinators to calculate

$$\begin{aligned}
\mathbb{E}(|L(\underline{x})|^p) &= C_p \mathbb{E}\big(\sigma_W^p(l_1(x_1), \dots, l_d(x_d))\big) \\
&\leq C_p \int_{\mathbb{R}_+^d} \Big(\sum_{j=1}^N c_j \underline{z}^{\underline{\alpha}^{(j)}} \Big)^p f_1^{x_1}(z_1) \dots f_d^{x_d}(z_d) d(z_1, \dots, z_d) \\
&\leq C(N,p) \sum_{j=1}^N c_j^p \prod_{i=1}^d \underbrace{\int_0^{+\infty} z_i^{p\alpha_i^{(j)}} f_i^{x_i}(z_i) dz_i}_{=: I_i^j}.
\end{aligned}$$

It remains to show that all the integrals I_i^j are finite. For $i \in \{1, \dots, d\}$ and $j \in \{1, \dots, N\}$ with $\alpha_i^{(j)} = 0$ we have $I_i^j = 1$. If $\alpha_i^{(j)} \neq 0$ it holds

$$\begin{aligned}
I_i^j &= \Big(\int_0^K + \int_K^{+\infty} \Big) z_i^{p\alpha_i^{(j)}} f_i^{x_i}(z_i) dz_i \\
&\leq K^{p\alpha_i^{(j)}} + C \int_K^{+\infty} z_i^{p\alpha_i^{(j)} - \eta_i} dz_i < +\infty,
\end{aligned}$$

where the integral in the last step is finite since $p\alpha_i^{(j)} - \eta_i < -1$ for all $i \in \{1, \dots, d\}$ and $j \in \{1, \dots, N\}$ with $\alpha_i^{(j)} \neq 0$. □

We close this section with three remarks on the assumptions and possible extensions of Theorem 5.6.1.

Remark 5.6.2. *The assumption given by Equation* (5.2) *is, for example, fulfilled for the d-dimensional Brownian sheet with $N = 1$, $c_1 = 1$ and $\alpha^{(1)} = (1/2, \dots, 1/2) \in \mathbb{R}_+^d$. Condition* (5.2) *also accomodates the GRFs we considered in the Lévy-Khinchin formula (see Theorem 5.4.6 and Assumption 5.4.4) with $N = d$, $c_1 = \dots = c_d = 1$ and $\underline{\alpha}^{(j)} = 1/2 \cdot \hat{e}_j$ for $j = 1, \dots, d$, where $\hat{e}_j$ is the j-th unit vector in $\mathbb{R}^d$. Further, this assumption is fulfilled for any stationary GRF W. Indeed, in case of a stationary GRF the assumption is satisfied for $\alpha^{(1)} = (\varepsilon, 0, \dots, 0)$ for any $\varepsilon > 0$ and, hence, Theorem 5.6.1 yields that every moment of the corresponding evaluated subordinated GRF exists, independently of the specific choice of the subordinators. This is consistent with Remark 5.4.8. The assumption on the Lévy subordinators in Equation* (5.3) *is natural and can be*

verified easily in many cases, see also [15, Assumption 3.7 and Remark 3.8]. For example, if for some non-negative integer $n \in \mathbb{N}$*, the* n*-th derivative of the characteristic function* $\phi_{l(x_i)}(\cdot)$ *is integrable over* $\mathbb{R}$*, then Equation* (5.3) *holds with* $\eta_i = n$*,* $K = 0$ *and* $C = \frac{1}{2\pi} \int_{-\infty}^{+\infty} |\frac{d^n}{dt^n} \phi_{l(x_i)}(t)| \, dt$ *(cf. [73, Lemma 12]).* ◆

Remark 5.6.3. *We point out that the statement of Theorem 5.6.1 remains valid if we consider Lévy distributions with discrete probability distribution which satisfy a discrete version of* (5.3)*: If the GRF* W *satisfies* (5.2) *and the evaluated discrete subordinators* $l_1(x_1), \ldots, l_d(x_d)$ *satisfy*

$$f_i^{x_i}(k) = \mathbb{P}(l_i(x_i) = k) \leq C|k|^{-\eta_i}, \text{ for } k \geq K \text{ and } i \in \{1, \ldots, d\}, \tag{5.4}$$

then we obtain that $\mathbb{E}(|L(x_1, \ldots, x_d)|^p) < \infty$ *for* $p \in [1, a)$ *with the real number* a *defined in Theorem 5.6.1.* ◆

Remark 5.6.4. *For the pointwise existence of moments given by Theorem 5.6.1, it is not necessary to restrict the subordinating processes to the class of Lévy subordinators. More generally, one could consider a GRF* W *satisfying* (5.2) *and general Lévy processes* $l_1, \ldots, l_d$ *satisfying* (5.3) *for* $|z| \geq K$*. In this case, Theorem 5.6.1 still holds for the random field* L *defined by* $L(\underline{x}) := W(|l_1(x_1)|, \ldots, |l_d(x_d)|)$*, for* $\underline{x} = (x_1, \ldots, x_d) \in [0, \mathbb{T}]_d$*.* ◆

5.7 Numerical examples

In the following, we present numerical experiments on the theoretical results given in this paper. The goal of this section is to use the knowledge on theoretical properties of the subordinated GRF to investigate existing numerical methods for the approximation of pointwise distributions (Subsection 5.7.1) as well as methods to verify or disprove the existence of moments of a random variable (Subection 5.7.2). The numerical methods may also be useful for a fitting of random fields to existing data in applications. All our numerical experiments have been performed with MATLAB.

5.7.1 Experiments on the Lévy-Khinchin formula

The Lévy-Khinchin-type formula (Theorem 5.4.6) allows access to the pointwise distribution of a subordinated GRF which motivates the investigation of numerical methods to approximate

the pointwise distribution. To be more precise, we use Corollary 5.4.7 to obtain a pointwise distributional representation of a subordinated GRF as the sum of one-dimensional Lévy processes with transformed Lévy triplets. We use this representation to investigate the performance of different methods to approximate the distribution of Lévy processes.

Assume $L = (W(l_1(x), l_2(y)),\ (x, y) \in [0, 1]^2)$ is a subordinated GRF where the GRF W satisfies Assumption 5.4.4 and the two subordinators l_1 and l_2 are characterized by the Lévy triplets $(\gamma_k, 0, \nu_k)$ for $k = 1, 2$. It follows by Corollary 5.4.7 that L admits the pointwise distributional representation

$$L(x, y) \stackrel{\mathcal{D}}{=} \tilde{l}_1(x) + \tilde{l}_2(y), \tag{5.5}$$

for $(x, y) \in [0, 1]^2$. Here, the processes $\tilde{l}_k$ on $[0, 1]$ are independent Lévy processes with triplets $(0, \sigma^2\gamma_k, \nu_k^{\#})$, for $k = 1, 2$, in the sense of the one-dimensional Lévy-Khinchin formula (see Theorem 5.2.1) and the Lévy measure $\nu_k^{\#}$ is defined by

$$\nu_k^{\#}([a, b]) := \int_0^{\infty} \int_a^b \frac{1}{\sqrt{2\pi\sigma^2 t}} \exp\left(-\frac{x^2}{2\sigma^2 t}\right) dx\, \nu_k(dt),$$

$a, b \in \mathbb{R}$ and $k = 1, 2$. We choose specific spatial points and use two different methods to approximate the distribution of the Lévy processes on the right hand side of (5.5): the compound Poisson approximation (CPA) (see [109, Section 8.2.1]) and the Fourier inversion method for Lévy processes (see [56] and [15]) which allows for a direct approximation of the density of the right hand side of (5.5). In order to investigate the performance of these two approaches, the corresponding results are then compared with samples of the subordinated GRF on the left hand side of Equation (5.5).

5.7.1.1 Compound Poisson approximation

We recall that a Gamma(a_G, b_G) process l_G has independent Gamma-distributed increments and $l_G(t)$ follows a Gamma$(a_G \cdot t, b_G)$ distribution. In our first example we choose Gamma$(4, 12)$ processes to subordinate the GRF W defined by $W(x, y) = \sqrt{x + y}\, \tilde{W}(x, y)$, for $(x, y) \in \mathbb{R}^2_+$, where $\tilde{W}$ is a Matérn-1.5-GRF with pointwise standard deviation $\sigma = 2$ (see Remark 5.4.5). We fix the evaluation point $(x, y) = (1, 1)$ and use the CPA method to obtain samples of the Lévy process on the right hand side of (5.5) which can then be compared with samples of the subordinated GRF. Figure 5.2 (left and middle) shows the corresponding histograms for 10.000 samples of each distribution. We observe an accurate fit of the samples generated by the different approaches: the first histogram, corresponding to the exact sampling of the

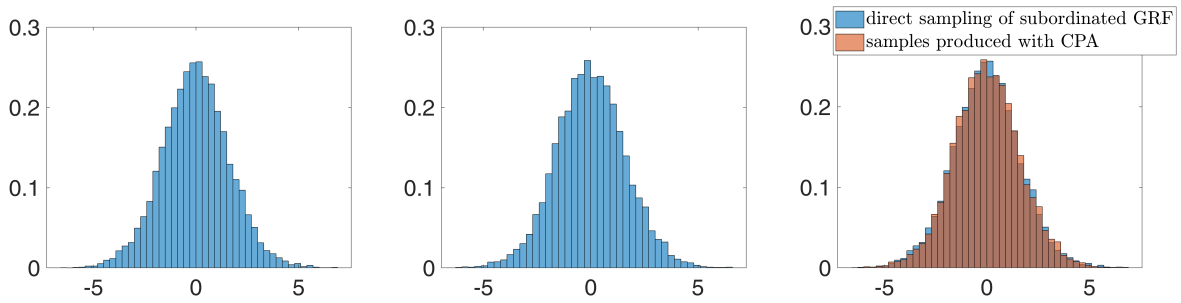

Figure 5.2: Samples of the subordinated GRF $W(l_1(1), l_2(1))$ (left), the sum of the corresponding transformed Lévy processes $\tilde{l}_1(1)+\tilde{l}_2(1)$ generated by the CPA method (middle) and both histograms in one plot (right).

subordinated GRF, displays the same characteristics as the histogram generated by CPA, which shows that the CPA method is appropriate to simulate the distribution of the right hand side of Equation (5.5).

5.7.1.2 Fourier inversion method

The second approach is to approximate the density function of the right hand side of (5.5) by the Fourier inversion (FI) method (see [56] and [15]) and compare it with samples of the subordinated GRF. Figure 5.3 illustrates the results for this approach where we used the evaluation point $(x, y) = (1, 1)$, the same GRF as in Subsection 5.7.1.1, Gamma$(4, 12)$ subordinators and 100.000 samples of the subordinated GRF. As one can see in Figure 5.3, the approximated

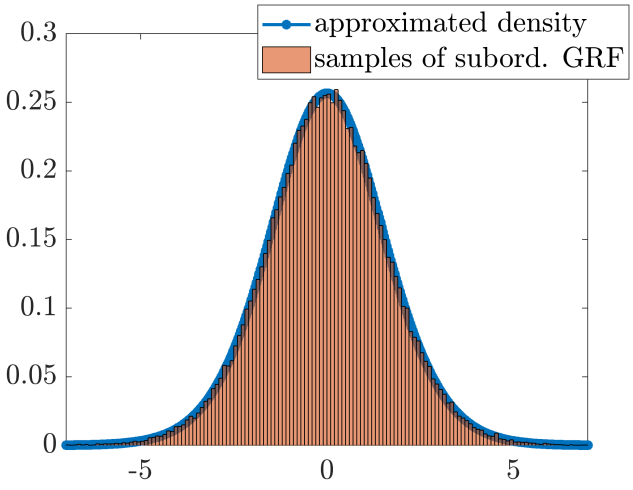

Figure 5.3: Samples of Gamma$(4, 12)$-subordinated GRF and approximated density (FI).

density of the right hand side of (5.5) perfectly matches the pointwise distribution of the

subordinated GRF. We want to confirm this observation by a Kolmogorov-Smirnov-Test (see for example [103, Section VII.4]). Figure 5.4 illustrates how the empirical CDF, obtained by sampling the subordinated GRF, converges to the target CDF which is approximated by the Fourier inversion method using Equation (5.5). A Kolmogorov-Smirnov-test with 10.000 samples and a level of significance of 5% is passed.

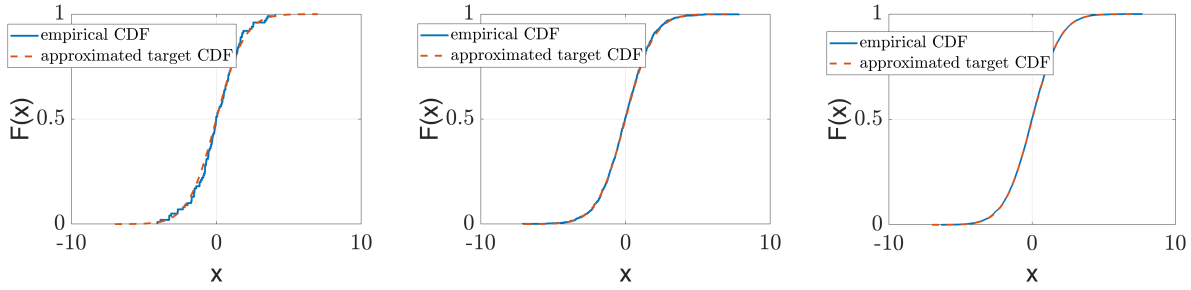

Figure 5.4: Approximated target CDF (FI) vs. empirical CDF using 100 (left), 1.000 (middle) and 10.000 (right) samples of the subordinated GRF with Gamma$(4, 12)$ subordinators.

In the next experiment we use a modified subordinator, which results in a less smooth pointwise density of the subordinated GRF. We repeat the experiment with Gamma$(0.5, 10)$ subordinators where the GRF, the evaluation point and the sample size remain unchanged. Figure 5.5 shows 100.000 samples of the subordinated GRF and the density of the process given by the right hand side of Equation (5.5) approximated via the Fourier Inversion method. As in

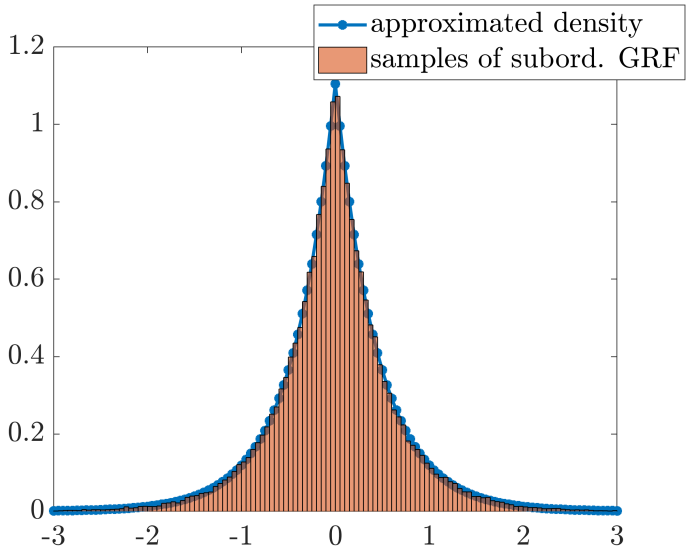

Figure 5.5: Samples of Gamma$(0.5, 10)$-subordinated GRF and approximated density (FI).

the first experiment, the results given by Figure 5.5 indicate that the approximated density of

the right hand side of (5.5) matches the pointwise distribution of the subordinated GRF. Figure 5.6 illustrates how the empirical CDF, obtained by sampling of the subordinated GRF, converges to the approximated target CDF of the right hand side of Equation (5.5), which is computed by the Fourier inversion method. A Kolmogorov-Smirnov-test with a level of significance of 5% is passed.

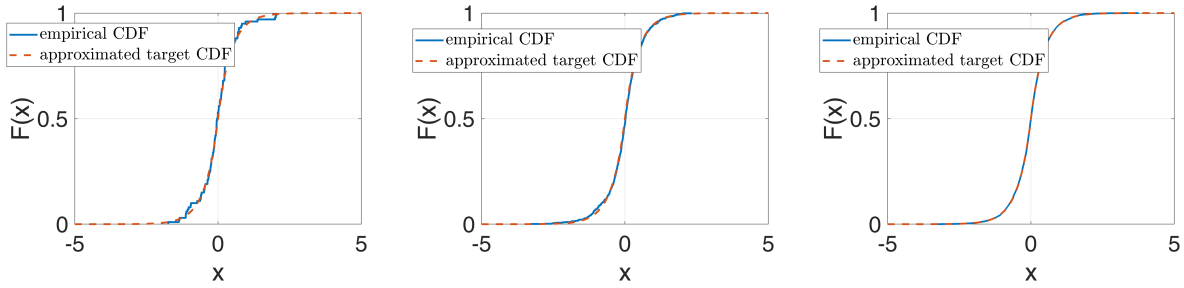

Figure 5.6: Approximated target CDF (FI) vs. empirical CDF using 100 (left), 1.000 (middle) and 10.000 (right) samples of the subordinated GRF with Gamma$(0.5, 10)$ subordinators.

5.7.2 Pointwise moments

Theorem 5.6.1 guarantees the existence of pointwise moments of the subordinated GRF if the GRF and the corresponding subordinators satisfy certain conditions. In the following numerical experiments, we investigate the results of different statistical methods to investigate numerically the existence of pointwise moments of a certain order in the specific situation of the subordinated Gaussian random field. We set $d = 2$ and assume W to be a Brownian sheet on $\mathbb{R}^2_+$. Further, we use Lévy processes with different stochastic regularity - in terms of the existence of moments - to subordinate the GRF W.

5.7.2.1 Statistical methods to test the existence of moments of a random variable

The existence of moments of a specific distribution is one of the most frequently formulated assumptions in statistical applications. For example, already the strong law of large numbers assumes finiteness of the first moment of the corresponding random variable. Nevertheless, in the literature only few statistical methods exist to verify or disprove the existence of moments, given a specific sample of random variables (see e.g. [92, 71, 99, 52, 53, 54]). One of the earlier methods to verify the existence of moments of a distribution was proposed in 1963 by Mandelbrot

(see [92] and [34]). It is based on the simple observation that the estimated (sample-)moments will converge to a certain value for an increasing sample size if the theoretical moment exists. On the other side, if the theoretical moment does not exist, the estimated moment will diverge or behave unstable when the sample size increases. However, this quite intuitive method is rather heuristic and depends highly on the experience of the researcher (see also [52]). Another popular direct way to investigate the existence of moments of a certain distribution is the sample-based estimation of a decay rate α for the corresponding density function proposed by Hill in [71]. However, the Hill-estimator requires a parameter $k > 0$ which specifies the sample values which are considered as the tail of the distribution and it turned out that the Hill-estimator is very sensitive to the choice of this parameter k. Further, the method makes the quite restrictive assumption that the underlying distribution is of Pareto-type (see [99, 52, 53] and [54]). In 2013, Fedotenkov proposed a bootstrap test for the existence of moments of a given distribution (see [52]). The test performs well for specific distributions, however, its accuracy deteriorates fast when moments of higher order are considered (see also [53]). Recently, Ng and Yau proposed another sample-based bootstrap test for the existence of moments which outperforms the previously mentioned methods for many distributions (see [99]). The test is based on a result from bootstrap asymptotic theory which states that the m out of n bootstrap sample mean (see [20]) converges weakly to a normal distribution. For a detailed description of the test statistic and further theoretical investigations we refer the interested reader to [99].

Based on these observations, we investigate the results of direct moment estimation via Monte Carlo (MC) and the bootstrap test proposed by Ng and Yau to analyze the existence of (pointwise) moments of the subordinated GRF.

For our numerical examples we choose three different Lévy distributions to subordinate the Brownian sheet W: a Poisson distribution, a Gamma distribution and a Student-t distribution. Therefore, we use a discrete and a continuous distribution where all moments are finite and a continuous distribution, which only admits a limited number of moments. Hence, we consider three fundamentally different situations. In all three experiments, we consider the evaluation point $\underline{x} = (x_1, x_2) = (1, 1) \in \mathbb{R}^2_+$ for the subordinated GRF L. Note that the two-dimensional Brownian sheet satisfies Equation (5.2) in Theorem 5.6.1 with $N = 1$, $c_1 = 1$ and $\underline{\alpha}^{(1)} = (1/2, 1/2)$.

5.7.2.2 Poisson-subordinated Brownian sheet

In this example, we use Poisson(3) processes to subordinate the two-dimensional Brownian sheet. It is easy to verify that condition (5.4) is satisfied for any $\eta_i > 0$, $i = 1, 2$, since point evaluations of a Poisson process are Poisson distributed. Theorem 5.6.1 implies the existence of

the p-th moment of the evaluated field $L(1,1)$ for any $p < \infty$ (see Remark 5.6.3). We estimate the p-th moment for $p \in \{4,6,8\}$ by a MC-estimation using M samples of the evaluated GRF $L(1,1)$ for different values of $M \in \mathbb{N}$, i.e.

$$\mathbb{E}(|L(1,1)|^p) \approx E_M(|L(1,1)|^p) = \frac{1}{M}\sum_{i=1}^{M} |L^{(i)}(1,1)|^p,$$

where $(L^{(i)}(1,1),\ i \geq 1)$ are i.i.d. samples of the evaluated field $L(1,1)$. As explained in Subsection 5.7.2.1, the MC-estimator $E_M(|L(1,1)|^p)$ is expected to converge for $M \to \infty$ if the p-th moment exists and one expects unstable behaviour if this is not the case. Figure 5.7 shows the development of the MC-estimator $E_M(|L(1,1)|^p)$ for the p-th moment as a function of the number of samples M. For every moment, we take 5 independent MC-runs to validate that they converge to the same value. As expected, Figure 5.7 shows a stable convergence of

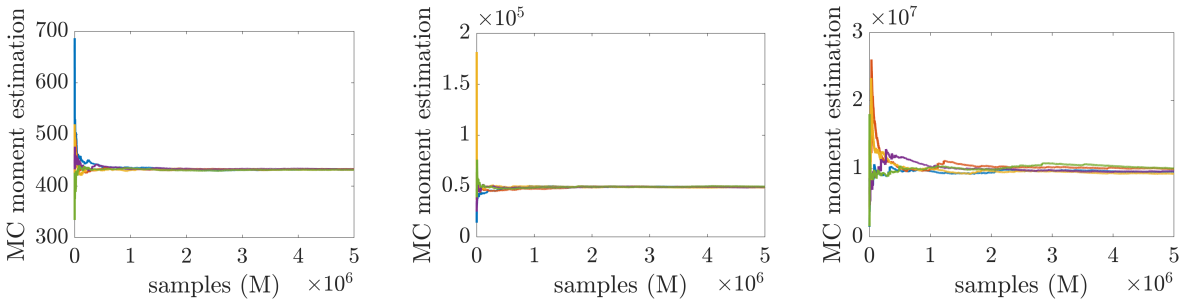

Figure 5.7: Five independent realizations of the MC-estimator $E_M(|L(1,1)|^p) \approx \mathbb{E}(|L(1,1)|^p)$ as a function of the sample numbers M with a Poisson(3)-subordinated Brownian sheet; $p = 4$ (left), $p = 6$ (middle), $p = 8$ (right).

the MC-estimator for a growing number of samples for every considered moment. Further, the different independent MC-runs converge to the same value - the theoretical p-th moment for $p \in \{4,6,8\}$.

In the next step, we perform the bootstrap test (see Subsection 5.7.2.1 and [99]). We test the existence of the p-th moment for $p \in \{1,2,3,4,5,6,7,8\}$ using $M = 10^7$ samples of the subordinated evaluated GRF $L(1,1)$. Hence, the null and alternative hypothesis are given by

$$H_0 : \mathbb{E}(|L(1,1)|^p) < +\infty \text{ vs. } H_1 : \mathbb{E}(|L(1,1)|^p) = +\infty,$$

for the different values of p. We choose the significance level $\alpha_s = 1\%$ and perform 100 independent test runs. Figure 5.8 shows the proportion of acceptance of the null hypothesis in the 100 test runs as a function of the considered moment $p \in \{1,2,3,4,5,6,7,8\}$. As we see in Figure 5.8, the bootstrap test accepts the null hypothesis H_0 in almost every test run for

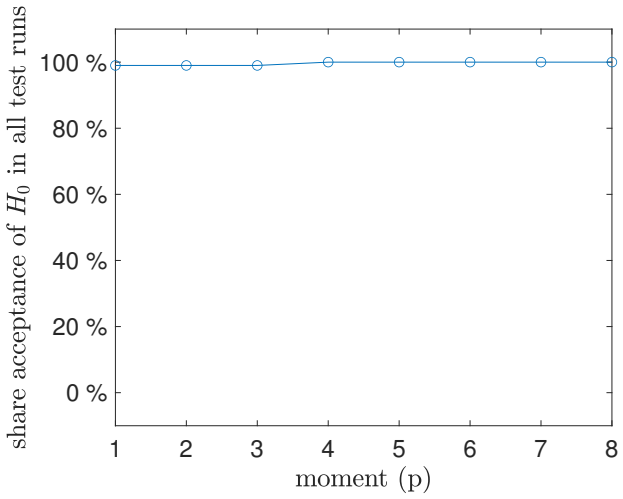

Figure 5.8: Results for 100 independent runs of the bootstrap test for the existence of the p-th moment using Poisson(3) processes to subordinate the Brownian sheet.

every considered moment $p \in \{1, 2, 3, 4, 5, 6, 7, 8\}$ which is in line with our expectatations since all these moments exist. We conclude that both approaches, the MC moment estimation and the bootstrap test, perform as expected in this experiment.

5.7.2.3 Gamma-subordinated Brownian sheet

In our second numerical example we consider Gamma processes to subordinate the Brownian sheet. We recall that, for $a_G, b_G > 0$, a Gamma(a_G, b_G)-distributed random variable admits the density function

$$x \mapsto \frac{b_G^{a_G}}{\Gamma(a_G)} x^{a_G - 1} \exp(-x b_G), \quad \text{for } x > 0,$$

where $\Gamma(\cdot)$ denotes the Gamma function. A Gamma process $(l(t))_{t \geq 0}$ has independent Gamma distributed increments and $l(t)$ follows a Gamma$(a_G \cdot t, b_G)$-distribution for $t > 0$. Therefore, condition (5.3) holds for any $\eta_i > 0$, for $i = 1, 2$ and, hence, Theorem 5.6.1 again implies the existence of every moment, i.e. $\mathbb{E}(|L(1,1)|^p) < \infty$ for any $p \geq 1$. We choose $a_G = 4$, $b_G = 10$ and estimate the p-th moment of $L(1,1)$ with $p \in \{4, 6, 8\}$ by a MC-estimation using a growing number of samples $M \in \mathbb{N}$. Figure 5.9 shows the development of the MC-estimator $E_M(|L(1,1)|^p)$ for the p-th moment as a function of the number of samples M. As in the first experiment, we take 5 independent MC-runs to validate the convergence to a unique value. In line with our expectations, the results show a stable convergence of the MC-estimations for

the different moments of this subordinated GRF.

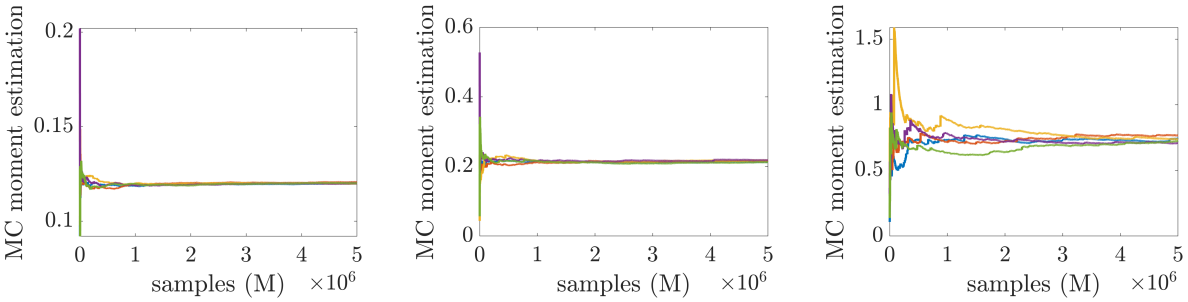

Figure 5.9: Five independent realizations of the MC-estimator $E_M(|L(1,1)|^p) \approx \mathbb{E}(|L(1,1)|^p)$ as a function of the sample numbers M with a Gamma$(4,10)$-subordinated Brownian sheet; $p = 4$ (left), $p = 6$ (middle), $p = 8$ (right).

In this experiment we again perform the bootstrap test for the existence of the p-th moment for $p \in \{1,2,3,4,5,6,7,8\}$ using $M = 10^7$ samples of the subordinated evaluated GRF $L(1,1)$. Hence, the null and alternative hypothesis are given by

$$H_0 : \mathbb{E}(|L(1,1)|^p) < +\infty \text{ vs. } H_1 : \mathbb{E}(|L(1,1)|^p) = +\infty,$$

for the different values of p. We choose the significance level $\alpha_s = 1\%$ and perform 100 independent test runs. Figure 5.10 shows the proportion of acceptance of the null hypothesis in the 100 test runs as a function of the considered moment $p \in \{1,2,3,4,5,6,7,8\}$. As in the

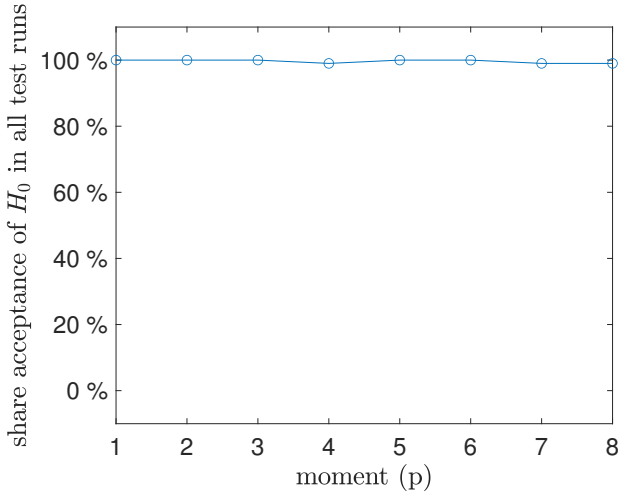

Figure 5.10: Results for 100 independent runs of the bootstrap test for the existence of the p-th moment using Gamma(4,10) processes to subordinate the Brownian sheet.

first experiment, the test results meet our expectations, since almost every test run accepts the

null hypothesis for any moment $p \in \{1, 2, 3, 4, 5, 6, 7, 8\}$.

5.7.2.4 Student t-subordinated Browinan Sheet

In our last experiment we consider a Lévy process where the pointwise distribution only admits a finite number of moments. The Student-t-distribution with three degress of freedom admits the density function

$$f_t(x) = \frac{\Gamma(2)}{\sqrt{3\pi}\Gamma(3/2)}\Big(1 + \frac{x^2}{3}\Big)^{-2}, \text{ for } x \in \mathbb{R}. \tag{5.6}$$

It follows by [78, Theorem 3] that a Student-t distributed random variable with three degrees of freedom is infinitely divisible. Hence, we can define Lévy processes l_j, for $j = 1, 2$, such that $l_j(1)$ follows a Student-t distribution with three degrees of freedom (see [108, Theorem 7.10]). Using these processes and the Brownian sheet W, we consider the subordinated GRF $L(x_1, x_2) := W(|l_1(x_1)|, |l_2(x_2)|)$ for $(x_1, x_2) \in [0, T_1] \times [0, T_2]$ (see Remark 5.6.4). For our numerical experiment we again evaluate the field at $(x_1, x_2) = (1, 1)$. Using (5.6) we obtain

$$f_t(x) \leq C|x|^{-4}, \text{for } x \in \mathbb{R}.$$

Therefore, condition (5.3) is satisfied for $\eta_i = 4$, for $i = 1, 2$, and it is violated for any $\eta_i > 4$ (see also Remark 5.6.4). Since the Brownian sheet satisfies condition (5.2) with $N = 1, c_1 = 1$ and $\underline{\alpha}^{(1)} = (1/2, 1/2)$, Theorem 5.6.1 yields that $\mathbb{E}(|L(1,1)|^p) < \infty$ for $p < 6$ and we expect that this boundary is sharp, i.e. we expect that $\mathbb{E}(|L(1,1)|^p) = \infty$ for $p \geq 6$.

We estimate the p-th moment for $p \in \{5, 6, 8\}$ with the MC-estimator $E_M(|L(1,1)|^p)$ with growing sample number $M \in \mathbb{N}$. In Figure 5.11 we see the development of the MC-estimator for the p-th moment as a function of the number of samples. For every moment, we take 5 independent MC-runs. The results indicate a convergence of the MC-estimations of the p-th moment for $p = 5$: in this case the estimation stabilizes with growning sample size and all 5 independent MC-estimations seem to converge to a unique value. However, for the higher moments $p = 6$ and $p = 8$, we see upward breakouts and instable behaviour of the corresponding MC-estimator for increasing sample sizes. Further, the 5 independent MC-runs do not indicate a convergence to a unique value. For all the considered moments $p \in \{5, 6, 8\}$, these results are in line with our expectations, since the p-th moment of the evaluated subordinated GRF $L(1,1)$ admits a p-th moment for $p < 6$ and this boundary is sharp (see Theorem 5.6.1).

We perform the bootstrap test for the existence of the p-th moment for $p \in \{1, 2, 3, 4, 4.5, 5,$

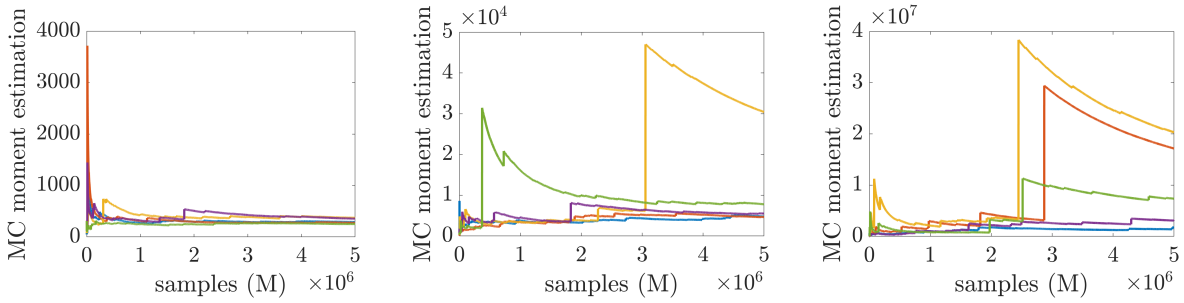

Figure 5.11: Five independent realizations of the MC-estimator $E_M(|L(1,1)|^p) \approx \mathbb{E}(|L(1,1)|^p)$ as a function of the sample numbers M with a Student-t-subordinated Brownian sheet; $p = 5$ (left), $p = 6$ (middle), $p = 8$ (right).

$5.2, 5.4, 5.6, 5.8, 6, 6.5, 7, 8\}$ using $M = 10^7$ samples of the subordinated GRF $L(1,1)$. Hence, the null and alternative hypothesis are again given by

$$H_0 : \mathbb{E}(|L(1,1)|^p) < +\infty \text{ vs. } H_1 : \mathbb{E}(|L(1,1)|^p) = +\infty,$$

for the different values of p. We choose the significance level $\alpha_s = 1\%$ and perform 100 independent test runs. Figure 5.12 shows the proportion of acceptance of the null hypothesis in the 100 test runs as a function of the considered moment p and the test statistic values for the 100 test runs. In all of the 100 test runs the null hypothesis is accepted for $p \in \{1, 2, 3, 4, 4.5, 5\}$.

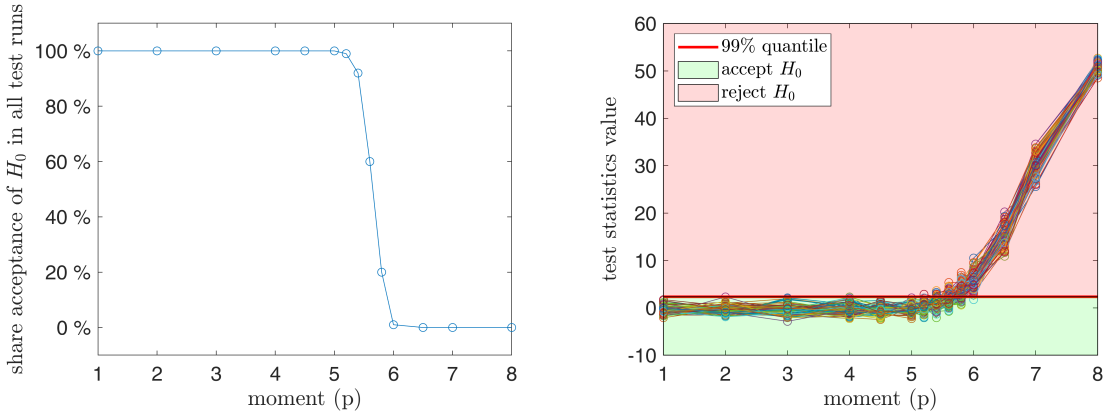

Figure 5.12: Results for 100 independent runs of the bootstrap test for the existence of the p-th moment using Student-t-distributed random variables as subordinators: share acceptance of H_0 (left), test statistic values for the test runs (right).

Further, in almost all of the 100 test runs H_0 is rejected for the cases $p \in \{6, 6.5, 7, 8\}$, which is absolutely in line with the theoretical results for this specific choice of the subordinated GRF. Only for $p \in (5, 6)$, the test rejects the null hypothesis in some of the test runs although

the theoretical moment exists. Overall, the test results for the existence of moments of the Student-t-subordinated GRF match our expectations based on Theorem 5.6.1.

Acknowledgements

The authors would like to thank two anonymous referees for their remarks, which led to a significant improvement of the manuscript.

Funding

Open Access funding enabled and organized by Projekt DEAL. Funded by Deutsche Forschungsgemeinschaft (DFG, German Research Foundation) under Germany's Excellence Strategy - EXC 2075 - 390740016.

Data availability

All data used in our experiments have been produced with MATLAB random number generators and no external datasets have been used. The datasets generated and analysed during the current study are available from the corresponding author on reasonable request.

Conflicts of interest

The authors declare that they have no conflict of interest.

Subordinated Gaussian random fields in elliptic partial differential equations

6

Robin Merkle[1] and Andrea Barth[1]

Published in Stochastics and Partial Differential Equations: Analysis and Computations (2022)
Reproduced with permission from Springer Nature
Reference: [96], Link: https://doi.org/10.1007/s40072-022-00246-w

Abstract: *To model subsurface flow in uncertain heterogeneous or fractured media an elliptic equation with a discontinuous stochastic diffusion coefficient — also called random field — may be used. In case of a one-dimensional parameter space, Lévy processes allow for jumps and display great flexibility in the distributions used. However, in various situations (e.g. microstructure modeling), a one-dimensional parameter space is not sufficient. Classical extensions of Lévy processes on two parameter dimensions suffer from the fact that they do not allow for spatial discontinuities (see for example [15]). In this paper a new subordination approach is employed (see also [95]) to generate Lévy-type discontinuous random fields on a two-dimensional spatial parameter domain. Existence and uniqueness of a (pathwise) solution to a general elliptic partial differential equation is proved and an approximation theory for the diffusion coefficient and the corresponding solution provided. Further, numerical examples using a Monte Carlo approach on a finite element discretization validate our theoretical results.*

[1]IANS/SimTech, University of Stuttgart, Stuttgart, Germany

6.1 Introduction

Over the last decade partial differential equations with stochastic operators/data/domain became a widely studied object. This branch of research is oftentimes called Uncertainty Quantification. Especially for problems where data is sparse or measurement errors are unavoidable, like subsurface flow problems, the theory provides an approach to quantify this uncertainty. There are two main approaches to discretize the uncertain problem: intrusive and non-intrusive methods. The former require the solution of a high dimensional partial differential equation, where the dimensionality depends on the smoothness of the random field or process (see for example [12], [55], [97] and the references therein). The latter consist of (essentially) sampling methods and require multiple solutions of a low dimensional problem (see, among others, [1], [14], [16], [110], [87], [112]). Up to date mainly Gaussian random fields were used to model the diffusivity in an elliptic equation (as a model for a subsurface flow problem). Gaussian random fields have the advantage that they may be used in both approaches and that they are stochastically very well understood objects. A great disadvantage is however, that the distributions underlying the field are Gaussian and therefore the model lacks flexibility, in the sense that the field cannot have pointwise marginal distributions with heavy-tails. Further, Gaussian random fields that are commonly used in applications, like Matérn fields, have $\mathbb{P}$-almost surely spatial continuous paths. In view of these limitations, some extensions of Gaussian models for the diffusivity in elliptic PDEs have been explored in the literature: The paper [87] presents a multilevel Monte Carlo method for elliptic equations with jump-diffusion coefficients for two-phase random media, where the diffusion coefficient assumes two different values on random domains. Discontinuous models for the diffusion coefficient in elliptic PDEs have also been used in the context of Bayesian inversion, where geometric priors or level-set priors are used as a model for the diffusion, see e.g. [75] and [76]. In the recent article [49], the diffusion coefficient of an elliptic PDE is modeled as a transformation of smoothed Lévy noise fields. The authors investigate the existence, integrability and approximation of the corresponding stochastic PDE solution. The presented model yields a high distributional flexibility of the diffusion coefficient, however, the considered fields are continuous in space.

In this paper we propose a two-dimensional subordinated Gaussian random field as stochastic diffusion coefficient in an elliptic equation. The subordinated Gaussian random field is a type of a (discontinuous) Lévy field. Different subordinators display unique patterns in the discontinuities and have varied marginal distributions (see [95]). Naturally the spatial regularity of a subordinated Gaussian random field depends on the subordinator. We prove existence and uniqueness of a solution to the elliptic equation in a pathwise sense and provide different discretization schemes.

We structured the rest of the paper as follows: In Section 6.2 we introduce a general pathwise existence and uniqueness result for a stochastic elliptic equation under mild assumptions on the coefficient. These assumptions accommodate the subordinated Gaussian random fields we introduce in Section 6.3. In Section 6.4 we approximate the specific diffusion coefficient which is used in this paper and show convergence of the elliptic equation with the approximated coefficient to the unapproximated solution in Section 6.5. Section 6.6 provides spatial approximation methods and in Section 6.7 numerical examples are presented.

6.2 The stochastic elliptic problem

In this section we introduce the framework of the general stochastic elliptic boundary value problem which allows for discontinuous diffusion coefficients. For the general setting and pathwise existence theory we follow [16]. In the following, let $(\Omega, \mathcal{F}, \mathbb{P})$ be a complete probability space. Let $(B, \|\cdot\|_B)$ be a Banach space and Z be a B valued random variable, i.e. a measurable function $Z : \Omega \to B$. The space $L^p(\Omega; B)$ contains all strongly measurable B-valued random variables with $\|Z\|_{L^p(\Omega;B)} < +\infty$, for $p \in [1, +\infty]$, where the norm is defined by

$$\|Z\|_{L^p(\Omega;B)} = \begin{cases} \mathbb{E}(\|Z\|_B^p)^{\frac{1}{p}} & , \text{ if } 1 \leq p < +\infty, \\ \operatorname{ess\,sup}_{\omega\in\Omega} \|Z\|_B & , \text{ if } p = +\infty. \end{cases}$$

6.2.1 Problem formulation

Let $\mathcal{D} \subset \mathbb{R}^d$ for $d \in \mathbb{N}$ be a bounded, connected Lipschitz domain. We consider the equation

$$-\nabla \cdot (a(\omega, \underline{x})\nabla u(\omega, \underline{x})) = f(\omega, \underline{x}) \text{ in } \Omega \times \mathcal{D}, \tag{6.1}$$

where $a : \Omega \times \mathcal{D} \to \mathbb{R}_+$ is a stochastic (jump-diffusion) coefficient and $f : \Omega \times \mathcal{D} \to \mathbb{R}$ is a (measurable) random source function. Further, we impose the following boundary conditions

$$u(\omega, \underline{x}) = 0 \text{ on } \Omega \times \Gamma_1, \tag{6.2}$$

$$a(\omega, \underline{x})\overrightarrow{n} \cdot \nabla u(\omega, \underline{x}) = g(\omega, \underline{x}) \text{ on } \Omega \times \Gamma_2, \tag{6.3}$$

where we assume to have a decomposition $\partial\mathcal{D} = \Gamma_1 \dot\cup \Gamma_2$ with two $(d-1)$-dimensional manifolds $\Gamma_1,\ \Gamma_2$ such that the exterior normal derivative $\overrightarrow{n} \cdot \nabla u$ on Γ_2 is well-defined for every $u \in C^1(\overline{\mathcal{D}})$. Here, $\overrightarrow{n}$ is the outward unit normal vector to Γ_2 and $g : \Omega \times \Gamma_2 \to \mathbb{R}$ a measurable function. Note that we just reduce the theoretical analysis to the case of homogeneous Dirichlet boundary conditions to simplify notation. The extension to the inhomogeneous case is straightforward.

We now state assumptions under which the elliptic boundary value problem has a unique solution.

Assumption 6.2.1.
Let $H := L^2(\mathcal{D})$. We assume that

i for any fixed $\underline{x} \in \mathcal{D}$ the mapping $\omega \mapsto a(\omega, \underline{x})$ is measurable, i.e. $a(\cdot, \underline{x})$ is a (real-valued) random variable,

ii for any fixed $\omega \in \Omega$ the mapping $a(\omega, \cdot)$ is $\mathcal{B}(\mathcal{D}) - \mathcal{B}(\mathbb{R}_+)$-measurable and it holds $a_-(\omega) := \operatorname{ess\,inf}_{\underline{x}\in\mathcal{D}} a(\omega, \underline{x}) > 0$ and $a_+(\omega) := \operatorname{ess\,sup}_{\underline{x}\in\mathcal{D}} a(\omega, \underline{x}) < +\infty$,

iii $\frac{1}{a_-} \in L^p(\Omega; \mathbb{R})$, $f \in L^q(\Omega; H)$ and $g \in L^q(\Omega; L^2(\Gamma_2))$ for some $p, q \in [1, +\infty]$ such that $r := (\frac{1}{p} + \frac{1}{q})^{-1} \geq 1$.

◆

Remark 6.2.2. *Note that Assumption 6.2.1 implies that the real-valued mappings $a_-, a_+ : \Omega \to \mathbb{R}$ are measurable. This can be seen as follows: For fixed $p \geq 1$ consider the mapping*

$$I_p : \Omega \to \mathbb{R},\ \omega \mapsto \|a(\omega, \cdot)\|_{L^p(\mathcal{D})} = \Big(\int_{\mathcal{D}} a(\omega, \underline{x})^p d\underline{x} \Big)^{1/p},$$

which is well-defined by Assumption 6.2.1. It follows from the definition of the Lebesgue integral and Assumption 6.2.1 i that the mapping $\omega \mapsto I_p(\omega)$ is $\mathcal{F} - \mathcal{B}(\mathbb{R})$ measurable. For a fixed $\omega \in \Omega$, by the embedding theorem for L^p spaces (see [2, Theorem 2.14]), we get

$$a_+(\omega) = \lim_{m\to\infty} \|a(\omega, \cdot)\|_{L^m(\mathcal{D})}.$$

Since this holds for all $\omega \in \Omega$ we obtain by [6, Lemma 4.29] that the mapping

$$\omega \mapsto a_+(\omega),$$

is $\mathcal{F} - \mathcal{B}(\mathbb{R})$-measurable. The measurability of $\omega \mapsto a_-(\omega)$ follows analogously. Note that we do not treat the random coefficient $a : \Omega \times \mathcal{D} \to \mathbb{R}$ as a $L^\infty(\mathcal{D})$-valued random variable, since $L^\infty(\mathcal{D})$ is not separable and therefore the strong measurability of the mapping $a : \Omega \to L^\infty(\mathcal{D})$ is only guaranteed in a very restrictive setting. Nevertheless, the measurability of the functions a_+ and a_- allows taking expectations of these real-valued random variables. In order to avoid confusion about that, we use the notation $\mathbb{E}(\operatorname{ess\,sup}_{\underline{x}\in\mathcal{D}} |\cdot|^s)^{1/s}$. ◆

6.2.2 Weak solution

We denote by $H^1(\mathcal{D})$ the Sobolev space on $\mathcal{D}$ with the norm $\|v\|_{H^1(\mathcal{D})} := (\|v\|^2_{L^2(\mathcal{D})} + \|\nabla v\|^2_{L^2(\mathcal{D})})^{1/2}$, for $v \in H^1(\mathcal{D})$ (see for example [50, Section 5.2]). Further, we denote by T the trace operator $T : H^1(\mathcal{D}) \to H^{\frac{1}{2}}(\partial\mathcal{D})$ where $Tv = v|_{\partial\mathcal{D}}$ for $v \in C^\infty(\overline{\mathcal{D}})$ (see [41]). We define the subspace $V \subset H^1(\mathcal{D})$ as

$$V := \{v \in H^1(\mathcal{D}) \mid Tv|_{\Gamma_1} = 0\},$$

with the standard Sobolev norm, i.e. $\|\cdot\|_V := \|\cdot\|_{H^1(\mathcal{D})}$. We identify $H = L^2(\mathcal{D})$ with its dual space H' and work on the Gelfand triplet $V \subset H \simeq H' \subset V'$. Hence, Assumption 6.2.1 guarantees that $f(\omega,\cdot) \in V'$ and $g(\omega,\cdot) \in H^{-\frac{1}{2}}(\Gamma_2)$ for $\mathbb{P}$-almost every $\omega \in \Omega$. We multiply Equation (6.1) by a test function $v \in V$, integrate by parts and use the boundary conditions (6.2) and (6.3) to obtain

$$\begin{aligned}\int_{\mathcal{D}} -\nabla\cdot(a(\omega,\underline{x})\nabla u(\omega,\underline{x}))v(\underline{x})d\underline{x} = &\int_{\mathcal{D}} a(\omega,\underline{x})\nabla u(\omega,\underline{x})\cdot\nabla v(\underline{x})d\underline{x} \\ &- \int_{\Gamma_2} g(\omega,\underline{x})[Tv](\underline{x})d\underline{x}.\end{aligned}$$

This leads to the following pathwise weak formulation of the problem: For any $\omega \in \Omega$, given $f(\omega,\cdot) \in V'$ and $g(\omega,\cdot) \in H^{-\frac{1}{2}}(\Gamma_2)$, find $u(\omega,\cdot) \in V$ such that

$$B_{a(\omega)}(u(\omega,\cdot), v) = F_\omega(v) \tag{6.4}$$

for all $v \in V$. The function $u(\omega,\cdot)$ is then called *pathwise weak solution* to problem (6.1) - (6.3). Here, the bilinear form $B_{a(\omega)}$ and the operator F_ω are given by

$$B_{a(\omega)} : V \times V \to \mathbb{R},\ (u,v) \mapsto \int_{\mathcal{D}} a(\omega,\underline{x})\nabla u(\underline{x})\cdot\nabla v(\underline{x})d\underline{x},$$

and

$$F_\omega : V \to \mathbb{R},\ v \mapsto \int_{\mathcal{D}} f(\omega, x)v(\underline{x})d\underline{x} + \int_{\Gamma_2} g(\omega, \underline{x})[Tv](\underline{x})d\underline{x},$$

for fixed $\omega \in \Omega$, where the integrals in F_ω are understood as the duality pairings:

$$\int_{\mathcal{D}} f(\omega, \underline{x})v(\underline{x})d\underline{x} = {}_{V'}\langle f(\omega, \cdot), v\rangle_V \text{ and}$$
$$\int_{\Gamma_2} g(\omega, \underline{x})[Tv](\underline{x})d\underline{x} = {}_{H^{-\frac{1}{2}}(\Gamma_2)}\langle g(\omega, \cdot), Tv\rangle_{H^{\frac{1}{2}}(\Gamma_2)},$$

for $v \in V$. For a proof of the following existence result we refer to [16, Theorem 2.5].

Theorem 6.2.3.
Under Assumption 6.2.1, there exists a unique pathwise weak solution $u(\omega, \cdot) \in V$ to problem (6.4) *for very $\omega \in \Omega$. Furthermore, $u \in L^r(\Omega; V)$ and*

$$\|u\|_{L^r(\Omega;V)} \leq C(a_-, \mathcal{D}, p)(\|f\|_{L^q(\Omega;H)} + \|g\|_{L^q(\Omega;L^2(\Gamma_2))}),$$

where $C(a_-, \mathcal{D}, p) > 0$ is a constant depending on a_-, p and the volume of $\mathcal{D}$. ◆

In addition to the existence of the solution, the following remark gives a rigorous justification for the measurability of the solution mapping

$$u : \Omega \to V,\ \omega \mapsto u(\omega, \cdot),$$

which maps any $\omega \in \Omega$ on the corresponding pathwise weak PDE solution.

Remark 6.2.4. *Let $(v_n,\ n \in \mathbb{N}) \subset V$ be an orthonormal basis of the separable Hilbert space V. For every $n \in \mathbb{N}$ we define the mapping*

$$J_n : \Omega \times V \to \mathbb{R}$$
$$(\omega, v) \mapsto \int_{\mathcal{D}} a(\omega, \underline{x})\nabla v(\underline{x}) \cdot \nabla v_n(\underline{x})d\underline{x} - \int_{\mathcal{D}} f(\omega, \underline{x})v_n(\underline{x})d\underline{x} - \int_{\Gamma_2} g(\omega, \underline{x})[Tv_n](\underline{x})d\underline{x}.$$

It is easy to see that this mapping is Carathéodory for any $n \in \mathbb{N}$, i.e. $J_n(\cdot, v)$ is $\mathcal{F}$-$\mathcal{B}(\mathbb{R})$-measurable for any fixed $v \in V$ and $J_n(\omega, \cdot)$ is continuous on V for any fixed $\omega \in \Omega$. We define

the correspondences

$$\phi_n(\omega) := \{v \in V \mid J_n(\omega, v) = 0\},$$

for every $n \in \mathbb{N}$*. It follows from [6, Corollary 18.8] that this correspondence has a measurable graph, i.e.*

$$\{(\omega, v) \in \Omega \times V \mid v \in \phi_n(\omega)\} \in \mathcal{F} \otimes \mathcal{B}(V).$$

Further, by Assumption 6.2.1 and the Lax-Milgram Lemma (see for example [67, Lemma 6.97] and [16, Theorem 2.5]) we know that for every fixed $\omega \in \Omega$*, there exists a unique solution* $u(\omega, \cdot) \in V$ *satisfying* (6.4) *for every* $v \in V$*. Therefore, we obtain for the graph of the solution mapping:*

$$\begin{aligned}\{(\omega, u(\omega, \cdot)) \mid \omega \in \Omega\} &= \{(\omega, v) \in \Omega \times V \mid J_n(\omega, v) = 0, \text{ for all } n \in \mathbb{N}\} \\ &= \bigcap_{n \in \mathbb{N}} \{(\omega, v) \in \Omega \times V \mid v \in \phi_n(\omega)\} \in \mathcal{F} \otimes \mathcal{B}(V).\end{aligned}$$

This implies for an arbitrary measurable set $\tilde{V} \in \mathcal{B}(V)$

$$\{(\omega, u(\omega, \cdot)) \mid \omega \in \Omega\} \cap \Omega \times \tilde{V} \in \mathcal{F} \otimes \mathcal{B}(V)$$

and therefore

$$\{\omega \in \Omega \mid u(\omega, \cdot) \in \tilde{V}\} \in \mathcal{F},$$

by the projection theorem (see [6, Theorem 18.25]), which gives the measurability of the solution mapping. ◆

6.3 Subordinated Gaussian random fields

A random field $W : \Omega \times \mathcal{D} \to \mathbb{R}$ is called an $\mathbb{R}$-valued *Gaussian random field (GRF)* if for any tuple $(\underline{x}_1, \dots, \underline{x}_n) \subset \mathcal{D}$ and any number $n \in \mathbb{N}$ the $\mathbb{R}^n$-valued random variable

$$[W(\underline{x}_1), \dots, W(\underline{x}_n)]^T : \Omega \to \mathbb{R}^n$$

is multivariate normally distributed (see [3, Section 1.2]). Here $\underline{x}^T$ denotes the transpose of the vector $\underline{x}$. We denote by

$$m(\underline{x}) := \mathbb{E}(W(\underline{x})),\ \underline{x} \in \mathcal{D},\ \text{and}$$
$$q(\underline{x}, \underline{y}) := \mathrm{Cov}(W(\underline{x}), W(\underline{y})),\ \underline{x}, \underline{y} \in \mathcal{D},$$

the associated mean and covariance function. The *covariance operator* $Q : L^2(\mathcal{D}) \to L^2(\mathcal{D})$ of W is defined by

$$Q(\psi)(\underline{x}) = \int_{\mathcal{D}} q(\underline{x}, \underline{y})\psi(\underline{y})d\underline{y} \text{ for } \underline{x} \in \mathcal{D}.$$

Further, if $\mathcal{D} \subset \mathbb{R}^d$ is compact and W is centered, i.e. $m \equiv 0$, there exists a decreasing sequence $(\lambda_i,\ i \in \mathbb{N})$ of real eigenvalues of Q with corresponding eigenfunctions $(e_i,\ i \in \mathbb{N}) \subset L^2(\mathcal{D})$ which form an orthonormal basis of $L^2(\mathcal{D})$ (see [3, Section 3.2] and [115, Theorem VI.3.2 and Chapter II.3]).

Example 6.3.1. *One important class of continuous GRFs is given by the Matérn family: for a given smoothness parameter $\nu > 1/2$, correlation parameter $r > 0$ and variance $\sigma^2 > 0$, the Matérn-ν covariance function is given by $q_M(\underline{x}, \underline{y}) = \rho_M(|\underline{x} - \underline{y}|_2)$, for $(\underline{x}, \underline{y}) \in \mathbb{R}^d_+ \times \mathbb{R}^d_+$, with*

$$\rho_M(s) = \sigma^2 \frac{2^{1-\nu}}{\Gamma(\nu)} \Big(\frac{2s\sqrt{\nu}}{r}\Big)^{\nu} K_\nu\Big(\frac{2s\sqrt{\nu}}{r}\Big),\ \textit{for } s \geq 0,$$

where $\Gamma(\cdot)$ is the Gamma function and $K_\nu(\cdot)$ is the modified Bessel function of the second kind (see [63, Section 2.2 and Proposition 1]). Here, $|\underline{x}|_2 := (\sum_{i=1}^d \underline{x}_i^2)^{\frac{1}{2}}$ denotes the Euclidean norm of the vector $\underline{x} \in \mathbb{R}^d$. A Matérn-$\nu$ GRF is a centered GRF with covariance function q_M. ◆

6.3.1 Construction of subordinated GRFs

Let $D > 0$ be fixed and $\mathcal{I} = [0, D]$ or $\mathcal{I} = \mathbb{R}_+$ with $\mathbb{R}_+ := [0, +\infty)$. A real-valued stochastic process $l = (l(t),\ t \in \mathcal{I})$ is said to be a *Lévy process* on $\mathcal{I}$ if $l(0) = 0$ $\mathbb{P}$-a.s., l has independent and stationary increments and l is stochastically continuous (see [8, Section 1.3]). One of the most important properties of Lévy processes is the so called *Lévy-Khinchin formula* (see [8, Th. 1.3.3]).

Theorem 6.3.2 (Lévy-Khinchin formula)**.**
Let l be a real-valued Lévy process on the interval $\mathcal{I} \subseteq \mathbb{R}_+$. There exist constants, $\gamma_l \in \mathbb{R}$, $\sigma_l^2 \in \mathbb{R}_+$ and a measure ν on $(\mathbb{R}, \mathcal{B}(\mathbb{R}))$ such that the characteristic function $\phi_{l(t)}$, for $t \in \mathcal{I}$, admits the representation

$$\begin{aligned}\phi_{l(t)}(u) &:= \mathbb{E}(\exp(iul(t))) \\ &= \exp\left(t\left(i\gamma_l u - \frac{\sigma_l^2}{2}u^2 + \int_{\mathbb{R}\setminus\{0\}} e^{iuy} - 1 - iuy\mathbb{1}_{\{|y|\leq 1\}}\nu(dy)\right)\right).\end{aligned}$$

◆

Motivated by Theorem 6.3.2 we denote by $(\gamma_l, \sigma_l^2, \nu)$ the characteristic triplet of the Lévy process l. A (Lévy-)subordinator is a Lévy process which is *non-decreasing* $\mathbb{P}$-a.s.. By [8, Theorem 1.3.15] it follows that the Lévy triplet of a Lévy subordinator always admits the form $(\gamma_l, 0, \nu)$ with a measure ν on $(\mathbb{R}, \mathcal{B}(\mathbb{R}))$ satisfying

$$\nu(-\infty, 0) = 0 \text{ and } \int_0^\infty \min(y, 1)\,\nu(dy) < \infty.$$

Remark 6.3.3. *Let $B = (B(t),\, t \geq 0)$ be a standard Brownian motion and $l = (l(t),\, t \geq 0)$ be a Lévy subordinator. The stochastic process defined by*

$$L(t) := B(l(t)),\ t \geq 0,$$

is called subordinated Brownian motion and is again a Lévy process (see [8, Theorem 1.3.25]). ◆

In [95] the authors propose a new approach to extend standard subordinated Lévy processes on a higher dimensional parameter space. Motivated by the rich class of subordinated Brownian motions, the authors construct discontinuous random fields by subordinating a GRF on a d-dimensional parameter domain by d one-dimensional Lévy subordinators. In case of a two-dimensional parameter space the construction is as follows: For a GRF $W : \Omega \times \mathbb{R}_+^2 \to \mathbb{R}$ and two (Lévy-)subordinators $l_1,\ l_2$ on $[0, D]$, with a finite $D > 0$, we define the real-valued random field

$$L(x, y) := W(l_1(x), l_2(y)),\ \text{for } x, y \in [0, D].$$

Figure 6.1 shows samples of a GRF with Martérn-1.5 covariance function and the corresponding subordinated field where we used Poisson and Gamma processes as subordinators.

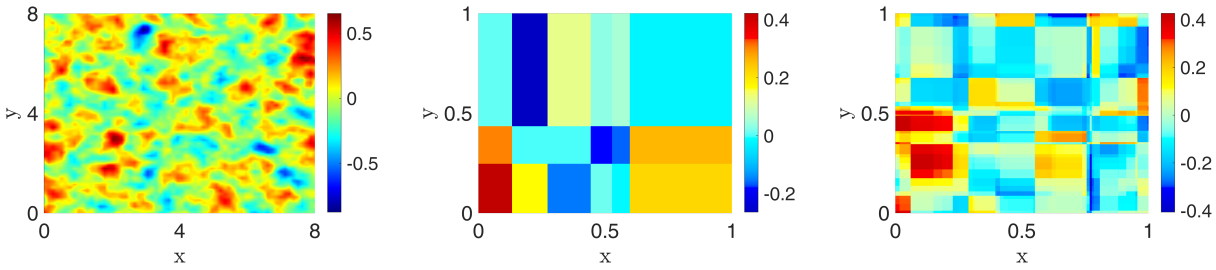

Figure 6.1: Sample of Matérn-1.5-GRF (left), Poisson-subordinated GRF (middle) and Gamma-subordinated GRF (right).

This construction yields a rich class of discontinuous random fields which also admit a Lévy-Khinchin-type formula. Further, the newly constructed random fields are also interesting for practical reasons, since formulas for the covariance functions can be derived which is very useful for applications, e.g. in statistical fitting. For a theoretical investigation of the constructed random fields we refer to [95].

6.3.2 Subordinated GRFs as diffusion coefficients in elliptic problems

In the following, we define the specific diffusion coefficient that we consider in problem (6.1) - (6.3). In order to allow discontinuities, we incorporate a subordinated GRF in the coefficient additionally to a Gaussian component. The construction of the coefficient is done so that Theorem 6.2.3 is applicable and, at the same time, the coefficient is as versatile as possible.

Definition 6.3.4.
We consider the domain $\mathcal{D} = (0, D)^2$ *with* $D < +\infty$[2]. *We define the jump-diffusion coefficient* a *in problem* (6.1) - (6.3) *with* $d = 2$ *as*

$$\begin{aligned} a &: \Omega \times \mathcal{D} \to (0, +\infty), \\ &(\omega, x, y) \mapsto \overline{a}(x, y) + \Phi_1(W_1(x, y)) + \Phi_2(W_2(l_1(x), l_2(y))), \end{aligned} \tag{6.5}$$

where

[2]For simplicity we choose a square domain, recangular ones may be considered in the same way

- $\overline{a} : \mathcal{D} \to (0, +\infty)$ *is deterministic, continuous and there exist constants* $\overline{a}_+, \overline{a}_- > 0$ *with* $\overline{a}_- \leq \overline{a}(x, y) \leq \overline{a}_+$ *for* $(x, y) \in \mathcal{D}$.
- $\Phi_1,\ \Phi_2 : \mathbb{R} \to [0, +\infty)$ *are continuous.*
- W_1 *and* W_2 *are zero-mean GRFs on* $\mathcal{D}$ *respectively on* $[0, +\infty)^2$ *with* $\mathbb{P}$*-a.s. continuous paths.*
- l_1 *and* l_2 *are Lévy subordinators on* $[0, D]$ *with Lévy triplets* $(\gamma_1, 0, \nu_1)$ *and* $(\gamma_2, 0, \nu_2)$ *which are independent of the GRFs* W_1 *and* W_2.

◆

Remark 6.3.5. *The first two assumptions ensure that the diffusion coefficient* a *is positive over the domain* $\mathcal{D}$. *To show the convergence of the approximated diffusion coefficient in Subsection 6.5.1 we have to impose independence of the GRFs* W_1 *and* W_2 *(see Assumption 6.5.2 and the proof of Theorem 6.5.5). This assumption is in the sense natural as also one-dimensional Lévy processes admit an additive decomposition into a continuous part and a pure-jump part which are stochastically independent (Lévy-Itô decomposition, see e.g. [8, Theorem 2.4.11]). For the same reason the assumption that the Lévy subordinators are independent of the GRFs is also natural (see for example [8, Section 1.3.2]).* ◆

In order to verify Assumption 6.2.1 *i* and *ii* we need the following lemma. For a proof we refer to [95, Lemma 3.2]).

Lemma 6.3.6.
For fixed $(x, y) \in \mathcal{D}$ *the mapping* $\omega \mapsto a(\omega, x, y)$ *is* $\mathcal{F} - \mathcal{B}(\mathbb{R}_+)$*-measurable. Further, for fixed* $\omega \in \Omega$, *the mapping* $(x, y) \mapsto a(\omega, x, y)$ *is* $\mathcal{B}(\mathcal{D}) - \mathcal{B}(\mathbb{R}_+)$*-measurable.* ◆

Definition 6.3.4 guarantees the existence of a pathwise weak solution to problem (6.1), as we prove in the following theorem.

Theorem 6.3.7.
Let a *be as in Definition 6.3.4 and let* $f \in L^q(\Omega; H),\ g \in L^q(\Omega; L^2(\Gamma_2))$ *for some* $q \in [1, +\infty)$. *Then there exists a unique pathwise weak solution* $u(\omega, \cdot) \in V$ *to problem* (6.1) *for* $\mathbb{P}$*-almost every* $\omega \in \Omega$. *Furthermore,* $u \in L^r(\Omega; V)$ *for all* $r \in [1, q)$ *and*

$$\|u\|_{L^r(\Omega;V)} \leq C(\overline{a}_-, \mathcal{D})(\|f\|_{L^q(\Omega;H)} + \|g\|_{L^q(\Omega;L^2(\Gamma_2))}),$$

where $C(\overline{a}_-, \mathcal{D}) > 0$ is a constant depending only on the indicated parameter and the volume of $\mathcal{D}$. ◆

Proof. In order to apply Theorem 6.2.3 we have to verify Assumption 6.2.1. We have $a_-(\omega) = \inf_{x\in\mathcal{D}} a(\omega, x) \geq \overline{a}_-$ for every fixed $\omega \in \Omega$ by Definition 6.3.4. Further, $W_2(\omega)$ is continuous on $K(\omega) := [0, l_1(\omega, D)] \times [0, l_2(\omega, D)]$ and therefore

$$\begin{aligned} a_+(\omega) &= \sup_{(x,y)\in\mathcal{D}} a(\omega, x, y) \\ &\leq \overline{a}_+ + \sup_{(x,y)\in\mathcal{D}} \Phi_1(W_1(\omega, x, y)) + \sup_{(x,y)\in K(\omega)} \Phi_2(W_2(\omega, x, y)) < +\infty. \end{aligned}$$

For $1 \leq r < q$ define $p := (\frac{1}{r} - \frac{1}{q})^{-1} > 0$. We observe that

$$0 \leq \frac{1}{a_-(\omega)} \leq \frac{1}{\overline{a}_-} < \infty,$$

$\mathbb{P}$-a.s. and hence $1/a_- \in L^p(\Omega; \mathbb{R})$. Therefore, Assumption 6.2.1 holds with $r = (1/p+1/q)^{-1}$ and the assertion follows by Theorem 6.2.3. □

6.4 Approximation of the diffusion coefficient

To simulate the solution to the elliptic equation we need to define a tractable approximation of the diffusion coefficient. Here, we face a new challenge regarding the GRF W_2 which is subordinated by the Lévy processes l_1 and l_2: Due to the fact that the Lévy subordinators in general can attain any value in $[0, +\infty)$ we have to consider (and approximate) the GRF W_2 on the *unbounded* domain $[0, +\infty)^2$. In most cases where elliptic PDEs of the form (6.1) have been considered with a random coefficient, the problem is stated on a bounded domain, see e.g. [16], [30], [29], [63], [65]. Many regularity results for GRFs formulated for a bounded parameter space cannot easily be transferred to an unbounded parameter space (see also [3, Chapter 1], especially the discussion on p. 13). Even the Karhunen-Loève expansion of a GRF requires compactness of the domain (see e.g. [3, Section 3.2]). We avoid an unbounded parameter domain by bounding the subordinators from above in Subsection 6.4.1. Furthermore, to show convergence of the solution in Section 6.5 we need to bound the diffusion coefficient from above by a deterministic upper bound A (see Theorem 6.5.11 and Remark 6.5.9). Note that the weaker assumption of L^p integrability of the pathwise upper bound a_+ instead of a deterministic upper bound A of the diffusion coefficient is not enough in this setting. The

reason being that the absence of a deterministic upper bound A would lead to an additional ω-dependence in the regularity constants in Assumption 6.5.7 which would be difficult to handle in the convergence theorem in Subsection 6.5.2 (see also Remark 6.5.9). Therefore, we cut off the diffusion coefficient at a deterministic level A (see Subsection 6.4.2). Subsequently we show that this induces an error in the solution approximation which can be controlled and which vanishes for growing A (see Subsection 6.5.1 and Theorem 6.5.1). Summarized, we derive an approximation in three steps: First, we bound the subordinators, and, second, we cut off the diffusion coefficient. Finally, we consider approximations of the GRFs and the subordinators and prove the convergence of this approximation of the diffusion coefficient under suitable assumptions.

6.4.1 First approximation: bounding the Lévy subordinators

For a fixed $K \in (0, +\infty)$, we define the cut-function $\chi_K : [0, +\infty) \to [0, K]$ as $\chi_K(z) := \min(z, K)$ for $z \in [0, +\infty)$. Instead of problem (6.1) we consider the following modified problem

$$-\nabla \cdot (a_K(\omega, \underline{x})\nabla u_K(\omega, \underline{x})) = f(\omega, \underline{x}) \text{ in } \Omega \times \mathcal{D}, \tag{6.6}$$

and impose the boundary conditions

$$u_K(\omega, \underline{x}) = 0 \text{ on } \Omega \times \Gamma_1, \tag{6.7}$$

$$a_K(\omega, \underline{x})\overrightarrow{n} \cdot \nabla u_K(\omega, \underline{x}) = g(\omega, \underline{x}) \text{ on } \Omega \times \Gamma_2. \tag{6.8}$$

Here, the diffusion coefficient is defined by

$$\begin{aligned} &a_K : \Omega \times \mathcal{D} \to (0, +\infty), \\ &(\omega, x, y) \mapsto \overline{a}(x, y) + \Phi_1(W_1(x, y)) + \Phi_2(W_2(\chi_K(l_1(x)), \chi_K(l_2(y)))). \end{aligned} \tag{6.9}$$

For functions $f \in L^q(\Omega; H)$ and $g \in L^q(\Omega; L^2(\Gamma_2))$ with $q \in [1, +\infty)$, there exists a weak solution $u_K \in L^r(\Omega; V)$ to problem (6.6) - (6.8) for $r \in [1, q)$ (see Theorem 6.3.7)[3].

Remark 6.4.1. *We note that the influence of this problem modification can be controlled: one*

[3]For simplicity we assume one fixed K for all spatial dimensions. The results in the subsequent sections hold for individual independent values in each spatial dimension as well.

may choose $K > 0$ *such that*

$$\mathbb{P}(\max(\sup_{x\in[0,D]} l_1(x), \sup_{y\in[0,D]} l_2(y)) \geq K) = \mathbb{P}(\max(l_1(D), l_2(D)) \geq K) < \varepsilon$$

for any $\varepsilon > 0$. *In other words, pathwise the modified problem coincides with the original one up to a set of samples, whose probability can be made arbitrarily small.* ◆

6.4.2 Second modification: diffusion cut-off

We consider again the cut function $\chi_A(z) := \min(z, A)$ for $z \in [0, +\infty)$ with a fixed positive number $A > 0$ and consider the following problem

$$-\nabla \cdot (a_{K,A}(\omega, \underline{x})\nabla u_{K,A}(\omega, \underline{x})) = f(\omega, \underline{x}) \text{ in } \Omega \times \mathcal{D}, \tag{6.10}$$

where we impose the boundary conditions

$$u_{K,A}(\omega, \underline{x}) = 0 \text{ on } \Omega \times \Gamma_1, \tag{6.11}$$

$$a_{K,A}(\omega, \underline{x})\overrightarrow{n} \cdot \nabla u_{K,A}(\omega, \underline{x}) = g(\omega, \underline{x}) \text{ on } \Omega \times \Gamma_. \tag{6.12}$$

The diffusion coefficient $a_{K,A}$ is defined by

$$\begin{aligned} &a_{K,A} : \Omega \times \mathcal{D} \to (0, +\infty), \\ &(\omega, x, y) \mapsto \chi_A\Big(\overline{a}(x, y) + \Phi_1(W_1(x, y)) + \Phi_2(W_2(\chi_K(l_1(x)), \chi_K(l_2(y))))\Big). \end{aligned} \tag{6.13}$$

Again, Theorem 6.3.7 applies in this case and yields the existence of a pathwise weak solution $u_{K,A} \in L^r(\Omega; V)$ for $r \in [1, q)$ if $f \in L^q(\Omega; H)$ and $g \in L^q(\Omega; L^2(\Gamma_2))$. The error of the modification vanishes for growing A as shown in the end of Section 6.5.1.

6.4.3 Approximation of GRF and subordinators

In the following, we show how to approximate the modified diffusion coefficient $a_{K,A}$ using approximations $W_1^{(\varepsilon W)} \approx W_1$, $W_2^{(\varepsilon W)} \approx W_2$ of the GRFs and $l_1^{(\varepsilon l)} \approx l_1$, $l_2^{(\varepsilon l)} \approx l_2$ of the Lévy subordinators. We aim to approximate the GRFs W_1 and W_2 in the diffusion coefficient by sampling on a discrete grid. These approximations may be extended to the whole domain using linear interpolation (see [64] and [65]). Certain regularity assumptions on the GRFs

then allow for a quantification of the corresponding approximation error (see Lemma 6.4.4). In [15], the authors considered approximations of general Lévy processes and quantified the approximation error in an $L^s(\Omega)$-sense uniformly in $x \in [0, D]$. Such an approximation may be obtained by piecewise constant approximations constructed from samples of the process $(l_j(x_i),\ i = 1, \dots, N_l)$ on a discrete grid $(x_i,\ i = 1, \dots, N_l) \subset [0, D]$ with $N_l \in \mathbb{N}$ grid points, for $j = 1, 2$ (see Section 6.7, [15] and [109]). Motivated by this, we formulate the following working assumptions on the covariance operators of the Gaussian fields, the subordinators and the data of the elliptic problem.

Assumption 6.4.2.
Let W_1 be a zero-mean GRF on $[0, D]^2$ and W_2 be a zero-mean GRF on $[0, K]^2$. We denote by $q_1 : [0, D]^2 \times [0, D]^2 \to \mathbb{R}$ and $q_2 : [0, K]^2 \times [0, K]^2 \to \mathbb{R}$ the covariance functions of these random fields and by Q_1, Q_2 the associated covariance operators defined by

$$Q_j\phi = \int_{[0,z_j]^2} q_j((x, y), (x', y'))\phi(x', y')d(x', y'),$$

for $\phi \in L^2([0, z_j]^2)$ with $z = (D, K)$ and $j = 1, 2$. We denote by $(\lambda_i^{(1)}, e_i^{(1)},\ i \in \mathbb{N})$ resp. $(\lambda_i^{(2)}, e_i^{(2)},\ i \in \mathbb{N})$ the eigenpairs associated to the covariance operators Q_1 and Q_2. In particular, $(e_i^{(1)},\ i \in \mathbb{N})$ resp. $(e_i^{(2)},\ i \in \mathbb{N})$ are ONBs of $L^2([0, D]^2)$ resp. $L^2([0, K]^2)$.

i We assume that the eigenfunctions are continuously differentiable and there exist positive constants $\alpha,\ \beta,\ C_e,\ C_\lambda > 0$ such that for any $i \in \mathbb{N}$ it holds

$$\begin{aligned} \|e_i^{(1)}\|_{L^\infty([0,D]^2)},\ \|e_i^{(2)}\|_{L^\infty([0,K]^2)} &\leq C_e, \\ \|\nabla e_i^{(1)}\|_{L^\infty([0,D]^2)},\ \|\nabla e_i^{(2)}\|_{L^\infty([0,K]^2)} &\leq C_e i^\alpha, \\ \sum_{i=1}^{\infty} (\lambda_i^{(1)} + \lambda_i^{(2)}) i^\beta &\leq C_\lambda < +\infty. \end{aligned}$$

ii There exist constants $\phi,\ \psi, C_{lip} > 0$ such that the continuous functions $\Phi_1,\ \Phi_2 : \mathbb{R} \to [0, +\infty)$ from Definition 6.3.4 satisfy

$$|\Phi_1'(x)| \leq \phi\, \exp(\psi|x|),\ |\Phi_2(x) - \Phi_2(y)| \leq C_{lip}\,|x - y| \text{ for } x, y \in \mathbb{R}.$$

In particular, $\Phi_1 \in C^1(\mathbb{R})$.

iii $f \in L^q(\Omega; H)$ and $g \in L^q(\Omega; L^2(\Gamma_2))$ for some $q \in (1, +\infty)$.

iv $\overline{a} : \mathcal{D} \to (0, +\infty)$ *is deterministic, continuous and there exist constants* $\overline{a}_+, \overline{a}_- > 0$ *with* $\overline{a}_- \leq \overline{a}(x, y) \leq \overline{a}_+$ *for* $(x, y) \in \mathcal{D}$.

v l_1 *and* l_2 *are Lévy subordinators on* $[0, D]$ *with Lévy triplets* $(\gamma_1, 0, \nu_1)$ *and* $(\gamma_2, 0, \nu_2)$ *which are independent of the GRFs* W_1 *and* W_2. *Further, we assume that we have approximations* $l_1^{(\varepsilon_l)}$, $l_2^{(\varepsilon_l)}$ *of these processes and there exist constants* $C_l > 0$ *and* $\eta > 1$ *such that for every* $s \in [1, \eta)$ *it holds*

$$\mathbb{E}(|l_j(x) - l_j^{(\varepsilon_l)}(x)|^s) \leq C_l \varepsilon_l,$$

for $\varepsilon_l > 0$, $x \in [0, D]$ *and* $j = 1, 2$.

◆

Remark 6.4.3. *Note that the first assumption on the eigenpairs of the GRFs is natural (see [16] and [63]). For example, the case that* Q_1, Q_2 *are Matérn covariance operators are included. Assumption 6.4.2 ii is necessary to be able to quantify the error of the approximation of the diffusion coefficient. Assumption 6.4.2 iii is necessary to ensure the existence of a solution and has already been formulated in Assumption 6.2.1. The last assumption ensures that we can approximate the Lévy subordinators in an* L^s*-sense. This can always be achieved under appropriate assumptions on the tails of the distribution of the subordinators, see [15, Assumption 3.6, Assumption 3.7 and Theorem 3.21].* ◆

For any numerical simulation we have to approximate the GRF as well as the subordinating Lévy processes, which results in an additional approximation of the coefficient $a_{K,A}$ given in Equation (6.13). In the following we want to quantify the error induced by this approximation.

It follows by an application of the Kolmogorov-Chentsov theorem ([35, Theorem 3.5]) that W_1 and W_2 can be assumed to have Hölder-continuous paths with Hölder exponent $b \in (0, (2\gamma k - 2)/(2k))$ for $0 < \gamma \leq \min(1, \beta/(2\alpha))$ and every $k \in \mathbb{N}$ (see the proof of [16, Lemma 3.5]). Further, it follows by an application of the Sobolev embedding theorem that $W_1 \in L^n(\Omega; C^{0,\gamma}([0, D]^2))$ and $W_2 \in L^n(\Omega; C^{0,\gamma}([0, K]^2))$, i.e.

$$\mathbb{E}\left(\Big(\sup_{z \neq z' \in [0,D]^2} \frac{|W_1(z) - W_1(z')|}{|z - z'|_2^\gamma}\Big)^n\right), \ \mathbb{E}\left(\Big(\sup_{z \neq z' \in [0,K]^2} \frac{|W_2(z) - W_2(z')|}{|z - z'|_2^\gamma}\Big)^n\right) < +\infty, \tag{6.14}$$

for every $n \in [1, +\infty)$ and $\gamma < \min(1, \beta/(2\,\alpha))$ (see [29, Proposition 3.1]).

Next, we prove a bound on the error of the approximated diffusion coefficient, where the

GRFs are approximated by a discrete evaluation and (bi-)linear interpolation between these points (see [64] and [65]).

Lemma 6.4.4.
We consider the discrete grids $G_1^{(\varepsilon_W)} = \{(x_i, x_j)|\ i,j = 0,\dots,M_{\varepsilon_W}^{(1)}\}$ *on* $[0,D]^2$ *and* $G_2^{(\varepsilon_W)} = \{(y_i, y_j)|\ i,j = 0,\dots,M_{\varepsilon_W}^{(2)}\}$ *on* $[0,K]^2$ *where* $(x_i,\ i = 0,\dots,M_{\varepsilon_W}^{(1)})$ *is an equidistant grid on* $[0,D]$ *with maximum step size* ε_W *and* $(y_i,\ i = 0,\dots,M_{\varepsilon_W}^{(2)})$ *is an equidistant grid on* $[0,K]$ *with maximum step size* ε_W*. Further, let* $W_1^{(\varepsilon_W)}$ *and* $W_2^{(\varepsilon_W)}$ *be approximations of the GRFs* $W_1,\ W_2$ *on the discrete grids* $G_1^{(\varepsilon_W)}$ *resp.* $G_2^{(\varepsilon_W)}$ *which are constructed by point evaluation of the random fields* W_1 *and* W_2 *on the grids and linear interpolation between the grid points. Under Assumption 6.4.2 i it holds for* $n \in [1,+\infty)$*:*

$$\|W_1 - W_1^{(\varepsilon_W)}\|_{L^n(\Omega;L^\infty([0,D]^2))} \leq C(D,n)\varepsilon_W^\gamma$$
$$\|W_2 - W_2^{(\varepsilon_W)}\|_{L^n(\Omega;L^\infty([0,K]^2))} \leq C(K,n)\varepsilon_W^\gamma$$

for $\gamma < \min(1, \beta/(2\alpha))$ *where* β *and* α *are the parameters from Assumption 6.4.2.* ◆

Proof. Note that for any fixed $\omega \in \Omega$ and $\mathcal{D}_{ij} := [x_i, x_{i+1}] \times [y_j, y_{j+1}]$ with $i,j \in \{1,\dots,M_{\varepsilon_W}^{(1)}\}$, it holds

$$\max_{(x,y)\in\mathcal{D}_{ij}} W_1^{(\varepsilon_W)}(x,y), \min_{(x,y)\in\mathcal{D}_{ij}} W_1^{(\varepsilon_W)}(x,y) \in \{W_1(x_i,y_j), W_1(x_{i+1},y_j), W_1(x_i,y_{j+1}), W_1(x_{i+1},y_{j+1})\}.$$

This holds since $W_1^{(\varepsilon_W)}$ is constructed by (bi-)linear interpolation of the GRF W_1 and the piecewise linear interpolants attain their maximum and minimum at the corners (the Hessian evaluated at the (unique) stationary point of the bilinear basis functions is always indefinite). Therefore, for a fixed $(x,y) \in [x_i, x_{i+1}] \times [y_j, y_{j+1}]$ it follows from the intermediate value theorem that $W_1^{(\varepsilon_W)}(x,y) = W_1(x',y')$ for appropriate $(x',y') \in [x_i, x_{i+1}] \times [y_j, y_{j+1}]$. Using this observation we estimate

$$
\begin{aligned}
&\|W_1 - W_1^{(\varepsilon_W)}\|^n_{L^n(\Omega;L^\infty([0,D]^2))} \\
&= \mathbb{E}\Big(\sup_{(x,y)\in[0,D]^2} |W_1(x,y) - W_1^{(\varepsilon_W)}(x,y)|^n \Big) \\
&\leq \mathbb{E}\Big(\sup_{\substack{(x,y),(x',y')\in[0,D]^2,\\ |(x,y)^T-(x',y')^T|_2\leq\sqrt{2}\varepsilon_W}} |W_1(x,y) - W_1(x',y')|^n \Big) \\
&= \varepsilon_W^{n\gamma}\, \mathbb{E}\Big(\sup_{\substack{(x,y),(x',y')\in[0,D]^2,\\ |(x,y)^T-(x',y')^T|_2\leq\sqrt{2}\varepsilon_W}} \frac{|W_1(x,y) - W_1(x',y')|^n}{\varepsilon_W^{n\gamma}} \Big) \\
&\leq 2^{\frac{n\gamma}{2}} \varepsilon_W^{n\gamma}\, \mathbb{E}\Big(\Big(\sup_{\substack{(x,y)\neq(x',y')\in[0,D]^2,\\ |(x,y)^T-(x',y')^T|_2\leq\sqrt{2}\varepsilon_W}} \frac{|W_1(x,y) - W_1(x',y')|}{|(x,y)^T - (x',y')^T|_2^\gamma} \Big)^n \Big) \\
&\leq 2^{\frac{n\gamma}{2}} \varepsilon_W^{n\gamma}\, \mathbb{E}\Big(\Big(\sup_{(x,y)\neq(x',y')\in[0,D]^2} \frac{|W_1(x,y) - W_1(x',y')|}{|(x,y)^T - (x',y')^T|_2^\gamma} \Big)^n \Big) \\
&\leq C(D)\varepsilon_W^{n\gamma},
\end{aligned}
$$

where we used Equation (6.14) in the last step. Equivalently the error bound for W_2 follows. □

Remark 6.4.5. *Note that Lemma 6.4.4 immediately implies for* $m \in [1, +\infty)$

$$
\begin{aligned}
\|W_1 - W_1^{(\varepsilon_W)}\|_{L^n(\Omega;L^m([0,D]^2))} &= \mathbb{E}\Big(\Big(\int_{[0,D]^2} |W_1(x,y) - W_1^{(\varepsilon_W)}(x,y)|^m d(x,y) \Big)^{\frac{n}{m}} \Big)^{\frac{1}{n}} \\
&\leq D^{\frac{2}{m}} \mathbb{E}\Big(\sup_{(x,y)\in[0,D]^2} |W_1(x,y) - W_1^{(\varepsilon_W)}(x,y)|^n \Big)^{\frac{1}{n}} \\
&= D^{\frac{2}{m}} \|W_1 - W_1^{(\varepsilon_W)}\|_{L^n(\Omega;L^\infty([0,D]^2))} \leq C(D,m,n)\varepsilon_W^\gamma.
\end{aligned}
$$

◆

6.4.4 Convergence to the modified diffusion coefficient

Given some approximations $W_1^{(\varepsilon_W)} \approx W_1,\ W_2^{(\varepsilon_W)} \approx W_2$ as in Lemma 6.4.4 and approximations $l_1^{(\varepsilon_l)} \approx l_1,\ l_2^{(\varepsilon_l)} \approx l_2$ as in Assumption 6.4.2 ν as well as some fixed constants $K, A > 0$,

we approximate the diffusion coefficient $a_{K,A}$ in (6.13) by $a_{K,A}^{(\varepsilon_W,\varepsilon_l)} : \Omega \times \mathcal{D} \to (0, +\infty)$ with

$$a_{K,A}^{(\varepsilon_W,\varepsilon_l)}(x,y) = \chi_A\Big(\overline{a}(x,y) + \Phi_1(W_1^{(\varepsilon_W)}(x,y)) + \Phi_2(W_2^{(\varepsilon_W)}(\chi_K(l_1^{(\varepsilon_l)}(x)), \chi_K(l_2^{(\varepsilon_l)}(y))))\Big) \quad (6.15)$$

for $(x,y) \in \mathcal{D}$. To prove a convergence result for this approximated coefficient (Theorem 6.4.8) we need the following two technical lemmas. The second can be proved by the use of [108, Proposition 1.16]. For a detailed proof we refer to [95].

Lemma 6.4.6.
For $n, m \in [1, +\infty)$ with $n \geq m$ and $\varphi \in L^n([0,D]^2 \times \Omega; \mathbb{R}, \lambda \otimes \mathbb{P})$, where λ denotes the Lebesgue measure on $(\mathbb{R}^2, \mathcal{B}(\mathbb{R}^2))$, it holds

$$\|\varphi\|_{L^n(\Omega;L^m([0,D]^2))} \leq C(D,n,m)\|\varphi\|_{L^n([0,D]^2\times\Omega;\mathbb{R})}.$$

◆

Proof. The case $n = m$ is trivial. For $n > m$ we use Hölder's inequality and obtain

$$\begin{aligned}
\|\varphi\|_{L^n(\Omega;L^m([0,D]^2))} &= \Big(\int_\Omega \Big(\int_{[0,D]^2} |\varphi(x,y)|^m d(x,y)\Big)^{\frac{n}{m}} d\mathbb{P}\Big)^{\frac{1}{n}} \\
&\leq \Big(\int_\Omega \Big(\int_{[0,D]^2} |\varphi(x)|^n d(x,y)\Big) D^{\frac{2(n-m)}{m}} d\mathbb{P}\Big)^{\frac{1}{n}} \\
&= D^{\frac{2}{m}-\frac{2}{n}} \|\varphi\|_{L^n([0,D]^2\times\Omega;\mathbb{R})}.
\end{aligned}$$

□

Lemma 6.4.7.
Let $W : \Omega \times \mathbb{R}^d_+ \to \mathbb{R}$ be a $\mathbb{P}$-a.s. continuous random field and let $Z : \Omega \to \mathbb{R}^d_+$ be a $\mathbb{R}^d_+$-valued random variable which is independent of the random field W. Further, let $\varphi : \mathbb{R} \to \mathbb{R}$ be a deterministic, continuous function. It holds

$$\mathbb{E}(\varphi(W(Z)) = \mathbb{E}(\zeta(Z)),$$

where $\zeta(z) := \mathbb{E}(\varphi(W(z))$ for deterministic $z \in \mathbb{R}^d_+$. ◆

Theorem 6.4.8.
Let $W_1^{(\varepsilon_W)} \approx W_1,\ W_2^{(\varepsilon_W)} \approx W_2$ be approximations of the GRFs on discrete grids as in Lemma 6.4.4. Further, let $1 \leq t \leq s < \eta$ and $0 < \gamma < \min(1, \beta/(2\alpha))$ such that $s\gamma \geq 2$. Under Assumption 6.4.2 we get the following error bound for the approximation of the diffusion coefficient:

$$\|a_{K,A} - a_{K,A}^{(\varepsilon_W,\, \varepsilon_l)}\|_{L^s(\Omega;L^t([0,D]^2))} \leq C(\varepsilon_W^\gamma + \varepsilon_l^{\frac{1}{s}}),$$

with a constant C which does not depend on the discretization parameters ε_W and ε_l. ◆

Proof. Since the cut function χ_A is Lipschitz continuous with Lipschitz constant 1 we calculate

$$\begin{aligned}
&\|a_{K,A} - a_{K,A}^{(\varepsilon_W,\, \varepsilon_l)}\|_{L^s(\Omega;L^t([0,D]^2))} \\
&\qquad \leq \|\Phi_1(W_1) - \Phi_1(W_1^{(\varepsilon_W)})\|_{L^s(\Omega;L^t([0,D]^2))} \\
&\qquad + \|\Phi_2(W_2(\chi_K(l_1), \chi_K(l_2))) - \Phi_2(W_2^{(\varepsilon_W)}(\chi_K(l_1^{(\varepsilon_l)}), \chi_K(l_2^{(\varepsilon_l)})))\|_{L^s(\Omega;L^t([0,D]^2))} \\
&\qquad =: I_1 + I_2
\end{aligned}$$

First, we consider I_1 and use Assumption 6.4.2 *ii* and the same calculation as in Remark 6.4.5 to get

$$I_1 \leq D^{\frac{2}{t}} \|\Phi_1(W_1) - \Phi_1(W_1^{(\varepsilon_W)})\|_{L^s(\Omega;L^\infty([0,D]^2))}.$$

The mean value theorem yields, for fixed $(x, y) \in [0, D]^2$ and an appropriately chosen value $\xi \in (\min(W_1(x,y), W_1^{(\varepsilon_W)}(x,y)), \max(W_1(x,y), W_1^{(\varepsilon_W)}(x,y)))$,

$$\begin{aligned}
|\Phi_1(W_1(x,y)) - \Phi_1(W_1^{(\varepsilon_W)}(x,y))| &\\
&= |\Phi_1'(\xi)|\, |W_1(x,y) - W_1^{(\varepsilon_W)}(x,y)| \\
&\leq \phi\, \exp(\psi|\xi|) |W_1(x,y) - W_1^{(\varepsilon_W)}(x,y)| \\
&\leq \phi\, \max\{\exp(\psi|W_1(x,y)|), \exp(\psi|W_1^{(\varepsilon_W)}(x,y)|)\} \\
&\qquad\qquad \times |W_1(x,y) - W_1^{(\varepsilon_W)}(x,y)|,
\end{aligned}$$

for $\mathbb{P}$-almost every $\omega \in \Omega$. As already mentioned in the proof of Lemma 6.4.4, for any $\omega \in \Omega$ and fixed $\mathcal{D}_{ij} := [x_i, x_{i+1}] \times [y_j, y_{j+1}]$ with $i, j \in \{1, \dots, M_{\varepsilon_W}^{(1)}\}$, it holds

$$\max_{(x,y)\in\mathcal{D}_{ij}} W_1^{(\varepsilon_W)}(x,y), \min_{(x,y)\in\mathcal{D}_{ij}} W_1^{(\varepsilon_W)}(x,y) \\ \in \{W_1(x_i,y_j), W_1(x_{i+1},y_j), W_1(x_i,y_{j+1}), W_1(x_{i+1},y_{j+1})\}.$$

Therefore, we obtain the pathwise estimate

$$\begin{aligned}
&\|\Phi_1(W_1) - \Phi_1(W_1^{(\varepsilon_W)})\|_{L^\infty([0,D]^2)} \\
&\le \max_{(x,y)\in[0,D]^2} \phi \, \max\{\exp(\psi|W_1(x,y)|), \exp(\psi|W_1^{(\varepsilon_W)}(x,y)|)\} \\
&\qquad\qquad \times \max_{(x,y)\in[0,D]^2} |W_1(x,y) - W_1^{(\varepsilon_W)}(x,y)| \\
&\le \phi \exp\big(\psi \, \max\{\max_{(x,y)\in[0,D]^2}|W_1(x,y)|, \max_{(x,y)\in[0,D]^2}|W_1^{(\varepsilon_W)}(x,y)|\}\big) \\
&\qquad\qquad \times \max_{(x,y)\in[0,D]^2}|W_1(x,y) - W_1^{(\varepsilon_W)}(x,y)| \\
&= \phi \, \exp\Big(\psi \max_{(x,y)\in[0,D]^2} |W_1(x,y)|\Big) \max_{(x,y)\in[0,D]^2} |W_1(x,y) - W_1^{(\varepsilon_W)}(x,y)|.
\end{aligned}$$

Finally, we obtain for any $n_1, n_2 \in [1, +\infty)$ with $1/n_1 + 1/n_2 = 1$ by Hölder's inequality

$$\begin{aligned}
I_1 &\le D^{\frac{2}{t}} \|\Phi_1(W_1) - \Phi_1(W_1^{(\varepsilon_W)})\|_{L^s(\Omega;L^\infty([0,D]^2))} \\
&\le D^{\frac{2}{t}} \phi \, \| \exp(\psi|W_1|)\|_{L^{sn_1}(\Omega;L^\infty([0,D]^2))} \, \|W_1 - W_1^{(\varepsilon_W)}\|_{L^{sn_2}(\Omega;L^\infty([0,D]^2))} \\
&\le C(D)\varepsilon_W^\gamma,
\end{aligned}$$

where we used Lemma 6.4.4 and the fact that $\| \exp(\psi|W_1|)\|_{L^{sn_1}(\Omega;L^\infty([0,D]^2))} < \infty$ (see [3, Theorem 2.1.1] and the proof of Theorem 6.5.5 for more details).

For the second summand we calculate:

$$\begin{aligned}
I_2 &\le \|\Phi_2(W_2(\chi_K(l_1), \chi_K(l_2))) - \Phi_2(W_2(\chi_K(l_1^{(\varepsilon_l)}), \chi_K(l_2^{(\varepsilon_l)})))\|_{L^s(\Omega;L^t([0,D]^2))} \\
&\quad + \|\Phi_2(W_2(\chi_K(l_1^{(\varepsilon_l)}), \chi_K(l_2^{(\varepsilon_l)}))) - \Phi_2(W_2^{(\varepsilon_W)}(\chi_K(l_1^{(\varepsilon_l)}), \chi_K(l_2^{(\varepsilon_l)})))\|_{L^s(\Omega;L^t([0,D]^2))} \\
&= I_3 + I_4.
\end{aligned}$$

We use the same calculation as in Remark 6.4.5 and the Lipschitz continuity of Φ_2 to calculate for the summand I_4

$$\begin{aligned}
I_4 &\leq D^{\frac{2}{t}} \|\Phi_2(W_2(\chi_K(l_1^{(\varepsilon_l)}), \chi_K(l_2^{(\varepsilon_l)}))) - \Phi_2(W_2^{(\varepsilon_W)}(\chi_K(l_1^{(\varepsilon_l)}), \chi_K(l_2^{(\varepsilon_l)})))\|_{L^s(\Omega;L^\infty([0,D]^2))} \\
&\leq C_{lip} D^{\frac{2}{t}} \|W_2(\chi_K(l_1^{(\varepsilon_l)}), \chi_K(l_2^{(\varepsilon_l)})) - W_2^{(\varepsilon_W)}(\chi_K(l_1^{(\varepsilon_l)}), \chi_K(l_2^{(\varepsilon_l)}))\|_{L^s(\Omega;L^\infty([0,D]^2))} \\
&\leq C_{lip} D^{\frac{2}{t}} \|W_2 - W_2^{(\varepsilon_W)}\|_{L^s(\Omega;L^\infty([0,K]^2))} \\
&\leq C_{lip} D^{\frac{2}{t}} C(K,s) \varepsilon_W^\gamma,
\end{aligned}$$

where we used Lemma 6.4.4. It remains to bound the summand I_3. We estimate using Lemma 6.4.6

$$\begin{aligned}
I_3 &= \|\Phi_2(W_2(\chi_K(l_1), \chi_K(l_2))) - \Phi_2(W_2(\chi_K(l_1^{(\varepsilon_l)}), \chi_K(l_2^{(\varepsilon_l)})))\|_{L^s(\Omega;L^t([0,D]^2))} \\
&\leq D^{\frac{2}{t}-\frac{2}{s}} \|\Phi_2(W_2(\chi_K(l_1), \chi_K(l_2))) - \Phi_2(W_2(\chi_K(l_1^{(\varepsilon_l)}), \chi_K(l_2^{(\varepsilon_l)})))\|_{L^s([0,D]^2\times\Omega)} \\
&= D^{\frac{2}{t}-\frac{2}{s}} \Big(\int_{[0,D]^2} \mathbb{E}\Big(|\Phi_2\big(W_2(\chi_K(l_1(x)), \chi_K(l_2(y)))\big) \\
&\qquad\qquad - \Phi_2(W_2(\chi_K(l_1^{(\varepsilon_l)}(x)), \chi_K(l_2^{(\varepsilon_l)}(y))))|^s \Big) d(x,y) \Big)^{\frac{1}{s}} \\
&\leq C_{lip} D^{\frac{2}{t}-\frac{2}{s}} \Big(\int_{[0,D]^2} \mathbb{E}(|W_2(\chi_K(l_1(x)), \chi_K(l_2(y))) \\
&\qquad\qquad - W_2(\chi_K(l_1^{(\varepsilon_l)}(x)), \chi_K(l_2^{(\varepsilon_l)}(y)))|^s) d(x,y) \Big)^{\frac{1}{s}}.
\end{aligned}$$

We know by Lemma 6.4.7 that it holds for $(x,y) \in [0,D]^2$

$$\begin{aligned}
&\mathbb{E}(|W_2(\chi_K(l_1(x)), \chi_K(l_2(y))) - W_2(\chi_K(l_1^{(\varepsilon_l)}(x)), \chi_K(l_2^{(\varepsilon_l)}(y)))|^s) \\
&\qquad = \mathbb{E}(\varphi(\chi_K(l_1(x)), \chi_K(l_2(y)), \chi_K(l_1^{(\varepsilon_l)}(x)), \chi_K(l_2^{(\varepsilon_l)}(y))))
\end{aligned}$$

where

$$\varphi(x,y,v,w) := \mathbb{E}(|W_2(x,y) - W_2(v,w)|^s).$$

For $(x,y) = (v,w)$ it holds $\varphi(x,y,v,w) = 0$ and for $(x,y) \neq (v,w) \in [0,K]^2$ we get

$$\begin{aligned}\varphi(x,y,v,w) &= |(x,y)^T - (v,w)^T|_2^{\gamma s}\, \mathbb{E}\Big(\frac{|W_2(x,y) - W_2(v,w)|^s}{|(x,y)^T - (v,w)^T|_2^{\gamma s}}\Big) \\ &\leq |(x,y)^T - (v,w)^T|_2^{\gamma s} \mathbb{E}\left(\Big(\sup_{z\neq z' \in [0,K]^2} \frac{|W_2(z) - W_2(z')|}{|z-z'|_2^{\gamma}}\Big)^s\right) \\ &\leq C(K)|(x,y)^T - (v,w)^T|_2^{\gamma s}\end{aligned}$$

by Equation (6.14). Further, we know from Hölder's inequality for $\gamma s \geq 2$ that it holds

$$\begin{aligned}|(x,y)^T - (v,w)^T|_2^{\gamma s} &= ((x-v)^2 + (y-w)^2)^{\frac{\gamma s}{2}} \\ &\leq 2^{\frac{\gamma s}{2}-1}(|x-v|^{\gamma s} + |y-w|^{\gamma s})\end{aligned}$$

and therefore we calculate

$$\begin{aligned}&\mathbb{E}(|W_2(\chi_K(l_1(x)), \chi_K(l_2(y))) - W_2(\chi_K(l_1^{(\varepsilon_l)}(x)), \chi_K(l_2^{(\varepsilon_l)}(y)))|^s) \\ &\leq 2^{\frac{\gamma s}{2}-1} C(K) \mathbb{E}(|\chi_K(l_1(x)) - \chi_K(l_1^{(\varepsilon_l)}(x))|^{\gamma s} + |\chi_K(l_2(y)) - \chi_K(l_2^{(\varepsilon_l)}(y))|^{\gamma s}) \\ &\leq 2^{\frac{\gamma s}{2}-1} C(K) \mathbb{E}(|l_1(x) - l_1^{(\varepsilon_l)}(x)|^{\gamma s} + |l_2(y) - l_2^{(\varepsilon_l)}(y)|^{\gamma s}) \\ &\leq 2^{\frac{\gamma s}{2}} C(K) C_l \varepsilon_l\end{aligned}$$

where we used the Lipschitz continuity of χ_K and Assumption 6.4.2 *v* in the last step. Therefore, we finally obtain

$$I_3 \leq C_{lip} D^{\frac{2}{t}} 2^{\frac{\gamma}{2}} C(K)^{\frac{1}{s}} C_l^{\frac{1}{s}} \varepsilon_l^{\frac{1}{s}} =: C(C_{lip}, D, t, \gamma, s, K, C_l)\varepsilon_l^{\frac{1}{s}}$$

which proves that

$$\|a_{K,A} - a_{K,A}^{(\varepsilon_W,\, \varepsilon_l)}\|_{L^s(\Omega; L^t([0,D]^2))} \leq C(D, K, C_{lip}, t, \gamma, s, C_l)(\varepsilon_W^{\gamma} + \varepsilon_l^{\frac{1}{s}}).$$

□

6.5 Convergence analysis

In this section we derive an error bound for the approximation of the solution. We split the error in two components: the first component is associated with the cut-off of the diffusion coefficient we described in Subsection 6.4.2. The second error contributor corresponds to the

approximation of the GRFs and the Lévy subordinators we considered in Subsection 6.4.4.

Let $r \in [1, q)$ with q as in Assumption 6.4.2 *iii* and denote by $u_K \in L^r(\Omega; V)$ the weak solution to problem (6.6) - (6.9). Further, let $u_{K,A}^{(\varepsilon_W,\varepsilon_l)} \in L^r(\Omega; V)$ be the weak solution to the problem

$$-\nabla \cdot (a_{K,A}^{(\varepsilon_W,\varepsilon_l)}(\omega, \underline{x}) \nabla u_{K,A}^{(\varepsilon_W,\varepsilon_l)}(\omega, \underline{x})) = f(\omega, \underline{x}) \text{ in } \Omega \times \mathcal{D}, \tag{6.16}$$

with boundary conditions

$$u_{K,A}^{(\varepsilon_W,\varepsilon_l)}(\omega, \underline{x}) = 0 \text{ on } \Omega \times \Gamma_1, \tag{6.17}$$

$$a_{K,A}^{(\varepsilon_W,\varepsilon_l)}(\omega, \underline{x}) \overrightarrow{n} \cdot \nabla u_{K,A}^{(\varepsilon_W,\varepsilon_l)}(\omega, x) = g(\omega, x) \text{ on } \Omega \times \Gamma_2. \tag{6.18}$$

Note that Theorem 6.3.7 also applies to the elliptic problem with coefficient $a_{K,A}^{(\varepsilon_W,\varepsilon_l)}$. The aim of this section is to quantify the error of the approximation $u_{K,A}^{(\varepsilon_W,\varepsilon_l)} \approx u_K$[4]. By the triangle inequality we obtain

$$\|u_K - u_{K,A}^{(\varepsilon_W,\varepsilon_l)}\| \leq \|u_K - u_{K,A}\| + \|u_{K,A} - u_{K,A}^{(\varepsilon_W,\varepsilon_l)}\| =: E_1 + E_2 \tag{6.19}$$

for any suitable norm $\|\cdot\|$. Here, $u_{K,A}$ is the solution to the truncated problem (6.10) - (6.13). We consider the two error contributions E_1 and E_2 separately in this section. The results presented in Subsections 6.5.1 and 6.5.2 prove the following theorem:

Theorem 6.5.1.
Under Assumptions 6.5.2 and 6.5.7 it holds

$$\|u_K - u_{K,A}^{(\varepsilon_W,\varepsilon_l)}\|_{L^r(\Omega;V)} \to 0 \text{ for } A \to +\infty,\ \varepsilon_W, \varepsilon_l \to 0,$$

for admissible values of $r \geq 2$ (see Remark 6.5.6 and Theorem 6.5.11). As a consequence, we obtain

$$\mathbb{P}(\|u_K - u_{K,A}^{(\varepsilon_W,\varepsilon_l)}\|_V > \delta) \to 0 \text{ for } A \to +\infty,\ \varepsilon_W, \varepsilon_l \to 0,$$

for any $\delta > 0$. Furthermore, it holds

$$\mathbb{P}(\{\omega \in \Omega \mid u_K(\omega) \neq u_{K,A} \text{ in } V\} = \mathbb{P}(\{\omega \in \Omega \mid \operatorname*{ess\,sup}_{(x,y)\in\mathcal{D}} a_K(\omega, x, y)\} > A\}) \to 0,$$

[4]The error of the approximation $u_K \approx u$ may be controlled as in Remark 6.4.1 but cannot be quantified for the solution.

for $A \to +\infty$. Therefore, the solution $u_{K,A}$ to the modified problem (6.10) - (6.12) *coincides with the solution u_K to problem* (6.6) - (6.8) *up to a set of samples, whose probability can be made arbitrarily small for growing A. With Remark 6.4.1 we conclude that the solution $u_{K,A}$ coincides with the solution u to problem* (6.1) - (6.3) *with diffusion coefficient a defined in Equation* (6.5) *up to a set of samples, whose probability can be made arbitrarily small for growing thresholds K and A.* ◆

6.5.1 Bound on E_1

Assumption 6.5.2.
We assume that the GRFs W_1 and W_2 occurring in the diffusion coefficient (6.5) *are stochastically independent.* ◆

The aim of this subsection is to show that the first error contributor E_1 in Equation (6.19) vanishes for increasing cut-off threshold A. The strategy consists of two separated steps: in the first step we show the stability of the solution, which means that the value E_1 can be controlled by the quality of the approximation of the diffusion coefficient $a_{K,A} \approx a_K$. In the second step, we show that the quality of the approximation of the diffusion coefficient can be controlled by the cut-off threshold A. The first step is given by Theorem 6.5.4. In order to prove it we need the following lemma.

Lemma 6.5.3.
For fixed cut-off levels A and K we consider the solution $u_K \in L^r(\Omega; V)$ and its approximation $u_{K,A} \in L^r(\Omega; V)$ for $r \in [1, q)$. It holds the pathwise estimate

$$\|u_K - u_{K,A}\|_V \leq a_{K,+} C(\overline{a}_-, \mathcal{D}) \|\nabla u_K - \nabla u_{K,A}\|_{L^2(\mathcal{D})},$$

for $\mathbb{P}$-almost every $\omega \in \Omega$. Here, the constant $C(\overline{a}_-, \mathcal{D})$ only depends on the indicated parameters and we define $a_{K,+}(\omega) := \max\{1, \operatorname{ess\,sup}_{(x,y)\in\mathcal{D}} a_K(\omega, x, y)\} < \infty$ for $\omega \in \Omega$. ◆

Proof. For a fixed $\omega \in \Omega$ we consider the variational problem: find a unique $\hat{w} \in V$ such that

$$B_{a_K}(\hat{w}, v) = \langle u_K - u_{K,A}, v \rangle_{L^2(\mathcal{D})},$$

for all $v \in V$. By the Lax-Milgram theorem there exists a unique solution $\hat{w} \in V$ with

$$\|\hat{w}\|_V \leq C'(\overline{a}_-, \mathcal{D})\|u_K - u_{K,A}\|_{L^2(\mathcal{D})},$$

(see Theorem 6.3.7 and [16, Theorem 2.5]). Therefore, we obtain by Hölder's inequality

$$\begin{aligned}
\|u_K - u_{K,A}\|^2_{L^2(\mathcal{D})} &= B_{a_K}(\hat{w}, u_K - u_{K,A}) \\
&= \langle a_K \nabla \hat{w}, \nabla u_K - \nabla u_{K,A} \rangle_{L^2(\mathcal{D})} \\
&\leq a_{K,+}\|\nabla \hat{w}\|_{L^2(\mathcal{D})}\|\nabla u_K - \nabla u_{K,A}\|_{L^2(D)} \\
&\leq \|u_K - u_{K,A}\|_{L^2(\mathcal{D})} a_{K,+} C'(\overline{a}_-, \mathcal{D})\|\nabla u_K - \nabla u_{K,A}\|_{L^2(\mathcal{D})} \\
&\leq \frac{1}{2}\|u_K - u_{K,A}\|^2_{L^2(\mathcal{D})} + a^2_{K,+} C'(\overline{a}_-, \mathcal{D})^2/2 \|\nabla u_K - \nabla u_{K,A}\|^2_{L^2(\mathcal{D})},
\end{aligned}$$

where we used Young's inequality in the last step. Finally, we obtain

$$\begin{aligned}
\|u_K - u_{K,A}\|^2_V &= \|u_K - u_{K,A}\|^2_{L^2(\mathcal{D})} + \|\nabla u_K - \nabla u_{K,A}\|^2_{L^2(\mathcal{D})} \\
&\leq (1 + a^2_{K,+} C'(\overline{a}_-, \mathcal{D})^2)\|\nabla u_K - \nabla u_{K,A}\|^2_{L^2(\mathcal{D})}.
\end{aligned}$$

□

Theorem 6.5.4.
Let $f \in L^q(\Omega; H)$ and $g \in L^q(\Omega; L^2(\Gamma_2))$ for some $q \in [1, +\infty)$. Further, for a given number $t \in (1, +\infty)$ we define the dual number $n := \frac{t}{t-1}$. Then, for any for $r \in [1, q/n)$, it holds

$$\begin{aligned}
\|u_K - u_{K,A}\|_{L^r(\Omega;V)} \leq C(\mathcal{D}, \overline{a}_-, r) \, &(\|f\|_{L^q(\Omega;H)} + \|g\|_{L^q(\Omega;\Gamma_2))}) \\
&\times \mathbb{E}(\operatorname*{ess\,sup}_{\underline{x} \in \mathcal{D}} |a_K(\underline{x}) - a_{K,A}(\underline{x})|^{rt})^{\frac{1}{rt}}
\end{aligned}$$

◆

Proof. By a direct calculation we obtain

$$\|\nabla u_K - \nabla u_{K,A}\|^2_{L^2(\mathcal{D})} \leq \frac{1}{\overline{a}_-} \int_{\mathcal{D}} a_{K,A} |\nabla u_K - \nabla u_{K,A}|^2_2 d(x, y).$$

Since u_K and $u_{K,A}$ are weak solutions of problem (6.6) - (6.9) resp. (6.10) - (6.13) it holds

$$\int_{\mathcal{D}} a_{K,A}\nabla u_{K,A}\cdot\nabla u_K d(x,y) = \int_{\mathcal{D}} a_K|\nabla u_K|_2^2 d(x,y),$$
$$\int_{\mathcal{D}} a_{K,A}|\nabla u_{K,A}|_2^2 d(x,y) = \int_{\mathcal{D}} a_K\nabla u_K\cdot\nabla u_{K,A} d(x,y),$$

$\mathbb{P}$-almost surely and therefore

$$\int_{\mathcal{D}} a_{K,A}|\nabla u_K - \nabla u_{K,A}|_2^2 d(x,y) = \int_{\mathcal{D}} (a_{K,A}-a_K)\nabla u_K(\nabla u_K - \nabla u_{K,A}) d(x,y).$$

We estimate using Hölder's inequality

$$\begin{aligned}\|\nabla u_K - \nabla u_{K,A}\|_{L^2(\mathcal{D})}^2 &\le \frac{1}{\overline{a}_-}\|a_K - a_{K,A}\|_{L^\infty(\mathcal{D})}\|\nabla u_K\|_{L^2(\mathcal{D})}\|\nabla u_K - \nabla u_{K,A}\|_{L^2(\mathcal{D})}\\ &\le \frac{1}{\overline{a}_-}\|a_K - a_{K,A}\|_{L^\infty(\mathcal{D})}\|u_K\|_V\|\nabla u_K - \nabla u_{K,A}\|_{L^2(\mathcal{D})}\end{aligned}$$

and therefore we obtain

$$\|\nabla u_K - \nabla u_{K,A}\|_{L^2(\mathcal{D})} \le \frac{1}{\overline{a}_-}\|a_K - a_{K,A}\|_{L^\infty(\mathcal{D})}\|u_K\|_V.$$

Using Lemma 6.5.3 we obtain the pathwise estimate

$$\|u_K - u_{K,A}\|_V \le C(\overline{a}_-,\mathcal{D})a_{K,+}\|a_K - a_{K,A}\|_{L^\infty(\mathcal{D})}\|u_K\|_V.$$

Using again Hölder's inequality we have

$$\|u_K - u_{K,A}\|_{L^r(\Omega;V)} \le C(\overline{a}_-,\mathcal{D})\mathbb{E}(\operatorname*{ess\,sup}_{\underline{x}\in\mathcal{D}}|a_K(\underline{x}) - a_{K,A}(\underline{x})|^{rt})^{\frac{1}{rt}}\mathbb{E}(a_{K,+}^{nr}\|u_K\|_V^{nr})^{\frac{1}{nr}}.$$

By assumption it holds $nr < q$. Therefore, we can choose a real number $\rho > 1$ such that $nr\rho < q$. We define the dual number $\rho' := \frac{\rho}{\rho-1} \in (1,+\infty)$ and use Hölder's inequality to calculate

$$\begin{aligned}\|u_K - u_{K,A}\|_{L^r(\Omega;V)} \le& C(\overline{a}_-,\mathcal{D})\mathbb{E}(\operatorname*{ess\,sup}_{\underline{x}\in\mathcal{D}}|a_K(\underline{x}) - a_{K,A}(\underline{x})|^{rt})^{\frac{1}{rt}}\\ &\times \mathbb{E}(a_{K,+}^{nr\rho'})^{\frac{1}{nr\rho'}}\|u_K\|_{L^{nr\rho}(\Omega;V)}.\end{aligned}$$

Obviously Theorem 6.3.7 applies also to problem (6.6) - (6.9). Therefore, since $nr\rho < q$ by

assumption we conclude

$$\begin{aligned}\|u_K - u_{K,A}\|_{L^r(\Omega;V)} \leq & C(\mathcal{D}, \overline{a}_-, r)\mathbb{E}(\operatorname*{ess\,sup}_{\underline{x}\in\mathcal{D}} |a_K(\underline{x}) - a_{K,A}(\underline{x})|^{rt})^{\frac{1}{rt}} \\ & \times (\|f\|_{L^q(\Omega;H)} + \|g\|_{L^q(\Omega;\Gamma_2))}),\end{aligned}$$

where we additionally used the fact that $\mathbb{E}(a_{K,+}^{nr\rho'})^{\frac{1}{nr\rho'}} < +\infty$ (see Theorem 6.5.5). □

In other words, finding a bound for the error contribution E_1 in Equation (6.19) reduces to quantifying the quality of the approximation of the diffusion coefficient $a_{K,A} \approx a_K$. For readability the proof of the following theorem can be found in the appendix at the end of this article.

Theorem 6.5.5.
For any $n \in (1, +\infty)$ it holds

$$\mathbb{E}(\operatorname*{ess\,sup}_{\underline{x}\in\mathcal{D}} a_K(\underline{x})^n)^{\frac{1}{n}} < +\infty.$$

Further, for any $\delta > 0$ there exists a constant $A = A(\delta, n) > 0$ such that

$$\mathbb{E}(\operatorname*{ess\,sup}_{\underline{x}\in\mathcal{D}} |a_K(\underline{x}) - a_{K,A}(\underline{x})|^n)^{1/n} < \delta.$$

◆

We close this subsection with the following remark on the convergence of the error contributor E_1 in Equation (6.19).

Remark 6.5.6. *From Theorem 6.5.4 together with Theorem 6.5.5 we obtain*

$$\|u_K - u_{K,A}\|_{L^r(\Omega;V)} \to 0, \text{ for } A \to \infty,$$

for every $r < q$. ◆

6.5.2 Bound on E_2

The aim is to bound the second term of Equation (6.19) given by

$$E_2 = \|u_{K,A} - u_{K,A}^{(\varepsilon_W,\varepsilon_l)}\|$$

in an appropriate norm. For technical reasons we have to impose an additional assumption on the solution of the truncated problem. The subsequent remarks discuss situations under which this assumption is fulfilled.

Assumption 6.5.7.
We assume that there exist constants $j_{reg} > 0$ and $k_{reg} \geq 2$ such that

$$C_{reg} := \mathbb{E}(\|\nabla u_{K,A}\|^{k_{reg}}_{L^{2+j_{reg}}(\mathcal{D})}) < +\infty. \tag{6.20}$$

◆

Since $u_{K,A} \in H^1(\mathcal{D})$ we already know that $\nabla u_{K,A} \in L^2(\mathcal{D})$. Assumption 6.5.7 requires a slightly higher integrability over the spatial domain. Since this is an assumption on the regularity of the solution $u_{K,A}$ we denote the above constant by C_{reg}.

Remark 6.5.8. *Note that Assumption 6.5.7 is fulfilled if there exists $\theta \in (0,1)$ such that*

$$\|u_{K,A}\|_{H^{1+\theta}(\mathcal{D})} \leq C(f,a) \tag{6.21}$$

with some constant $C(f,a)$ with $\mathbb{E}(C(f,a)^{k_{reg}}) < \infty$. This is true since for any $\rho \geq 2$ and an arbitrary function $\varphi \in H^{1+\theta}(\mathcal{D})$ the inequality

$$\|\nabla\varphi\|_{L^\rho(\mathcal{D})} \leq C\|\nabla\varphi\|_{H^{1-\frac{2}{\rho}}(\mathcal{D})} \leq C\|\varphi\|_{H^{2-\frac{2}{\rho}}(\mathcal{D})}$$

holds for $\theta := 1 - \frac{2}{\rho}$ (see [39, Theorem 6.7]). Here, the constant $C = C(\mathcal{D},\theta)$ depends only on the indicated parameters. Hence, the condition (6.21) *implies Equation* (6.20) *with $j_{reg} = \frac{2\theta}{1-\theta}$.* ◆

Remark 6.5.9. *Note that there are several results about higher integrability of the gradient of the solution to an elliptic PDE of the form* (6.10) - (6.13)*. For instance [105] yields that the solution $u_{K,A}$ has $H^{1+\delta/(2\pi)}$ regularity with $\delta = \min(1, \overline{a}_-, A^{-1})$ under mixed boundary conditions and under the assumption that $a_{K,A}$ is piecewise constant (see [105, Theorem 7.3]). This corresponds to*

the case where no Gaussian noise is considered (i.e. $\Phi_1 \equiv 0$) and $\overline{a}$ is constant. Another important result is given in [43]. It follows by [43, Theorem 1] that under the assumption that there exists $q > 2$ with $f \in L^q(\mathcal{D})$ $\mathbb{P}$-a.s. there exists a constant $C = C(\mathcal{D}, \|f\|_{L^q(\mathcal{D})}, \overline{a}_-, A)$ and a positive number $\vartheta = \vartheta(\mathcal{D}, \|f\|_{L^q(\mathcal{D})}, \overline{a}_-, A) > 0$ only depending on the indicated parameters, such that:

$$\|\nabla u_{K,A}\|_{L^{2+\vartheta}(\mathcal{D})} \leq C. \tag{6.22}$$

In particular, if the right hand side f of the problem is deterministic, then ϑ and the constant C in (6.22) *are deterministic and one immediately obtains*

$$\mathbb{E}(\|\nabla u_{K,A}\|^{k_{reg}}_{L^{2+\vartheta}(\mathcal{D})}) < +\infty,$$

for any $k_{reg} \geq 1$ and a deterministic, positive constant $\vartheta > 0$. ◆

Next, we show that for a given approximation of the diffusion coefficient, the resulting error contributor E_2 is bounded by the approximation error of the diffusion coefficient. Similar to the corresponding assertion we gave in Subsection 6.5.1 we need the following lemma for the proof of this error bound. For a proof we refer to Lemma 6.5.3.

Lemma 6.5.10.
For fixed cut-off levels A, K and fixed approximation parameters $\varepsilon_W, \varepsilon_l$ we consider the PDE solutions $u_{A,K} \in L^r(\Omega; V)$ and $u_{K,A}^{(\varepsilon_W,\varepsilon_l)} \in L^r(\Omega; V)$ for $r \in [1, q)$. It holds the pathwise estimate

$$\|u_{K,A} - u_{K,A}^{(\varepsilon_W,\varepsilon_l)}\|_V \leq a_{K,+} C(\overline{a}_-, \mathcal{D}) \|\nabla u_{K,A} - \nabla u_{K,A}^{(\varepsilon_W,\varepsilon_l)}\|_{L^2(\mathcal{D})},$$

for $\mathbb{P}$-almost every $\omega \in \Omega$. Here, constant $C(\overline{a}_-, \mathcal{D})$ depends only on the indicated parameters and $a_{K,+}(\omega) := \max\{1, \operatorname{ess\,sup}_{(x,y)\in\mathcal{D}} a_K(\omega, x, y)\} < \infty$ for $\omega \in \Omega$. ◆

Theorem 6.5.11.
Let $r \geq 2$ and $b, c \in [1, +\infty]$ be given such that it holds

$$rc\gamma \geq 2 \text{ and } 2b \leq rc < \eta$$

with a fixed real number $\gamma \in (0, \min(1, \beta/(2\alpha))$. Here, the parameters η, α and β are determined by the GRFs W_1, W_2 and the Lévy subordinators l_1, l_2 (see Assumption 6.4.2).

Let $m, n \in [1, +\infty]$ be real numbers such that

$$\frac{1}{m} + \frac{1}{c} = \frac{1}{n} + \frac{1}{b} = 1,$$

and let $k_{reg} \geq 2$ and $j_{reg} > 0$ be the regularity specifiers given by Assumption 6.5.7. If it holds that

$$n < 1 + \frac{j_{reg}}{2} \text{ and } rm < k_{reg},$$

then the approximated solution $u_{K,A}^{(\varepsilon_W,\varepsilon_l)}$ converges to the solution $u_{K,A}$ of the truncated problem for $\varepsilon_W, \varepsilon_l \to 0$ and it holds

$$\begin{aligned}\|u_{K,A} - u_{K,A}^{(\varepsilon_W,\varepsilon_l)}\|_{L^r(\Omega;V)} &\leq C(\overline{a}_-, \mathcal{D}, r) C_{reg} \|a_{K,A}^{(\varepsilon_W,\varepsilon_l)} - a_{K,A}\|_{L^{rc}(\Omega;L^{2b}(\mathcal{D}))} \\ &\leq C_{reg} C(\overline{a}_-, \mathcal{D}, r)(\varepsilon_W^{\gamma} + \varepsilon_l^{\frac{1}{rc}}).\end{aligned}$$

◆

Proof. By a direct calculation we obtain the pathwise estimate

$$\|\nabla u_{K,A} - \nabla u_{K,A}^{(\varepsilon_W,\varepsilon_l)}\|_{L^2(\mathcal{D})}^2 \leq \frac{1}{\overline{a}_-} \int_{\mathcal{D}} a_{K,A}^{(\varepsilon_W,\varepsilon_l)} (|\nabla u_{K,A} - \nabla u_{K,A}^{(\varepsilon_W,\varepsilon_l)}|_2^2) d\underline{x}.$$

Since $u_{K,A}$ (resp. $u_{K,A}^{(\varepsilon_W,\varepsilon_l)}$) is the weak solution to problem (6.10) - (6.13) (resp. (6.16) - (6.18)) we have

$$\begin{aligned}\int_D a_{K,A}^{(\varepsilon_W,\varepsilon_l)} \nabla u_{K,A}^{(\varepsilon_W,\varepsilon_l)} \cdot \nabla u_{K,A} d\underline{x} &= \int_{\mathcal{D}} a_{K,A} |\nabla u_{K,A}|_2^2 d\underline{x}, \\ \int_{\mathcal{D}} a_{K,A}^{(\varepsilon_W,\varepsilon_l)} |\nabla u_{K,A}^{(\varepsilon_W,\varepsilon_l)}|_2^2 d\underline{x} &= \int_{\mathcal{D}} a_{K,A} \nabla u_{K,A} \cdot \nabla u_{K,A}^{(\varepsilon_W,\varepsilon_l)} d\underline{x}\end{aligned}$$

$\mathbb{P}$-a.s. and therefore

$$\begin{aligned}&\int_D a_{K,A}^{(\varepsilon_W,\varepsilon_l)} |\nabla u_{K,A} - \nabla u_{K,A}^{(\varepsilon_W,\varepsilon_l)}|_2^2 d\underline{x} \\ &= \int_{\mathcal{D}} (a_{K,A}^{(\varepsilon_W,\varepsilon_l)} - a_{K,A}) \nabla u_{K,A} \cdot (\nabla u_{K,A} - \nabla u_{K,A}^{(\varepsilon_W,\varepsilon_l)}) d\underline{x}.\end{aligned}$$

Using Hölder's inequality we calculate

$$\begin{aligned}&\|\nabla u_{K,A} - \nabla u_{K,A}^{(\varepsilon_W,\varepsilon_l)}\|_{L^2(\mathcal{D})}^2\\ &\leq \frac{1}{\overline{a}_-}\|(a_{K,A}^{(\varepsilon_W,\varepsilon_l)} - a_{K,A})\nabla u_{K,A}\|_{L^2(\mathcal{D})}\|\nabla u_{K,A} - \nabla u_{K,A}^{(\varepsilon_W,\varepsilon_l)}\|_{L^2(\mathcal{D})}\end{aligned}$$

and therefore

$$\|\nabla u_{K,A} - \nabla u_{K,A}^{(\varepsilon_W,\varepsilon_l)}\|_{L^2(\mathcal{D})} \leq \frac{1}{\overline{a}_-}\|(a_{K,A}^{(\varepsilon_W,\varepsilon_l)} - a_{K,A})\nabla u_{K,A}\|_{L^2(\mathcal{D})},$$

Next, we apply Lemma 6.5.10 to obtain the following estimate.

$$\|u_{K,A} - u_{K,A}^{(\varepsilon_W,\varepsilon_l)}\|_V \leq C(\overline{a}_-,\mathcal{D})a_{K,+}\|(a_{K,A}^{(\varepsilon_W,\varepsilon_l)} - a_{K,A})\nabla u_{K,A}\|_{L^2(\mathcal{D})}$$

Hence, it remains to bound the norm $\|(a_{K,A}^{(\varepsilon_W,\varepsilon_l)} - a_{K,A})\nabla u_{K,A}\|_{L^2(\mathcal{D})}$. By Hölder's inequality we obtain

$$\begin{aligned}&\|(a_{K,A}^{(\varepsilon_W,\varepsilon_l)} - a_{K,A})\nabla u_{K,A}\|_{L^2(\mathcal{D})}\\ &\leq \|a_{K,A}^{(\varepsilon_W,\varepsilon_l)} - a_{K,A}\|_{L^{2b}(\mathcal{D})}\|\nabla u_{K,A}\|_{L^{2n}(\mathcal{D})}.\end{aligned}$$

Applying Hölder's inequality once more we estimate

$$\begin{aligned}&\|u_{K,A} - u_{K,A}^{(\varepsilon_W,\varepsilon_l)}\|_{L^r(\Omega;V)}\\ &\leq C(\overline{a}_-,\mathcal{D})\|a_{K,A}^{(\varepsilon_W,\varepsilon_l)} - a_{K,A}\|_{L^{rc}(\Omega;L^{2b}(\mathcal{D}))}\mathbb{E}(a_{K,+}^{rm}\|\nabla u_{K,A}\|_{L^{2n}(\mathcal{D})}^{rm})^{\frac{1}{rm}}\end{aligned}$$

By assumption it holds $rm < k_{reg}$. Hence, we can choose a real number $\rho > 1$ such that $rm\rho < k_{reg}$. We define the dual number $\rho' := \frac{\rho}{1-\rho} \in (1, +\infty)$ and use Hölder's inequality to obtain

$$\mathbb{E}(a_{K,+}^{rm}\|\nabla u_{K,A}\|_{L^{2n}(\mathcal{D})}^{rm})^{\frac{1}{rm}} \leq \mathbb{E}(a_{K,+}^{rm\rho'})^{\frac{1}{rm\rho'}}\|\nabla u_{K,A}\|_{L^{rm\rho}(\Omega;L^{2n}(\mathcal{D}))} \leq C(\mathcal{D},r)C_{reg},$$

where we again used the fact that $\mathbb{E}(a_{K,+}^{nr\rho'})^{\frac{1}{nr\rho'}} < +\infty$ (see Theorem 6.5.5) together with Assumption 6.5.7. Finally we obtain the estimate

$$\begin{aligned}\|u_{K,A} - u_{K,A}^{(\varepsilon_W,\varepsilon_l)}\|_{L^r(\Omega;V)} &\leq C(\overline{a}_-,\mathcal{D},r)C_{reg}\|a_{K,A}^{(\varepsilon_W,\varepsilon_l)} - a_{K,A}\|_{L^{rc}(\Omega;L^{2b}(\mathcal{D}))}\\ &\leq C_{reg}C(\overline{a}_-,\mathcal{D},r)(\varepsilon_W^{\gamma} + \varepsilon_l^{\frac{1}{rc}}),\end{aligned}$$

where we applied Theorem 6.4.8 in the last estimate. □

We close this section with a remark on how to choose the parameters A, ε_W and ε_l to obtain an approximation error smaller than any given threshold $\delta > 0$.

Remark 6.5.12. *For any given parameter K large enough (see Remark 6.4.1), we choose a positive number $A > 0$ such that the first error contributor satisfies $E_1 = \|u_K - u_{K,A}\|_{L^r(\Omega;V)} < \delta/2$ (see Theorem 6.5.4 and Theorem 6.5.5). Afterwards, under the assumptions of Theorem 6.5.11, we may choose the approximation parameters ε_W and ε_l small enough, such that the second error contributor satisfies $E_2 = \|u_{K,A} - u_{K,A}^{(\varepsilon_W,\varepsilon_l)}\|_{L^r(\Omega;V)} < \delta/2$. Hence, we get an overall error smaller than δ (see Equation* (6.19)*).* ◆

6.6 Pathwise sample-adapted finite element approximation

We want to approximate the solution u to the problem (6.1) - (6.3) with diffusion coefficient a given by Equation (6.5) using a pathwise finite element (FE) approximation of the solution $u_{K,A}^{(\varepsilon_W,\varepsilon_l)}$ of problem (6.16) - (6.18) where the approximated diffusion coefficient $a_{K,A}^{(\varepsilon_W,\varepsilon_l)}$ is given by (6.15). Therefore, for almost all $\omega \in \Omega$, we have to find a function $u_{K,A}^{(\varepsilon_W,\varepsilon_l)}(\omega,\cdot) \in V$ such that it holds

$$\begin{aligned} B_{a_{K,A}^{(\varepsilon_W,\varepsilon_l)}(\omega)}(u_{K,A}^{(\varepsilon_W,\varepsilon_l)}(\omega,\cdot), v) &:= \int_{\mathcal{D}} a_{K,A}^{(\varepsilon_W,\varepsilon_l)}(\omega,\underline{x})\nabla u_{K,A}^{(\varepsilon_W,\varepsilon_l)}(\omega,\underline{x}) \cdot \nabla v(\underline{x}) d\underline{x} \\ &= \int_{\mathcal{D}} f(\omega,\underline{x}) v(\underline{x}) d\underline{x} + \int_{\Gamma_2} g(\omega,\underline{x})[Tv](\underline{x}) d\underline{x} =: F_\omega(v), \end{aligned} \tag{6.23}$$

for every $v \in V$. Here, $K, A, \varepsilon_W, \varepsilon_l$ are fixed approximation parameters. In order to solve this variational problem numerically we consider a standard Galerkin approach with linear elements and assume $\mathcal{V} = (V_\ell,\ \ell \in \mathbb{N}_0)$ to be a sequence of finite-dimensional subspaces $V_\ell \subset V$ with $\dim(V_\ell) = d_\ell$ for $\ell \in \mathbb{N}_0$. We denote by $(h_\ell,\ \ell \in \mathbb{N}_0)$ the corresponding sequence of refinement sizes which is assumed to decrease monotonically to zero for $\ell \to \infty$. Let $\ell \in \mathbb{N}_0$ be fixed and denote by $\{v_1^{(\ell)}, \dots, v_{d_\ell}^{(\ell)}\}$ a basis of V_ℓ. The (pathwise) discrete version of (6.23) reads:

Find $u_{K,A,\ell}^{(\varepsilon_W,\varepsilon_l)}(\omega,\cdot) \in V_\ell$ such that

$$B_{a_{K,A}^{(\varepsilon_W,\varepsilon_l)}(\omega)}(u_{K,A,\ell}^{(\varepsilon_W,\varepsilon_l)}(\omega,\cdot), v_i^{(\ell)}) = F_\omega(v_i^{(\ell)}) \text{ for all } i = 1, \dots, d_\ell.$$

We expand the function $u_{K,A,\ell}^{(\varepsilon_W,\varepsilon_l)}(\omega,\cdot)$ with respect to the basis $\{v_1^{(\ell)},\dots,v_{d_\ell}^{(\ell)}\}$:

$$u_{K,A,\ell}^{(\varepsilon_W,\varepsilon_l)}(\omega,\cdot)=\sum_{i=1}^{d_\ell} c_i v_i^{(\ell)},$$

where the coefficient vector $\mathbf{c}=(c_1,\dots,c_{d_\ell})^T\in\mathbb{R}^{d_\ell}$ is determined by the linear equation system

$$\mathbf{B}(\omega)\mathbf{c}=\mathbf{F}(\omega),$$

with a stochastic stiffness matrix $\mathbf{B}(\omega)_{i,j}=B_{a_{K,A}^{(\varepsilon_W,\varepsilon_l)}(\omega)}(v_i^{(\ell)},v_j^{(\ell)})$ and load vector $\mathbf{F}(\omega)_i=F_\omega(v_i^{(\ell)})$ for $i,j=1,\dots,d_\ell$.

Remark 6.6.1. *Let $(\mathcal{K}_\ell,\ \ell\in\mathbb{N}_0)$ be a sequence of triangulations on $\mathcal{D}$ and denote by $\theta_\ell>0$ the minimum interior angle of all triangles in $\mathcal{K}_\ell$. We assume $\theta_\ell\geq\theta>0$ for a positive constant θ and define the maximum diameter of the triangulation $\mathcal{K}_\ell$ by $h_\ell:=\max_{K\in\mathcal{K}_\ell}\operatorname{diam}(K)$, for $\ell\in\mathbb{N}_0$. Further, we define the finite dimensional subspaces by $V_\ell:=\{v\in V\mid v|_K\in\mathcal{P}_1,K\in\mathcal{K}_\ell\}$, where $\mathcal{P}_1$ denotes the space of all polynomials up to degree one. The convergence of the FE method is determined by the regularity of the solution: If we assume that for $\mathbb{P}$-almost all $\omega\in\Omega$ it holds $u_{K,A}^{(\varepsilon_W,\varepsilon_l)}(\omega,\cdot)\in H^{1+\kappa_a}(\mathcal{D})$ for some positive number $\kappa_a>0$, the pathwise discretization error is bounded by Céa's lemma $\mathbb{P}$-a.s. by*

$$\|u_{K,A}^{(\varepsilon_W,\varepsilon_l)}(\omega,\cdot)-u_{K,A,\ell}^{(\varepsilon_W,\varepsilon_l)}(\omega,\cdot)\|_V\leq C_{\theta,\mathcal{D}}\frac{A}{\overline{a}_-}\|u_{K,A}^{(\varepsilon_W,\varepsilon_l)}(\omega,\cdot)\|_{H^{1+\kappa_a}(\mathcal{D})}h_\ell^{\min(\kappa_a,1)},$$

(see [16, Section 4] and [67, Chapter 8]). If the bound $\|u_{K,A}^{(\varepsilon_W,\varepsilon_l)}\|_{L^2(\Omega;H^{1+\kappa_a}(\mathcal{D}))}\leq C_u=C_u(K,A)$ is finite for the fixed approximation parameters K,A, we immediately obtain

$$\|u_{K,A}^{(\varepsilon_W,\varepsilon_l)}-u_{K,A,\ell}^{(\varepsilon_W,\varepsilon_l)}\|_{L^2(\Omega;V)}\leq C_{\theta,\mathcal{D}}\frac{A}{\overline{a}_-}C_u h_\ell^{\min(\kappa_a,1)}.$$

We note that, by construction of our random field, we always obtain an interface geometry with fixed angles and bounded jump height, which have great influence on the solution regularity, see e.g. [105]. ◆

For general elliptic jump-diffusion problems, one obtains a discretization error of order $\kappa_a\in(1/2,1)$. In general, we cannot expect the full order of convergence $\kappa_a=1$ for discontinuous diffusion coefficients. Without special treatment of the interfaces with respect

to the triangulation, one cannot expect a convergence rate which is higher than $\kappa_a = 1/2$ for the deterministic interface problem (see [10] and [16]). The convergence of the FE method may be improved by the use of triangulations which are adapted to the discontinuities. This is explained in more detail in the following subsection.

6.6.1 Sample-adapted triangulations

In [16], the authors suggest sample-adapted triangulations to improve the convergence rate of the FE approximation: Consider a fixed $\omega \in \Omega$ and assume that the discontinuities of the diffusion coefficient are described by the partition $\mathcal{T}(\omega) = (\mathcal{T}_i,\ i = 1, \dots, \tau(\omega))$ of the domain $\mathcal{D}$ where $\tau(\omega)$ describes the number of elements in the partition. We consider finite-dimensional subspaces $\hat{V}_\ell(\omega) \subset V$ with (stochastic) dimension $\hat{d}_\ell(\omega) \in \mathbb{N}$. We denote by $\hat{\theta}_\ell(\omega)$ the minimal interior angle within $\mathcal{K}_\ell(\omega)$ and assume the existence of a positive number $\theta > 0$ such that $\inf\{\hat{\theta}_\ell(\omega) \mid \ell \in \mathbb{N}_0\} \geq \theta$ for $\mathbb{P}$-almost all $\omega \in \Omega$. Assume that $\mathcal{K}_\ell(\omega)$ is a triangulation of $\mathcal{D}$ which is adjusted to the partition $\mathcal{T}(\omega)$ in the sense that for every $i = 1, \dots, \tau(\omega)$ it holds

$$\partial\mathcal{T}_i \subset \bigcup_{\kappa \in \mathcal{K}_\ell(\omega)} \partial\kappa \text{ and } \hat{h}_\ell(\omega) := \max_{K \in \mathcal{K}_\ell(\omega)} \operatorname{diam}(K) \leq \overline{h}_\ell,$$

for all $\ell \in \mathbb{N}_0$, where $(\overline{h}_\ell,\ \ell \in \mathbb{N}_0)$ is a deterministic, decreasing sequence of refinement thresholds which converges to zero (see Figure 6.2).

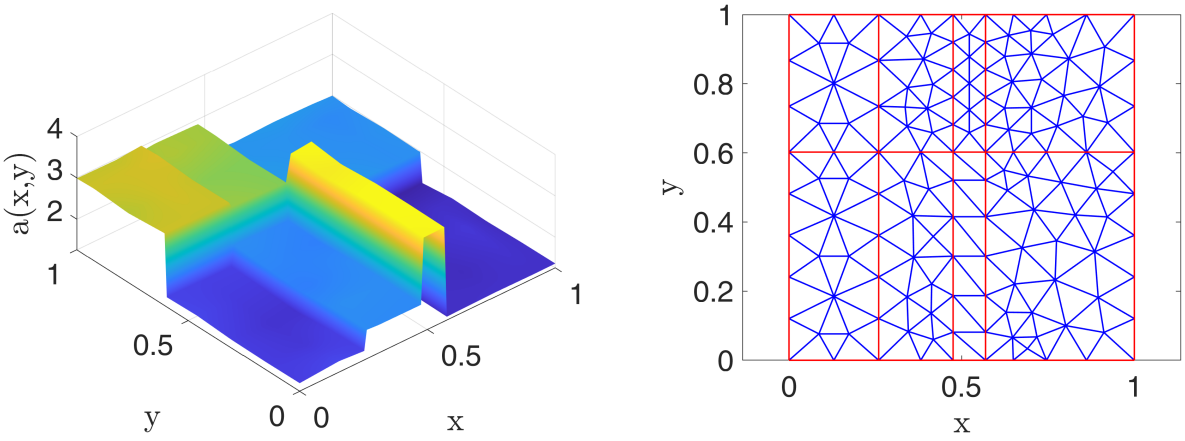

Figure 6.2: A sample of a Poisson-subordinated Matérn-1.5-GRF (left) with corresponding sample-adapted triangulations (right).

Sample-adapted triangulations lead to an improved convergence rate for elliptic problems

with discontinuous coefficients (see [16, Section 4.1] and Section 6.7). This is especially true for jump-diffusion coefficients with polygonal jump geometry, which is the case for the subordinated GRF considered in this paper (see Figure 6.2, [16], [31]). The question arises whether mean squared convergence rates can be derived analytically (cf. Assumption 6.7.1). While it is not possible to prove convergence rates for the mean squared error for our diffusion coefficient in general due to the regularity of the stochastic solution, in practice one can (at least) recover the convergence rates of the deterministic jump-diffusion problem in the strong error (see Section 6.7, [16, Section 4.1] and [31, Section 2]). In fact, in the non-adapted case it is possible to get even better convergence rates than expected for some examples.

6.7 Numerical examples

In the following experiments we work on the domain $\mathcal{D} = (0,1)^2$ and use a FE method with hat-function basis as described in Section 6.6. Here, we distinguish between the *standard* FEM approach with standard triangulations and the *sample-adapted* FEM approach. The aim of our numerical experiments is to compare the sample-adapted with the non-adapted approach and investigate how different Lévy subordinators and GRFs influence the strong convergence rate. In our first example we use Poisson processes with low intensity to investigate the superiority of the presented sample-adapted triangulation. In the second example we use Poisson subordinators with a significantly higher intensity. Besides Poisson subordinators we also use Gamma processes which have infinite activity.

6.7.1 Strong error approximation

Remark 6.6.1 and Subsection 6.6.1 motivate the following assumption on the approximation error of the FE method for non-adapted and adapted triangulations for the rest of this paper (see [16, Assumption 4.4]).

Assumption 6.7.1.
There exist deterministic constants $\hat{C}_u, C_u, \hat{\kappa}_a, \kappa_a > 0$ such that for any $\varepsilon_W, \varepsilon_l > 0$ and any $\ell \in \mathbb{N}_0$, the finite element approximation errors of $\hat{u}_{K,A,\ell}^{(\varepsilon_W,\varepsilon_l)} \approx u_{K,A}^{(\varepsilon_W,\varepsilon_l)}$ in the (sample-adapted)

subspaces $\hat{V}_\ell$, respectively $u_{K,A,\ell}^{(\varepsilon_W,\varepsilon_l)} \approx u_{K,A}^{(\varepsilon_W,\varepsilon_l)}$ in V_ℓ, are bounded by

$$\|u_{K,A}^{(\varepsilon_W,\varepsilon_l)} - \hat{u}_{K,A,\ell}^{(\varepsilon_W,\varepsilon_l)}\|_{L^2(\Omega;V)} \leq \hat{C}_u \mathbb{E}(\hat{h}_\ell^{2\hat{\kappa}_a})^{1/2}, \text{ respectively,}$$
$$\|u_{K,A}^{(\varepsilon_W,\varepsilon_l)} - u_{K,A,\ell}^{(\varepsilon_W,\varepsilon_l)}\|_{L^2(\Omega;V)} \leq C_u h_\ell^{\kappa_a},$$

where the constants $\hat{C}_u, C_u$ may depend on a, f, g, K, A but are independent of $\hat{h}_\ell, h_\ell, \hat{\kappa}_a$ and κ_a. ◆

In each numerical experiment we choose a problem dependent cut-off level K for the subordinators in (6.9) large enough so that its influence is negligible (see Remark 6.4.1). Further, we choose the cut-off level for the diffusion coefficient A in (6.13) large enough such that it has no influence in numerical experiments, e.g. $A = 50$ and therefore the error induced by the error contributor E_1 in (6.19) can be neglected in our experiments. We estimate the strong error using a standard Monte Carlo estimator. Assume that a sequence of (sample-adapted) finite-dimensional subspaces $(\hat{V}_\ell,\ \ell \in \mathbb{N}_0) \subset V$ is given where we use the notation of Section 6.6. For readability we only treat the case of pathwise sample-adapted finite element approximations in the rest of the theoretical consideration in this subsection. We would like to point out, however, that similar arguments lead to the corresponding results for standard FE approximations.

Under the assumptions of Theorem 6.5.11 and Assumption 6.7.1 we obtain

$$\begin{aligned}\|u_{K,A} - \hat{u}_{K,A,\ell}^{(\varepsilon_W,\varepsilon_l)}\|_{L^2(\Omega;V)} &\leq \|u_{K,A} - u_{K,A}^{(\varepsilon_W,\varepsilon_l)}\|_{L^2(\Omega;V)} + \|u_{K,A}^{(\varepsilon_W,\varepsilon_l)} - \hat{u}_{K,A,\ell}^{(\varepsilon_W,\varepsilon_l)}\|_{L^2(\Omega;V)} \\ &\leq C(\varepsilon_W^\gamma + \varepsilon_l^{\frac{1}{2c}} + \mathbb{E}(\hat{h}_\ell^{2\hat{\kappa}_a})^{1/2}),\end{aligned} \tag{6.24}$$

with a constant $C = C(C_{reg}, D, \overline{a}_-, \hat{C}_u)$. Therefore, in order to equilibrate all error contributions, we choose the approximation parameters ε_W and ε_l in the following way:

$$\varepsilon_W \simeq \mathbb{E}(\hat{h}_\ell^{2\hat{\kappa}_a})^{1/(2\gamma)} \text{ and } \varepsilon_l \simeq \mathbb{E}(\hat{h}_\ell^{2\hat{\kappa}_a})^c. \tag{6.25}$$

For readability, we omit the cut-off parameters K and A in the following and use the notation $\hat{u}_{\ell,\varepsilon_W,\varepsilon_l} = \hat{u}_{K,A,\ell}^{(\varepsilon_W,\varepsilon_l)}$. Choosing the approximation parameters $\varepsilon_W, \varepsilon_l$ according to (6.25), we can investigate the strong error convergence rate by a Monte Carlo estimation of the left hand side of (6.24): for a fixed natural number $M \in \mathbb{N}$ we approximate

$$\|u_{K,A} - \hat{u}_{K,A,\ell}^{(\varepsilon_W,\varepsilon_l)}\|_{L^2(\Omega;V)}^2 = \|u_{K,A} - \hat{u}_{\ell,\varepsilon_W,\varepsilon_l}\|_{L^2(\Omega;V)}^2 \approx \frac{1}{M}\sum_{i=1}^{M} \|u_{ref}^{(i)} - \hat{u}_{\ell,\varepsilon_W,\varepsilon_l}^{(i)}\|_V^2, \tag{6.26}$$

where $(u_{ref}^{(i)},\ i = 1, \dots, M)$ are i.i.d. realizations of the stochastic reference solution $u_{ref} \approx u_{K,A}$ and $(\hat{u}_{\ell,\varepsilon_W,\varepsilon_l}^{(i)},\ i = 1 \dots, M)$ are i.i.d. realizations of the FE approximation $\hat{u}_{\ell,\varepsilon_W,\varepsilon_l}$ of the PDE solution on the FE subspace $\hat{V}_\ell$. In all examples we choose the sample number M so that the standard deviation of the MC samples is smaller than 10% of the MC estimator itself.

6.7.2 PDE parameters

In all of our numerical examples we choose $\overline{a} \equiv 1/10$, $f \equiv 10$, $\Phi_1 = 1/100 \exp(\cdot)$ and $\Phi_2 = 5\,|\cdot|$. Further, we impose mixed Dirichlet-Neumann boundary conditions if nothing else is explicitly mentioned. To be precise, we split the domain boundary $\partial\mathcal{D}$ by $\Gamma_1 = \{0,1\} \times [0,1]$ and $\Gamma_2 = (0,1) \times \{0,1\}$ and impose the pathwise mixed Dirichlet-Neumann boundary conditions

$$u_{K,A} = \begin{cases} 0.1 & \text{on } \{0\} \times [0,1] \\ 0.3 & \text{on } \{1\} \times [0,1] \end{cases} \text{ and } a_{K,A}\overrightarrow{n} \cdot \nabla u_{K,A} = 0 \text{ on } \Gamma_2,$$

for $\omega \in \Omega$.

We choose W_1 to be a Matérn-1.5-GRF on $\mathcal{D}$ with correlation length $r_1 = 0.5$ and different variance parameters σ_1^2. Further, we set W_2 to be a Matérn-1.5-GRF on $[0,K]^2$ which is independent of W_1 with different variances σ_2^2 and correlation lengths r_2. We use a reference grid with 801×801 equally spaced points on the domain $\mathcal{D}$ for interpolation and prolongation.

6.7.3 Poisson subordinators

In this section we use Poisson processes to subordinate the GRF W_2 in the diffusion coefficient in (6.5). We consider both, high and low intensity Poisson processes and vary the boundary conditions. Further, using Poisson subordinators allows for a detailed investigation of the approximation error caused by approximating the Lévy subordinators l_1 and l_2 according to Assumption 6.4.2 *v*.

6.7.3.1 The two approximation methods

Using Poisson processes as subordinators allows for two different simulation approaches in the numerical examples: the first approach is an exact and grid-independent simulation of a Poisson process using for example the *Method of Exponential Spacings* or the *Uniform Method*

(see [109, Section 8.1.2]). On the other hand, one may also work with approximations of the Poisson processes satisfying Assumption 6.4.2 *v*.

We recall that a Poisson(λ) process l is a Lévy process with $l(t) \sim \text{Poiss}(t\lambda)$ for $t > 0$, i.e. it admits the discrete density

$$\mathbb{P}(l(t) = k) = e^{-t\lambda}\frac{(t\lambda)^k}{k!}, \text{ for } k \in \mathbb{N}_0.$$

We sample the values of the Poisson(λ) processes l_1 and l_2 on an equidistant grid $\{x_i,\ i = 0, \dots, N_l\}$ with $x_0 = 0$ and $x_{N_l} = 1$ and step size $|x_{i+1} - x_i| \leq \varepsilon_l \leq 1$ for all $i = 0, \dots, N_l - 1$. Further, we approximate the stochastic processes by a piecewise constant extension $l_j^{(\varepsilon_l)} \approx l_j$ of the values on the grid:

$$l_j^{(\varepsilon_l)}(x) = \begin{cases} l_j(x_i) & x \in [x_i, x_{i+1}) \text{ for } i = 0, \dots, N_l - 1, \\ l_j(x_{N_l-1}) & x = 1. \end{cases}$$

for $j = 1, 2$. Since the Poisson process has independent, Poisson distributed increments, values of the Poisson process at the discrete points $\{x_i,\ i = 0, \dots, N_l\}$ can be generated by adding independent Poisson distributed random variables. In the following we refer to this approach as the *approximation approach* to simulate a Poisson process. Note that in this case Assumption 6.4.2 *v* holds with $\eta = +\infty$. In fact, for any $s \in [1, +\infty)$ we obtain for $j = 1, 2$ and an arbitrary $x \in [0, 1)$ with $x \in [x_i, x_{i+1})$:

$$\mathbb{E}(|l_j(x) - l_j^{(\varepsilon_l)}(x)|^s) = \mathbb{E}(|l_j(x) - l_j(x_i)|^s) \leq \mathbb{E}(|l_j(x_{i+1} - x_i)|^s) \leq \mathbb{E}(|l_j(\varepsilon_l)|^s),$$

which is independent of the specific $x \in [0, 1)$. Note that this also holds for $x = D = 1$ and therefore

$$\sup_{x \in [0,1]} \mathbb{E}(|l_j(x) - l_j^{(\varepsilon_l)}(x)|^s) \leq \mathbb{E}(|l_j(\varepsilon_l)|^s).$$

For a Poisson process with parameter λ we obtain

$$\mathbb{E}(|l_j(\varepsilon_l)|^s) = e^{-\lambda\varepsilon_l}\sum_{k=0}^{\infty} k^s \frac{(\lambda\varepsilon_l)^k}{k!} \leq \varepsilon_l \sum_{k=1}^{\infty} k^s \frac{\lambda^k}{k!} \leq C_l\varepsilon_l,$$

where the series converges by the ratio test.

Since the Poisson process allows for both approaches - approximation and exact simulation of the process - the use of these processes are suitable to investigate the additional error in

the approximation of the PDE solution resulting from an approximation of the subordinators. Note that the main difference of the proposed approaches is that the approximation approach is grid dependent and the exact simulation of the Poisson process is not. The differences in the computational costs for the two approaches are insignificant in our numerical examples.

6.7.3.2 Poisson subordinators: low intensity and mixed boundary conditions

In this example we choose l_1 and l_2 to be Poisson(1) subordinators. Further, the variance parameter of the GRF W_1 is set to be $\sigma_1^2 = 1.5^2$ and the variance and correlation parameters of the GRF W_2 are given by $\sigma_2^2 = 0.3^2$ and $r_2 = 1$.

For independent Poisson(1) subordinators l_1 and l_2 we choose $K = 8$ as the cut-off parameter (see (6.9)). With this choice we obtain

$$\mathbb{P}(\sup_{t\in[0,1]} l_j(t) > K) = \mathbb{P}(l_j(1) > K) \approx 1.1252e{-}06,$$

for $j = 1, 2$, such that this cut-off has no influence in the numerical example. Note that for Matérn-1.5-GRFs we can expect $\gamma = 1$ in Equation (6.14) (see e.g. [110, Chapter 5], [63, Proposition 9] and [30, Section 2.3]).

We approximate the GRFs W_1 and W_2 by the circulant embedding method (see [64] and [65]) to obtain approximations $W_1^{(\varepsilon_W)} \approx W_1$ and $W_2^{(\varepsilon_W)} \approx W_2$ as in Lemma 6.4.4. Since $\eta = +\infty$ and $f \in L^q(\Omega; H)$ for every $q \geq 1$ we choose for any positive $\delta > 0$

$$r = 2,\ c = b = 1 + \delta$$

to obtain from Theorem 6.5.11

$$\|u_{K,A} - u_{K,A}^{(\varepsilon_W,\varepsilon_l)}\|_{L^2(\Omega;V)} \leq C_{reg}\frac{C(D)}{\overline{a}_-}(\varepsilon_W + \varepsilon_l^{\frac{1}{2c}}),$$

where we have to assume that $j_{reg} \geq 2((1+\delta)/\delta - 1)$ and $k_{reg} \geq 2(1+\delta)/\delta$ for the regularity constants j_{reg}, k_{reg} given in Assumption 6.5.7. For $\delta = 0.05$ we obtain

$$\|u_{K,A} - u_{K,A}^{(\varepsilon_W,\varepsilon_l)}\|_{L^2(\Omega;V)} \leq C_{reg}\frac{C(D)}{\overline{a}_-}(\varepsilon_W + \varepsilon_l^{\frac{1}{2.01}}). \tag{6.27}$$

Therefore, we get $\gamma = 1$ and $c = 2.01/2$ in the equilibration formula (6.25).

Figure 6.3 shows two different samples of the diffusion coefficient and the corresponding FE approximations of the PDE solution. The FE discretization parameters are given by $h_\ell =$

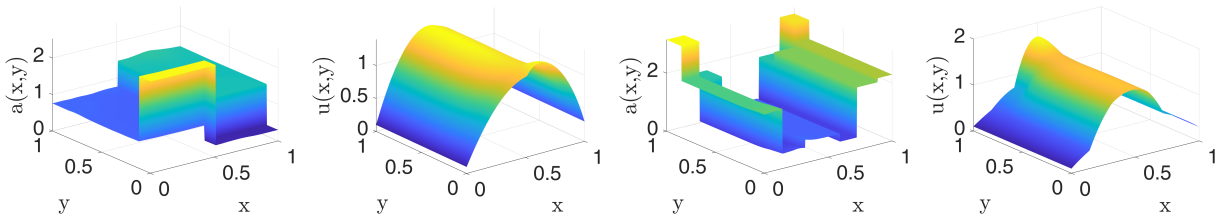

Figure 6.3: Different samples of the diffusion coefficient with Poisson(1) subordinators and the corresponding PDE solutions with mixed Dirichlet-Neumann boundary conditions.

$0.4 \cdot 2^{-(\ell-1)}$ for $l = 1, \dots, 7$. We set $u_{ref} = \hat{u}_{7,\varepsilon_W,\varepsilon_l}$, where the approximation parameters ε_W and ε_l are choosen according to (6.25) and we compute $M = 100$ samples to estimate the strong error by the Monte Carlo estimator (see Equation (6.26)). In this experiment we investigate the strong error convergence rate for the sample-adapted FE approach as well as convergence rate for the non-adapted FE approach (see Section 6.6). In Subsection 6.7.3.1 we described two approaches to simulate Poisson subordinators. We run this experiment with both approaches: first, we approximate the Poisson process via sampling on an equidistant level-dependent grid and, in a second run of the experiment, we simulate the Poisson subordinators exactly using the Uniform Method described in [109, Section 8.1.2]. The convergence results for the both approaches for this experiment are given in the Figure 6.4.

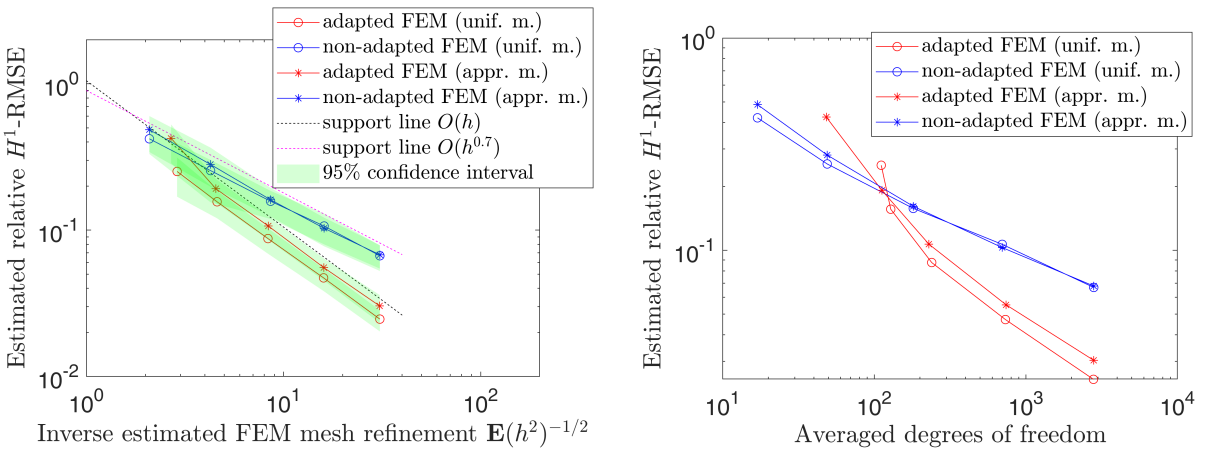

Figure 6.4: Convergence results for Poisson(1) subordinators using the approximation approach and the Uniform Method with mixed Dirichlet-Neumann boundary conditions.

We see a convergence rate of approximately 0.7 for the standard FEM discretization and full order convergence ($\hat{\kappa}_a \approx 1$) for the sample-adapted approach. On the right hand side of Figure 6.4 on sees that the sample-adapted approach is more efficient in terms of computational effort if we consider the error-to-(averaged)DOF-plot. Only on the first level the standard FEM

approach seems to be more efficient (pre-asymptotic behaviour). If we compare the results for the approximation method with the Uniform Method (see Subsection 6.7.3.1), we find that, while the convergence rates are the same, the constant of the error in the sample-adapted approach is slightly smaller for the Uniform Method. This shift is exactly the additional error resulting from an approximation of the subordinators in the approximation approach. We also see that, compared to the approximation approach, on the lower levels the averaged degrees of freedom in the sample-adapted FEM approach is slightly higher if we simulate the Poisson subordinators exactly. This is caused by the fact that in this case we do not approximate the discontinuities of the field which are generated by the Poisson processes. This results in a higher average number of degrees of freedom on the lower levels because discontinuities are more likely close to each other.

6.7.3.3 Poisson subordinators: low intensity and homogeneous Dirichlet boundary conditions

Next, we consider the elliptic PDE under homogeneous Dirichlet boundary conditions. All other parameters remain as in Subsection 6.7.3.2. Figure 6.5 shows samples of the diffusion coefficient and the corresponding FE approximation of the PDE solution. We estimate the

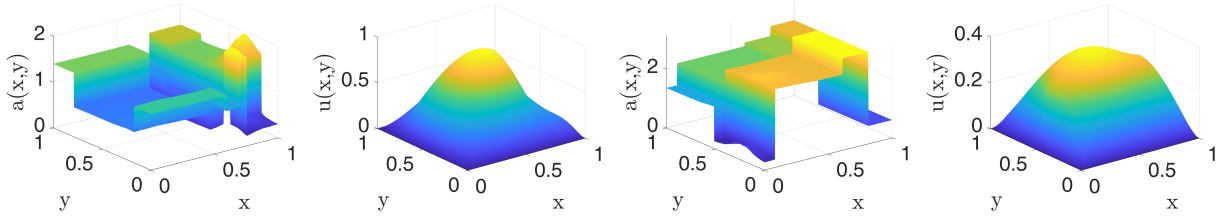

Figure 6.5: Different samples of the diffusion coefficient with Poisson(1) subordinators and the corresponding PDE solutions with homogeneous Dirichlet boundary conditions.

strong error convergence rate for this problem in the same way as in the previous example using $M = 250$ samples and we use the approximation approach to simulate the Poisson subordinators (see Subsection 6.7.3.1). Convergence results are given in Figure 6.6. As in the experiment with mixed Dirichlet-Neumann boundary conditions we obtain convergence order of $\kappa_a \approx 0.7$ for the standard FEM approach and full order convergence for the sample-adapted approach. Also in case of homogeneous Dirichlet boundary conditions the sample-adapted FEM is more efficient in terms of the averaged number of degrees of freedom.

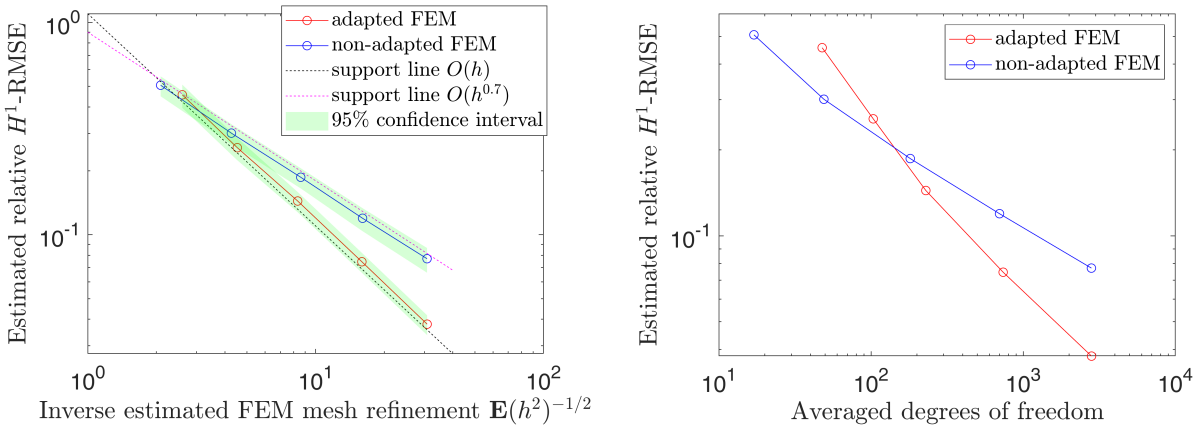

Figure 6.6: Convergence results for Poisson(1) subordinators using the approximation approach and homogeneous Dirichlet boundary conditions.

6.7.3.4 Poisson subordinators: high intensity and mixed boundary conditions

In this section we want to consider subordinators with higher intensity, resulting in a higher number of discontinuities in the diffusion coefficient. Therefore, we consider l_1 and l_2 to be Poisson(5) processes. We set $K = 1$ in the diffusion coefficient (6.9) and consider the downscaled process

$$\tilde{l}_j(t) = \frac{1}{15} l_j(t),$$

for $t \in [0,1]$ and $j = 1,2$. With this choice it is reasonable to expect that this cut-off has no numerical influence since

$$\mathbb{P}\big(\sup_{t\in[0,1]} \frac{l_j(t)}{15} > 1\big) = \mathbb{P}(l_j(1) > 15) \approx 6.9008e{-}05,$$

for $j = 1,2$. The reason we consider the downscaled process is that otherwise we would have to simulate the GRF W_2 on the domain $[0,15]^2$ which is very time consuming. Note that the downscaling of the subordinators has no effect on the jump activity. The variance parameter of the field W_1 is chosen to be $\sigma_1^2 = 1$ and the parameters of the GRF W_2 are set to be $\sigma_2^2 = 0.3^2$ and $r_2 = 0.5$. Figure 6.7 shows samples of the coefficient and the corresponding pathwise FEM solution.

As in the first experiment, we again run this experiment using both methods described in Subsection 6.7.3.1: the approximation approach using Poisson-distributed increments and the Uniform Method. We use the discretization steps $h_\ell = 0.1 \cdot 1.7^{-(\ell-1)}$ for $\ell = 1,\dots,7$ and

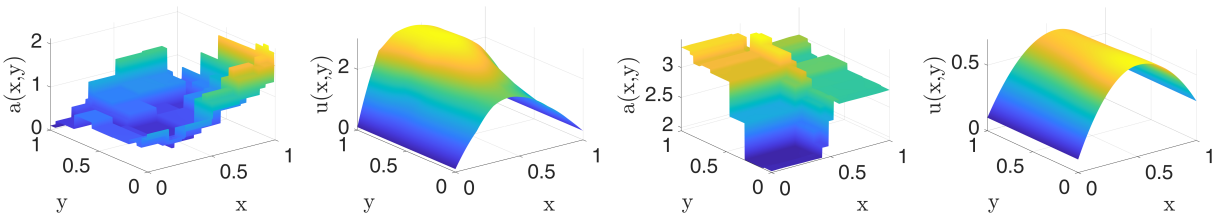

Figure 6.7: Different samples of the diffusion coefficient with Poisson(5) subordinators and the corresponding PDE solutions with mixed Dirichlet-Neumann boundary conditions.

$M = 150$ samples.

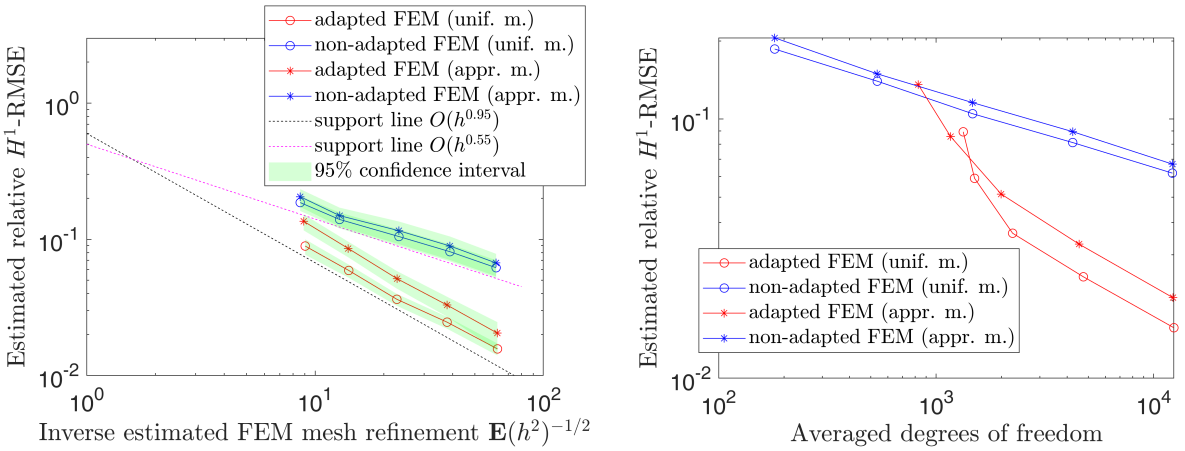

Figure 6.8: Convergence results for Poisson(5) subordinators using the approximation approach and the Uniform Method with mixed Dirichlet-Neumann boundary conditions.

In Figure 6.8 we see that we get almost full order convergence for the sample-adapted FE method for both approximation approaches of the Poisson processes. Compared to the low-intensity examples with Poisson(1) subordinators given in Subsection 6.7.3.2 and 6.7.3.3, we get a slightly lower convergence rate of approximately 0.55 for the standard FEM approach. This holds for both approximation methods of the Poisson subordinators. Hence, we see that the way how the Poisson subordinators are simulated seems to have no effect on the convergence rate.

6.7.3.5 Poisson subordination of a GRF with short correlation length: high intensity and mixed boundary conditions

In our construction of the jump-diffusion coefficient, the jumps are generated by the subordinated GRF. To be precise, the number of spatial jumps is determined by the subordinators and

the jump intensities (in terms of the differences in height between the jumps) are essentially determined by the GRF W_2. This fact allows to control the jump intensities of the diffusion coefficient by the correlation parameter of the underlying GRF W_2. In the following experiment we want to investigate the influence of the jump intensities of the diffusion coefficient on the convergence rates.

In Subsection 6.7.3.4 we subordinated a Matérn-1.5-GRF with pointwise standard deviation $\sigma_2^2 = 0.3^2$ and a correlation length of $r_2 = 0.5$. In the following experiment we set the standard deviation of the GRF W_2 to $\sigma_2^2 = 0.5^2$ and the correlation length to $r_2 = 0.1$ and leave all the other parameters unchanged. Figure 6.9 compares the resulting GRF with the field W_2 with parameters $\sigma_2^2 = 0.3^2$ and $r_2 = 0.5$ which we used in Subsection 6.7.3.4.

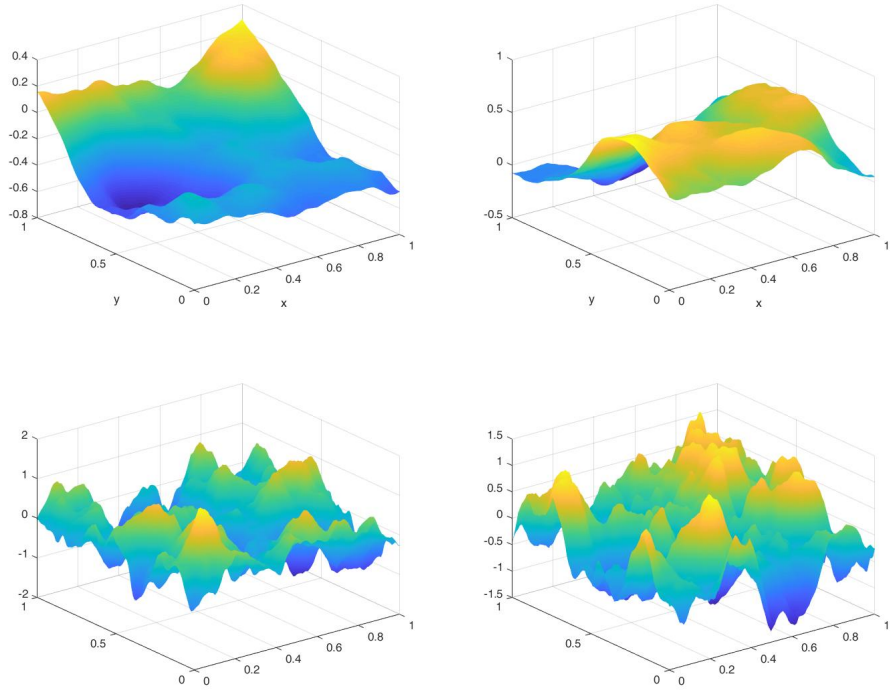

Figure 6.9: Samples of a Matérn-1.5-GRF with $\sigma_2^2 = 0.3^2$, $r_2 = 0.5$ (top) and with parameters $\sigma_2^2 = 0.5^2$, $r_2 = 0.1$ (bottom).

Subordinating the GRF with small correlation length (bottom plots in Figure 6.9) result in higher jump intensities in the diffusion coefficient as the subordination of the GRF with higher correlation length (top plots in Figure 6.9). Figure 6.10 shows samples of the diffusion coefficient and the corresponding PDE solutions where the parameters of W_2 are $\sigma_2^2 = 0.5^2$ and $r_2 = 0.1$.

As expected, the resulting jump coefficient shows jumps with a higher intensity compared to the jump coefficient in the previous experiment where we used the GRF W_2 with parameters

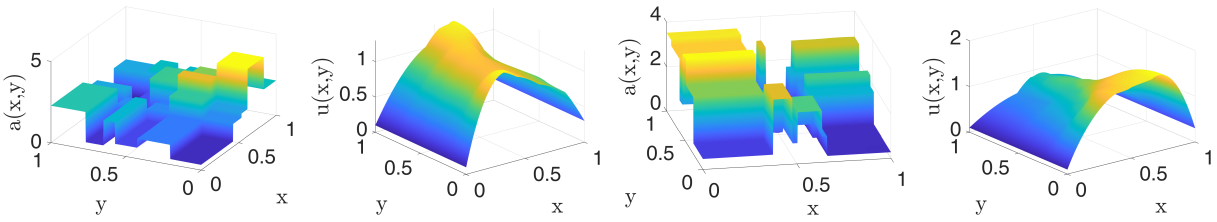

Figure 6.10: Different samples of the diffusion coefficient with Poisson(5) subordinators and the corresponding PDE solutions with mixed Dirichlet-Neumann boundary conditions and small correlation length $r_2 = 0.1$ of the GRF W_2.

$\sigma_2^2 = 0.3^2$ and $r_2 = 0.5$ (see Figure 6.7).

We estimate the strong error convergence rate using this high-intensity jump coefficient using $M = 200$ samples and approximate the Poisson subordinators by the Uniform Method.

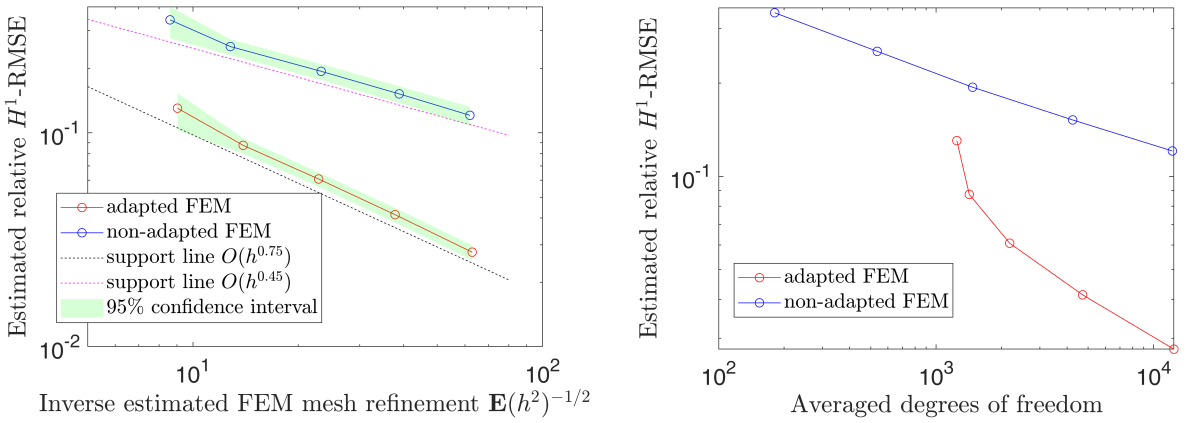

Figure 6.11: Convergence results for Poisson(5) subordinators using the Uniform Method with mixed Dirichlet-Neumann boundary conditions and GRF parameters $\sigma_2^2 = 0.5^2$ and $r_2 = 0.1$.

Figure 6.11 shows that for the GRF W_2 with small correlation length the convergence rates are reduced for both approaches: the standard FEM approach and the sample-adapted version. We cannot preserve full order convergence in the sample-adapted FEM but observe a convergence rate of approximately 0.75. In the non-adapted approach we obtain a convergence rate of approximately 0.45. Looking at the error-to-(averaged)DOF-plot on the right hand side of Figure 6.11 we see that still the sample-adapted approach is by a large margin more efficient in terms of computational effort. This experiment confirms our expectations since the FEM convergence rate has been shown to be strongly influenced by the regularity of the jump-diffusion coefficient (see e.g. [16] and [105]).

6.7.4 Gamma subordinators

In order to also consider Lévy subordinators with infinite activity we take Gamma processes to subordinate the GRF in the remaining numerical examples. We set the standard deviation of the GRF W_1 to be $\sigma_1^2 = 1.5^2$ and we choose $\sigma_2^2 = 0.3^2$ and $r_2 = 1$ for the Matérn-1.5-GRF W_2 and leave the other parameters unchanged.

For $a_G, b_G > 0$, a Gamma(a_G, b_G)-distributed random variable admits the density function

$$x \mapsto \frac{b_G^{a_G}}{\Gamma(a_G)} x^{a_G - 1} \exp(-x b_G), \quad \text{for } x > 0,$$

where $\Gamma(\cdot)$ denotes the Gamma function. A Gamma process $(l(t), t \geq 0)$ has independent Gamma distributed increments. Being precise, $l(t) - l(s) \sim$ Gamma$(a_G \cdot (t-s), b_G)$ for $0 < s < t$ (see [109, Chapter 8]). The following lemma is essential to approximate the Gamma processes.

Lemma 6.7.2.
Let Z be a Gamma(a_G, b_G) distributed random variable for positive parameters $a_G, b_G > 0$. It holds

$$\mathbb{E}(Z^n) = b_G^{-n} \frac{\Gamma(a_G + n)}{\Gamma(a_G)},$$

for all $n \in \mathbb{N}_0$. ◆

Proof. We calculate

$$\begin{aligned}
\mathbb{E}(Z^n) &= \frac{b_G^{a_G}}{\Gamma(a_G)} \int_0^\infty x^{n + a_G - 1} \exp(-x b_G) dx \\
&= \frac{b_G^{a_G}}{\Gamma(a_G)} \frac{\Gamma(a_G + n)}{b_G^{a_G + n}} \int_0^\infty \frac{b_G^{a_G + n}}{\Gamma(a_G + n)} x^{n + a_G - 1} \exp(-x b_G) dx \\
&= b_G^{-n} \frac{\Gamma(a_G + n)}{\Gamma(a_G)},
\end{aligned}$$

where we used that the integral over the Gamma density equals one in the last step. □

In our numerical experiments we choose l_j to be a Gamma$(4, 10)$ process for $j = 1, 2$. Since increments of a Gamma process are Gamma-distributed random variables it is straightforward to generate values of a Gamma process on grid points $(x_i)_{i=0}^{N_l} \subset [0, 1]$ with $|x_{i+1} - x_i| \leq \varepsilon_l$

for $i = 0, \dots, N_l - 1$. We then use the piecewise constant extension of the simulated values $\{l_j(x_i),\ i = 0, \dots, N_l - 1,\ j = 1, 2\}$ to approximate the Lévy subordinators:

$$l_j^{(\varepsilon_l)}(x) = \begin{cases} l_j(x_i) & x \in [x_i, x_{i+1}) \text{ for } i = 0, \dots, N_l - 1, \\ l_j(x_{N_l - 1}) & x = 1. \end{cases}$$

for $j = 1, 2$. Note that in this case Assumption 6.4.2 v is fulfilled for any fixed $\eta < +\infty$. To see that we consider a fixed $s \in \mathbb{N}$ with $s \leq \eta$ and calculate for an arbitrary $x \in [0, 1)$ with $x \in [x_i, x_{i+1})$:

$$\begin{aligned} \mathbb{E}(|l_j(x) - l_j^{(\varepsilon_l)}(x)|^s) &\leq \mathbb{E}(|l_j(x_{i+1}) - l_j(x_i)|^s) \\ &\leq \mathbb{E}(|l_j(\varepsilon_l)|^s) \\ &= b_G^{-s} \frac{\Gamma(a_G \varepsilon_l + s)}{\Gamma(a_G \varepsilon_l)} \\ &= b_G^{-s} \prod_{i=1}^{s-1} (a_G \varepsilon_l + i) a_G \varepsilon_l \\ &\leq C_l \varepsilon_l. \end{aligned}$$

Figure 6.12 shows samples of the jump-diffusion coefficient with Gamma$(4, 10)$ subordinators and corresponding FE solution where we used mixed Dirichlet-Neumann boundary conditions.

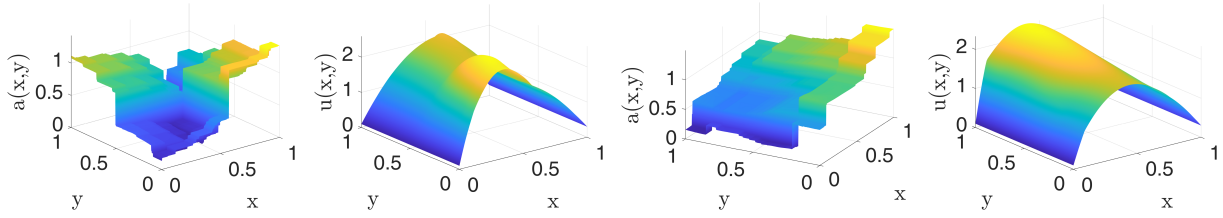

Figure 6.12: Different samples of the diffusion coefficient with Gamma$(4, 10)$ subordinators and the corresponding PDE solutions with mixed Dirichlet-Neumann boundary conditions.

We set the diffusion cut-off to $K = 2$ since in this case we obtain

$$\mathbb{P}(\sup_{t \in [0,1]} l_j(t) \geq 2) = \mathbb{P}(l_j(1) \geq 2) \approx 3.2042e{-}06,$$

for $j = 1, 2$. The use of infinite-activity Gamma subordinators in the diffusion coefficient does not allow anymore for a sample-adapted approach to solve the PDE problem. Hence, we only use the standard FEM approach to solve the PDE samplewise and estimate the strong error

convergence. We use $M = 200$ samples to estimate the strong error on the levels $\ell = 1, \dots, 5$ where we set the non-adaptive FEM solution $u_{7,\varepsilon_W,\varepsilon_l}$ on level $L = 7$ to be the reference solution. We choose the FEM discretization steps to be $h_\ell = 0.4 \cdot 2^{-(\ell-1)}$ for $\ell = 1, \dots, 7$.

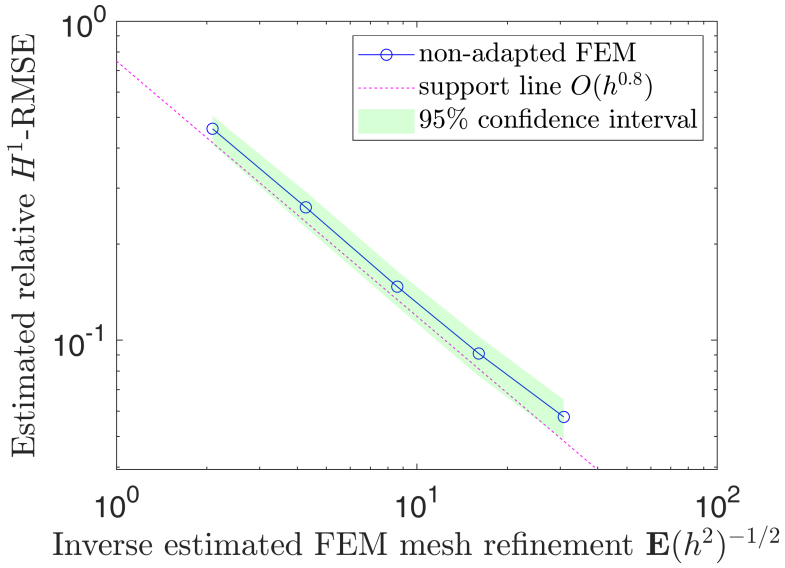

Figure 6.13: Convergence results for Gamma$(4, 10)$ subordinators with mixed Dirichlet-Neumann boundary conditions.

Figure 6.13 shows a convergence rate of approximately 0.8 for the standard-FEM approach. Since we do not treat the discontinuities in a special way we cannot expect full order convergence. In fact, the given convergence is comparably good since in general we cannot prove a higher convergence order than 0.5 for the standard deterministic FEM approach without special treatment of the discontinuities (see [10] and [16]). The convergence rate of approximately 0.8 in this example is based on the comparatively large correlation length of the underlying GRF W_2 (see 6.7.3.5).

In Subsection 6.7.3.5 we investigated the effect of a rougher diffusion coefficient on the convergence rate for Poisson(5) subordinators. In the following experiment we follow a similar strategy and use a shorter correlation length in the GRF W_2 which is subordinated by Gamma processes. Therefore, we choose the parameters of the Matérn-1.5-GRF W_2 to be $\sigma_2^2 = 0.3^2$ and $r_2 = 0.05$. Figure 6.14 shows a comparison of the resulting GRFs W_2 with the different correlation lengths.

In Figure 6.15, the GRF with small correlation length results in higher jumps of the diffusion coefficient and stronger deformations of the corresponding PDE solution compared to the previous example (see Figure 6.12).

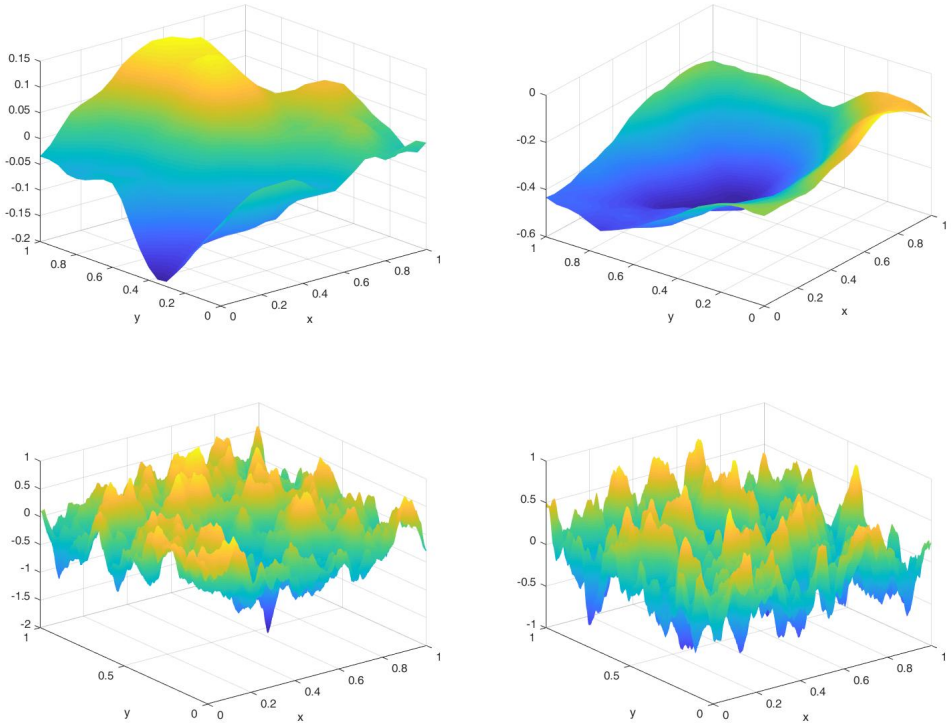

Figure 6.14: Samples of a Matérn-1.5-GRF with correlation length $r_2 = 1$ (top) and with correlation length $r_2 = 0.05$ (bottom).

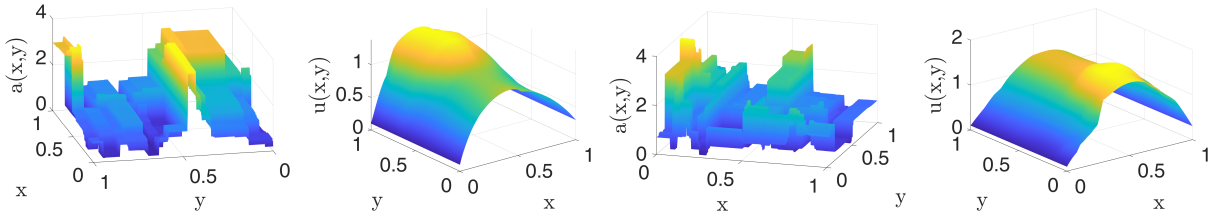

Figure 6.15: Different samples of the diffusion coefficient with Gamma$(4, 10)$ subordinators and the corresponding PDE solutions with mixed Dirichlet-Neumann boundary conditions where the correlation length of W_2 is $r_2 = 0.05$.

We estimate the strong error taking $M = 200$ samples where we use the non-adapted FEM solution $u_{9,\varepsilon_W,\varepsilon_l}$ on level $L = 9$ as reference solution and choose the FEM discretization steps to be $h_\ell = 0.1 \cdot 1.5^{-(\ell-1)}$ for $\ell = 1, \dots, 9$. Figure 6.16 shows the convergence on the levels $\ell = 1, \dots, 6$.

We observe a convergence rate of approximately 0.45 which is significantly smaller than the rate of approximately 0.8 we obtained in the example where we used a GRF W_2 with

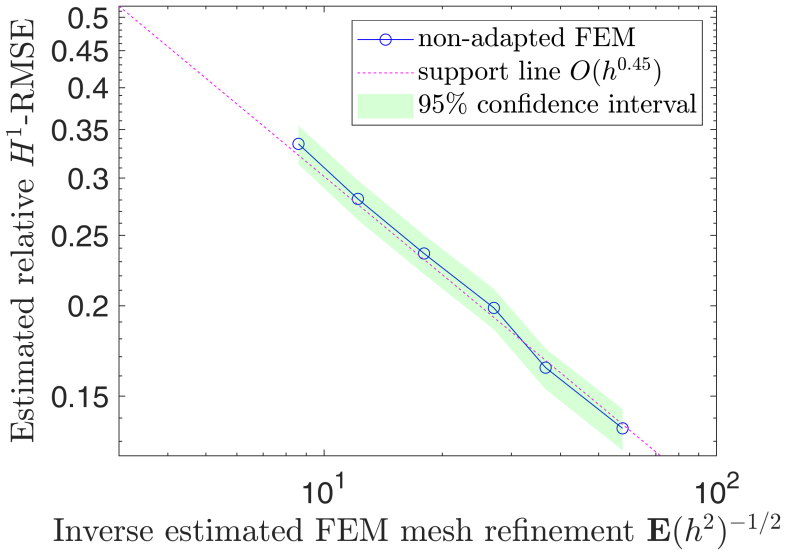

Figure 6.16: Convergence results for Gamma$(4, 10)$ subordinators with mixed Dirichlet-Neumann boundary conditions where the correlation length of W_2 is $r_2 = 0.05$.

correlation length $r_2 = 1$ (see Figure 6.13). This again confirms that, for subordinated GRFs, the convergence rate of the FE method is highly dependent on the correlation length of the underlying GRF W_2 and the resulting jump-intensity of the diffusion coefficient.

6.8 Appendix: Proof of Theorem 6.5.5

Theorem 6.8.1 (Theorem 6.5.5)**.**
For any $\delta > 0$ and any $n \in (1, +\infty)$ there exists a constant $A = A(\delta, n) > 0$ such that

$$\mathbb{E}(\operatorname*{ess\,sup}_{\underline{x} \in \mathcal{D}} |a_K(\underline{x}) - a_{K,A}(\underline{x})|^n)^{1/n} < \delta.$$

◆

Proof. *Step 1: Tail estimation for the coefficient*
By Assumption 6.4.2 *ii*, the functions Φ_1, Φ_2 from Definition 6.3.4 fulfill

$$|\Phi_1'(x)| \leq \phi \exp(\psi|x|), \ |\Phi_2(x) - \Phi_2(y)| \leq C_{lip}|x - y|,$$

for $x, y \in \mathbb{R}$. By the mean value theorem, for any $x \in \mathbb{R}$ there exists a real number $\xi \in \mathbb{R}$

with $|\xi| \leq |x|$ such that it holds

$$\begin{aligned} |\Phi_1(x)| &\leq C(1 + |x|\Phi_1'(\xi)) \leq C(1 + |x|\phi \exp(\psi|\xi|)) \\ &\leq C(1 + |x|\phi \exp(\psi|x|)) \leq \tilde{\phi} \exp(\tilde{\psi}|x|), \end{aligned} \tag{6.28}$$

for positive constants $\tilde{\phi}$ and $\tilde{\psi}$ which are independent of $x \in \mathbb{R}$.

Since the GRFs W_1 and W_2 are $\mathbb{P}$-a.s. bounded on $\mathcal{D}$ resp. on $[0, K]^2$ it follows from [3, Theorem 2.1.1] that $\mu_1 := \mathbb{E}(\sup_{(x,y)\in\mathcal{D}} W_1(x, y)) < +\infty$ and

$$\mathbb{P}(\|W_1\|_{L^\infty(\mathcal{D})} > m) \leq 2\,\mathbb{P}(\sup_{(x,y)\in\mathcal{D}} W_1(x, y) > m) \leq 2 \exp\Big(-\frac{(m - \mu_1)^2}{2\sigma_{\mathcal{D}}^2}\Big), \tag{6.29}$$

for $m > \mu_1$ with a finite constant $\sigma_{\mathcal{D}}^2$ defined by

$$\sigma_{\mathcal{D}}^2 := \sup_{(x,y)\in\mathcal{D}} \mathbb{E}(W_1(x, y)^2) = \sum_{i=1}^{\infty} \lambda_i^{(1)} e_i^{(1)}(x, y)^2 \leq C_e^2 \sum_{i=1}^{\infty} \lambda_i^{(1)} < +\infty,$$

by Assumption 6.4.2 *i.* For a given $\varepsilon \in (0, 1)$ we choose the real number A such that it holds

$$A > 3\,\tilde{\phi}\, \exp\Big(\tilde{\psi}(\sqrt{2\sigma_{\mathcal{D}}^2 |\ln(\varepsilon/2)|} + \mu_1)\Big). \tag{6.30}$$

With this choice we obtain the bound

$$\mathbb{P}(\sup_{(x,y)\in\mathcal{D}} \Phi_1(W_1(x, y)) > A/3) \leq \varepsilon. \tag{6.31}$$

This can be seen by the following calculation

$$\begin{aligned} \mathbb{P}(\sup_{(x,y)\in\mathcal{D}} \Phi_1(W_1(x, y)) > A/3) &\leq \mathbb{P}(\sup_{(x,y)\in\mathcal{D}} \tilde{\phi} \exp(\tilde{\psi}|W_1(x, y)|) > A/3) \\ &= \mathbb{P}(\|W_1\|_{L^\infty(\mathcal{D})} > 1/\tilde{\psi}\, \ln(A/(3\tilde{\phi}))) \\ &\leq 2\, \exp\Big(-\frac{(1/\tilde{\psi}\, \ln(A/(3\tilde{\phi})) - \mu_1)^2}{2\sigma_{\mathcal{D}}^2}\Big) \\ &\leq \varepsilon, \end{aligned}$$

where we used (6.28) in the first step, the estimate (6.29) in the third step and condition (6.30) in the last step.

Obviously, an estimation as in Equation (6.29) holds for the GRF W_2:

$$\begin{aligned}\mathbb{P}(\|W_2\|_{L^\infty([0,K]^2)} > m) &\leq 2\,\mathbb{P}(\sup_{(x,y)\in[0,K]^2} W_2(x,y) > m)\\ &\leq 2\exp\Big(-\frac{(m-\mu_2)^2}{2\sigma_K^2}\Big),\end{aligned} \tag{6.32}$$

for $m > \mu_2$ with $\mu_2 := \mathbb{E}(\sup_{(x,y)\in[0,K]^2} W_2(x,y)) < +\infty$ and

$$\sigma_K^2 := \sup_{(x,y)\in[0,K]^2} \mathbb{E}(W_2(x,y)^2) = \sum_{i=1}^{\infty} \lambda_i^{(2)} e_i^{(2)}(x,y)^2 \leq C_e^2 \sum_{i=1}^{\infty} \lambda_i^{(2)} < +\infty.$$

By the Lipschitz continuity of Φ_2 we conclude the existence of a constant $\phi_2 > 0$ such that

$$|\Phi_2(x)| \leq \phi_2(1+|x|), \tag{6.33}$$

for $x \in \mathbb{R}$. If we again fix a positive $\varepsilon \in (0,1)$ and choose the real number A such that

$$A > 3\phi_2\Big(\sqrt{2\sigma_K^2|\ln(\varepsilon/2)|} + \mu_2 + 1\Big),$$

we obtain the following bound

$$\mathbb{P}(\sup_{(x,y)\in[0,K]^2} \Phi_2(W_2(x,y)) > A/3) \leq \varepsilon. \tag{6.34}$$

This can be seen by the following calculation:

$$\begin{aligned}\mathbb{P}(\sup_{(x,y)\in[0,K]^2} \Phi_2(W_2(x,y)) > A/3) &\leq \mathbb{P}(\phi_2(1+\|W_2\|_{L^\infty([0,K]^2)}) > A/3)\\ &\leq \mathbb{P}(\|W_2\|_{L^\infty([0,K]^2)} > A/(3\phi_2) - 1)\\ &\leq 2\,\exp\Big(-\frac{(A/(3\phi_2)-1-\mu_2)^2}{2\sigma_K^2}\Big)\\ &\leq \varepsilon.\end{aligned}$$

Step 2: Finite moments of the coefficient

In this step we want to show that for any $n \in [1,+\infty)$ it holds

$$\mathbb{E}(\operatorname*{ess\,sup}_{\underline{x}\in\mathcal{D}} |a_K(\underline{x})|^n) =: C_{a_K}(n,K,D) < +\infty. \tag{6.35}$$

We use the definition of the coefficient a_K in (6.9) and Hölder's inequality to calculate

$$\begin{aligned}
&\mathbb{E}(\operatorname*{ess\,sup}_{\underline{x}\in\mathcal{D}} |a_K(\underline{x})|^n) \\
&\leq \mathbb{E}(|\overline{a}_+ + \sup_{(x,y)\in\mathcal{D}} \Phi_1(W_1(x,y)) + \sup_{(x,y)\in[0,K]^2} \Phi_2(W_2(x,y))|^n) \\
&\leq 3^{\frac{n-1}{n}} \Big(\overline{a}_+^n + \mathbb{E}(\sup_{(x,y)\in\mathcal{D}} \Phi_1(W_1(x,y))^n) + \mathbb{E}(\sup_{(x,y)\in[0,K]^2} \Phi_2(W_2(x,y))^n)\Big) \\
&= 3^{\frac{n-1}{n}} (\overline{a}_+^n + I_1 + I_2).
\end{aligned}$$

Therefore, it remains to show that it holds $I_1, I_2 < +\infty$.

By Fubini's theorem, for every nonnegative random variable X it holds

$$\mathbb{E}(X) = \int_\Omega X \, d\mathbb{P} = \int_\Omega \int_0^\infty \mathbb{1}_{\{X\geq c\}} dc \, d\mathbb{P} = \int_0^\infty \mathbb{P}(X \geq c) dc$$

if the right hand side exists. We use this fact and Equation (6.28) to estimate for I_1:

$$\begin{aligned}
I_1 &\leq \tilde{\phi}^n \mathbb{E}(\exp(\tilde{\psi} n \|W_1\|_{L^\infty(\mathcal{D})}) \\
&= \tilde{\phi}^n \int_0^\infty \mathbb{P}(\exp(\tilde{\psi} n \|W_1\|_{L^\infty(\mathcal{D})}) > c) dc \\
&= \tilde{\phi}^n \int_0^\infty \mathbb{P}(\|W_1\|_{L^\infty(\mathcal{D})} > \ln(c)/(\tilde{\psi} n)) dc \\
&= \tilde{\phi}^n \tilde{\psi} n \int_{-\infty}^{+\infty} \exp(\tilde{\psi} n c) \mathbb{P}(\|W_1\|_{L^\infty(\mathcal{D})} > c) dc \\
&\leq \tilde{\phi}^n \tilde{\psi} n \Big(\frac{1}{\tilde{\psi} n} + \mu_1 \exp(\tilde{\psi} n \mu_1) + \int_{\mu_1}^\infty 2 \exp(\tilde{\psi} n c - \frac{(c-\mu_1)^2}{2\sigma_{\mathcal{D}}^2}) dc\Big) < +\infty,
\end{aligned}$$

where we split the integral and used Equation (6.29) in the last step. In a similar way, we use Equation (6.33) to calculate for the second summand I_2:

$$\begin{aligned}
I_2 &\leq \phi_2^n \mathbb{E}((1 + \|W_2\|_{L^\infty([0,K]^2)})^n) \\
&= \phi_2^n \int_0^\infty \mathbb{P}((1 + \|W_2\|_{L^\infty([0,K]^2)})^n > c) dc \\
&= \phi_2^n \int_0^\infty \mathbb{P}(\|W_2\|_{L^\infty([0,K]^2)} > c^{\frac{1}{n}} - 1) dc \\
&= \phi_2^n n \int_{-1}^\infty (c+1)^{n-1} \mathbb{P}(\|W_2\|_{L^\infty([0,K]^2)} > c) dc \\
&\leq \phi_2^n n \Big((\mu_2 + 1)^n + 2 \int_{\mu_2}^\infty (c+1)^{n-1} \exp(-\frac{(c-\mu_2)^2}{2\sigma_K^2}) dc\Big) < +\infty,
\end{aligned}$$

where we used Equation (6.32) in the last step. This proves Equation (6.35).

Step 3: Estimate for the approximation of the diffusion coefficient.

Now, let $\delta \in (0,1)$ be arbitrary. Choose $A = A(\delta) > 0$ such that

$$A > \max\left\{3\overline{a}_+, 3\,\tilde{\phi}\,\exp\left(\tilde{\psi}(\sqrt{2\sigma_D^2|\ln(\varepsilon/2)|}+\mu_1)\right), 3\phi_2\left(\sqrt{2\sigma_K^2|\ln(\varepsilon/2)|}+\mu_2+1\right)\right\}$$

for $\varepsilon := 1-\sqrt{1-(\delta^{2s}/C_{a_K}(2s,K,D))}$.

We estimate using Hölder's inequality:

$$\begin{aligned}\mathbb{E}(\operatorname*{ess\,sup}_{\underline{x}\in\mathcal{D}}|a_K(\underline{x})-a_{K,A}(\underline{x})|^s) &\le \mathbb{E}(\|a_K\|^s_{L^\infty(\mathcal{D})}\mathbb{1}_{\{\|a_K\|_{L^\infty(\mathcal{D}))}\ge A\}})\\ &\le \mathbb{E}(\|a_K\|^{2s}_{L^\infty(\mathcal{D})})^{\frac{1}{2}}\mathbb{P}(\operatorname*{ess\,sup}_{\underline{x}\in\mathcal{D}}|a_K(\underline{x})|\ge A)^{\frac{1}{2}}\\ &= C_{a_K}(2s,K,D)^{\frac{1}{2}}\mathbb{P}(\operatorname*{ess\,sup}_{\underline{x}\in\mathcal{D}}|a_K(\underline{x})|\ge A)^{\frac{1}{2}}\end{aligned}$$

For the second factor we estimate using the independence of W_1 and W_2

$$\begin{aligned}&\mathbb{P}(\operatorname*{ess\,sup}_{\underline{x}\in\mathcal{D}}|a_K(\underline{x})|\ge A)\\ &= 1-\mathbb{P}(\operatorname*{ess\,sup}_{\underline{x}\in\mathcal{D}}|a_K(\underline{x})|\le A)\\ &\le 1-\mathbb{P}(\|\Phi_1(W_1)\|_{L^\infty(\mathcal{D})}\le A/3)\cdot\mathbb{P}(\|\Phi_2(W_2)\|_{L^\infty([0,K]^2)}\le A/3)\\ &\le 1-(1-\mathbb{P}(\|\Phi_1(W_1)\|_{L^\infty(\mathcal{D})}\ge A/3))\cdot(1-\mathbb{P}(\|\Phi_2(W_2)\|_{L^\infty([0,K]^2)}\ge A/3))\\ &\le 1-(1-\varepsilon)^2\\ &\le \delta^{2s}/C_{a_K}(2s,K,D),\end{aligned}$$

where we used Equations (6.31) and (6.34) in the fourth step and therefore we obtain

$$\mathbb{E}(\operatorname*{ess\,sup}_{\underline{x}\in\mathcal{D}}|a_K(\underline{x})-a_{K,A}(\underline{x})|^s)^{1/s}\le\delta.$$

□

Acknowledgements

Funded by Deutsche Forschungsgemeinschaft (DFG, German Research Foundation) under Germany's Excellence Strategy - EXC 2075 - 390740016. The authors would like to thank

two anonymous referees for their remarks, which led to a significant improvement of the manuscript.

Funding

Open Access funding enabled and organized by Projekt DEAL.

Availability of data and materials

All data used in our experiments have been produced with MATLAB random number generators and no external datasets have been used. The datasets generated and analysed during the current study are available from the corresponding author on reasonable request.

Multilevel Monte Carlo estimators for elliptic PDEs with Lévy-type diffusion coefficient

7

Robin Merkle[1] and Andrea Barth[1]

Published in BIT Numerical Mathematics (2022)
Reproduced with permission from Springer Nature
Reference: [93], Link: https://doi.org/10.1007/s10543-022-00912-4

Abstract: *General elliptic equations with spatially discontinuous diffusion coefficients may be used as a simplified model for subsurface flow in heterogeneous or fractured porous media. In such a model, data sparsity and measurement errors are often taken into account by a randomization of the diffusion coefficient of the elliptic equation which reveals the necessity of the construction of flexible, spatially discontinuous random fields. Subordinated Gaussian random fields are random functions on higher dimensional parameter domains with discontinuous sample paths and great distributional flexibility. In the present work, we consider a random elliptic partial differential equation (PDE) where the discontinuous subordinated Gaussian random fields occur in the diffusion coefficient. Problem specific multilevel Monte Carlo (MLMC) finite element methods are constructed to approximate the mean of the solution to the random elliptic PDE. We prove a-priori convergence of a standard MLMC estimator and a modified MLMC - control variate estimator and validate our results in various numerical examples.*

[1]IANS/SimTech, University of Stuttgart, Stuttgart, Germany

7.1 Introduction

Partial differential equations with random operators / data / domain are widely studied. For problems with sparse data or where measurement errors are unavoidable, uncertainties may be quantified using stochastic models. Methods to quantify uncertainty could be divided into two different branches: intrusive and non-intrusive. The former requires solving a high dimensional partial differential equation, where part of the dimensionality stems from the smoothness of the random field or process (see among others [12], [55], [97] and the references therein). The latter are (essentially) sampling methods and require repeated solutions of lower dimensional problems (see, among others, [1], [14], [16], [110], [87], [112]). Among the sampling method the multilevel Monte Carlo approach has been successfully established to lower the computational complexity for various uncertain problems, to the point where (depending on the dimension) it is asymptotically as costly as a single solve of the deterministic partial differential equation on a fine discretization level (see [14], [16], [30] and [59]). In the cited papers mostly Gaussian random fields were used as diffusivity coefficients in the elliptic equation. Gaussian random fields are stochastically very well understood objects and they may be used in both approaches. The distributions underlying the field are, however, Gaussian and therefore the model lacks flexibility, in the sense that fields cannot have pointwise marginal distributions having heavy-tails. Furthermore, Gaussian random fields with Matérn-type covariance operators have $\mathbb{P}$-almost surely spatial continuous paths. There are some extensions in the literature (see, for example, [16], [87] and [49]).

In this paper we investigate multilevel Monte Carlo methods for an elliptic PDE where the coefficient is given by a subordinated Gaussian random field. The subordinated Gaussian random field is a type of a (discontinuous) Lévy field. Different subordinators display unique patterns in the discontinuities and have varied marginal distributions (see [95]). Existence and uniqueness of pathwise solutions to the problem was demonstrated in [96]. Spatial regularity of the solution depends on the subordinated Gaussian random field which itself depends on the subordinator. The discontinuities in the spatial domain pose additional difficulty in the pathwise discretization. A sample-adapted approach was considered in [96], but is limited to certain subordinators. Here we investigate not only the limitations of a sample-adapted approach in multilevel sampling, but also a control variates ansatz as presented first in [101].

We structured the rest of the paper as follows: In Section 7.2 we introduce a general stochastic elliptic equation and its weak solution under mild assumptions on the coefficient. These assumptions accommodate the subordinated Gaussian random fields we introduce in Section 7.3. In Section 7.4 we approximate the diffusion coefficient and state a convergence result of the elliptic equation with the approximated coefficient to the unapproximated solution. In

Section 7.5 we discuss spatial approximation methods, which are needed for the multilevel Monte Carlo methods introduced in Section 7.6 and its control variates variant in Section 7.7. Numerical examples are presented in the last section.

7.2 The stochastic elliptic problem

In this section, we briefly introduce the general stochastic elliptic boundary value problem with random diffusion coefficient and define the corresponding weak solution. This provide the theoretical framework for Section 7.4, where stochastic elliptic PDEs with a specific *discontinuous* random coefficient are considered. For more details on the existence, uniqueness and measurability of the solution to the considered PDE, we refer the reader to [96] and [16]. For the rest of this paper we assume that a complete probability space $(\Omega, \mathcal{F}, \mathbb{P})$ is given. Let $(H, (\cdot,\cdot)_H)$ be a Hilbert space. A H-valued random variable is a measurable function $Z : \Omega \to H$. The space $L^p(\Omega; H)$ contains all strongly measurable functions $Z : \Omega \to H$ with $\|Z\|_{L^p(\Omega;H)} < \infty$, for $p \in [1, +\infty]$, where the norm is defined by

$$\|Z\|_{L^p(\Omega;H)} := \begin{cases} \mathbb{E}(\|Z\|_H^p)^{\frac{1}{p}} & , \text{ if } 1 \leq p < +\infty, \\ \operatorname{ess\,sup}_{\omega\in\Omega} \|Z\|_H & , \text{ if } p = +\infty. \end{cases}$$

For a H-valued random variable $Z \in L^1(\Omega; H)$ we define the *expectation* by the Bochner integral $\mathbb{E}(Z) := \int_\Omega Z \, d\mathbb{P}$. Further, for a square-integrable, H-valued random variable $Z \in L^2(\Omega; H)$, the *variance* is defined by $\mathrm{Var}(Z) := \|Z - \mathbb{E}(Z)\|^2_{L^2(\Omega;H)}$. We refer to [35], [77], [79] or [104] for more details on general probability theory and Hilbert space-valued random variables.

7.2.1 Problem formulation

Let $\mathcal{D} \subset \mathbb{R}^d$, for $d \in \mathbb{N}$, be a bounded, connected Lipschitz domain. We set $H := L^2(\mathcal{D})$ and consider the elliptic PDE

$$-\nabla \cdot (a(\omega, \underline{x})\nabla u(\omega, \underline{x})) = f(\omega, \underline{x}) \text{ in } \Omega \times \mathcal{D}, \tag{7.1}$$

where we impose the following boundary conditions

$$u(\omega, \underline{x}) = 0 \text{ on } \Omega \times \Gamma_1, \tag{7.2}$$

$$a(\omega, \underline{x}) \overrightarrow{n} \cdot \nabla u(\omega, \underline{x}) = g(\omega, \underline{x}) \text{ on } \Omega \times \Gamma_2. \tag{7.3}$$

Here, we split the domain boundary in two $(d-1)$-dimensional manifolds $\Gamma_1,\ \Gamma_2$, i.e. $\partial\mathcal{D} = \Gamma_1 \dot{\cup} \Gamma_2$, where we assume that Γ_1 is of positive measure and that the exterior normal derivative $\overrightarrow{n} \cdot \nabla v$ on Γ_2 is well-defined for every $v \in C^1(\overline{\mathcal{D}})$. The mapping $a : \Omega \times \mathcal{D} \to \mathbb{R}$ is a measurable, positive and stochastic (jump-diffusion) coefficient and $f : \Omega \times \mathcal{D} \to \mathbb{R}$ is a measurable random source function. Further, $\overrightarrow{n}$ is the outward unit normal vector to Γ_2 and $g : \Omega \times \Gamma_2 \to \mathbb{R}$ a measurable function. Note that we just reduce the theoretical analysis to the case of homogeneous Dirichlet boundary conditions on Γ_1 to simplify notation. One could also consider non-homogeneous Dirichlet boundary conditions, since such a problem can always be considered as a version of (7.1) - (7.3) with modified source term and Neumann data (see also [16, Remark 2.1]).

7.2.2 Weak solution

In this subsection, we introduce the pathwise weak solution of problem (7.1) - (7.3) following [96]. We denote by $H^1(\mathcal{D})$ the Sobolev space on $\mathcal{D}$ equipped with the norm

$$\|v\|_{H^1(\mathcal{D})} = \left(\int_D |v(\underline{x})|^2 + |\nabla v(\underline{x})|_2^2 d\underline{x} \right)^{\frac{1}{2}}, \text{ for } v \in H^1(\mathcal{D}),$$

with the Euclidean norm $|\underline{x}|_2 := (\sum_{i=1}^d \underline{x}_i^2)^{\frac{1}{2}}$, for $\underline{x} \in \mathbb{R}^d$ (see for example [50, Section 5.2] for an introduction to Sobolev spaces). We denote by T the trace operator $T : H^1(\mathcal{D}) \to H^{\frac{1}{2}}(\partial\mathcal{D})$ where $Tv = v|_{\partial\mathcal{D}}$ for $v \in C^\infty(\overline{\mathcal{D}})$ (see [41]) and we introduce the solution space $V \subset H^1(\mathcal{D})$ by

$$V := \{v \in H^1(\mathcal{D}) \mid Tv|_{\Gamma_1} = 0\},$$

where we take over the standard Sobolev norm, i.e. $\|\cdot\|_V := \|\cdot\|_{H^1(\mathcal{D})}$. We identify H with its dual space H' and work on the Gelfand triplet $V \subset H \simeq H' \subset V'$.

We multiply Equation (7.1) by a test function $v \in V$ and integrate by parts (see e.g. [113, Section 6.3]) to obtain the following pathwise weak formulation of the problem: For $\mathbb{P}$-almost

all $\omega \in \Omega$, given $f(\omega, \cdot) \in V'$ and $g(\omega, \cdot) \in H^{-\frac{1}{2}}(\Gamma_2)$, find $u(\omega, \cdot) \in V$ such that

$$B_{a(\omega)}(u(\omega, \cdot), v) = F_\omega(v) \tag{7.4}$$

for all $v \in V$. The function $u(\omega, \cdot)$ is then called pathwise weak solution to problem (7.1) - (7.3). The bilinear form $B_{a(\omega)}$ and the operator F_ω are defined by

$$\begin{aligned} B_{a(\omega)}(u, v) &:= \int_{\mathcal{D}} a(\omega, \underline{x}) \nabla u(\underline{x}) \cdot \nabla v(\underline{x}) d\underline{x}, \text{ and} \\ F_\omega(v) &:= \int_{\mathcal{D}} f(\omega, x) v(\underline{x}) d\underline{x} + \int_{\Gamma_2} g(\omega, \underline{x}) [Tv](\underline{x}) d\underline{x}, \end{aligned}$$

for $u, v \in V$ and fixed $\omega \in \Omega$, where the integrals in F_ω are understood as the duality pairings:

$$\begin{aligned} \int_{\mathcal{D}} f(\omega, \underline{x}) v(\underline{x}) d\underline{x} &= {}_{V'}\langle f(\omega, \cdot), v \rangle_V \text{ and} \\ \int_{\Gamma_2} g(\omega, \underline{x}) [Tv](\underline{x}) d\underline{x} &= {}_{H^{-\frac{1}{2}}(\Gamma_2)}\langle g(\omega, \cdot), Tv \rangle_{H^{\frac{1}{2}}(\Gamma_2)}. \end{aligned}$$

7.3 Subordinated Gaussian random fields

In [95], the authors proposed a new subordination approach to construct discontinuous Lévy-type random fields: the *subordinated Gaussian random field*. Motivated by the subordinated Brownian motion, the subordinated Gaussian Random field is constructed by replacing the spatial variables of a Gaussian random field (GRF) W on a general d-dimensional domain $\mathcal{D} \subset \mathbb{R}^d$ by d independent Lévy subordinators (see [95], [109], [8]). For $d = 2$, the detailed construction is as follows: For two positive horizons $T_1, T_2 < +\infty$, we define the domain $\mathcal{D} = [0, T_1] \times [0, T_2]$. We consider a GRF $W = (W(x, y),\ (x, y) \in \mathbb{R}^2_+)$ with $\mathbb{P}$-a.s. continuous paths and assume two independent Lévy subordinators $l_1 = (l_1(x),\ x \in [0, T_1])$ and $l_2 = (l_2(y),\ y \in [0, T_2])$ are given (see [95] and [8]). The subordinated GRF is then defined by

$$L(x, y) = W(l_1(x), l_2(y)), \text{ for } (x, y) \in [0, T_1] \times [0, T_2]. \tag{7.5}$$

The corresponding random field $L = (L(x, y),\ (x, y) \in [0, T_1], \times [0, T_2])$ is in general discontinuous on the spatial domain $\mathcal{D}$.

Figure 7.1 demonstrates how the subordinators l_1 and l_2 create discontinuities in the subordi-

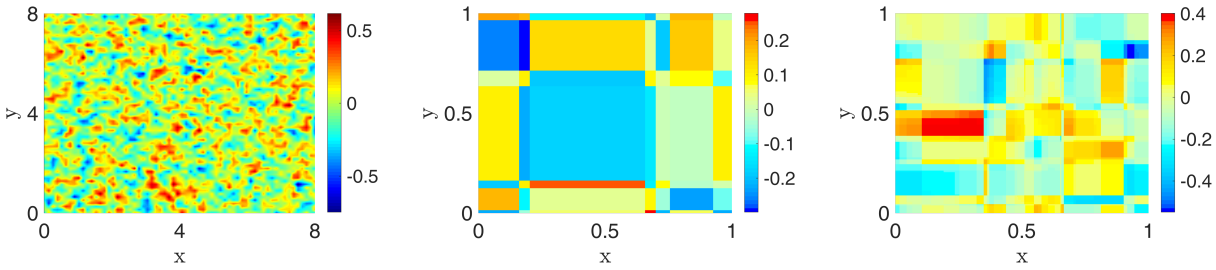

Figure 7.1: Sample of a Matérn-1.5-GRF (left) and a corresponding Poisson-subordinated GRF (middle) and Gamma-subordinated GRF (right).

nated GRF. In the presented samples, the underlying GRF is a Matérn-1.5 GRF. We recall that, for a given smoothness parameter $\nu_M > 1/2$, correlation parameter $r_M > 0$ and variance $\sigma_M^2 > 0$, the Matérn-ν_M covariance function on $\mathbb{R}_+^d \times \mathbb{R}_+^d$ is given by $q_M(\underline{x}, \underline{y}) = \rho_M(|\underline{x}-\underline{y}|_2)$, for $(\underline{x}, \underline{y}) \in \mathbb{R}_+^d \times \mathbb{R}_+^d$, with

$$\rho_M(s) = \sigma_M^2 \frac{2^{1-\nu_M}}{\Gamma(\nu_M)} \Big(\frac{2s\sqrt{\nu_M}}{r_M} \Big)^{\nu_M} K_{\nu_M} \Big(\frac{2s\sqrt{\nu_M}}{r_M} \Big), \text{ for } s \geq 0,$$

where $\Gamma(\cdot)$ is the Gamma function and $K_\nu(\cdot)$ is the modified Bessel function of the second kind (see [63, Section 2.2 and Proposition 1]). A Matérn-ν_M GRF is a centered GRF with covariance function q_M. It has been shown in [95] that the subordinated GRF constructed in (7.5) is separately measurable. Further, the corresponding random fields display great distributional flexibility, allow for a Lévy-Khinchin-type formula and formulas for their covariance functions can be derived which makes them attractive for applications. We refer the interested reader to [95] for a theoretical investigation of the constructed random fields.

7.4 The subordinated GRF in the elliptic model equation

In this section we incorporate the subordinated GRF in the diffusion coefficient of the elliptic PDE (7.1) - (7.3). Further, we show how to approximate the diffusion coefficient and state the most important results on the approximation of the corresponding PDE solution following [96]. For the proofs and a more detailed study of subordinated GRFs in the elliptic model equation we refer the reader to [96].

7.4.1 Subordinated GRFs in the diffusion coefficient

It follows from the Lévy-Itô decomposition that any Lévy process on a one-dimensional (time) domain can be additively decomposed into a deterministic drift part, a continuous noise part and a pure-jump process (see [8, Section 2.4]). Motivated by this, we construct the diffusion coefficient a in the elliptic PDE as follows (cf. [96, Definition 3.4]).

Definition 7.4.1.
We consider the domain $\mathcal{D} = (0, D)^2$ with $D < +\infty$[2]. We define the jump-diffusion coefficient a in problem (7.1) - (7.3) with $d = 2$ as

$$\begin{aligned} &a : \Omega \times \mathcal{D} \to (0, +\infty), \\ &(\omega, x, y) \mapsto \overline{a}(x, y) + \Phi_1(W_1(x, y)) + \Phi_2(W_2(l_1(x), l_2(y))), \end{aligned} \tag{7.6}$$

where

- *$\overline{a} : \mathcal{D} \to (0, +\infty)$ is deterministic, continuous and there exist constants $\overline{a}_+, \overline{a}_- > 0$ with $\overline{a}_- \leq \overline{a}(x, y) \leq \overline{a}_+$ for $(x, y) \in \mathcal{D}$.*
- *$\Phi_1,\ \Phi_2 : \mathbb{R} \to [0, +\infty)$ are continuous .*
- *W_1 and W_2 are zero-mean GRFs on $\mathcal{D}$ respectively on $[0, +\infty)^2$ with $\mathbb{P}$-a.s. continuous paths.*
- *l_1 and l_2 are Lévy subordinators on $[0, D]$.*

◆

It follows by a pathwise application of the Lax-Milgram lemma that the elliptic model problem (7.1) - (7.3) with the diffusion coefficient constructed in Definition 7.4.1 has a unique pathwise weak solution. For a proof we refer to [96, Theorem 3.7].

Theorem 7.4.2.
Let a be as in Definition 7.4.1 and let $f \in L^q(\Omega; H),\ g \in L^q(\Omega; L^2(\Gamma_2))$ for some $q \in [1, +\infty)$. Then there exists a unique pathwise weak solution $u(\omega, \cdot) \in V$ to problem (7.1) - (7.3) for $\mathbb{P}$-almost

[2]For simplicity we chose a square domain, rectangular ones may be considered in the same way.

every $\omega \in \Omega$. *Furthermore,* $u \in L^r(\Omega; V)$ *for all* $r \in [1, q)$ *and*

$$\|u\|_{L^r(\Omega;V)} \leq C(\overline{a}_-, \mathcal{D})(\|f\|_{L^q(\Omega;H)} + \|g\|_{L^q(\Omega;L^2(\Gamma_2))}),$$

where $C(\overline{a}_-, \mathcal{D}) > 0$ *is a constant depending only on the indicated parameters.* ◆

7.4.2 Problem modification

Theorem 7.4.2 guarantees the existence of a unique solution u to problem (7.1) - (7.3) for the specific diffusion coefficient a constructed in Definition 7.4.1. However, accessing this pathwise weak solution numerically is a different matter. Here, we face several challenges: The first difficulty is related to the domain on which the GRF W_2 is defined. The Lévy subordinators l_1 and l_2 can in general attain any value in $[0, +\infty)$. Hence, it is necessary to consider the GRF W_2 on the unbounded domain $[0, +\infty)^2$. However, most regularity and approximation results on GRFs are formulated for the case of a parameter space which is at least bounded and cannot easily be extended to unbounded domains (see e.g. [3, Chapter 1]). Therefore, we modify the diffusion coefficient a from Definition 7.4.1 and cut the Lévy subordinators at a deterministic threshold $K > 0$ depending on the choice of the subordinator. The resulting problem then coincides with the original problem up to a set of samples, whose probability can be made arbitrary small (see [96, Remark 4.1]). Furthermore, we have to bound the diffusion coefficient itself by a deterministic upper bound A in order to show the convergence of the solution (see [96, Section 5] for details). Therefore, we also cut the diffusion coefficient at a deterministic level $A > 0$. It can be shown that this induces an additional error in the solution approximation which can be controlled and vanishes for growing threshold A (see [96, Section 5.1, esp. Theorem 5.4 and Theorem 5.5]). The two described modifications of the original problem (7.1) - (7.3) are formalized in this subsection.

We define the cut function $\chi_K(z) := \min(z, K)$, for $z \in [0, +\infty)$, with a positive number $K > 0$. Further, for fixed numbers $K, A > 0$, we consider the following problem

$$-\nabla \cdot (a_{K,A}(\omega, \underline{x}) \nabla u_{K,A}(\omega, \underline{x})) = f(\omega, \underline{x}) \text{ in } \Omega \times \mathcal{D}, \tag{7.7}$$

where we impose the boundary conditions

$$u_{K,A}(\omega, \underline{x}) = 0 \text{ on } \Omega \times \Gamma_1, \tag{7.8}$$

$$a_{K,A}(\omega, \underline{x}) \overrightarrow{n} \cdot \nabla u_{K,A}(\omega, \underline{x}) = g(\omega, \underline{x}) \text{ on } \Omega \times \Gamma_. \tag{7.9}$$

The diffusion coefficient $a_{K,A}$ is defined by [3]

$$a_{K,A} : \Omega \times \mathcal{D} \to (0, +\infty),$$
$$(\omega, x, y) \mapsto \chi_A\Big(\overline{a}(x, y) + \Phi_1(W_1(x, y)) + \Phi_2(W_2(\chi_K(l_1(x)), \chi_K(l_2(y))))\Big), \quad (7.10)$$

where we assume that the functions $\overline{a}$, Φ_1, Φ_2, the GRFs W_1, W_2 and the Lévy subordinators l_1, l_2 are as described in Definition 7.4.1. Again, Theorem 7.4.2 applies in this case and yields the existence of a pathwise weak solution $u_{K,A} \in L^r(\Omega; V)$, for $r \in [1, q)$, if $f \in L^q(\Omega; H)$ and $g \in L^q(\Omega; L^2(\Gamma_2))$. In [96], the authors investigated in detail how this modification affects the solution u of the original problem and how the resulting error can be controlled by the choice of the deterministic thresholds K and A. Therefore, from now on we decide to consider problem (7.7) - (7.10) for a fixed choice of K and A and focus on the approximation of the GRFs W_1, W_2 and the Lévy subordinators l_1, l_2 in the following. We come back on the choice of K and A in specific situations in Section 7.8.

7.4.3 Approximation of the GRFs and the Lévy subordinators and convergence of the approximated solution

In order to approximate the random solution $u_{K,A}$ of problem (7.7) - (7.10) we have to generate samples from the GRFs $W_1,\ W_2$ and the Lévy subordinators $l_1,\ l_2$ to obtain samples of the diffusion coefficient $a_{K,A}$ defined in Equation (7.10). However, the GRFs $W_1,\ W_2$ and the Lévy subordinators $l_1,\ l_2$ may in general not be simulated exactly and, hence, appropriate approximations have to be used. Therefore, we have to impose some additional assumptions on the GRFs and the Lévy subordinators. We summarize our working assumptions in the following (cf. [96, Assumption 4.2]).

Assumption 7.4.3.
Let W_1 be a zero-mean GRF on $[0, D]^2$ and W_2 be a zero-mean GRF on $[0, K]^2$. We denote by $q_1 : [0, D]^2 \times [0, D]^2 \to \mathbb{R}$ and $q_2 : [0, K]^2 \times [0, K]^2 \to \mathbb{R}$ the covariance functions of these random fields and by Q_1, Q_2 the associated covariance operators defined by

$$Q_j\phi = \int_{[0,z_j]^2} q_j((x, y), (x', y'))\phi(x', y')d(x', y'),$$

[3] We assume one fixed K for all spatial dimensions to keep notation simple. However, the results presented in the subsequent sections also hold for individual values in each spatial dimension.

for $\phi \in L^2([0, z_j]^2)$ *with* $z = (D, K)$ *and* $j = 1, 2$. *We denote by* $(\lambda_i^{(1)}, e_i^{(1)},\ i \in \mathbb{N})$ *resp.* $(\lambda_i^{(2)}, e_i^{(2)},\ i \in \mathbb{N})$ *the eigenpairs associated to the covariance operators* Q_1 *and* Q_2. *In particular,* $(e_i^{(1)},\ i \in \mathbb{N})$ *resp.* $(e_i^{(2)},\ i \in \mathbb{N})$ *are orthonormal bases of* $L^2([0, D]^2)$ *resp.* $L^2([0, K]^2)$.

i We assume that the eigenfunctions are continuously differentiable and there exist positive constants $\alpha,\ \beta,\ C_e,\ C_\lambda > 0$ *such that for any* $i \in \mathbb{N}$ *it holds*

$$\begin{aligned} \|e_i^{(1)}\|_{L^\infty([0,D]^2)},\ \|e_i^{(2)}\|_{L^\infty([0,K]^2)} &\leq C_e, \\ \|\nabla e_i^{(1)}\|_{L^\infty([0,D]^2)},\ \|\nabla e_i^{(2)}\|_{L^\infty([0,K]^2)} &\leq C_e i^\alpha, \\ \sum_{i=1}^{\infty} (\lambda_i^{(1)} + \lambda_i^{(2)}) i^\beta &\leq C_\lambda < +\infty. \end{aligned}$$

ii There exist constants $\phi,\ \psi, C_{lip} > 0$ *such that the continuous functions* $\Phi_1,\ \Phi_2 : \mathbb{R} \to [0, +\infty)$ *from Definition 7.4.1 satisfy*

$$|\Phi_1'(x)| \leq \phi\, \exp(\psi|x|),\ |\Phi_2(x) - \Phi_2(y)| \leq C_{lip}\, |x - y| \text{ for } x, y \in \mathbb{R}.$$

In particular, $\Phi_1 \in C^1(\mathbb{R})$.

iii $f \in L^q(\Omega; H)$ *and* $g \in L^q(\Omega; L^2(\Gamma_2))$ *for some* $q \in (1, +\infty)$.

iv l_1 *and* l_2 *are Lévy subordinators on* $[0, D]$ *which are independent of the GRFs* W_1 *and* W_2. *Further, we assume that we have approximations* $l_1^{(\varepsilon_l)},\ l_2^{(\varepsilon_l)}$ *of these processes and there exist constants* $C_l > 0$ *and* $\eta > 1$ *such that for every* $s \in [1, \eta)$ *it holds*

$$\mathbb{E}(|l_j(x) - l_j^{(\varepsilon_l)}(x)|^s) \leq C_l \varepsilon_l,$$

for $\varepsilon_l > 0$, $x \in [0, D]$ *and* $j = 1, 2$.

◆

The first assumption on the eigenpairs of the GRFs is natural (see [16] and [63]). Assumption 7.4.3 *ii* is necessary to be able to quantify the error of the approximation of the diffusion coefficient and Assumption 7.4.3 *iii* guarantees the existence of a solution. The last assumption ensures that we can approximate the Lévy subordinators with a controllable L^s-error. Here, the parameter ε_l may be interpreted as the maximum stepsize of the grid on $[0, D]$ on which the piecewise constant approximation $l_j^{(\varepsilon_l)}$ of the Lévy process l_j is defined (see Section 7.8). The prescribed error bound may then always be achieved under appropriate assumptions on

the tails of the distribution of the Lévy subordinators, see [15, Assumption 3.6, Assumption 3.7 and Theorem 3.21].

For technical reasons we have to work under the following assumption on the integrability of the gradient of the solution $\nabla u_{K,A}$ of problem (7.7) - (7.10) (cf. [96, Assumption 5.7]). This assumption is necessary to prove convergence of the approximation to the solution $u_{K,A}$ in Theorem 7.4.5. Its origin lies in the fact that we cannot approximate the Lévy subordinators in an $L^s(\Omega; L^\infty([0,D]))$-sense due to the discontinuities. To showcase this consider a Poisson process with constant jump size 1 (cf. [109, Section 5.3.1]): for almost every path, a piecewise constant approximation of the process on an equidistant grid leads to a pathwise error of at least 1 measured in the $L^\infty([0,D])$-norm. Note that the approximation property given by Assumption 7.4.3 (iv) is weaker than an approximation in the $L^s(\Omega; L^\infty([0,D]))$-norm.

Assumption 7.4.4.
We assume that there exist constants $j_{reg} > 0$ and $k_{reg} \geq 2$ such that

$$C_{reg} := \mathbb{E}(\|\nabla u_{K,A}\|^{k_{reg}}_{L^{2+j_{reg}}(\mathcal{D})}) < +\infty.$$

◆

There are several results on higher integrability of the gradient of the solution to an elliptic PDE of the form (7.7) - (7.10) which guarantee the condition of Assumption 7.4.4. We refer to [96, Section 5.2] and especially Remark 5.8 and Remark 5.9 therein for more details.

We now turn to the final approximation of the diffusion coefficient using approximations $W_1^{(\varepsilon_W)} \approx W_1, W_2^{(\varepsilon_W)} \approx W_2$ of the GRFs and $l_1^{(\varepsilon_l)} \approx l_1, l_2^{(\varepsilon_l)} \approx l_2$ of the Lévy subordinators (see Assumption 7.4.3): We consider discrete grids $G_1^{(\varepsilon_W)} = \{(x_i, x_j) |\, i,j = 0,\dots,M^{(1)}_{\varepsilon_W}\}$ on $[0,D]^2$ and $G_2^{(\varepsilon_W)} = \{(y_i, y_j) |\, i,j = 0,\dots,M^{(2)}_{\varepsilon_W}\}$ on $[0,K]^2$ where $(x_i,\ i = 0,\dots,M^{(1)}_{\varepsilon_W})$ is an equidistant grid on $[0,D]$ with maximum step size ε_W and $(y_i,\ i = 0,...,M^{(2)}_{\varepsilon_W})$ is an equidistant grid on $[0,K]$ with maximum step size ε_W. Further, let $W_1^{(\varepsilon_W)}$ and $W_2^{(\varepsilon_W)}$ be approximations of the GRFs $W_1,\ W_2$ on the discrete grids $G_1^{(\varepsilon_W)}$ resp. $G_2^{(\varepsilon_W)}$ which are constructed by point evaluation of the random fields W_1 and W_2 on the grid points and linear interpolation between the them. Such an approximation may be obtained, for example, by the circulant embedding method (cf. [64] and [65]).

We approximate the diffusion coefficient $a_{K,A}$ from Equation (7.10) by

$a_{K,A}^{(\varepsilon_W,\varepsilon_l)} : \Omega \times \mathcal{D} \to (0, +\infty)$ with

$$\begin{aligned} &a_{K,A}^{(\varepsilon_W,\varepsilon_l)}(x,y) \\ &= \chi_A\Big(\overline{a}(x,y) + \Phi_1(W_1^{(\varepsilon_W)}(x,y)) + \Phi_2(W_2^{(\varepsilon_W)}(\chi_K(l_1^{(\varepsilon_l)}(x)), \chi_K(l_2^{(\varepsilon_l)}(y))))\Big) \end{aligned} \tag{7.11}$$

for $(x,y) \in \mathcal{D}$. Further, we denote by $u_{K,A}^{(\varepsilon_W,\varepsilon_l)} \in L^r(\Omega; V)$, with $r \in [1, q)$, the weak solution to the corresponding elliptic problem

$$-\nabla \cdot (a_{K,A}^{(\varepsilon_W,\varepsilon_l)}(\omega, \underline{x}) \nabla u_{K,A}^{(\varepsilon_W,\varepsilon_l)}(\omega, \underline{x})) = f(\omega, \underline{x}) \text{ in } \Omega \times \mathcal{D}, \tag{7.12}$$

with boundary conditions

$$u_{K,A}^{(\varepsilon_W,\varepsilon_l)}(\omega, \underline{x}) = 0 \text{ on } \Omega \times \Gamma_1, \tag{7.13}$$

$$a_{K,A}^{(\varepsilon_W,\varepsilon_l)}(\omega, \underline{x}) \overrightarrow{n} \cdot \nabla u_{K,A}^{(\varepsilon_W,\varepsilon_l)}(\omega, x) = g(\omega, x) \text{ on } \Omega \times \Gamma_2. \tag{7.14}$$

Note that Theorem 7.4.2 also applies to the elliptic problem with coefficient $a_{K,A}^{(\varepsilon_W,\varepsilon_l)}$. We are now able to state the most important result on the convergence of the approximated solution $u_{K,A}^{(\varepsilon_W,\varepsilon_l)}$ to $u_{K,A}$. For a proof we refer the reader to [96, Theorem 5.11].

Theorem 7.4.5.
Assume $q > 2$ in Assumption 7.4.3. Let $r \in [2, q)$ and $b, c \in [1, +\infty]$ be given such that it holds

$$rc\gamma \geq 2 \text{ and } 2b \leq rc < \eta$$

with a fixed real number $\gamma \in (0, \min(1, \beta/(2\alpha))$. Here, the parameters η, α and β are determined by the GRFs W_1, W_2 and the Lévy subordinators l_1, l_2 (see Assumption 7.4.3).

Let $m, n \in [1, +\infty]$ be real numbers such that

$$\frac{1}{m} + \frac{1}{c} = \frac{1}{n} + \frac{1}{b} = 1,$$

and let $k_{reg} \geq 2$ and $j_{reg} > 0$ be the regularity specifiers given by Assumption 7.4.4. If it holds that

$$n < 1 + \frac{j_{reg}}{2} \text{ and } rm < k_{reg},$$

then the approximated solution $u_{K,A}^{(\varepsilon_W,\varepsilon_l)}$ converges to the solution $u_{K,A}$ of the truncated problem

for $\varepsilon_W, \varepsilon_l \to 0$ *and it holds*

$$\begin{aligned}\|u_{K,A} - u_{K,A}^{(\varepsilon_W,\varepsilon_l)}\|_{L^r(\Omega;V)} &\leq C(\overline{a}_-, \mathcal{D}, r) C_{reg} \|a_{K,A}^{(\varepsilon_W,\varepsilon_l)} - a_{K,A}\|_{L^{rc}(\Omega;L^{2b}(\mathcal{D}))} \\ &\leq C_{reg} C(\overline{a}_-, \mathcal{D}, r)(\varepsilon_W^{\gamma} + \varepsilon_l^{\frac{1}{rc}}).\end{aligned}$$

◆

This result is essential since it guarantees the convergence of the approximated solution $u_{K,A}^{(\varepsilon_W,\varepsilon_l)}$ to the solution $u_{K,A}$ with a controllable upper bound on the error. Further, the error estimate given by Theorem 7.4.5 will be used in the error equilibration for the MLMC estimator in Section 7.6. It allows to balance the errors resulting from the approximation of the diffusion coefficient and the finite element (FE) error resulting from the pathwise numerical approximation of the PDE solution.

7.5 Pathwise finite element approximation

In this section, we describe the numerical method which is used to compute pathwise approximations of the solution to the considered elliptic PDE following [96, Section 6]. We use a FE approach with standard triangulations and sample-adapted triangulations of the spatial domain, which is described in the following.

7.5.1 The standard pathwise finite element approximation

We approximate the solution u to problem (7.1) - (7.3) with diffusion coefficient a given by Equation (7.6) using a pathwise FE approximation of the solution $u_{K,A}^{(\varepsilon_W,\varepsilon_l)}$ of problem (7.12) - (7.14) with the approximated diffusion coefficient $a_{K,A}^{(\varepsilon_W,\varepsilon_l)}$ given by (7.11). Therefore, for almost all $\omega \in \Omega$, we aim to approximate the function $u_{K,A}^{(\varepsilon_W,\varepsilon_l)}(\omega, \cdot) \in V$ such that it holds

$$\begin{aligned}&B_{a_{K,A}^{(\varepsilon_W,\varepsilon_l)}(\omega)}(u_{K,A}^{(\varepsilon_W,\varepsilon_l)}(\omega,\cdot), v) := \int_{\mathcal{D}} a_{K,A}^{(\varepsilon_W,\varepsilon_l)}(\omega, \underline{x}) \nabla u_{K,A}^{(\varepsilon_W,\varepsilon_l)}(\omega, \underline{x}) \cdot \nabla v(\underline{x}) d\underline{x} \\ &= \int_{\mathcal{D}} f(\omega, \underline{x}) v(\underline{x}) d\underline{x} + \int_{\Gamma_2} g(\omega, \underline{x})[Tv](\underline{x}) d\underline{x} =: F_\omega(v), \end{aligned} \tag{7.15}$$

for every $v \in V$ with fixed approximation parameters $K, A, \varepsilon_W, \varepsilon_l$. We compute a numerical approximation of the solution to this variational problem using a standard Galerkin approach

with linear elements: assume $\mathcal{V} = (V_\ell,\ \ell \in \mathbb{N}_0)$ is a sequence of finite-dimensional subspaces $V_\ell \subset V$ with increasing $\dim(V_\ell) = d_\ell$. Further, we denote by $(h_\ell,\ \ell \in \mathbb{N}_0)$ the corresponding refinement sizes which are assumed to converge monotonically to zero for $\ell \to \infty$. Let $\ell \in \mathbb{N}_0$ be fixed and denote by $\{v_1^{(\ell)}, \dots, v_{d_\ell}^{(\ell)}\}$ a basis of V_ℓ. The (pathwise) discrete version of (7.15) reads: Find $u_{K,A,\ell}^{(\varepsilon_W,\varepsilon_l)}(\omega,\cdot) \in V_\ell$ such that

$$B_{a_{K,A}^{(\varepsilon_W,\varepsilon_l)}(\omega)}(u_{K,A,\ell}^{(\varepsilon_W,\varepsilon_l)}(\omega,\cdot), v_i^{(\ell)}) = F_\omega(v_i^{(\ell)}) \text{ for all } i = 1,\dots,d_\ell.$$

Expanding the function $u_{K,A,\ell}^{(\varepsilon_W,\varepsilon_l)}(\omega,\cdot)$ with respect to the basis $\{v_1^{(\ell)}, \dots, v_{d_\ell}^{(\ell)}\}$ yields the representation

$$u_{K,A,\ell}^{(\varepsilon_W,\varepsilon_l)}(\omega,\cdot) = \sum_{i=1}^{d_\ell} c_i v_i^{(\ell)},$$

where the coefficient vector $\mathbf{c} = (c_1,\dots,c_{d_\ell})^T \in \mathbb{R}^{d_\ell}$ is determined by the linear equation system

$$\mathbf{B}(\omega)\mathbf{c} = \mathbf{F}(\omega),$$

with a stochastic stiffness matrix $\mathbf{B}(\omega)_{i,j} = B_{a_{K,A}^{(\varepsilon_W,\varepsilon_l)}(\omega)}(v_i^{(\ell)}, v_j^{(\ell)})$ and load vector $\mathbf{F}(\omega)_i = F_\omega(v_i^{(\ell)})$ for $i,j = 1,\dots,d_\ell$.

Let $(\mathcal{K}_\ell,\ \ell \in \mathbb{N}_0)$ be a sequence of triangulations on $\mathcal{D}$ and denote by $\theta_\ell > 0$ the minimum interior angle of all triangles in $\mathcal{K}_\ell$. We assume $\theta_\ell \geq \theta > 0$ for a positive constant θ and define the maximum diameter of the triangulation $\mathcal{K}_\ell$ by $h_\ell := \max_{K\in\mathcal{K}_\ell} \operatorname{diam}(K)$, for $\ell \in \mathbb{N}_0$ as well as the finite dimensional subspaces by $V_\ell := \{v \in V \mid v|_K \in \mathcal{P}_1, K \in \mathcal{K}_\ell\}$, where $\mathcal{P}_1$ denotes the space of all polynomials up to degree one. If we assume that for $\mathbb{P}$-almost all $\omega \in \Omega$ it holds $u_{K,A}^{(\varepsilon_W,\varepsilon_l)}(\omega,\cdot) \in H^{1+\kappa_a}(\mathcal{D})$ for some positive number $\kappa_a > 0$, and that there exists a finite bound $\|u_{K,A}^{(\varepsilon_W,\varepsilon_l)}\|_{L^2(\Omega;H^{1+\kappa_a}(\mathcal{D}))} \leq C_u = C_u(K,A)$ for the fixed approximation parameters K, A, we immediately obtain the following estimate using Céa's lemma (see [16, Section 4], [96, Section 6], [67, Chapter 8])

$$\|u_{K,A}^{(\varepsilon_W,\varepsilon_l)} - u_{K,A,\ell}^{(\varepsilon_W,\varepsilon_l)}\|_{L^2(\Omega;V)} \leq C_{\theta,\mathcal{D}} \frac{A}{\overline{a}_-} C_u h_\ell^{\min(\kappa_a,1)}.$$

By construction of the subordinated GRF, we always obtain an interface geometry with fixed angles and bounded jump height in the diffusion coefficient, which have great influence on the solution regularity, see e.g. [105]. Note that, for general deterministic interface problems,

one obtains a pathwise discretization error of order $\kappa_a \in (1/2, 1)$ and in general one cannot expect the full order of convergence $\kappa_a = 1$ without special treatment of the discontinuities of the diffusion coefficient (see [10] and [16]). The convergence may be improved by the use of sample-adapted triangulations.

7.5.2 Sample-adapted triangulations

In [16], the authors suggest sample-adapted triangulations to improve the convergence of the FE approximation for elliptic jump-diffusion coefficients. This approach is also used in this paper and the convergence of the corresponding FE method is compared to the performance with the use of standard triangulations. The construction of the sample-adapted triangulations is explained in the following. Consider a fixed $\omega \in \Omega$ and assume that the discontinuities of the diffusion coefficient are described by the partition $\mathcal{T}(\omega) = (\mathcal{T}_i,\ i = 1, \dots, \tau(\omega))$ of the domain $\mathcal{D}$ with $\tau(\omega) \in \mathbb{N}$ and $\mathcal{T}_i \subset \mathcal{D}$. Assume that $\mathcal{K}_\ell(\omega)$ is a triangulation of $\mathcal{D}$ which is adjusted to the partition $\mathcal{T}(\omega)$ in the sense that for every $i = 1, \dots, \tau(\omega)$ it holds

$$\partial\mathcal{T}_i \subset \bigcup_{\kappa \in \mathcal{K}_\ell(\omega)} \partial\kappa \text{ and } \hat{h}_\ell(\omega) := \max_{K \in \mathcal{K}_\ell(\omega)} \operatorname{diam}(K) \leq \overline{h}_\ell,$$

for all $\ell \in \mathbb{N}_0$, where $(\overline{h}_\ell,\ \ell \in \mathbb{N}_0)$ is a deterministic, decreasing sequence of refinement thresholds which converges to zero. We denote by $\hat{V}_\ell(\omega) \subset V$ the corresponding finite-dimensional subspaces with dimension $\hat{d}_\ell(\omega) \in \mathbb{N}$. Figure 7.2 illustrates the adapted triangulation for a sample of the diffusion coefficient where we used a Poisson(5)-subordinated Matérn-1.5-GRF.

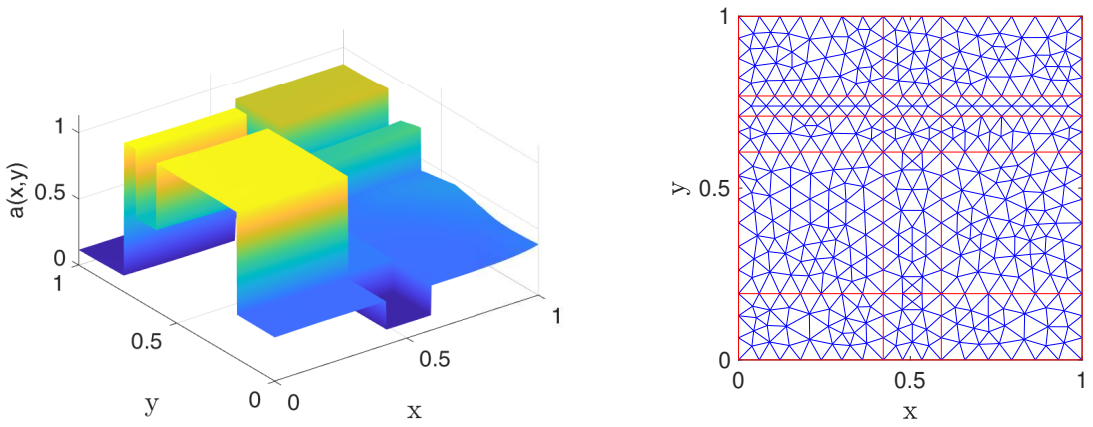

Figure 7.2: Sample of the diffusion coefficient using a Poisson-subordinated Matérn-1.5-GRF (left) with corresponding sample-adapted triangulation (right).

The sample-adapted approach leads to an improved sample-wise convergence rate for the elliptic PDE with discontinuous diffusion coefficient (see e.g. [16, Section 4.1]). This is particularly true in the situation of jump-diffusion coefficients with polygonal jump geometry, which is the case for the diffusion coefficients considered in this paper (see Figure 7.2, [16], [31], [96, Sections 6 and 7]). However, one should also mention that the sample-adapted approach causes additional computational costs since adapted meshes have to be constructed for each single sample of the diffusion coefficient. This might inflate the computational costs especially in situations of jump coefficients with many interfaces or jumps which are closely located to each other (see also Section 7.7 and Subsection 7.8.3).

While mean squared convergence rates cannot be derived theoretically in our general setting due to the stochastic regularity of the PDE solutions, in practice one at least recovers the convergence rates of the deterministic jump-diffusion problem in the strong error, which also has been investigated numerically in [96]. This observation, together with the comments in the end of Subsection 7.5.1, motivate the following assumption for the remaining theoretical analysis (see [96, Assumption 7.1]).

Assumption 7.5.1.
There exist deterministic constants $\hat{C}_u, C_u, \hat{\kappa}_a, \kappa_a > 0$ such that for any $\varepsilon_W, \varepsilon_l > 0$ and any $\ell \in \mathbb{N}_0$, the FE approximation errors of $\hat{u}_{K,A,\ell}^{(\varepsilon_W,\varepsilon_l)} \approx u_{K,A}^{(\varepsilon_W,\varepsilon_l)}$ in the (sample-adapted) subspaces $\hat{V}_\ell$, respectively $u_{K,A,\ell}^{(\varepsilon_W,\varepsilon_l)} \approx u_{K,A}^{(\varepsilon_W,\varepsilon_l)}$ in V_ℓ, are bounded by

$$\begin{aligned}
&\|u_{K,A}^{(\varepsilon_W,\varepsilon_l)} - \hat{u}_{K,A,\ell}^{(\varepsilon_W,\varepsilon_l)}\|_{L^2(\Omega;V)} \leq \hat{C}_u \mathbb{E}(\hat{h}_\ell^{2\hat{\kappa}_a})^{1/2}, \text{ respectively,} \\
&\|u_{K,A}^{(\varepsilon_W,\varepsilon_l)} - u_{K,A,\ell}^{(\varepsilon_W,\varepsilon_l)}\|_{L^2(\Omega;V)} \leq C_u h_\ell^{\kappa_a},
\end{aligned}$$

where the constants $\hat{C}_u, C_u$ may depend on a, f, g, K, A but are independent of $\hat{h}_\ell, h_\ell, \hat{\kappa}_a$ and κ_a. ◆

We remark that we expect $1 \geq \hat{\kappa}_a \geq \kappa_a > 0$ in Assumption 7.5.1 due to the observations given in the beginning of Subsection 7.5.2 (see also [96], [16] and Section 7.8).

Remark 7.5.2. *Assumption 7.4.4 on the integrability of the solution gradient and Assumption 7.5.1 on the convergence rate of the FE method are presented independently. We point out that both assumptions highly depend on the Sobolev regularity of the solution which dictates the integrability of the solution gradient (see for example [96, Remark 5.8]) and controls the convergence rate of the FE method (see for example [96, Remark 6.1]). Hence, both assumptions depend on the regularity of the solution, which itself is related to the specific choice of diffusion coefficient and, therefore,*

depends on Assumption 7.4.3. To describe the relation of these three assumptions is not possible in an explicit manner in the general stochastic setting considered, but one should keep in mind that they are not independent from each other. ◆

7.6 MLMC estimation of the solution

In this section we construct a multilevel Monte Carlo (MLMC) estimator for the expectation $\mathbb{E}(u_{K,A})$ of the PDE solution and prove an a-priori bound for the approximation error. We start with the introduction of a general singlelevel Monte Carlo (SLMC) estimation since the MLMC estimator is an extension of this approach.

The next lemma follows by the definition of the inner product on the Sobolev space $H^1(\mathcal{D})$ and will be useful in our theoretical investigations.

Lemma 7.6.1.
For independent, centered V-valued random variables Z_1 and Z_2 it holds

$$\mathbb{E}((Z_1, Z_2)_V) = 0.$$

◆

Proof. We use the definition of the inner product on $V \subset H^1(\mathcal{D})$ together with the independence of Z_1 and Z_2 to calculate

$$\mathbb{E}((Z_1, Z_2)_V) = \int_{\mathcal{D}} \mathbb{E}(\partial_x Z_1)\mathbb{E}(\partial_x Z_2) + \mathbb{E}(\partial_y Z_1)\mathbb{E}(\partial_y Z_2) + \mathbb{E}(Z_1)\mathbb{E}(Z_2) d(x,y) = 0.$$

□

Let $(u^{(i)},\ i \in \mathbb{N}) \subset L^2(\Omega; V)$ be a sequence of i.i.d. random variables and $M \in \mathbb{N}$ a fixed sample number. The *singlelevel Monte Carlo* estimator for the approximation of the mean $\mathbb{E}(u^{(1)})$ is defined by

$$E_M(u^{(1)}) := \frac{1}{M} \sum_{i=1}^{M} u^{(i)} \approx \mathbb{E}(u^{(1)}),$$

and we have the following standard result (see also [14] and [16]).

Lemma 7.6.2.
Let $M \in \mathbb{N}$ and $(u^{(i)},\ i \in \mathbb{N}) \subset L^2(\Omega; V)$ be a sequence of i.i.d. random variables. It holds

$$\|\mathbb{E}(u^{(1)}) - E_M(u^{(1)})\|_{L^2(\Omega;V)} = \sqrt{\frac{\mathrm{Var}(u^{(1)})}{M}} \leq \frac{\|u^{(1)}\|_{L^2(\Omega;V)}}{\sqrt{M}} \text{ and}$$
$$\|E_M(u^{(1)})\|_{L^2(\Omega;V)} \leq \|u^{(1)}\|_{L^2(\Omega;V)}.$$

◆

One major disadvantage of the SLMC estimator described above is the slow convergence of the (statistical) error for increasing sample numbers M (see Lemma 7.6.2 and [57]). Multilevel Monte Carlo (MLMC) uses multigrid concepts to reduce the computational complexity for the estimation of the mean compared to the singlelevel approach. The idea is to compute samples of FE approximations with different accuracy where one takes many samples of FE approximations with lower accuracy (and lower computationally costs) and less samples of FE approximations with higher accuracy (and higher computational cost), see also [57] and [59].

For fixed parameters K, A the goal is to approximate the value $\mathbb{E}(u_{K,A})$. For ease of notation, we focus here on the sample-adapted discretization with the corresponding approximation $\hat{u}_{K,A,\ell}^{(\varepsilon_W,\varepsilon_l)}$ with average refinement parameter $\mathbb{E}(\hat{h}_\ell^{2\hat{\kappa}_a})^{1/2}$ and convergence rate $\hat{\kappa}_a$ in this section (see Assumption 7.5.1). However, the reader should always keep in mind that all results also hold in the case of standard triangulations where $\mathbb{E}(\hat{h}_\ell^{2\hat{\kappa}_a})^{1/2}$ should be replaced by $h_\ell^{\kappa_a}$. We remind that the approximation parameters $\varepsilon_W > 0$ and $\varepsilon_l > 0$ correspond to the stepsize of the discrete grids on which the approximations $W_j^{(\varepsilon_W)} \approx W_j$ of the GRFs and $l_j^{(\varepsilon_l)} \approx l_j$ of the Lévy subordinators are defined, for $j = 1, 2$ (see Subsection 7.4.3).

Assume a maximum level $L \in \mathbb{N}$ is given. We consider finite-dimensional subspaces $(\hat{V}_\ell,\ \ell = 0, \dots, L)$ of V with refinement sizes $\hat{h}_0 > \cdots > \hat{h}_L > 0$ and approximation parameters $\varepsilon_{W,0} > \cdots > \varepsilon_{W,L}$ for the GRFs and $\varepsilon_{l,0} > \cdots > \varepsilon_{l,L}$ for the Lévy subordinators. Since we fix the parameters K and A in this analysis, we omit them in the following and use the notation $\hat{u}_{\varepsilon_{W,\ell},\varepsilon_{l,\ell},\ell} := \hat{u}_{K,A,\ell}^{(\varepsilon_{W,\ell},\varepsilon_{l,\ell})}$ for the FEM approximation of $u_{K,A}^{(\varepsilon_{W,\ell},\varepsilon_{l,\ell})}$ on $\hat{V}_\ell$, for $\ell = -1, \dots, L$, where we set $\hat{u}_{\varepsilon_{W,-1},\varepsilon_{l,-1},-1} := 0$. If we expand the expectation on the finest level in a telescopic sum we obtain the following representation

$$\mathbb{E}(\hat{u}_{\varepsilon_{W,L},\varepsilon_{l,L},L}) = \sum_{\ell=0}^{L} \mathbb{E}(\hat{u}_{\varepsilon_{W,\ell},\varepsilon_{l,\ell},\ell} - \hat{u}_{\varepsilon_{W,\ell-1},\varepsilon_{l,\ell-1},\ell-1}). \tag{7.16}$$

This motivates the multilevel Monte Carlo estimator, which estimates the left hand side of Equation (7.16) by singlelevel Monte Carlo estimations of each summand on the right hand side

(see [57]). To be precise, let M_ℓ be a natural number for $\ell = 0, ..., L$. The multilevel Monte Carlo estimator of $\hat{u}_{\varepsilon_{W,L},\varepsilon_{l,L},L}$ is then defined by

$$\begin{aligned} E^L(\hat{u}_{\varepsilon_{W,L},\varepsilon_{l,L},L}) &:= \sum_{\ell=0}^{L} E_{M_\ell}(\hat{u}_{\varepsilon_{W,\ell},\varepsilon_{l,\ell},\ell} - \hat{u}_{\varepsilon_{W,\ell-1},\varepsilon_{l,\ell-1},\ell-1}), \\ &= \sum_{\ell=0}^{L} \frac{1}{M_\ell} \sum_{i=1}^{M_\ell} (\hat{u}^{(i,\ell)}_{\varepsilon_{W,\ell},\varepsilon_{l,\ell},\ell} - \hat{u}^{(i,\ell)}_{\varepsilon_{W,\ell-1},\varepsilon_{l,\ell-1},\ell-1}) \end{aligned}$$

where $(\hat{u}^{(i,\ell)}_{\varepsilon_{W,\ell},\varepsilon_{l,\ell},\ell})_{i=1}^{M_\ell}$ (resp. $(\hat{u}^{(i,\ell)}_{\varepsilon_{W,\ell-1},\varepsilon_{l,\ell-1},\ell-1})_{i=1}^{M_\ell}$) are M_ℓ i.i.d. copies of the random variable $\hat{u}_{\varepsilon_{W,\ell},\varepsilon_{l,\ell},\ell}$ (resp. $\hat{u}_{\varepsilon_{W,\ell-1},\varepsilon_{l,\ell-1},\ell-1}$) for $\ell = 0, \dots, L$ (see also [57]). The following result gives an a-priori bound on the MLMC error. Similar formulations can be found, for example, in [14], [1] and [16].

Theorem 7.6.3.
We set $r = 2$ and assume $q > 2$ in Assumption 7.4.3. Further, let $b, c \geq 1$ be given such that Theorem 7.4.5 holds. For $L \in \mathbb{N}$, let $\hat{h}_\ell > 0$, M_ℓ, $\varepsilon_{W,\ell} > 0$ and $\varepsilon_{l,\ell} > 0$ be the level-dependent approximation parameters for $\ell = 0, ..., L$ such that $\hat{h}_\ell$, $\varepsilon_{W,\ell}$, and $\varepsilon_{l,\ell}$ are decreasing with respect to ℓ. It holds

$$\begin{aligned} \|\mathbb{E}(u_{K,A}) - E^L(\hat{u}_{\varepsilon_{W,L},\varepsilon_{l,L},L})\|_{L^2(\Omega;V)} \leq C\Big(&\varepsilon_{W,L}^{\gamma} + \varepsilon_{l,L}^{\frac{1}{2c}} + \mathbb{E}(\hat{h}_L^{2\hat{\kappa}_a})^{1/2} + \frac{1}{\sqrt{M_0}} \\ &+ \sum_{\ell=0}^{L-1} \frac{\varepsilon_{W,\ell}^{\gamma} + \varepsilon_{l,\ell}^{\frac{1}{2c}} + \mathbb{E}(\hat{h}_\ell^{2\hat{\kappa}_a})^{1/2}}{\sqrt{M_{\ell+1}}}\Big), \end{aligned}$$

where $C > 0$ is a constant which is independent of L and the level-dependent approximation parameters. Note that the numbers $\gamma > 0$ and $c \geq 1$ are determined by the GRFs resp. the subordinators (cf. Theorem 7.4.5). ◆

Proof. We estimate

$$\begin{aligned} \|\mathbb{E}(u_{K,A}) - E^L(\hat{u}_{\varepsilon_{W,L},\varepsilon_{l,L},L})\|_{L^2(\Omega;V)} &\leq \|\mathbb{E}(u_{K,A}) - \mathbb{E}(\hat{u}_{\varepsilon_{W,L},\varepsilon_{l,L},L})\|_{L^2(\Omega;V)} \\ &\quad + \|\mathbb{E}(\hat{u}_{\varepsilon_{W,L},\varepsilon_{l,L},L}) - E^L(\hat{u}_{\varepsilon_{W,L},\varepsilon_{l,L},L})\|_{L^2(\Omega;V)} \\ &=: I_1 + I_2. \end{aligned}$$

We use the triangular inequality, Theorem 7.4.5 and Assumption 7.5.1 to obtain

$$I_1 \leq \mathbb{E}(\|u_{K,A} - \hat{u}_{\varepsilon_{W,L},\varepsilon_{l,L},L}\|_V) \leq C_{reg} C(\overline{a}_-, \mathcal{D})(\varepsilon_{W,L}^{\gamma} + \varepsilon_{l,L}^{\frac{1}{2c}}) + \hat{C}_u \mathbb{E}(\hat{h}_L^{2\hat{\kappa}_a})^{\frac{1}{2}}.$$

For the second term we use the definition of the MLMC estimator E^L and Lemma 7.6.2 to obtain

$$\begin{aligned} I_2 &\leq \sum_{\ell=0}^{L} \Big(\frac{\mathrm{Var}(\hat{u}_{\varepsilon_{W,\ell},\varepsilon_{l,\ell},\ell} - \hat{u}_{\varepsilon_{W,\ell-1},\varepsilon_{l,\ell-1},\ell-1})}{M_\ell} \Big)^{1/2} \\ &\leq \sum_{\ell=0}^{L} \frac{1}{\sqrt{M_\ell}} \Big(\|\hat{u}_{\varepsilon_{W,\ell},\varepsilon_{l,\ell},\ell} - u_{K,A}\|_{L^2(\Omega;V)} + \|u_{K,A} - \hat{u}_{\varepsilon_{W,\ell-1},\varepsilon_{l,\ell-1},\ell-1}\|_{L^2(\Omega;V)} \Big). \end{aligned}$$

Similar as for the first summand I_1 we apply Theorem 7.4.5 and Assumption 7.5.1 to get

$$\|\hat{u}_{\varepsilon_{W,\ell},\varepsilon_{l,\ell},\ell} - u_{K,A}\|_{L^2(\Omega;V)} \leq C_{reg} C(\overline{a}_-, \mathcal{D})(\varepsilon_{W,\ell}^{\gamma} + \varepsilon_{l,\ell}^{\frac{1}{2c}}) + \hat{C}_u \mathbb{E}(\hat{h}_\ell^{2\hat{\kappa}_a})^{\frac{1}{2}},$$

for $\ell = 0, \dots, L$ and for $\ell = -1$ it follows from Theorem 7.4.2 that

$$\|u_{K,A}\|_{L^2(\Omega;V)} \leq C(\overline{a}_-, \mathcal{D})(\|f\|_{L^q(\Omega;H)} + \|g\|_{L^q(\Omega;L^2(\Gamma_2))}),$$

since $q > 2$. Finally, we calculate

$$\begin{aligned} &I_1 + I_2 \\ &\leq C_{reg} C(\overline{a}_-, \mathcal{D}) \Big(\varepsilon_{W,L}^{\gamma} + \varepsilon_{l,L}^{\frac{1}{2c}} + \frac{\varepsilon_{W,0}^{\gamma} + \varepsilon_{l,0}^{\frac{1}{2c}}}{\sqrt{M_0}} + \sum_{\ell=1}^{L} \frac{1}{\sqrt{M_\ell}} (\varepsilon_{W,\ell}^{\gamma} + \varepsilon_{l,\ell}^{\frac{1}{2c}} + \varepsilon_{W,\ell-1}^{\gamma} + \varepsilon_{l,\ell-1}^{\frac{1}{2c}}) \Big) \\ &+ \hat{C}_u \Big(\mathbb{E}(\hat{h}_L^{2\hat{\kappa}_a})^{\frac{1}{2}} + \frac{\mathbb{E}(\hat{h}_0^{2\hat{\kappa}_a})^{1/2}}{\sqrt{M_0}} + \sum_{\ell=1}^{L} \frac{1}{\sqrt{M_\ell}} (\mathbb{E}(\hat{h}_\ell^{2\hat{\kappa}_a})^{\frac{1}{2}} + \mathbb{E}(\hat{h}_{\ell-1}^{2\hat{\kappa}_a})^{\frac{1}{2}}) \Big) \\ &+ \frac{1}{\sqrt{M_0}} C(\overline{a}_-, \mathcal{D})(\|f\|_{L^q(\Omega;H)} + \|g\|_{L^q(\Omega;L^2(\Gamma_2))}) \\ &\leq C \Big(\varepsilon_{W,L}^{\gamma} + \varepsilon_{l,L}^{\frac{1}{2c}} + \mathbb{E}(\hat{h}_L^{2\hat{\kappa}_a})^{1/2} + \frac{1}{\sqrt{M_0}} + \sum_{\ell=0}^{L-1} \frac{\varepsilon_{W,\ell}^{\gamma} + \varepsilon_{l,\ell}^{\frac{1}{2c}} + \mathbb{E}(\hat{h}_\ell^{2\hat{\kappa}_a})^{1/2}}{\sqrt{M_{\ell+1}}} \Big), \end{aligned}$$

where we used the monotonicity of $(\varepsilon_{W,\ell})_{\ell=0}^L$, $(\varepsilon_{l,\ell})_{\ell=0}^L$ and $(\hat{h}_\ell)_{\ell=0}^L$. □

The error estimate of Theorem 7.6.3 allows for an equilibration of the error contributions resulting from the approximation of the diffusion coefficient and the approximation of the pathwise solution with the FE method which then leads to a higher computational efficiency

compared to the singlelevel approach. This leads in general to the strategy that one takes only few of the accurate, but expensive samples for large $\ell \in \{0, \dots, L\}$ and one generates more on the cheap, but less accurate samples on the lower levels, which can be seen in the following corollary (see also [16, Section 5], [57] and [59]).

Corollary 7.6.4.
Let the assumptions of Theorem 7.6.3 hold. For $L \in \mathbb{N}$ and given (stochastic) refinement parameters $\hat{h}_0 > \cdots > \hat{h}_L > 0$ choose $\varepsilon_{W,\ell} > 0$ and $\varepsilon_{l,\ell} > 0$ such that

$$\varepsilon_{W,\ell} \simeq \mathbb{E}(\hat{h}_\ell^{2\hat{\kappa}_a})^{1/(2\gamma)} \text{ and } \varepsilon_{l,\ell} \simeq \mathbb{E}(\hat{h}_\ell^{2\hat{\kappa}_a})^c, \tag{7.17}$$

and sample numbers $M_\ell \in \mathbb{N}$ according to

$$M_0 \simeq \mathbb{E}(\hat{h}_L^{2\hat{\kappa}_a})^{-1} \text{ and } M_\ell \simeq \mathbb{E}(\hat{h}_L^{2\hat{\kappa}_a})^{-1}\mathbb{E}(\hat{h}_{\ell-1}^{2\hat{\kappa}_a})(\ell+1)^{2(1+\xi)} \text{ for } \ell = 1, \dots, L, \tag{7.18}$$

for some positive parameter $\xi > 0$. Then, it holds

$$\|\mathbb{E}(u_{K,A}) - E^L(\hat{u}_{\varepsilon_{W,L},\varepsilon_{l,L},L})\|_{L^2(\Omega;V)} = \mathcal{O}(\mathbb{E}(\hat{h}_L^{2\hat{\kappa}_a})^{1/2}).$$

◆

Proof. We use Theorem 7.6.3 together with Equation (7.17) and Equation (7.18) to obtain

$$\begin{aligned}
&\|\mathbb{E}(u_{K,A}) - E^L(\hat{u}_{\varepsilon_{W,L},\varepsilon_{l,L},L})\|_{L^2(\Omega;V)} \\
&\qquad \le C\Big(\varepsilon_{W,L}^{\gamma} + \varepsilon_{l,L}^{\frac{1}{2c}} + \mathbb{E}(\hat{h}_L^{2\hat{\kappa}_a})^{1/2} + \frac{1}{\sqrt{M_0}} + \sum_{\ell=0}^{L-1} \frac{\varepsilon_{W,\ell}^{\gamma} + \varepsilon_{l,\ell}^{\frac{1}{2c}} + \mathbb{E}(\hat{h}_\ell^{2\hat{\kappa}_a})^{1/2}}{\sqrt{M_{\ell+1}}}\Big) \\
&\qquad \le C\mathbb{E}(\hat{h}_L^{2\hat{\kappa}_a})^{1/2}\Big(4 + \sum_{\ell=1}^{L} \frac{1}{(\ell+1)^{1+\xi}}\Big) \le C(4 + \zeta(1+\xi))\mathbb{E}(\hat{h}_L^{2\hat{\kappa}_a})^{1/2},
\end{aligned}$$

where $\zeta(\cdot)$ denotes the Riemann zeta function. □

7.7 Multilevel Monte Carlo with control variates

The jump discontinuities in the coefficient $a_{K,A}$ of the elliptic problem (7.7) - (7.10) have a negative impact on the FE convergence due to the low regularity of the solution (see Section 7.5 and [96]). In Subsection 7.5.2 we presented one possible approach to enhance the FE

convergence for discontinuous diffusion coefficients: the sample-adapted FE approach with triangulations adjusted to the discontinuities. However, this approach may be computationally not feasible anymore if one has many jump interfaces. For instance, using subordinators with high jump activity (e.g. Gamma subordinators) may result in a very high number of discontinuities making the construction of sample-adapted triangulations extremely expensive. Besides the usage of adapted triangulations, *variance reduction* techniques can also be used to improve the computational efficiency of the MLMC estimation of the mean of the PDE solution, as we see in this section. We start with an introduction to a specific variance reduction technique, the *control variates* (CV), and show subsequently how we use a control variate in our setting (cf. [101]).

7.7.1 Control variates as a variance reduction technique

Assume Y is a real-valued, square integrable random variable and $(Y_i,\ i \in \mathbb{N})$ is a sequence of i.i.d. random variables which follow the same distribution as Y. For a fixed number of samples $M \in \mathbb{N}$, the SLMC estimator for the estimation of the expectation $\mathbb{E}(Y)$ is given by $E_M(Y) = M^{-1}\sum_{i=1}^{M} Y_i$ (see Section 7.6) and we have the following representation for the statistical error (see Lemma 7.6.2):

$$\|\mathbb{E}(Y) - E_M(Y)\|_{L^2(\Omega;\mathbb{R})} = \sqrt{\frac{\mathrm{Var}(Y)}{M}}. \tag{7.19}$$

The use of control variates aims to reduce the statistical error of a MC estimation by reducing the variance on the right hand side of (7.19). Assume we are given another real valued, square integrable random variable X with known expectation $\mathbb{E}(X)$ and a corresponding sequence of i.i.d. random variables $(X_i,\ i \in \mathbb{N})$ following the same distribution as X. For a given number of samples $M \in \mathbb{N}$, the control variate estimator is then defined by

$$E_M^{CV}(Y) = \frac{1}{M}\sum_{i=1}^{M} Y_i - (X_i - \mathbb{E}(X)),$$

(see, for example, [62, Section 4.1]). The estimator $E_M^{CV}(Y)$ is unbiased for the estimation of $\mathbb{E}(Y)$ and the standard deviation is

$$\begin{aligned}\mathrm{Var}(E_M^{CV}(Y))^{1/2} &= \|\mathbb{E}(Y) - E_M^{CV}(Y)\|_{L^2(\Omega;\mathbb{R})} \\ &= \sqrt{\frac{\mathrm{Var}(Y) + \mathrm{Var}(X) - 2\,\mathrm{Cov}(X,Y)}{M}},\end{aligned}$$

where $\mathrm{Cov}(X,Y)$ denotes the covariance of the random variables X and Y. Hence, the standard deviation of the estimator $E_M^{CV}(Y)$, i.e. the statistical error, is smaller than the standard deviation of the SLMC estimator $E_M(Y)$ if the random variables X and Y are highly correlated (see [62, Section 4.1.1]).

In [101], the authors presented a MLMC-CV combination for the estimation of the mean of the solution to the problem (7.1) - (7.3), where the diffusion coefficient a is modeled as a lognormal GRF. They use a smoothed version of the GRF and the pathwise solution to the corresponding PDE problem to construct a highly-correlated control variate. The considered GRFs have at least continuous paths leading to continuous diffusion coefficients. In the following, we show how we use a similar approach for our discontinuous diffusion coefficients to enhance the efficiency of the MLMC estimator for the case of subordinators with high jump activity.

7.7.2 Smoothing the diffusion coefficient

In this section we construct the control variate which is used to enhance the MLMC estimation of the mean of the solution to (7.7) - (7.10) for subordinators with high jump activity. Our approach is motivated by [101].

For a positive smoothing parameter $\nu_s > 0$ we consider the Gaussian kernel on $\mathbb{R}^2$:

$$\phi_{\nu_s}(x,y) = e^{-\frac{x^2+y^2}{2\nu_s^2}}(2\pi\nu_s^2)^{-1}, \text{ for } (x,y) \in \mathbb{R}^2.$$

Further, we identify the jump-diffusion coefficient $a_{K,A}$ from Equation (7.10) with its extended version on the domain $\mathbb{R}^2$, where we set $a_{K,A}(x,y) = 0$ for $(x,y) \in \mathbb{R}^2 \setminus \mathcal{D}$, and define the smoothed version $a_{K,A}^{(\nu_s)}$ by convolution with the Gaussian kernel:

$$a_{K,A}^{(\nu_s)}(x,y) = \int_{\mathbb{R}^2} \phi_{\nu_s}(x',y') a_{K,A}(x-x', y-y') d(x',y') \\ = \int_{\mathbb{R}^2} \phi_{\nu_s}(x-x', y-y') a_{K,A}(x',y') d(x',y'), \text{ for } (x,y) \in \mathcal{D}.$$

Obviously, Theorem 7.4.2 applies also to the elliptic PDE (7.7) - (7.9) with smoothed coefficient $a_{K,A}^{(\nu_s)}$, which guarantees the existence of a solution $u_{K,A}^{(\nu_s)} \in L^r(\Omega; V)$, for $r \in [1, q)$, with $f \in L^q(\Omega; H)$ and $g \in L^q(\Omega; L^2(\Gamma_2))$, and yields the bound

$$\|u_{K,A}^{(\nu_s)}\|_{L^r(\Omega;V)} \leq C(\overline{a}_-, \mathcal{D}, \nu_s)(\|f\|_{L^q(\Omega;H)} + \|g\|_{L^q(\Omega;L^2(\Gamma_2))}). \tag{7.20}$$

If the smoothing parameter ν_s is small, the solution corresponding to the smoothed coefficient $a_{K,A}^{(\nu_s)}$ is highly correlated with the solution to the PDE with (unsmoothed) diffusion coefficient $a_{K,A}$. Therefore, the smoothed solution is a reasonable choice as a control variate in the MLMC estimator since it is highly correlated with the solution to the rough problem and easy to approximate using the FE method due to the high regularity compared to the rough problem (see also [101] and [67, Sections 8 and 9]). Figure 7.3 shows a sample of the diffusion coefficient and smoothed versions using a Gaussian kernel with different smoothness parameters.

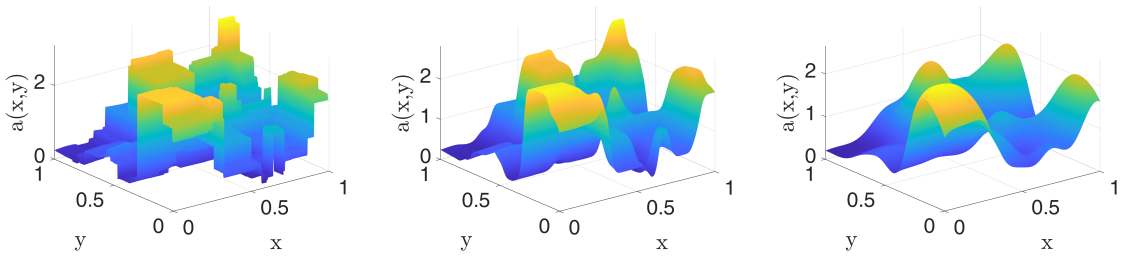

Figure 7.3: Sample of the diffusion coefficient $a_{K,A}$ using a Gamma-subordinated Matérn GRF (left), smoothed versions of the coefficient using Gaussian kernel smoothing with smoothness parameter $\nu_s = 0.02$ (middle) and $\nu_s = 0.06$ (right).

7.7.3 MLMC-CV estimator

Next, we define the MLMC-CV estimator following [101]. We fix a positive smoothing parameter $\nu_s > 0$. We assume $L \in \mathbb{N}$ and consider finite-dimensional subspaces $(\hat{V}_\ell,\ \ell = 0, \dots, L)$ of V with refinement sizes $\hat{h}_0 > \cdots > \hat{h}_L > 0$ and approximation parameters $\varepsilon_{W,0} > \cdots > \varepsilon_{W,L}$ for the GRFs and $\varepsilon_{l,0} > \cdots > \varepsilon_{l,L}$ for the Lévy subordinators (see Subsection 7.5.2). To

unify notation, we focus here again on the sample-adapted discretization with corresponding approximation $\hat{u}_{K,A,\ell}^{(\varepsilon_W,\varepsilon_l)}$ with averaged refinement parameter $\mathbb{E}(\hat{h}_\ell^{2\hat{\kappa}_a})^{1/2}$ and convergence rate $\hat{\kappa}_a$ for the theoretical analysis of the estimator (see Assumption 7.5.1 and Section 7.6) and point out again that similar results hold for the non-adapted FE approach. Since we again fix the parameters K and A in this analysis, we omit them in the following and use the notation $\hat{u}_{\varepsilon_{W,\ell},\varepsilon_{l,\ell},\ell} := \hat{u}_{K,A,\ell}^{(\varepsilon_{W,\ell},\varepsilon_{l,\ell})}$ for the FEM approximation on $\hat{V}_\ell$, for $\ell = 0,\dots,L$. Similar, we denote by $\hat{u}_{\varepsilon_{W,\ell},\varepsilon_{l,\ell},\ell}^{(\nu_s)} := \hat{u}_{K,A,\ell}^{(\nu_s,\varepsilon_{W,\ell},\varepsilon_{l,\ell})}$, for $\ell = 0,\dots,L$, the (pathwise) solution to problem (7.1) - (7.3) with diffusion coefficient $a_{K,A}^{(\nu_s,\varepsilon_{W,\ell},\varepsilon_{l,\ell})}$ as the smoothed version of the coefficient $a_{K,A}^{(\varepsilon_{W,\ell},\varepsilon_{l,\ell})}$ constructed in (7.11). We define the CV basis experiment by

$$\hat{u}_{\varepsilon_{W,\ell},\varepsilon_{l,\ell},\ell}^{CV} := \hat{u}_{\varepsilon_{W,\ell},\varepsilon_{l,\ell},\ell} - (\hat{u}_{\varepsilon_{W,\ell},\varepsilon_{l,\ell},\ell}^{(\nu_s)} - \mathbb{E}(u_{K,A}^{(\nu_s)})), \text{ for } \ell = 0,\dots,L, \tag{7.21}$$

and we set $\hat{u}_{\varepsilon_{W,-1},\varepsilon_{l,-1},-1}^{CV} = 0$. For the moment, we assume that the expectation $\mathbb{E}(u_{K,A}^{(\nu_s)})$ of the solution to the smoothed problem is known. Later, we elaborate more on appropriate approximations of this expectation (see Remark 7.7.7). The MLMC-CV estimator for the estimation of the expectation of the solution is then defined by

$$E^{CV,L}(\hat{u}_{\varepsilon_{W,L},\varepsilon_{l,L},L}^{CV}) := \sum_{\ell=0}^{L} E_{M_\ell}(\hat{u}_{\varepsilon_{W,\ell},\varepsilon_{l,\ell},\ell}^{CV} - \hat{u}_{\varepsilon_{W,\ell-1},\varepsilon_{l,\ell-1},\ell-1}^{CV}),$$

with sample sizes $M_\ell \in \mathbb{N}$ for $\ell = 0,\dots,L$.

Remark 7.7.1. *The smoothness parameter ν_s controls the variance reduction achieved in the MLMC-CV estimator and its optimal choice remains an open question (see [101]). This parameter shifts variance from the rough problem to the smoothed problem within the MLMC-CV estimator. Too large choices of ν_s lead to a small correlation between the rough and the smoothed problem which might result in a poor variance reduction in the MLMC-CV estimator. On the other hand, choosing ν_s too small might result in high costs for the computation of the CV (see also Remark 7.7.7). Therefore, the smoothness parameter should be chosen to balance these two viewpoints, which is highly problem dependent (see Subsection 7.8.3 and [101]).* ◆

7.7.4 Convergence of the MLMC-CV estimator

For the theoretical investigation of the MLMC-CV estimator we extend Assumption 7.5.1 by the following assumption on the mean-square convergence rate of the pathwise FE method for the smoothed problem.

Assumption 7.7.2.
There exist deterministic constants $\hat{C}_{u,s}, C_{u,s}$ such that for any $\varepsilon_W, \varepsilon_l > 0$ and any $\ell \in \mathbb{N}_0$, the FE approximation errors of $\hat{u}_{K,A,\ell}^{(\nu_s,\varepsilon_W,\varepsilon_l)} \approx u_{K,A}^{(\nu_s,\varepsilon_W,\varepsilon_l)}$ in the subspaces $\hat{V}_\ell$, respectively $u_{K,A,\ell}^{(\nu_s,\varepsilon_W,\varepsilon_l)} \approx u_{K,A}^{(\nu_s,\varepsilon_W,\varepsilon_l)}$ in V_ℓ, are bounded by

$$\|u_{K,A}^{(\nu_s,\varepsilon_W,\varepsilon_l)} - \hat{u}_{K,A,\ell}^{(\nu_s,\varepsilon_W,\varepsilon_l)}\|_{L^2(\Omega;V)} \leq \hat{C}_{u,s}\mathbb{E}(\hat{h}_\ell^2)^{1/2}, \text{ respectively,}$$
$$\|u_{K,A}^{(\nu_s,\varepsilon_W,\varepsilon_l)} - u_{K,A,\ell}^{(\nu_s,\varepsilon_W,\varepsilon_l)}\|_{L^2(\Omega;V)} \leq C_{u,s}h_\ell,$$

where the constants $\hat{C}_{u,s}, C_{u,s}$ may depend on a, f, g, K, A but are independent of $\hat{h}_\ell$ and h_ℓ. Further, we assume that Assumption 7.4.4 also holds for the solution $u_{K,A}^{(\nu_s)}$ corresponding to the elliptic PDE with the smoothed coefficient $a_{K,A}^{(\nu_s)}$. ◆

Note that this assumption is natural since we expect (pathwise) full order convergence of the linear FE method for the smoothed elliptic PDE (see also [1], [14], [16], [101] and [67, Section 8.5] together with [50, Section 6.3]). The assumption on the integrability of the gradient of the solution corresponding to the smoothed problem is also natural under Assumption 7.4.4, since the solution has a higher regularity than the solution $u_{K,A}$ to the elliptic problem with the jump-diffusion coefficient $a_{K,A}$. The following lemma states that the approximation error of the smoothed coefficient can be bounded by the approximation error of the rough diffusion coefficient.

Lemma 7.7.3.
For $t > 1$ and fixed parameters $\nu_s, K, A > 0$ and any $\varepsilon_W, \varepsilon_l > 0$ it holds for $\mathbb{P}$-almost every $\omega \in \Omega$

$$\|a_{K,A}^{(\nu_s)} - a_{K,A}^{(\nu_s,\varepsilon_W,\varepsilon_l)}\|_{L^t(\mathcal{D})}^t \leq C(t,\nu_s,\mathcal{D})\|a_{K,A} - a_{K,A}^{(\varepsilon_W,\varepsilon_l)}\|_{L^t(\mathcal{D})}^t,$$

with a constant $C = C(t,\nu_s,\mathcal{D})$ which depends only on the indicated parameters. ◆

Proof. Let $t' > 1$ such that $1/t + 1/t' = 1$. We calculate using Hölder's inequality and

the integrability of the Gaussian kernel ϕ_{ν_s}

$$\begin{aligned}
&\|a_{K,A}^{(\nu_s)} - a_{K,A}^{(\nu_s,\varepsilon_W,\varepsilon_l)}\|_{L^t(\mathcal{D})}^t \\
&\leq \int_{\mathcal{D}} \Big(\int_{\mathbb{R}^2} |\phi_{\nu_s}(x',y')(a_{K,A}(x-x',y-y') \\
&\qquad\qquad - a_{K,A}^{(\varepsilon_W,\varepsilon_l)}(x-x',y-y'))|d(x',y')\Big)^t d(x,y) \\
&\leq \int_{\mathcal{D}} \Big(\int_{\mathbb{R}^2} |a_{K,A}(x-x',y-y') - a_{K,A}^{(\varepsilon_W,\varepsilon_l)}(x-x',y-y')|^t d(x',y')\Big) \\
&\qquad\qquad \times \Big(\int_{\mathbb{R}^2} \phi_{\nu_s}(x',y')^{t'} d(x',y')\Big)^{t/t'} d(x,y) \\
&\leq C(t,\nu_s,\mathcal{D})\|a_{K,A} - a_{K,A}^{(\varepsilon_W,\varepsilon_l)}\|_{L^t(\mathcal{D})}^t.
\end{aligned}$$

□

In order to proof the convergence of the MLMC-CV estimator we need the following error bound on the approximation of the solution of the smoothed problem (cf. Theorem 7.4.5). As expected, this error bound depends on the approximation parameters ε_W of the GRFs and ε_l of the Lévy subordinators in the same way as the error bound of the unsmoothed problem in Theorem 7.4.5.

Theorem 7.7.4.
Assume $q > 2$ in Assumption 7.4.3. Let $r \in [2,q)$ and $b, c \in [1,+\infty]$ be given such that it holds

$$rc\gamma \geq 2 \text{ and } 2b \leq rc < \eta$$

with a fixed real number $\gamma \in (0, \min(1, \beta/(2\alpha))$. Here, the parameters η, α and β are determined by the GRFs W_1, W_2 and the Lévy subordinators l_1, l_2 (see Assumption 7.4.3).

Let $m, n \in [1,+\infty]$ be real numbers such that

$$\frac{1}{m} + \frac{1}{c} = \frac{1}{n} + \frac{1}{b} = 1,$$

and let $k_{reg} \geq 2$ and $j_{reg} > 0$ be the regularity specifiers given by Assumption 7.4.4. If it holds that

$$n < 1 + \frac{j_{reg}}{2} \text{ and } rm < k_{reg},$$

then the approximated solution $u_{K,A}^{(\nu_s,\varepsilon_W,\varepsilon_l)}$ of the smoothed problem converges to the solution $u_{K,A}^{(\nu_s)}$

of the truncated smoothed problem for $\varepsilon_W, \varepsilon_l \to 0$ and it holds

$$\begin{aligned}\|u_{K,A}^{(\nu_s)} - u_{K,A}^{(\nu_s,\varepsilon_W,\varepsilon_l)}\|_{L^r(\Omega;V)} &\leq C(\overline{a}_-, \mathcal{D}, r) C_{reg} \|a_{K,A}^{(\nu_s,\varepsilon_W,\varepsilon_l)} - a_{K,A}^{(\nu_s)}\|_{L^{rc}(\Omega;L^{2b}(\mathcal{D}))} \\ &\leq C_{reg} C(\overline{a}_-, \mathcal{D}, r, \nu_s)(\varepsilon_W^{\gamma} + \varepsilon_l^{\frac{1}{rc}}).\end{aligned}$$

◆

Proof. This theorem follows by the same arguments used in [96, Theorem 5.11] together with Lemma 7.7.3. □

We are now able to prove the following a-priori bound on the mean-square error of the MLMC-CV estimator, similar to Theorem 7.6.3.

Theorem 7.7.5.
We set $r = 2$ and assume $q > 2$. Further, let $b, c \geq 1$ be given such that Theorem 7.4.5 (and Theorem 7.7.4) hold. For $L \in \mathbb{N}$, let $\hat{h}_\ell > 0$, M_ℓ, $\varepsilon_{W,\ell} > 0$ and $\varepsilon_{l,\ell} > 0$ be the level-dependent approximation parameters, for $\ell = 0, ..., L$, such that $\hat{h}_\ell$, $\varepsilon_{W,\ell}$, and $\varepsilon_{l,\ell}$ decrease with respect to ℓ. It holds

$$\begin{aligned}\|\mathbb{E}(u_{K,A}) - E^{CV,L}(\hat{u}^{CV}_{\varepsilon_{W,L},\varepsilon_{l,L},L})\|_{L^2(\Omega;V)} \leq C\Big(&\varepsilon_{W,L}^{\gamma} + \varepsilon_{l,L}^{\frac{1}{2c}} + \mathbb{E}(\hat{h}_L^{2\hat{\kappa}_a})^{1/2} + \frac{1}{\sqrt{M_0}} \\ &+ \sum_{\ell=0}^{L-1} \frac{\varepsilon_{W,\ell}^{\gamma} + \varepsilon_{l,\ell}^{\frac{1}{2c}} + \mathbb{E}(\hat{h}_\ell^{2\hat{\kappa}_a})^{1/2}}{\sqrt{M_{\ell+1}}}\Big),\end{aligned}$$

where $C > 0$ is a constant which is independent of L and the level-dependent approximation parameters. Note that the numbers $\gamma > 0$ and $c \geq 1$ are determined by the GRFs resp. the subordinators (cf. Theorem 7.4.5 and Theorem 7.7.4). ◆

Proof. We split the error by

$$\begin{aligned}\|\mathbb{E}(u_{K,A}) - E^{CV,L}(\hat{u}^{CV}_{\varepsilon_{W,L},\varepsilon_{l,L},L})\|_{L^2(\Omega;V)} &\leq \|\mathbb{E}(u_{K,A}) - \mathbb{E}(\hat{u}^{CV}_{\varepsilon_{W,L},\varepsilon_{l,L},L})\|_{L^2(\Omega;V)} \\ &\quad + \|\mathbb{E}(\hat{u}^{CV}_{\varepsilon_{W,L},\varepsilon_{l,L},L}) - E^{CV,L}(\hat{u}^{CV}_{\varepsilon_{W,L},\varepsilon_{l,L},L})\|_{L^2(\Omega;V)} \\ &=: I_1 + I_2.\end{aligned}$$

For the first term we estimate using Theorem 7.4.5 and Assumption 7.5.1 together with Theorem

7.7.4 and Assumption 7.7.2 to obtain

$$\begin{aligned}
I_1 &\leq \mathbb{E}(\|u_{K,A} - \hat{u}_{\varepsilon_{W,L},\varepsilon_{l,L},L}\|_V) + \mathbb{E}(\|\hat{u}^{(\nu_s)}_{\varepsilon_{W,L},\varepsilon_{l,L},L} - u^{(\nu_s)}_{K,A}\|_V) \\
&\leq \|u_{K,A} - u^{(\varepsilon_{W,L},\varepsilon_{l,L})}_{K,A}\|_{L^2(\Omega;V)} + \|u^{(\varepsilon_{W,L},\varepsilon_{l,L})}_{K,A} - \hat{u}_{\varepsilon_{W,L},\varepsilon_{l,L},L}\|_{L^2(\Omega;V)} \\
&+ \|u^{(\nu_s)}_{K,A} - u^{(\nu_s,\varepsilon_{W,L},\varepsilon_{l,L})}_{K,A}\|_{L^2(\Omega;V)} + \|u^{(\nu_s,\varepsilon_{W,L},\varepsilon_{l,L})}_{K,A} - \hat{u}^{(\nu_s)}_{\varepsilon_{W,L},\varepsilon_{l,L},L}\|_{L^2(\Omega;V)} \\
&\leq C_{reg} C(\overline{a}_-, \mathcal{D}, \nu_s)(\varepsilon^{\gamma}_{W,L} + \varepsilon^{\frac{1}{2c}}_{l,L}) + \hat{C}_u \mathbb{E}(\hat{h}^{2\hat{\kappa}_a}_L)^{\frac{1}{2}} + \hat{C}_{u,s}\mathbb{E}(\hat{h}^2_L)^{1/2} \\
&\leq C_{reg} C(\overline{a}_-, \mathcal{D}, \nu_s)(\varepsilon^{\gamma}_{W,L} + \varepsilon^{\frac{1}{2c}}_{l,L}) + \tilde{C}\mathbb{E}(\hat{h}^{2\hat{\kappa}_a}_L)^{\frac{1}{2}}.
\end{aligned}$$

For the second term we use the definition of the MLMC-CV estimator $E^{CV,L}$ and Lemma 7.6.2 to estimate

$$\begin{aligned}
I_2 &\leq \sum_{\ell=0}^{L} \|\mathbb{E}(\hat{u}^{CV}_{\varepsilon_{W,\ell},\varepsilon_{l,\ell},\ell} - \hat{u}^{CV}_{\varepsilon_{W,\ell-1},\varepsilon_{l,\ell-1},\ell-1}) - E_{M_\ell}(\hat{u}^{CV}_{\varepsilon_{W,\ell},\varepsilon_{l,\ell},\ell} - \hat{u}^{CV}_{\varepsilon_{W,\ell-1},\varepsilon_{l,\ell-1},\ell-1})\|_{L^2(\Omega;V)} \\
&= \sum_{\ell=0}^{L} \Big(\frac{\mathrm{Var}(\hat{u}^{CV}_{\varepsilon_{W,\ell},\varepsilon_{l,\ell},\ell} - \hat{u}^{CV}_{\varepsilon_{W,\ell-1},\varepsilon_{l,\ell-1},\ell-1})}{M_\ell}\Big)^{1/2} \\
&\leq \sum_{\ell=0}^{L} \frac{1}{\sqrt{M_\ell}} \|\hat{u}^{CV}_{\varepsilon_{W,\ell},\varepsilon_{l,\ell},\ell} - \hat{u}^{CV}_{\varepsilon_{W,\ell-1},\varepsilon_{l,\ell-1},\ell-1}\|_{L^2(\Omega;V)} \\
&\leq \sum_{\ell=0}^{L} \frac{1}{\sqrt{M_\ell}} \Big(\|\hat{u}^{CV}_{\varepsilon_{W,\ell},\varepsilon_{l,\ell},\ell} - u_{K,A} + (u^{(\nu_s)}_{K,A} - \mathbb{E}(u^{(\nu_s)}_{K,A}))\|_{L^2(\Omega;V)} \\
&\qquad + \|u_{K,A} - (u^{(\nu_s)}_{K,A} - \mathbb{E}(u^{(\nu_s)}_{K,A})) - \hat{u}^{CV}_{\varepsilon_{W,\ell-1},\varepsilon_{l,\ell-1},\ell-1}\|_{L^2(\Omega;V)}\Big).
\end{aligned}$$

We estimate each term in this summand with the same strategy as we did for the term I_1 using Theorem 7.4.5 and Assumption 7.5.1 together with Theorem 7.7.4 and Assumption 7.7.2 to obtain

$$\begin{aligned}
&\|\hat{u}^{CV}_{\varepsilon_{W,\ell},\varepsilon_{l,\ell},\ell} - u_{K,A} + (u^{(\nu_s)}_{K,A} - \mathbb{E}(u^{(\nu_s)}_{K,A}))\|_{L^2(\Omega;V)} \\
&\qquad \leq \|\hat{u}_{\varepsilon_{W,\ell},\varepsilon_{l,\ell},\ell} - u_{K,A}\|_{L^2(\Omega,V)} + \|u^{(\nu_s)}_{K,A} - \hat{u}^{(\nu_s)}_{\varepsilon_{W,\ell},\varepsilon_{l,\ell},\ell}\|_{L^2(\Omega;V)} \\
&\qquad \leq C_{reg} C(\overline{a}_-, \mathcal{D}, \nu_s)(\varepsilon^{\gamma}_{W,\ell} + \varepsilon^{\frac{1}{2c}}_{l,\ell}) + \tilde{C}\mathbb{E}(\hat{h}^{2\hat{\kappa}_a}_\ell)^{\frac{1}{2}},
\end{aligned}$$

for $\ell = 0, \dots, L$ and for $\ell = -1$ we get by Theorem 7.4.2 and Equation (7.20)

$$\begin{aligned}
\|u_{K,A} - (u^{(\nu_s)}_{K,A} - \mathbb{E}(u^{(\nu_s)}_{K,A}))\|_{L^2(\Omega;V)} &\leq \|u_{K,A}\|_{L^2(\Omega;V)} + \mathrm{Var}(u^{(\nu_s)}_{K,A})^{\frac{1}{2}} \\
&\leq C(\overline{a}_-, \mathcal{D}, \nu_s)(\|f\|_{L^q(\Omega;H)} + \|g\|_{L^2(\Omega;L^2(\Gamma_2))}).
\end{aligned}$$

Together, we obtain

$$
\begin{aligned}
&I_1 + I_2 \leq \\
&C_{reg} C(\overline{a}_-, \mathcal{D}, \nu_s)\Big(\varepsilon_{W,L}^{\gamma} + \varepsilon_{l,L}^{\frac{1}{2c}} + \frac{\varepsilon_{W,0}^{\gamma} + \varepsilon_{l,0}^{\frac{1}{2c}}}{\sqrt{M_0}} + \sum_{\ell=1}^{L} \frac{1}{\sqrt{M_\ell}}(\varepsilon_{W,\ell}^{\gamma} + \varepsilon_{l,\ell}^{\frac{1}{2c}} + \varepsilon_{W,\ell-1}^{\gamma} + \varepsilon_{l,\ell-1}^{\frac{1}{2c}})\Big) \\
&+ \tilde{C}\Big(\mathbb{E}(\hat{h}_L^{2\hat{\kappa}_a})^{\frac{1}{2}} + \frac{\mathbb{E}(\hat{h}_0^{2\hat{\kappa}_a})^{1/2}}{\sqrt{M_0}} + \sum_{\ell=1}^{L} \frac{1}{\sqrt{M_\ell}}(\mathbb{E}(\hat{h}_\ell^{2\hat{\kappa}_a})^{\frac{1}{2}} + \mathbb{E}(\hat{h}_{\ell-1}^{2\hat{\kappa}_a})^{\frac{1}{2}})\Big) \\
&+ \frac{1}{\sqrt{M_0}} C(\overline{a}_-, \mathcal{D}, \nu_s)(\|f\|_{L^q(\Omega;H)} + \|g\|_{L^q(\Omega;L^2(\Gamma_2))}) \\
&\leq C\Big(\varepsilon_{W,L}^{\gamma} + \varepsilon_{l,L}^{\frac{1}{2c}} + \mathbb{E}(\hat{h}_L^{2\hat{\kappa}_a})^{1/2} + \frac{1}{\sqrt{M_0}} + \sum_{\ell=0}^{L-1} \frac{\varepsilon_{W,\ell}^{\gamma} + \varepsilon_{l,\ell}^{\frac{1}{2c}} + \mathbb{E}(\hat{h}_\ell^{2\hat{\kappa}_a})^{1/2}}{\sqrt{M_{\ell+1}}}\Big),
\end{aligned}
$$

where we used monotonicity of $(\varepsilon_{W,\ell})_{\ell=0}^{L}$, $(\varepsilon_{l,\ell})_{\ell=0}^{L}$ and $(\hat{h}_\ell)_{\ell=0}^{L}$ in the last step. □

As it is the case for the a-priori error bound for the MLMC estimator (see Theorem 7.6.3), Theorem 7.7.5 allows for an equilibration of all error contributions resulting from the approximation of the diffusion coefficient and the approximation of the pathwise solution by the FE method, which can be seen by the following corollary.

Corollary 7.7.6.
Let the assumptions of Theorem 7.7.5 hold. For $L \in \mathbb{N}$ and given (stochastic) refinement parameters $\hat{h}_0 > \cdots > \hat{h}_L > 0$ choose $\varepsilon_{W,\ell} > 0$ and $\varepsilon_{l,\ell} > 0$ such that

$$\varepsilon_{W,\ell} \simeq \mathbb{E}(\hat{h}_\ell^{2\hat{\kappa}_a})^{1/(2\gamma)} \text{ and } \varepsilon_{l,\ell} \simeq \mathbb{E}(\hat{h}_\ell^{2\hat{\kappa}_a})^{c},$$

and sample numbers $M_\ell \in \mathbb{N}$ such that for some positive parameter $\xi > 0$ it holds

$$M_0 \simeq \mathbb{E}(\hat{h}_L^{2\hat{\kappa}_a})^{-1} \text{ and } M_\ell \simeq \mathbb{E}(\hat{h}_L^{2\hat{\kappa}_a})^{-1}\mathbb{E}(\hat{h}_{\ell-1}^{2\hat{\kappa}_a})(\ell+1)^{2(1+\xi)} \text{ for } \ell = 1, \ldots, L.$$

Then, it holds

$$\|\mathbb{E}(u_{K,A}) - E^{CV,L}(\hat{u}^{CV}_{\varepsilon_{W,L},\varepsilon_{l,L},L})\|_{L^2(\Omega;V)} = \mathcal{O}(\mathbb{E}(\hat{h}_L^{2\hat{\kappa}_a})^{1/2}).$$

◆

Proof. See Corollary 7.6.4. □

We want to emphasize that Theorem 7.7.5 and Corollary 7.7.6 imply the same asymptotical convergence of the MLMC-CV estimator as the MLMC estimator which has been considered in Section 7.6. However, it is to be expected that the MLMC-CV estimator is more efficient due to the samplewise correction by the control variate and the resulting variance reduction on the different levels. We close this section with a remark on how to compute the mean of the control variate.

Remark 7.7.7. *Unlike we assumed the CV mean $\mathbb{E}(u_{K,A}^{(\nu_s)})$ is in general unknown for fixed parameters $K, A,$ and $\nu_s > 0$. Corollary 7.7.6 yields that it is sufficient to approximate the CV mean with any estimator which is convergent with order $\mathbb{E}(h_L^{2\hat{\kappa}_a})^{1/2}$. In fact, we denote by*

$$Est_{CV}^{L}(u_{K,A}^{(\nu_s)}) \approx \mathbb{E}(u_{K,A}^{(\nu_s)}),$$

the realization of the desired estimator and we assume the existence of a constant $C_{CV} > 0$ such that it holds

$$\|Est_{CV}^{L}(u_{K,A}^{(\nu_s)}) - \mathbb{E}(u_{K,A}^{(\nu_s)})\|_{L^2(\Omega;V)} \leq C_{CV}\mathbb{E}(\hat{h}_L^{2\hat{\kappa}_a})^{1/2},$$

in the notation of Theorem 7.7.5. Further, instead of the basis experiment $\hat{u}^{CV}_{\varepsilon_{W,\ell},\varepsilon_{l,\ell},\ell}$ from (7.21) we consider

$$\tilde{u}^{CV}_{\varepsilon_{W,\ell},\varepsilon_{l,\ell},\ell} := \hat{u}_{\varepsilon_{W,\ell},\varepsilon_{l,\ell},\ell} - (\hat{u}^{(\nu_s)}_{\varepsilon_{W,\ell},\varepsilon_{l,\ell},\ell} - Est_{CV}^{L}(u_{K,A}^{(\nu_s)})), \text{ for } \ell = 0, \dots, L,$$

and we set $\tilde{u}^{CV}_{\varepsilon_{W,-1},\varepsilon_{l,-1},-1} = 0$ and denote the corresponding MLMC-CV estimator by $E^{CV,L}(\tilde{u}^{CV}_{\varepsilon_{W,L},\varepsilon_{l,L},L})$. Then, by Corollary 7.7.6, it holds

$$\begin{aligned}
&\|\mathbb{E}(u_{K,A}) - E^{CV,L}(\tilde{u}^{CV}_{\varepsilon_{W,L},\varepsilon_{l,L},L})\|_{L^2(\Omega;V)} \\
&\leq \|\mathbb{E}(u_{K,A}) - E^{CV,L}(\hat{u}^{CV}_{\varepsilon_{W,L},\varepsilon_{l,L},L})\|_{L^2(\Omega;V)} + \|Est_{CV}^{L}(u_{K,A}^{(\nu_s)}) - \mathbb{E}(u_{K,A}^{(\nu_s)})\|_{L^2(\Omega;V)} \\
&= \mathcal{O}(\mathbb{E}(\hat{h}_L^{2\hat{\kappa}_a})^{1/2}).
\end{aligned}$$

For example, the CV mean could be estimated by another MLMC estimator on the level L where the parameters are chosen according to Corollary 7.7.6. ◆

7.8 Numerical examples

In the following section we present numerical examples for the estimation of the mean of the solution to the elliptic PDE (7.7) - (7.10). We perform convergence tests with the proposed multilevel Monte Carlo estimators defined in Section 7.6 and Section 7.7. In our numerical examples, we consider different levels $L \in \mathbb{N}$ and choose the sample numbers $(M_\ell,\ \ell = 0, \dots, L)$ and the level dependent approximation parameters for the GRFs $(\varepsilon_{W,\ell},\ \ell = 0, \dots, L)$ and the subordinators $(\varepsilon_{l,\ell},\ \ell = 0, \dots, L)$ according to Corollary 7.6.4 resp. Corollary 7.7.6 if nothing else is explicitly mentioned. Our numerical examples aim to compare the performance of the MLMC estimator with non-adapted triangulations with the MLMC estimator which uses sample-adapted triangulations. Further, we compare the performance of the standard MLMC estimator with the MLMC-CV estimator for high-intensity subordinators whose sample paths possess a comparatively high number of jump discontinuities. This results in a high number of jumps in the diffusion coefficient and, therefore, the sample-adapted triangulations are not feasible anymore. All our numerical experiments are performed in MATLAB R2021a on a workstation with 16 GB memory and Intel quadcore processor with 3.4 GHz.

7.8.1 PDE parameters

In our numerical examples we consider the domain $\mathcal{D} = (0,1)^2$ and choose $\overline{a} \equiv 1/10$, $f \equiv 10$, $\Phi_1 = 1/100 \exp(\cdot)$ and $\Phi_2 = 5\,|\cdot|$ for the diffusion coefficient in (7.10) if nothing else is explicitly mentioned. Further, we impose the following mixed Dirichlet-Neumann boundary conditions: we split the domain boundary $\partial\mathcal{D}$ by $\Gamma_1 = \{0,1\} \times [0,1]$ and $\Gamma_2 = (0,1) \times \{0,1\}$ and impose the pathwise mixed Dirichlet-Neumann boundary conditions

$$u_{K,A} = \begin{cases} 0.1 & \text{on } \{0\} \times [0,1] \\ 0.3 & \text{on } \{1\} \times [0,1] \end{cases} \text{ and } a_{K,A} \overrightarrow{n} \cdot \nabla u_{K,A} = 0 \text{ on } \Gamma_2,$$

for $\omega \in \Omega$. We use a reference grid with 401×401 equally spaced points on the domain $\mathcal{D}$ for interpolation and prolongation. The GRFs W_1 and W_2 are set to be a Matérn-1.5-GRFs on $\mathcal{D}$ (resp. on $[0,K]^2$) with varying correlation lengths and variance parameters. Note that for Matérn-1.5-GRFs we can expect $\gamma = 1$ in Theorem 7.4.5 (see [96, Section 7], [110, Chapter 5], [30]). We simulate the GRFs W_1 and W_2 by the circulant embedding method (see [64] and [65]) to obtain approximations $W_1^{(\varepsilon_W)} \approx W_1$ and $W_2^{(\varepsilon_W)} \approx W_2$ as described in Section 7.4.3. In the experiments, we choose the diffusion cut-off A in (7.10) large enough such that it has no

influence on the numerical experiments for our choice of the GRFs, e.g. $A = 100$ and choose the cut-off level K for each experiment individually depending on the specific choice of the subordinator.

7.8.2 Numerical examples for the MLMC estimator

In this section we conduct experiments with the MLMC estimator introduced in Section 7.6. We consider subordinators with different intensity and GRFs with varying correlation lengths in order to cover problems with different solution regularity. The comparatively low jump activity of the subordinators used in this section (see also Subsection 7.8.3) allows the application of the pathwise sample-adapted approach introduced in Subsection 7.5.2 which can then be compared with the performance of the MLMC estimator with standard triangulations. During this section, we refer to these approaches with *adapted FEM MLMC* and *non-adapted FEM MLMC*. In our experiments, we use Poisson processes to subordinate the GRF W_2 in the diffusion coefficient in (7.10). We consider both, Poisson processes with high and low intensity parameter leading to a different number of jumps in the diffusion coefficient. For the simulation of the Poisson processes we have two options: the processes may be approximated under Assumption 7.4.3 *iv* but they may also be simulated exactly (see Subsection 7.8.2.1). Hence, using Poisson subordinators allows for a detailed investigation of the approximation error caused by the approximation of the Lévy subordinators l_1 and l_2. This will be explained briefly in the following subsection (see also [96, Section 7.3.1]).

7.8.2.1 The two approximation methods

We simulate the Poisson processes by two conceptional different approaches: the first approach is an exact and grid-independent simulation of a Poisson process using the *Uniform Method* (see [109, Section 8.1.2]). On the other hand, we may simulate approximations of the Poisson processes satisfying Assumption 7.4.3 *iv* in the following way (see [96, Section 7.3.1]): We sample values of the Poisson(λ) processes l_1 and l_2 on an equidistant grid $\{x_i,\ i = 0, ..., N_l\}$ with $x_0 = 0$ and $x_{N_l} = 1$ and step size $|x_{i+1} - x_i| \leq \varepsilon_l \leq 1$ for all $i = 0, \dots, N_l - 1$ and approximate the stochastic processes by a piecewise constant extension $l_j^{(\varepsilon_l)} \approx l_j$ of the values on the grid:

$$l_j^{(\varepsilon_l)}(x) = \begin{cases} l_j(x_i) & x \in [x_i, x_{i+1}) \text{ for } i = 0, ..., N_l - 1, \\ l_j(x_{N_l - 1}) & x = 1. \end{cases}$$

for $j = 1, 2$. Since the Poisson process has independent, Poisson distributed increments, values of the Poisson process at the discrete points $\{x_i,\ i = 0, \dots, N_l\}$ may be generated by adding independent Poisson distributed random variables with appropriately scaled intensity parameters. For the rest of this paper, we refer to this approach as the *approximation approach* to simulate a Poisson process. Comparing the results of the MLMC experiments using the two described approaches for the simulation of the Poisson processes allows conclusions to be drawn on the numerical influence of an additional approximation of the subordinator (see Subsection 7.8.2.2). This is further important especially for situations in which the choice of the subordinators does not allow for an exact simulation of the process.

Note that Poisson processes satisfy Assumption 7.4.3 *iv* with $\eta = +\infty$ (see [96, Section 7.3.1]). Since $\gamma = 1$ (see Subection 7.8.1), $\eta = +\infty$ and $f \in L^q(\Omega; H)$ for every $q \geq 1$ we choose for any positive $\delta > 0$

$$r = 2,\ c = b = 1 + \delta$$

to obtain from Theorem 7.4.5

$$\|u_{K,A} - u_{K,A}^{(\varepsilon_W, \varepsilon_l)}\|_{L^2(\Omega;V)} \leq C_{reg} C(\overline{a}_-, \mathcal{D})(\varepsilon_W + \varepsilon_l^{\frac{1}{2c}}),$$

where we have to assume that $j_{reg} > 2((1+\delta)/\delta - 1)$ and $k_{reg} > 2(1+\delta)/\delta$ for the regularity constants $j_{reg},\ k_{reg}$ given in Assumption 7.4.4 since it is not possible to verify this rigorously for our diffusion coefficient (see also [96, Subsection 5.2]). For $\delta = 0.5$ we obtain

$$\|u_{K,A} - u_{K,A}^{(\varepsilon_W, \varepsilon_l)}\|_{L^2(\Omega;V)} \leq C_{reg} C(\overline{a}_-, \mathcal{D})(\varepsilon_W + \varepsilon_l^{\frac{1}{3}}).$$

Therefore, we get $\gamma = 1$ and $c = 1.5$ in the equilibration formula (7.17) for the numerical examples with the Poisson subordinators.

7.8.2.2 Poisson(1) subordinators

In our first numerical example we use Poisson(1) - subordinators. With this choice, we get on average one jump in each direction of the diffusion coefficient. The variance and the correlation parameters for the GRF W_1 (resp. W_2) are set to be $\sigma_1^2 = 1.5^2$ and $r_1 = 0.5$ (resp. $\sigma_2^2 = 0.1^2$ and $r_2 = 0.5$). Figure 7.4 shows samples of the diffusion coefficient and the corresponding PDE solution.

The cut-off threshold K for the subordinators in (7.10) is chosen to be $K = 8$. With this

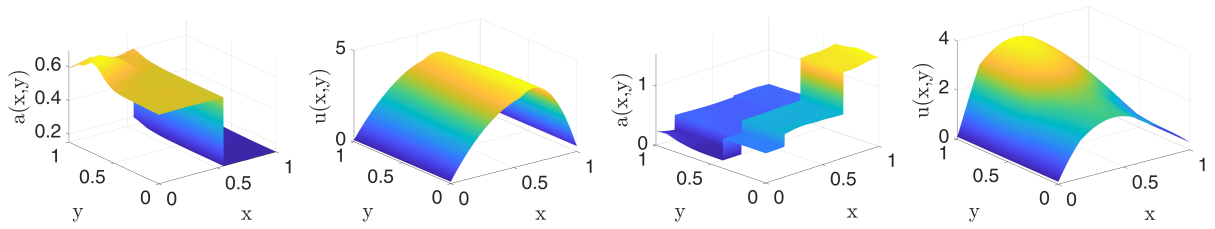

Figure 7.4: Different samples of the diffusion coefficient with Poisson(1) subordinators and the corresponding PDE solutions with mixed Dirichlet-Neumann boundary conditions.

choice we obtain

$$\mathbb{P}(\sup_{t\in[0,1]} l_j(t) > K) = \mathbb{P}(l_j(1) > K) \approx 1.1252e{-}06,$$

for $j = 1, 2$, such that this cut-off has a negligible influence in the numerical example. We compute the RMSE $\|\mathbb{E}(u_{K,A}) - E^L(\hat{u}_{\varepsilon_{W,L},\varepsilon_{l,L},L})\|_{L^2(\Omega;V)}$ for the sample-adapted and the non-adapted approach using 10 independent runs of the MLMC estimator on the levels $L = 1, \ldots, 5$, where we set $\overline{h}_\ell = h_\ell = 0.3 \cdot 1.7^{-(\ell-1)}$, for $\ell = 1, \ldots, 5$. Further, we use a reference solution computed on level 7 with singlelevel Monte Carlo using the FE method with adapted triangulations. We run this experiment with both approaches for the simulation of the subordinators introduced in Subsection 7.8.2.1: the approximation approach and the Uniform Method.

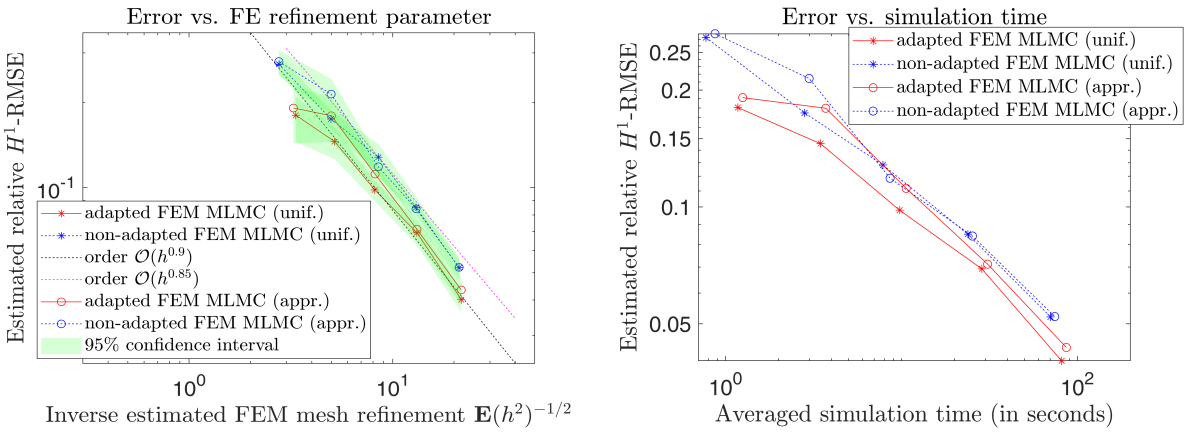

Figure 7.5: Convergence of the MLMC estimator for Poisson(1) subordinators (left) and time-to-error plot (right).

The left graph of Figure 7.5 shows almost full order convergence of the adapted FEM MLMC method and a slightly slower convergence of the non-adapted FEM MLMC approach. Closer

inspection of the figure shows that the choice of the simulation method of the subordinator does not affect the convergence rate of the MLMC estimator: where the Uniform Method yields a slightly smaller RMSE compared to the approximation approach in the sample-adapted case, the behaviour is almost the same for both simulation techniques in the non-adapted FEM MLMC method. The right hand side of Figure 7.5 demonstrates a slightly improved efficiency of adapted FEM MLMC compared to non-adapted FEM MLMC. The advantage of the sample-adapted approach can be further emphasized by the use of subordinators with a higher jump intensity and different correlation lengths of the underlying GRF, as we see in the following subsections.

7.8.2.3 Poisson(5) subordinators - smooth underlying GRF

In the second numerical example we increase the jump-intensity of the subordinators and investigate the effect on the performance of the MLMC estimators. We use Poisson(5) subordinators leading to an expected number of 5 jumps in each direction in the diffusion coefficient. The variance and the correlation parameter for the GRF W_1 (resp. W_2) are set to be $\sigma_1^2 = 0.5^2$ and $r_1 = 0.5$ (resp. $\sigma_2^2 = 0.3^2$ and $r_2 = 0.5$). Figure 7.6 shows samples of the diffusion coefficient and the corresponding PDE solution.

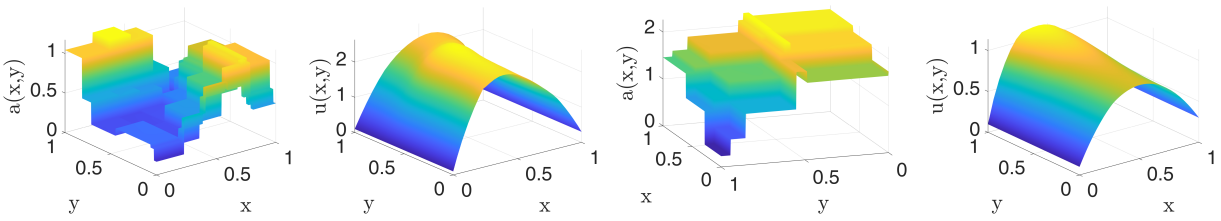

Figure 7.6: Different samples of the diffusion coefficient with Poisson(5) subordinators and the corresponding PDE solutions with mixed Dirichlet-Neumann boundary conditions.

The cut-off threshold K for the subordinators in (7.10) is chosen to be $K = 15$. With this choice we obtain

$$\mathbb{P}(\sup_{t\in[0,1]} l_j(t) > 15) = \mathbb{P}(l_j(1) > 15) \approx 6.9008e{-}05,$$

for $j = 1, 2$, such that this cut-off has a negligible influence in the numerical example. In order to avoid an expensive simulation of the GRF W_2 on the domain $[0, 15]^2$ we set $K = 1$ instead and consider the downscaled processes

$$\tilde{l}_j(t) = \frac{1}{15} l_j(t),$$

for $t \in [0,1]$ and $j = 1,2$. Note that this has no effect on the expected number of jumps of the processes. We use the Uniform Method to simulate the Poisson subordinators and estimate the RMSE of the MLMC estimators for the sample-adapted and the non-adapted approach using 10 independent MLMC runs on the levels $L = 1,\dots,5$, where we set $\overline{h}_\ell = h_\ell = 0.2 \cdot 1.7^{-(\ell-1)}$ for $\ell = 1,\dots,5$. Further, we use a reference solution computed on level 7 with singlelevel Monte Carlo using the FE method with adapted triangulations.

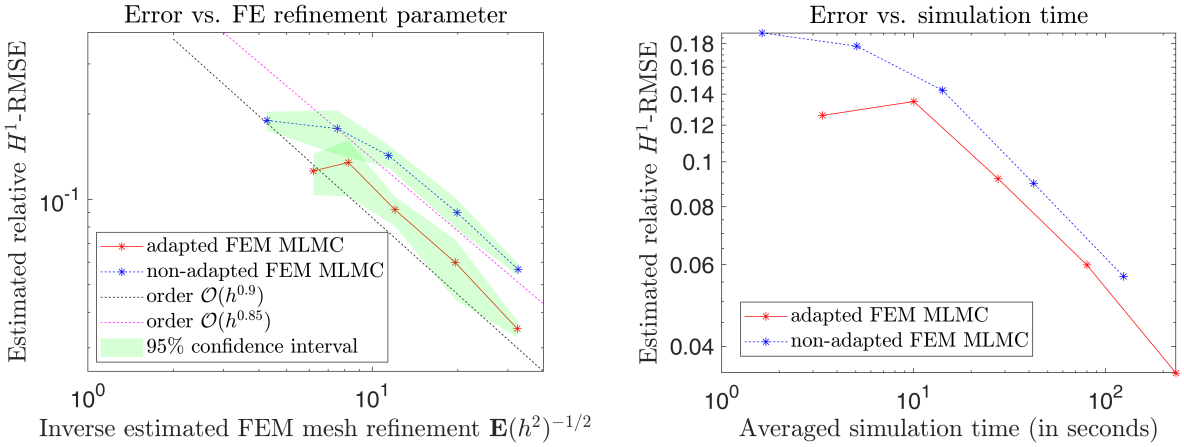

Figure 7.7: Convergence of the MLMC estimator for Poisson(5) subordinators (left) and time-to-error plot (right).

Figure 7.7 shows almost full order convergence of the adapted FEM MLMC method and a slightly slower convergence for the non-adapted FEM MLMC approach. The right hand side of Figure 7.7 demonstrates a higher efficiency of the sample-adapted approach. However, one has to mention that differences in the performance of the estimators are rather small due to the comparatively high convergence rate for the non-adapted MLMC approach of approximately 0.85. This is due to the fact that the jumps in the diffusion coefficient are comparatively small on account of the high correlation length of the underlying GRF W_2. We will see in the following subsection that an increased intensity of the jump heights in the diffusion coefficient has a significant negative influence on the performance of the non-adapted FEM MLMC approach.

7.8.2.4 Poisson(5) subordinators - rough underlying GRF

In the jump-diffusion coefficient (see (7.10)), the jumps are generated by the subordinated GRF in the following way: the number of spatial jumps is determined by the subordinators and the jump heights (measured in the differences in diffusion values across a jump) are essentially determined by the GRF W_2 and its correlation length. Hence, we may control the jump heights

in the diffusion coefficient by the correlation parameter of the underlying GRF W_2. In the following experiment we investigate the influence of the jump heights in the diffusion coefficient on the convergence rates of the MLMC estimators.

In Subsection 7.8.2.3 we subordinated a Matérn-1.5-GRF with correlation length $r_2 = 0.5$ by Poisson(5) processes. In the following experiment we set the correlation length of the GRF W_2 to $r_2 = 0.1$ and leave all the other parameters unchanged. Figure 7.8 presents samples of the resulting GRFs with the different correlation lengths.

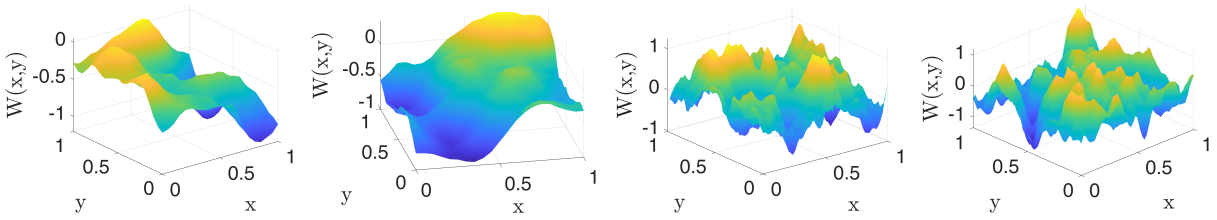

Figure 7.8: Different samples of Matérn-1.5-GRFs with correlation lengths $r = 0.5$ (left) and $r = 0.1$ (right).

By construction of the diffusion coefficient, the subordination of GRFs with small correlation lengths (right plots in Figure 7.8) results in higher jump heights in the diffusion coefficient as the subordination of GRFs with higher correlation lengths (left plots in Figure 7.8). This relationship is demonstrated in Figure 7.9 (cf. Figure 7.6).

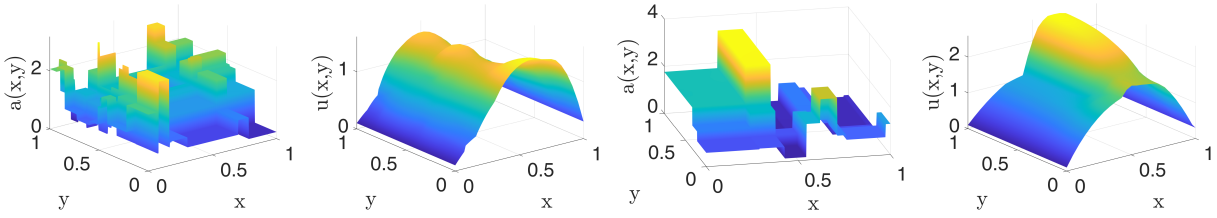

Figure 7.9: Different samples of the diffusion coefficient with Poisson(5) subordinators and small correlation length in the underlying GRF and the corresponding PDE solutions with mixed Dirichlet-Neumann boundary conditions.

We use the Uniform Method to compute the RMSE of the MLMC estimators for the sample-adapted and the non-adapted approach using 10 independent MLMC runs on the levels $L = 1, \dots, 5$, where we set $\overline{h}_\ell = h_\ell = 0.2 \cdot 1.7^{-(\ell-1)}$ for $\ell = 1, \dots, 5$. Further, we use a reference solution computed on level 7 with singlelevel Monte Carlo using the FE method with adapted triangulations. Figure 7.10 reveals that the increased jump heights in the diffusion coefficient have a negative impact on the convergence rates of both estimators: the adapted and the non-adapted FEM MLMC approach. We obtain a convergence rate of approximately 0.85 for the

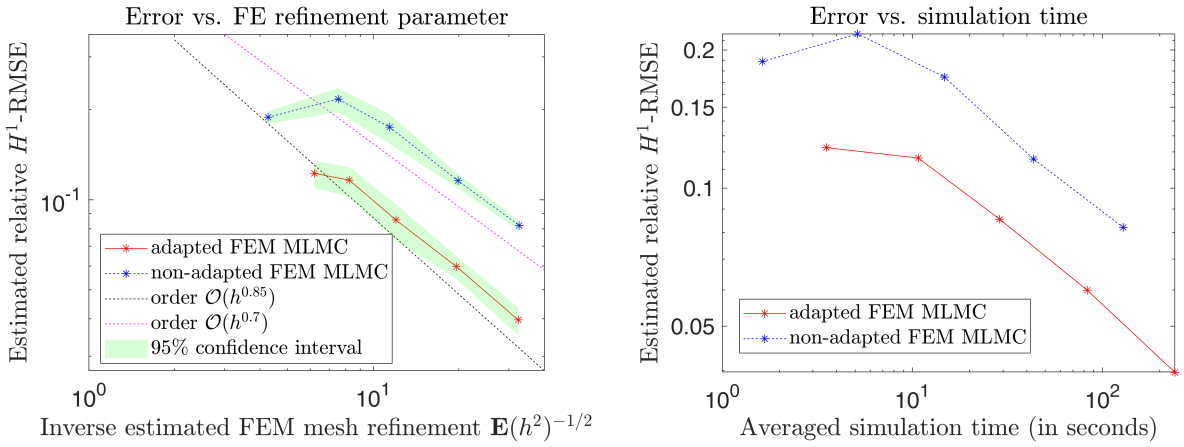

Figure 7.10: Convergence of the MLMC estimator for Poisson(5) subordinators and small correlation length in the underlying GRF (left) and time-to-error plot (right).

adapted FEM MLMC estimator and a smaller rate of approximately 0.7 for the MLMC estimator with non-adapted triangulations. Compared to the experiment discussed in Subsection 7.8.2.3, where we used Poisson(5) subordinators and a higher correlation length in the underlying GRF, we observe that both convergence rates are smaller in the current example. This matches our expectations since the FEM convergence rate has been shown to be influenced by the regularity of the jump-diffusion coefficient (see e.g. [16] and [105]). It is also important to mention that the RMSE is significantly smaller for the adapted FEM MLMC estimator due to the increased jump heights in this example. The higher efficiency of the sample-adapted approach is also demonstrated in the time-to-error plot on the right hand side of Figure 7.10: In this example we see a significant improvement in the time-to-error plot for the adapted FEM MLMC approach compared to the non-adapted FEM MLMC estimator.

7.8.3 Numerical examples for the MLMC-CV estimator

In the following section, we present numerical examples for the MLMC-CV estimator introduced in Section 7.7. In Subsection 7.8.2 we considered Poisson subordinators and compared the non-adapted FEM MLMC estimator with the sample-adapted approach and saw that the latter leads to an improved performance of the estimator. However, this approach is computationally not feasible anymore if we consider subordinators with infinite activity, i.e. which have infinitely many jumps on any finite interval. One example of an infinite activity process is the Gamma process (see also [109, Section 5.3]). The aim of this section is to compare the (non-adapted FEM) MLMC estimator with the MLMC-CV estimator for diffusion coefficients with Gamma-

subordinated GRFs.

7.8.3.1 Gamma subordinators

We approximate the Gamma processes in the same way as we approximate the Poisson subordinators in the approximation approach (see Subsection 7.8.2.1) and obtain a valid approximation in the sense of Assumption 7.4.3 *iv* for any $\eta < +\infty$ (see [96, Section 7.4] and [9]). In our numerical experiments we choose l_1 and l_2 to be Gamma$(4, 10)$ processes. We set the diffusion cut-off to $K = 2$ to obtain

$$\mathbb{P}(\sup_{t\in[0,1]} l_j(t) \geq K) = \mathbb{P}(l_j(1) \geq 2) \approx 3.2042e{-}06,$$

for $j = 1, 2$. Hence, the influence of the subordinator cut-off is again negligible in our numerical experiments. Due to the high jump intensity we have to choose a sufficiently small smoothness parameter ν_s since otherwise important detailed information of the diffusion coefficient might be unused. In our two numerical examples, we choose $\nu_s = 0.01$. This leads to a performance improvement in the MLMC-CV estimator for Gamma$(4, 10)$ subordinators, as we see in our numerical experiments (see also Remark 7.7.1).

7.8.3.2 MLMC-CV vs. MLMC for infinite activity subordinators

In our numerical examples, the variance of the W_1 is set to be $\sigma_1^2 = 1.5^2$ and the correlation length is defined by $r_1 = 0.5$. The parameters of the GRF W_2 are varied in the experiments. Since we aim to compare the performance of the MLMC estimator with the MLMC-CV estimator we use optimal sample numbers in the numerical experiments in this subsection: Assume level dependent FE discretization sizes h_ℓ are given, for $\ell = 1, \ldots, L$ with fixed $L \in \mathbb{N}$. Further, we denote by VAR_ℓ the (estimated) variances of $u_{\varepsilon_{W,\ell},\varepsilon_{l,\ell},\ell} - u_{\varepsilon_{W,\ell-1},\varepsilon_{l,\ell-1},\ell-1}$ (resp. $u^{CV}_{\varepsilon_{W,\ell},\varepsilon_{l,\ell},\ell} - u^{CV}_{\varepsilon_{W,\ell-1},\varepsilon_{l,\ell-1},\ell-1}$ for the MLMC-CV estimator). The optimal sample numbers are then given by the formula

$$M_\ell = h_L^{-2}\sqrt{VAR_\ell}h_\ell \sum_{i=1}^{L} \sqrt{VAR_i}h_i^{-1}, \text{ for } \ell = 1, \ldots, L,$$

since this choice minimizes the variance of the MLMC(-CV) estimator for fixed computational costs (see [59, Section 1.3]). As discussed in Remark 7.7.7, the expectation of the mean of the control variate $\mathbb{E}(u^{(\nu_s)}_{K,A})$ is usually not known explicitly and needs to be approximated

separately. We estimate $\mathbb{E}(u_{K,A}^{(\nu_s)})$ by a realization of a non-adapted FEM MLMC estimator on level L (see Section 7.6), which is of sufficient accuracy as discussed in Remark 7.7.7.

In the following numerical example we choose $\sigma_2^2 = 0.3^2$ and $r_2 = 0.05$ for the GRF W_2. Figure 7.11 shows samples of the diffusion coefficient and the corresponding PDE solutions. We

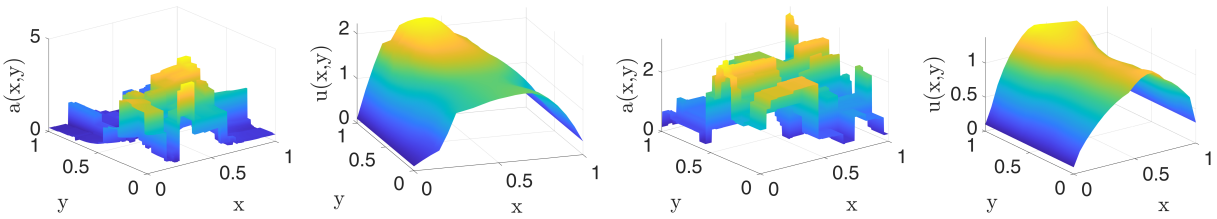

Figure 7.11: Different samples of the diffusion coefficient with Gamma$(4, 10)$ subordinators with small correlation length in the underlying GRF together with the corresponding PDE solutions with mixed Dirichlet-Neumann boundary conditions.

define the level dependent FE discretization parameters $h_\ell = 0.3 \cdot 1.7^{-(\ell-1)}$ for $\ell = 1, \dots, 5$ and compare the MLMC estimator with the MLMC-CV estimator. We perform 10 independent MLMC runs on the levels $L = 1, \dots, 5$ to estimate the RMSE where we use a reference solution on level 7 computed by singlelevel Monte Carlo. The results are given in the following figure. Figure 7.12 shows a similar convergence rate of approximately 0.75 for the MLMC and

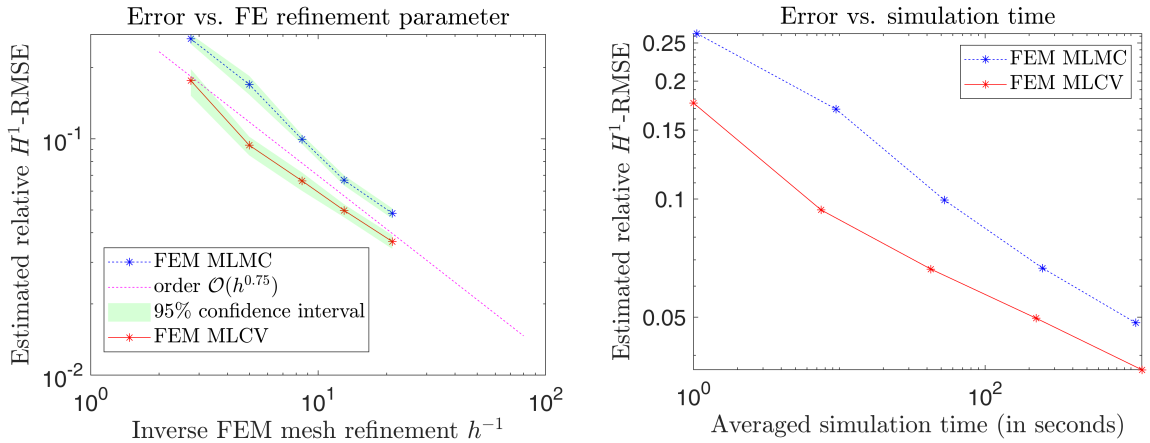

Figure 7.12: Convergence of the MLMC and the MLMC-CV estimator for Gamma$(4, 10)$ subordinators with small noise and small correlation length in the underlying GRF (left) and time-to-error plot (right).

the MLMC-CV estimator. However, the sample-wise correction by the smooth PDE problem in the MLMC-CV estimator improves the approximation which yields significantly smaller values for the RMSE on the different levels compared to the standard MLMC estimator. The efficiency improvement obtained by the control variate is further demonstrated on the right hand side

of Figure 7.12: The time-to-error plot demonstrates that the computational effort which is necessary to achieve a certain accuracy is significantly smaller for the MLMC-CV estimator compared to the standard MLMC estimator. Note that the computation of the expectation of the solution to the smoothed problem $\mathbb{E}(u_{K,A}^{(\nu_s)})$ is included in the simulation time of the MLMC-CV estimator.

In our last numerical example we choose $\Phi_1 = 0.2\exp(\cdot)$, $\Phi_2 = 3|\cdot|$ and $\sigma_2^2 = 0.5^2$, $r_2 = 0.2$ for the GRF W_2 and leave all other parameters unchanged. This leads to diffusion coefficient which is more noise accentuated has slightly reduced jump heights (see also Subsection 7.8.2.4) as can be seen in Figure 7.13.

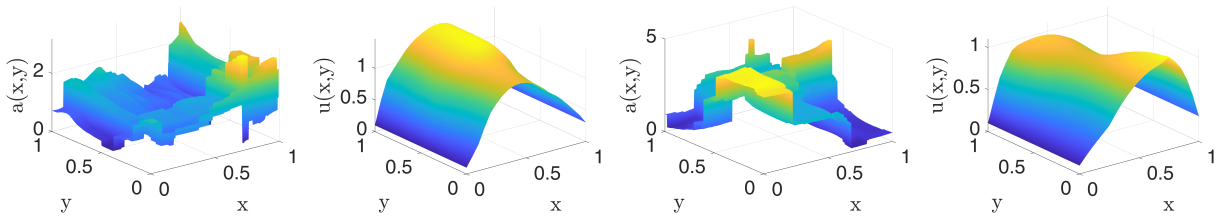

Figure 7.13: Different samples of the diffusion coefficient with Gamma$(4, 10)$ subordinators with strong noise and higher correlation length in the underlying GRF together with the corresponding PDE solutions with mixed Dirichlet-Neumann boundary conditions.

As in the last experiment, we define the level dependent FE discretization parameters $h_\ell = 0.3 \cdot 1.7^{-(\ell-1)}$ for $\ell = 1, \dots, 5$ and compare the MLMC estimator with the MLMC-CV estimator. We use 10 independent MLMC runs on the levels $L = 1, \dots, 5$ to estimate the RMSE and use a singlelevel Monte Carlo estimation on level 7 as reference solution. The results are given in Figure 7.14.

The reduced jump heights together with the emphasized (continuous) noise in the diffusion coefficient leads to a slightly improved convergence rate of approximately 0.85 for the estimators in this example (cf. Figure 7.12). As in the first experiment, we see that the usage of the control variate yields a significant improvement which is reflected in smaller values for the RMSE on the different levels compared to the standard MLMC approach. As expected, the right hand side of Figure 7.14 shows an improved efficiency of the MLMC-CV estimator compared to the standard MLMC estimator without control variates.

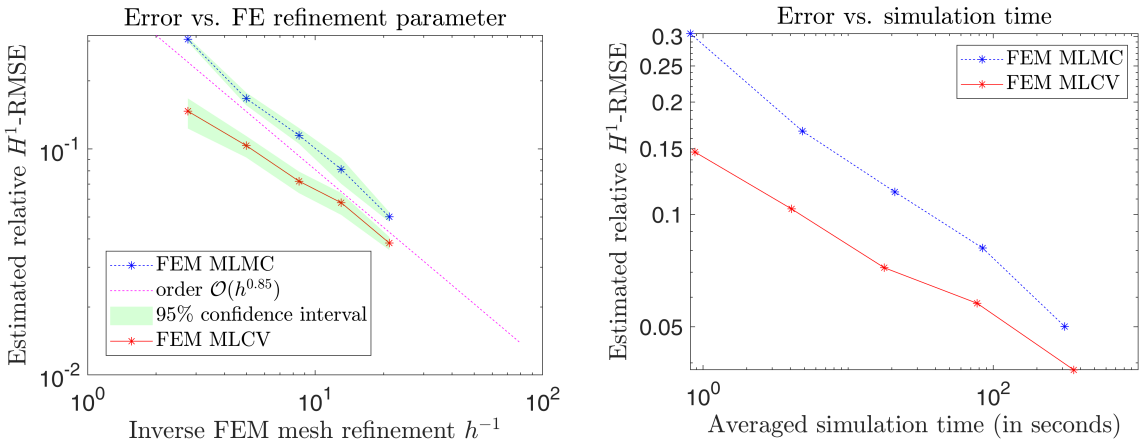

Figure 7.14: Convergence of the MLMC and the MLMC-CV estimator for Gamma$(4, 10)$ subordinators with strong noise and underlying GRF with higher correlation length (left) and time-to-error plot (right).

7.8.4 Numerical examples: summary

In our numerical experiments we presented a varied choice of subordinators and parameters of the GRFs. As expected, we see that the convergence rate of the MLMC estimator deteriorates if the jump heights, i.e. the contrast in the diffusion coefficient, increases. We get a convergence rate of approximatively 0.9 (resp. 0.85) for the adapted (resp. non-adapted) FEM MLMC estimator in the examples with Poisson(1) subordinators (see Subsection 7.8.2.2). While similar rates have been observed in the first example with Poisson(5) subordinators (see Subsection 7.8.2.3), we obtain smaller convergence rates for both approaches with Poisson(5) subordinators, but a GRF W_2 with smaller correlation parameter r_2, leading to a higher contrast in the samples of the diffusion coefficient. Here, we get a convergence rate of approximatively 0.85 (resp. 0.7) for the adapted (resp. non-adapted) FEM MLMC estimator. Further, the absolute difference between the respective RMSE values (i.e. the advantage of adapted FEM MLMC over non-adapted FEM MLMC) increases significantly in this example (see Subsection 7.8.2.4). In contrast to the sample adapted MLMC estimator, we cannot expect an improved convergence rate in the MLMC-CV estimator. However, the standard deviation of the MLMC-CV estimator is reduced by the variance reduction effect caused by the control variate which is demonstrated in the numerical examples in Subsection 7.8.3.

Acknowledgements

Funded by Deutsche Forschungsgemeinschaft (DFG, German Research Foundation) under Germany's Excellence Strategy - EXC 2075 - 390740016.

Funding

Open Access funding enabled and organized by Projekt DEAL.

On properties and applications of Gaussian subordinated Lévy fields

8

Robin Merkle[1] and Andrea Barth[1]

Submitted to Methodology and Computing in Applied Probability,
Reference: [94], preprint available under: https://arxiv.org/pdf/2208.01278.pdf

Abstract: *We consider Gaussian subordinated Lévy fields (GSLFs) that arise by subordinating Lévy processes with positive transformations of Gaussian random fields on some spatial domain $\mathcal{D} \subset \mathbb{R}^d$, $d \geq 1$. The resulting random fields are distributionally flexible and have in general discontinuous sample paths. Theoretical investigations of the random fields include pointwise distributions, possible approximations and their covariance function. As an application, a random elliptic PDE is considered, where the constructed random fields occur in the diffusion coefficient. Further, we present various numerical examples to illustrate our theoretical findings.*

8.1 Introduction

Ample applications that are modeled stochastically require stochastic processes or random fields, which allow for discontinuities or possess higher distributional flexibility than the standard Gaussian model (see for example [72], [109] and [118]). In case of a one-dimensional parameter domain, where the parameter often represents time, Lévy processes are widely used (see e.g. [109] for some applications in finance). For higher-dimensional parameter domains, some extensions of the Gaussian model have been proposed in the literature: The authors of [49] consider (smoothed) Lévy noise fields with high distributional flexibility and

[1]IANS/SimTech, University of Stuttgart, Stuttgart, Germany

continuous realizations in the context of random PDEs. In [16], the authors propose a general random field model which allows for spatial discontinuities with flexible jump geometries. However, in its general form, it not easy to investigate theoretical properties of the random field itself. In the context of Bayesian inversion, the level set approach combined with Gaussian random fields is often used as a discontinuous random field model (see, e.g. [76], [45] and [46]). The distributional flexibility of the resulting model is, however, again restricted since the stochasticity is governed by the Gaussian field. Another extension of the Gaussian model has been investigated in the recent paper [95]. The construction is motivated by the subordinated Brownian motion, which is a Brownian motion time-changed by a Lévy subordinator (i.e. a non-decreasing Lévy process). As a generalization, the authors consider Gaussian random fields on a higher-dimensional parameter domain subordinated by several independent Lévy subordinators. The constructed random fields allow for spatial jumps and display great distributional flexibility. However, the jump geometry is restricted in the sense that the jump interfaces are always rectangular.

In this paper, we investigate another specific class of discontinuous random fields: the Gaussian subordinated Lévy fields (GSLF). Motivated by the subordination of standard Lévy processes, the GSLF is constructed by subordination of a general real-valued Lévy process by a transformation of a Gaussian random field. It turns out that the resulting fields allow for spatial discontinuities with flexible jump geometries, are distributionally flexible and relatively easy to simulate. Besides a theoretical investigation of the constructed random fields, we present numerical examples and introduce a possible application of the fields in the diffusion coefficient of an elliptic model equation. Such a problem arises, for instance, in models for subsurface/groundwater flow in heterogeneous/porous media (see [16], [36], [98] and the references therein).

The rest of the paper is structured as follows: In Section 8.2 we shortly introduce Lévy processes and Gaussian random fields, which are crucial for the definition of the GSLF in Section 8.3. The pointwise distribution of the random fields are investigated in Section 8.4, where we derive a formula for its (pointwise) characteristic function. Section 8.5 deals with numerical approximations of the GSLF, including an investigation of the approximation error and the pointwise distribution of the approximated fields. Our theoretical investigations are concluded in Section 8.6, where we derive a formula for the covariance function. In Section 8.7, we present various numerical examples which validate and illustrate the theoretical findings of the previous sections. Section 8.8 concludes the paper and highlights the application of the GSLF in the context of random elliptic PDEs, exploring theoretical as well as numerical aspects.

8.2 Preliminaries

In the following section, we give a short introduction to Lévy processes and Gaussian random fields following [95] since they are crucial elements for the construction of the Gaussian subordinated Lévy field. For more details we refer the reader to [3, 108, 8]. Throughout the paper, we assume that $(\Omega, \mathcal{F}, \mathbb{P})$ is a complete probability space.

8.2.1 Lévy processes

We consider an Borel-measurable index set $\mathcal{T} \subseteq \mathbb{R}_+ := [0, +\infty)$. A *stochastic process* $X = (X(t),\ t \in \mathcal{T})$ on $\mathcal{T}$ is a family of random variables on the probability space $(\Omega, \mathcal{F}, \mathbb{P})$.

Definition 8.2.1.
A stochastic process l on $\mathcal{T} = [0, +\infty)$ is said to be a Lévy process if

i $l(0) = 0$ $\mathbb{P}$*-a.s.,*

ii l *has independent increments, i.e. for each* $0 \leq t_1 \leq t_2 \leq \cdots \leq t_{n+1}$ *the random variables* $(l(t_{j+1}) - l(t_j),\ 1 \leq j \leq n)$ *are mutually independent,*

iii l *has stationary increments, i.e. for each* $0 \leq t_1 \leq t_2 \leq \cdots \leq t_{n+1}$ *it holds* $l(t_{j+1}) - l(t_j) \stackrel{\mathcal{D}}{=} l(t_{j+1} - t_j) - l(0) \stackrel{\mathcal{D}}{=} l(t_{j+1} - t_j)$*, where* $\stackrel{\mathcal{D}}{=}$ *denotes equivalence in distribution,*

iv l *is stochastically continuous, i.e. for all* $a > 0$ *and for all* $s \geq 0$ *it holds*

$$\lim_{t \to s} \mathbb{P}(|l(t) - l(s)| > a) = 0.$$

◆

The well known *Lévy-Khinchin formula* yields a parametrization of the class of Lévy processes by the so called *Lévy triplet* (γ_l, b, ν). A proof can be found, for example, in [8, Th. 1.3.3 and p. 29].

Theorem 8.2.2 (Lévy-Khinchin formula)**.**
Let l be a real-valued Lévy process on $\mathcal{T} \subseteq \mathbb{R}_+ := [0, +\infty)$. There exist parameters $\gamma_l \in \mathbb{R}$, $b \in \mathbb{R}_+$ and a measure ν on $\mathbb{R}$ such that the characteristic function $\phi_{l(t)}$ of the Lévy process l

admits the representation

$$\phi_{l(t)}(\xi) := \mathbb{E}(\exp(i\xi l(t))) = \exp(t\psi(\xi)),\ \xi \in \mathbb{R},$$

for $t \in \mathcal{T}$. Here, ψ denotes the characteristic exponent of l which is given by

$$\psi(\xi) = i\gamma_l \xi - \frac{b}{2}\xi^2 + \int_{\mathbb{R}\setminus\{0\}} e^{i\xi y} - 1 - i\xi y \mathbb{1}_{\{|y|\leq 1\}}(y)\nu(dy),\ \xi \in \mathbb{R}.$$

Further, the measure ν satisfies

$$\int_{\mathbb{R}} \min(y^2, 1)\, \nu(dy) < \infty,$$

and is called Lévy measure and (γ_l, b, ν) is called Lévy triplet. ◆

8.2.2 Gaussian random fields

A random field defined over the Borel set $\mathcal{D} \subset \mathbb{R}^d$ is a family of real-valued random variables on the probability space $(\Omega, \mathcal{F}, \mathbb{P})$ parametrized by $\underline{x} \in \mathcal{D}$. The Gaussian random field defines an important example (see [3, Sc. 1.2]):

Definition 8.2.3.
A random field $(W(\underline{x}),\ \underline{x} \in \mathcal{D})$ on a d-dimensional domain $\mathcal{D} \subset \mathbb{R}^d$ is said to be a Gaussian random field (GRF) if, for any $\underline{x}^{(1)}, \ldots, \underline{x}^{(n)} \in \mathcal{D}$ with $n \in \mathbb{N}$, the n-dimensional random variable $(W(\underline{x}^{(1)}), \ldots, W(\underline{x}^{(n)}))$ follows a multivariate Gaussian distribution. In this case, we define the mean function $\mu_W(\underline{x}^{(i)}) := \mathbb{E}(W(\underline{x}^{(i)}))$ and the covariance function $q_W(\underline{x}^{(i)}, \underline{x}^{(j)}) := \mathbb{E}((W(\underline{x}^{(i)}) - \mu_W(\underline{x}^{(i)}))(W(\underline{x}^{(j)}) - \mu_W(\underline{x}^{(j)})))$, for $\underline{x}^{(i)},\ \underline{x}^{(j)} \in \mathcal{D}$. The GRF W is called centered, if $\mu_W(\underline{x}) = 0$ for all $\underline{x} \in \mathcal{D}$. ◆

Note that every GRF is determined uniquely by its mean and covariance function. The GRFs considered in this paper are assumed to be mean-square continuous, which is a common assumption (cf. [3]). We denote by $Q : L^2(\mathcal{D}) \to L^2(\mathcal{D})$ the *covariance operator* of W which is defined by

$$Q(\psi)(\underline{x}) = \int_{\mathcal{D}} q_W(\underline{x}, \underline{y})\psi(\underline{y})d\underline{y}, \text{ for } \underline{x} \in \mathcal{D},$$

for $\psi \in L^2(\mathcal{D})$. Here, $L^2(\mathcal{D})$ denotes the Lebesgue space of all square integrable functions

over $\mathcal{D}$ (see for example [2]). If $\mathcal{D}$ is compact, it is well known that there exists a decreasing sequence $(\lambda_i,\ i \in \mathbb{N})$ of real eigenvalues of Q with corresponding eigenfunctions $(e_i,\ i \in \mathbb{N}) \subset L^2(\mathcal{D})$ which form an orthonormal basis of $L^2(\mathcal{D})$ (see [3, Section 3.2] and [115, Theorem VI.3.2 and Chapter II.3]). A GRF W is called *stationary* if the mean function μ_W is constant and the covariance function $q_W(\underline{x}^{(1)}, \underline{x}^{(2)})$ only depends on the difference $\underline{x}^{(1)} - \underline{x}^{(2)}$ of the values $\underline{x}^{(1)},\ \underline{x}^{(2)} \in \mathcal{D}$ and a stationary GRF W is called *isotropic* if the covariance function $q_W(\underline{x}^{(1)}, \underline{x}^{(2)})$ only depends on the Euclidean length $|\underline{x}^{(1)} - \underline{x}^{(2)}|_2$ of the difference of the values $\underline{x}^{(1)},\ \underline{x}^{(2)} \in \mathcal{D}$ (see [3], p. 102 and p. 115).

Example 8.2.4. *The Matérn-GRFs are a class of continuous GRFs which are commonly used in applications. For a certain smoothness parameter $\nu > 1/2$, correlation parameter $r > 0$ and variance $\sigma^2 > 0$, the Matérn-ν covariance function is defined by $q_M(\underline{x}, \underline{y}) = \rho_M(|\underline{x} - \underline{y}|_2)$, for $(\underline{x}, \underline{y}) \in \mathbb{R}^d_+ \times \mathbb{R}^d_+$, with*

$$\rho_M(s) = \sigma^2 \frac{2^{1-\nu}}{\Gamma(\nu)} \Big(\frac{2s\sqrt{\nu}}{r}\Big)^{\nu} K_\nu\Big(\frac{2s\sqrt{\nu}}{r}\Big), \text{ for } s \geq 0.$$

Here, $\Gamma(\cdot)$ is the Gamma function and $K_\nu(\cdot)$ is the modified Bessel function of the second kind (see [63, Section 2.2 and Proposition 1]). A Matérn-ν GRF is a centered GRF with covariance function q_M. ◆

8.3 The Gaussian subordinated Lévy field

In this section we define Gaussian subordinated Lévy fields. Since their construction is motivated by the subordination of standard Lévy processes we shortly repeat this procedure: If l denotes a Lévy process and S denotes a Lévy subordinator (i.e. a non-decreasing Lévy process), which is independent of l, the time-changed process

$$t \mapsto l(S(t)),\ t \geq 0,$$

is called subordinated Lévy process. It can be shown that this process is again a Lévy process (cf. [8, Theorem 1.3.25]).

In order to construct the GSLF we consider a domain $\mathcal{D} \subset \mathbb{R}^d$ with $1 \leq d \in \mathbb{N}$. Let $l = (l(t),\ t \geq 0)$ be a Lévy process, $W : \Omega \times \mathcal{D} \to \mathbb{R}$ be an $\mathcal{F} \otimes \mathcal{B}(\mathcal{D})$-$\mathcal{B}(\mathbb{R})$-measurable GRF which is independent of l and $F : \mathbb{R} \to \mathbb{R}_+$ be a measurable, non-negative function. The

Gaussian subordinated Lévy field is defined by

$$L(\underline{x}) = l(F(W(\underline{x}))), \text{ for } \underline{x} \in \mathcal{D}.$$

Note that assuming the GRF W to have continuous paths is sufficient to ensure joint measurability (see [6, Lemma 4.51]). Since the Lévy process l is in general discontinuous, the GSLF L has in general discontinuous paths. This is demonstrated in Figure 8.1, which shows samples of the GSLF.

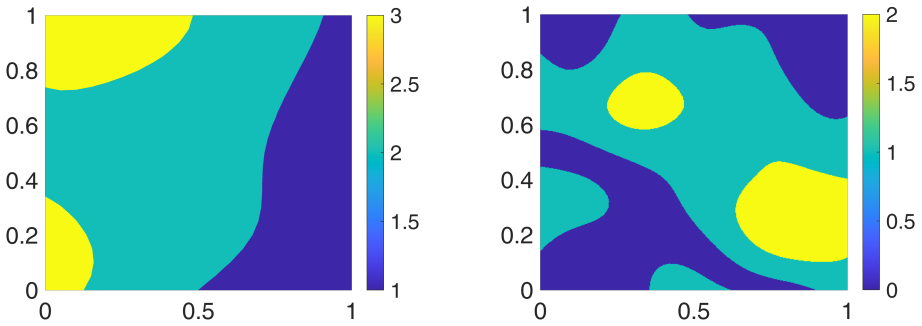

Figure 8.1: Sample of a Matérn-1.5-GRF-subordinated Poisson process.

Remark 8.3.1. *Discontinuous random fields often serve as prior model to solve inverse problems with a Bayesian approach as an alternative to the standard Gaussian prior (see e.g. [76, 72]). In these situations, the prior model is often set to be a Gaussian(-related) level-set function. One way to construct such a prior model is as follows:*

$$u(\underline{x}) = \sum_{i=1}^{n} u_i \mathbb{1}_{D_i}(\underline{x}), \ \underline{x} \in \mathcal{D},$$

where $n \in \mathbb{N}$, $(u_i, \ i = 1, \dots, n) \subset \mathbb{R}$ *are fixed and*

$$D_i = \{\underline{x} \in \mathcal{D} \mid c_{i-1} \leq W(\underline{x}) < c_i\},$$

with fixed levels $(c_i, \ i = 1, \dots, n) \subset \mathbb{R}$ *and a GRF* W *(see e.g. [46, 45]). The GSLF, as defined above, may be interpreted as a generalization of the Gaussian level-set function.* ◆

Remark 8.3.2. *It is easy to see that the GSLF is measurable: A Lévy process* $l : \Omega \times \mathbb{R}_+ \to \mathbb{R}$ *has càdlàg paths and, hence, is* $\mathcal{F} \otimes \mathcal{B}(\mathbb{R}_+) - \mathcal{B}(\mathbb{R})$*-measurable (see [106, Chapter 1, Theorem*

30] and [108, Chapter 6]). Further, since F and W are measurable by assumption, the mapping

$$(\omega, \underline{x}) \mapsto F(W(\omega, \underline{x})),\ (\omega, \underline{x}) \in \Omega \times \mathcal{D},$$

is $\mathcal{F} \otimes \mathcal{B}(\mathcal{D}) - \mathcal{B}(\mathbb{R}_+)$-measurable. It follows now by [6, Lemma 4.49], that the mapping

$$(\omega, \underline{x}) \mapsto (\omega, F(W(\omega, \underline{x}))),\ (\omega, \underline{x}) \in \Omega \times \mathcal{D},$$

is $\mathcal{F} \otimes \mathcal{B}(\mathcal{D}) - \mathcal{F} \otimes \mathcal{B}(\mathbb{R}_+)$-measurable. Therefore, the GSLF

$$(\omega, \underline{x}) \mapsto l(\omega, F(W(\omega, \underline{x}))),\ (\omega, \underline{x}) \in \Omega \times \mathcal{D},$$

is $\mathcal{F} \otimes \mathcal{B}(\mathcal{D}) - \mathcal{B}(\mathbb{R})$-measurable (cf. [6, Lemma 4.22]). ◆

8.4 The pointwise characteristic function of a GSLF

In the following section we derive a formula for the pointwise characteristic function of the GSLF, which determines the pointwise distribution entirely. Such a formula is especially valuable in applications, where distributions of a random field have to be fitted to data observed from real-world phenomena. We start with a technical lemma on the computation of expectations of functionals of the GSLF.

Lemma 8.4.1.
Let $l = (l(t),\ t \geq 0)$ be a stochastic process with a.s. càdlàg paths and W_+ be a real-valued, non-negative random variable which is stochastically independent of l. Further, let $g : \mathbb{R} \to \mathbb{R}$ be a continuous function. It holds

$$\mathbb{E}(g(l(W_+))) = \mathbb{E}(m(W_+)),$$

with $m(z) := \mathbb{E}(g(l(z)))$ for $z \in \mathbb{R}_+$. ◆

Proof. The proof follows the same arguments as the proof of [95, Lemma 4.1]. □

Remark 8.4.2. *Note that Lemma 8.4.1 also holds for complex-valued, continuous and bounded functions $g : \mathbb{R} \to \mathbb{C}$ (cf. [95, Remark 4.2]). Further, we emphasize that Lemma 8.4.1 also holds for an $\mathbb{R}_+^d$-valued random variable W_+ and a random field $(l(\underline{t}),\ \underline{t} \in \mathbb{R}_+^d)$, independent of W_+,*

which is a.s. càdlàg in each variable, i.e. for $\mathbb{P}$-almost all $\omega \in \Omega$, it holds

$$\lim_{n\to\infty} l(t_1^{(n)}, \dots, t_d^{(n)}) = l(t_1, \dots, t_d),$$

for $t_j^{(n)} \searrow t_j$, for $n \to \infty$, $j = 1, \dots, d$, and any $\underline{t} = (t_1, \dots, t_d) \in \mathbb{R}_+^d$. ◆

With Lemma 8.4.1 at hand, we are able to derive a formula for the pointwise characteristic funciton of the GSLF.

Corollary 8.4.3.
Let $l = (l(t),\ t \geq 0)$ be a Lévy process with Lévy triplet (γ_l, b, ν) and $W = (W(\underline{x}),\ \underline{x} \in \mathcal{D})$ be an independent GRF with pointwise mean $\mu_W(\underline{x}) = \mathbb{E}(W(\underline{x}))$ and variance $\sigma_W(\underline{x})^2 := \mathrm{Var}(W(\underline{x}))$ for $\underline{x} \in \mathcal{D}$. Further, let $F : \mathbb{R} \to \mathbb{R}_+$ be measurable. It holds

$$\begin{aligned}\phi_{l(F(W(\underline{x})))}(\xi) &= \mathbb{E}\Big(\exp(i\xi\, l(F(W(\underline{x}))))\Big) \\ &= \frac{1}{\sqrt{2\pi\sigma_W(\underline{x})^2}} \int_{\mathbb{R}} \exp\Big(F(y)\psi(\xi) - \frac{(y-\mu_W(\underline{x}))^2}{2\sigma_W(\underline{x})^2}\Big) dy,\end{aligned}$$

for $\underline{x} \in \mathcal{D}$, where ψ denotes the characteristic exponent of l defined by

$$\psi(\xi) = i\gamma_l\xi - \frac{b}{2}\xi^2 + \int_{\mathbb{R}\setminus\{0\}} e^{i\xi y} - 1 - i\xi y \mathbb{1}_{\{|y|\leq 1\}}(y)\nu(dy),\ \xi \in \mathbb{R}.$$

◆

Proof. We consider a fixed $\underline{x} \in \mathcal{D}$ and use Lemma 8.4.1 with $g(\cdot) := \exp(i\xi\cdot)$ and $W_+ := F(W(\underline{x}))$ to calculate

$$\mathbb{E}\Big(\exp(i\xi\, l(F(W(\underline{x}))))\Big) = \mathbb{E}(g(l(W_+)) = \mathbb{E}(m(W_+)) = \mathbb{E}(m(F(W(\underline{x})))),$$

where m is defined through

$$m(z) = \mathbb{E}(\exp(i\xi l(z)) = \exp(z\,\psi(\xi)),\ z \in \mathbb{R}_+,$$

by the Lévy-Khinchin formula (see Theorem 8.2.2). Hence, we obtain

$$\begin{aligned}\mathbb{E}\Big(\exp(i\xi\, l(F(W(\underline{x}))))\Big) &= \mathbb{E}\Big(\exp(F(W(\underline{x}))\psi(\xi))\Big) \\ &= \frac{1}{\sqrt{2\pi\sigma_W(\underline{x})^2}}\int_{\mathbb{R}}\exp\Big(F(y)\psi(\xi) - \frac{(y-\mu_W(\underline{x}))^2}{2\sigma_W(\underline{x})^2}\Big)dy.\end{aligned}$$

□

8.5 Approximation of the fields

The GSLF may in general not be simulated exactly since in most situations it is not possible to draw exact samples of the corresponding GRF and the Lévy process. The question arises how the GSLF may be approximated and if the corresponding approximation error may be quantified. In this section we answer both questions. We prove an approximation result for the GSLF where we approximate the GRF and the Lévy process separately. To be more precise, we approximate the Lévy processes using a piecewise constant càdlàg approximation on a discrete grid (see e.g. [15] and the remainder of the current section). The GRF may be approximated by a truncated Karhuen-Loève-expansion or using values of the GRF simulated on a discrete grid, e.g. via circulant embedding (see, e.g. [16, 1, 112] resp. [64, 65]). Naturally, we have to start with some assumptions on the regularity of the GRF and the approximability of the Lévy process. For simplicity, we consider centered GRFs in this subsection.

Assumption 8.5.1.
Let W be a zero-mean GRF on the compact domain $\mathcal{D}$. We denote by $q_W : \mathcal{D}\times\mathcal{D}\to\mathbb{R}$ the corresponding covariance function and by $((\lambda_i, e_i),\ i\in\mathbb{N})$ the eigenpairs associated to the corresponding covariance operator Q as introduced in Section 8.2.2. In particular, $(e_i,\ i\in\mathbb{N})$ is an orthonormal basis of $L^2(\mathcal{D})$.

i We assume that the eigenfunctions are continuously differentiable and there exist positive constants $\alpha,\ \beta,\ C_e,\ C_\lambda > 0$ such that for any $i\in\mathbb{N}$ it holds

$$\|e_i\|_{L^\infty(\mathcal{D})} \le C_e, \|\nabla e_i\|_{L^\infty(\mathcal{D})} \le C_e i^\alpha,\ \sum_{i=1}^{\infty}\lambda_i i^\beta \le C_\lambda < +\infty.$$

ii $F:\mathbb{R}\to\mathbb{R}_+$ is Lipschitz continuous and globally bounded by $C_F > 0$, i.e. $F(x) < C_F,\ x\in\mathbb{R}$.

iii l *is a Lévy process on* $[0, C_F]$ *with Lévy triplet* (γ_l, b, ν) *which is independent of* W*. Further, we assume there exists a constant* $\eta > 1$ *and càdlàg approximations* $l^{(\varepsilon_l)}$ *of this process such that for every* $s \in [1, \eta)$ *it holds*

$$\mathbb{E}(|l(t) - l^{(\varepsilon_l)}(t)|^s) \leq C_l \varepsilon_l,\ t \in [0, C_F), \tag{8.1}$$

for $\varepsilon_l > 0$ *and*

$$\mathbb{E}(|l(t)|^s) \leq C_l t^\delta,\ t \in [0, C_F), \tag{8.2}$$

with $\delta \in (0, 1]$ *and a constant* $C_l > 0$*.*

◆

We continue with a remark on Assumption 8.5.1.

Remark 8.5.2. *Assumtion 8.5.1 i is natural for GRFs and guarantees certain regularity properties for the paths of the GRF (see e.g. [16, 96, 29]). Equation* (8.1) *ensures that we can approximate the Lévy subordinators in an* L^s*-sense. This can be achieved under appropriate assumptions on the tails of the distribution of the Lévy processes, see [15, Assumption 3.6, Assumption 3.7, Theorem 3.21] and [96, Section 7]). There are several results in the direction of condition* (8.2)*. For example, in [90] and [37], the authors formulate general assumptions on the Lévy measure which guarantee Equation* (8.2) *and similar properties. Further, in [90] the authors explicitly derive the rate* δ *in Equation* (8.2) *for several Lévy processes. In [23, Proposition 2.3], an exact polynomial time-dependence of the absolute moments of a Lévy process under the assumption that the absolute moment of the Lévy process exists up to a certain order was proven. In order to illustrate* (8.2)*, we present a short numerical example: for three different Lévy processes, we estimate* $\mathbb{E}(|l(t)|^s)$ *for* $t = 2^i$ *with* $i \in \{1, 0, -1, \ldots, -16\}$ *using* 10^7 *samples of the process* l *and different values for the exponent* $s \geq 1$*. The results are shown in Figure 8.2, where the estimated moments* $\mathbb{E}(|l(t)|^s)$ *are plotted against the time parameter* t*. The results clearly indicate that* $\mathbb{E}(|l(t)|^s) = \mathcal{O}(t)$*,* $t \to 0$ *which implies* (8.2) *with* $\delta = 1$ *in the considered examples.* ◆

We close this subsection with a remark on a possible way to construct approximations of Lévy processes.

Remark 8.5.3. *One way to construct a càdlàg approximation* $l^{(\varepsilon_l)} \approx l$ *is a piecewise constant extension of the values of the process on a discrete grid: assume* $\{t_i,\ i = 0 \ldots, N_l\}$*, with* $t_0 = 0$

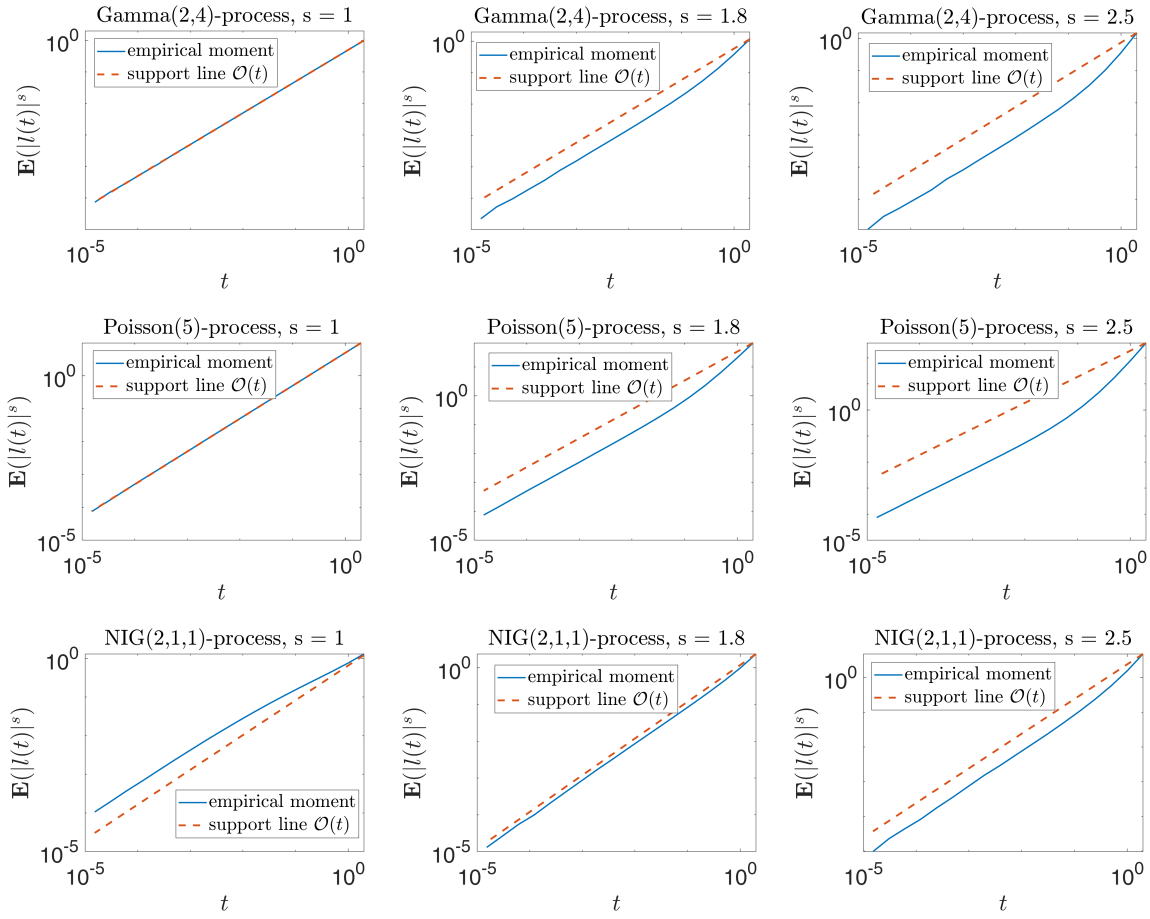

Figure 8.2: Estimated s-moment for different Lévy processes and different values of s. Top: Gamma(2,4) process, middle: Poisson(5) process, bottom: NIG(2,1,1) process.

and $t_{N_l} = C_F$ *is a grid on* $[0, C_F]$ *with* $|t_{i+1} - t_i| = t_{i+1} - t_i = \varepsilon_l > 0$ *for* $i = 0, \dots, N_l - 1$ *and* $\{l(t_i),\ i = 0, \dots, N_l\}$ *are the values of the process* l *on this grid. We define*

$$l^{(\varepsilon_l)}(t) = \sum_{i=1}^{N_l} \mathbb{1}_{[t_{i-1}, t_i)}(t)\, l(t_{i-1}),\ t \in [0, C_F).$$

Such a construction yields an admissible approximation in the sense of Assumption 8.5.1 iii for many Lévy processes (see e.g. [96, Section 7] for the case of Poisson and Gamma processes). Note that the values of the process on the grid may be simulated easily for many Lévy processes using the independent and stationary increment property. ◆

8.5.1 Approximation of the GRF

In this subsection, we shortly introduce two possible approaches to approximate the GRF W. Both approaches are admissible for the construction of approximations of the GSLF in Subsection 8.5.2. In the following and for the rest of the section, we consider $\mathcal{D} = [0, D]^d$. Assumption 8.5.1 allows conclusions to be drawn on the spatial regularity of the GRF W. The next lemma on the approximation of the GRF W follows from the regularity properties of W (see [96, Lemma 4.4] and [29]).

Lemma 8.5.4.
Consider the discrete grid $G^{(\varepsilon_W)} = \{(x_{i^{(1)}}, \dots, x_{i^{(d)}}) |\ i^{(1)}, \dots, i^{(d)} = 0, \dots, M_{\varepsilon_W}\}$ *on* $\mathcal{D}$ *where* $(x_i,\ i = 0, \dots, M_{\varepsilon_W})$ *is an equidistant grid on* $[0, D]$ *with maximum step size* ε_W. *Further, let* $W^{(\varepsilon_W)}$ *be an approximation of the GRF* W *on the discrete grids* $G^{(\varepsilon_W)}$ *which is constructed by point evaluation of the random field* W *on the grid and multilinear interpolation between the grid points. Under Assumption 8.5.1 i, it holds for* $n \in [1, +\infty)$*:*

$$\|W - W^{(\varepsilon_W)}\|_{L^n(\Omega; L^\infty(\mathcal{D}))} \leq C(D, n, d)\varepsilon_W^\gamma$$

for $\gamma < \min(1, \beta/(2\alpha))$, *where* β *and* α *are the parameters from Assumption 8.5.1 i.* ◆

It follows by the Karhunen-Loève-Theorem (see e.g. [3, Section 3.2]) that the GRF W admits the representation

$$W(\underline{x}) = \sum_{i=1}^{\infty} \sqrt{\lambda_i} Z_i e_i(\underline{x}),\ \underline{x} \in \mathcal{D},$$

with i.i.d. $\mathcal{N}(0, 1)$-distributed random variables $(Z_i,\ i \in \mathbb{N})$ and the sum converges in the mean-square sense, uniformly in $\underline{x} \in \mathcal{D}$. The Karhunen-Loève expansion (KLE) motivates another approach to approximate the GRF W: For a fixed cut-off index $N \in \mathbb{N}$, we define the approximation W^N by

$$W^N(\underline{x}) = \sum_{i=1}^{N} \sqrt{\lambda_i} Z_i e_i(\underline{x}),\ \underline{x} \in \mathcal{D}. \tag{8.3}$$

Under Assumption 8.5.1 we can quantify the corresponding approximation error (cf. [16, Theorem 3.8]).

Lemma 8.5.5.
Let Assumption 8.5.1 i hold. Then, it holds for any $N \in \mathbb{N}$ and $n \in [1, +\infty)$:

$$\|W - W^N\|_{L^n(\Omega;L^\infty(\mathcal{D}))} \leq C(D, n, d) N^{-\frac{\beta}{2}}.$$

◆

Proof. It follows by [16, Theorem 3.8] that

$$\|W - W^N\|^2_{L^n(\Omega;L^\infty(\mathcal{D}))} \leq C(D, n, d) \sum_{i=N+1}^{\infty} \lambda_i,$$

for all $N \in \mathbb{N}$. We use Assumption 8.5.1 *i* to compute

$$\sum_{i=N+1}^{\infty} \lambda_i = \sum_{i=N+1}^{\infty} \lambda_i i^\beta i^{-\beta} \leq N^{-\beta} \sum_{i=N+1}^{\infty} \lambda_i i^\beta \leq C_\lambda N^{-\beta},$$

which finishes the proof. □

In the following, we denote by W^N an approximation of the GRF of W. The notation is clear if we approximate the GRF by the truncated KLE. If we approximate W by sampling on a discrete grid (cf. Lemma 8.5.4), then we use $\varepsilon_W = 1/N$ and abuse notation to write $W^N = W^{(1/N)}$. Regardless of the choice between these two approaches, we thus obtain an approximation $W^N \approx W$ with

$$\|W - W^N\|_{L^n(\Omega;L^\infty(\mathcal{D}))} \leq C(D, n, d) R(N), \tag{8.4}$$

for $N \in \mathbb{N}$ and $n \in [1, +\infty)$, where $R(N) = N^{-\gamma}$ if we approximate the GRF by discrete sampling and $R(N) = N^{-\frac{\beta}{2}}$ if we approximate it by the KLE approach.

8.5.2 Approximation of the GSLF

We are now able to quantify the approximation error for the GSLF where both components, the Lévy process and the GRF, are approximated.

Theorem 8.5.6.
Let Assumption 8.5.1 hold and assume an approximation $W^N \approx W$ of the GRF is given, as introduced in Subsection 8.5.1. For a given real number $1 \leq p < \eta$ and a globally Lipschitz

continuous function $g : \mathbb{R} \to \mathbb{R}$, it holds

$$\|g(l^{(\varepsilon_l)}(F(W^N))) - g(l(F(W)))\|_{L^p(\Omega;L^p(\mathcal{D}))} \leq C(\varepsilon_l^{\frac{1}{p}} + R(N)^{\frac{\delta}{p}}),$$

for $N \in \mathbb{N}$ and $\varepsilon_l > 0$, where δ is the positive constant from (8.2). ◆

Proof. We calculate using Fubini's theorem and the triangle inequality

$$\begin{aligned}
&\|g(l^{(\varepsilon_l)}(F(W^N))) - g(l(F(W)))\|_{L^p(\Omega;L^p(\mathcal{D}))} \\
&\leq \|g(l^{(\varepsilon_l)}(F(W^N))) - g(l(F(W^N)))\|_{L^p(\Omega\times\mathcal{D})} \\
&\quad + \|g(l(F(W^N))) - g(l(F(W)))\|_{L^p(\Omega\times\mathcal{D})} \\
&=: I_1 + I_2
\end{aligned}$$

Further, we use the Lipschitz continuity of g together with Lemma 8.4.1 to obtain for any $\underline{x} \in \mathcal{D}$

$$\begin{aligned}
&\mathbb{E}(|g(l^{(\varepsilon_l)}(F(W^N(\underline{x})))) - g(l(F(W^N(\underline{x}))))|^p) \\
&\leq C_g \mathbb{E}(|l^{(\varepsilon_l)}(F(W^N(\underline{x}))) - l(F(W^N(\underline{x})))|^p) \\
&= \mathbb{E}(m(F(W^N(\underline{x})))
\end{aligned}$$

with

$$m(z) = \mathbb{E}(|l(z) - l^{(\varepsilon_l)}(z)|^p) \leq C_l \varepsilon_l$$

for $z \in [0, C_F)$ by Assumption 8.5.1 *iii.* Therefore, we obtain

$$\mathbb{E}(|g(l^{(\varepsilon_l)}(F(W^N(\underline{x})))) - g(l(F(W^N(\underline{x}))))|^p) \leq C_l \varepsilon_l,$$

for all $\underline{x} \in \mathcal{D}$ and, hence,

$$\begin{aligned}
I_1^p &= \int_{\mathcal{D}} \mathbb{E}(|g(l^{(\varepsilon_l)}(F(W^N(\underline{x})))) - g(l(F(W^N(\underline{x}))))|^p) d\underline{x} \\
&\leq D^d C_l \varepsilon_l.
\end{aligned}$$

For the second summand we calculate using Lemma 8.4.1 and Remark 8.4.2 with $\tilde{l}(t_1, t_2) := l(t_1) - l(t_2)$ and $\tilde{W}_+ := (F(W(\underline{x})), F(W^N(\underline{x})))$

$$\mathbb{E}(|l(F(W(\underline{x}))) - l(F(W^N(\underline{x})))|^p) = \mathbb{E}(\tilde{m}(F(W(\underline{x})), F(W^N(\underline{x})))),$$

with

$$\tilde{m}(t_1, t_2) = \mathbb{E}(|l(t_1) - l(t_2)|^p),\ t_1, t_2 \in [0, C_F).$$

For $C_F > t_1 \geq t_2 \geq 0$, the stationarity of l together with Assumption 8.5.1 *iii* yields

$$\tilde{m}(t_1, t_2) = \mathbb{E}(|l(t_1 - t_2)|^p) \leq C_l |t_1 - t_2|^\delta.$$

Further, for $0 \leq t_1 \leq t_2 < C_F$ we have

$$\tilde{m}(t_1, t_2) = \mathbb{E}(|l(t_2) - l(t_1)|^p) = \mathbb{E}(|l(t_2 - t_1)|^p) \leq C_l |t_2 - t_1|^\delta.$$

Overall, we obtain for any $\omega \in \Omega$ the pathwise estimate

$$\tilde{m}(F(W(\underline{x})), F(W^N(\underline{x}))) \leq C_l |F(W(\underline{x})) - F(W^N(\underline{x}))|^\delta,$$

for any $\underline{x} \in \mathcal{D}$. We apply Hölder's inequality and Equation (8.4) to obtain

$$\begin{aligned}
\mathbb{E}(|l(F(W(\underline{x}))) - l(F(W^N(\underline{x})))|^p) &= \mathbb{E}(\tilde{m}(F(W(\underline{x})), F(W^N(\underline{x})))), \\
&\leq C_l \mathbb{E}(|F(W(\underline{x})) - F(W^N(\underline{x}))|^\delta) \\
&\leq C_l \mathbb{E}(|F(W(\underline{x})) - F(W^N(\underline{x}))|)^\delta \\
&\leq C_l C_F \mathbb{E}(|W(\underline{x}) - W^N(\underline{x})|)^\delta \\
&\leq C_l C_F C(D, d)^\delta R(N)^\delta,
\end{aligned}$$

for any $\underline{x} \in \mathcal{D}$. Finally, we use the Lipschitz contnuity of g to obtain:

$$\begin{aligned}
I_2^p &= \int_{\mathcal{D}} \mathbb{E}(|g(l(F(W^N(\underline{x})))) - g(l(F(W(\underline{x}))))|^p) d\underline{x} \\
&\leq C(C_l, D, d, \delta, C_F, C_g) R(N)^\delta.
\end{aligned}$$

Overall, we end up with

$$\|g(l^{(\varepsilon_l)}(F(W^N))) - g(l(F(W)))\|_{L^p(\Omega; L^p(\mathcal{D}))} \leq C(C_l, D, d, \delta, C_F, C_g, p)(\varepsilon_l^{\frac{1}{p}} + R(N)^{\frac{\delta}{p}}).$$

□

8.5.3 The pointwise distribution of the approximated GSLF

In Section 8.4 we investigated the pointwise distribution of a GSLF and derived a formula for its pointwise characteristic function. In Section 8.5, we demonstrated how approximations of the Lévy process l and the underlying GRF W may be used to approximate the GSLF and quantified the approximation error. This is of great importance especially in applications, since it is in general not possible to simulate the GRF or the Lévy process on their continuous parameter domains. The question arises how such an approximation affects the pointwise distribution of the field. For this purpose, we prove in the following a formula for the pointwise charateristic function of the approximated GSLF.

Corollary 8.5.7.
We consider a GSLF with Lévy process l and an independent GRF W. Let $l^{(\varepsilon_l)} \approx l$ be a càdlàg approximation of the Lévy process and $W^N \approx W$ be an approximation of the GRF, where we assume that the mean function μ_W of the GRF W is known and does not need to be approximated. For $\underline{x} \in \mathcal{D}$, the pointwise characteristic function of the approximated GSLF is given by

$$\phi_{l^{(\varepsilon_l)}(F(W^N(\underline{x})))}(\xi) = \mathbb{E}\Big(\exp(i\xi l^{(\varepsilon_l)}(F(W^N(\underline{x}))))\Big) = \mathbb{E}(\rho_{l^{(\varepsilon_l)}}(F(W^N(\underline{x})),\xi)),\ \xi \in \mathbb{R},$$

where

$$\rho_{l^{(\varepsilon_l)}}(t,\xi) = \mathbb{E}(\exp(i\xi l^{(\varepsilon_l)}(t))),$$

denotes the pointwise characteristic function of $l^{(\varepsilon_l)}$. Further, consider the discrete grid $\{t_i,\ i = 0,\dots,N_l\}$ with $t_0 = 0$, $t_{N_l} = C_F$ and $|t_{i+1} - t_i| = \varepsilon_l$, for $i = 0,\dots,N_\ell - 1$.

If the Lévy process is approximated according to Remark 8.5.3 and the GRF is approximated with the truncated KLE, that is

$$W^N(\underline{x}) = \mu_W(\underline{x}) + \sum_{i=1}^{N} \sqrt{\lambda_i} Z_i e_i(\underline{x}) \approx \mu_W(\underline{x}) + \sum_{i=1}^{\infty} \sqrt{\lambda_i} Z_i e_i(\underline{x}) = W(\underline{x}),\ \underline{x} \in \mathcal{D},$$

with some $N \in \mathbb{N}$, i.i.d. standard normal random variables $(Z_i,\ i \in \mathbb{N})$ and eigenbasis $((\lambda_i, e_i),\ i \in \mathbb{N})$ corresponding to the covariance operator Q of W (cf. Section 8.5.1) and

$F(\cdot) < C_F$, we obtain

$$\phi_{l^{(\varepsilon_l)}(F(W^N(\underline{x})))}(\xi) = \frac{1}{\sqrt{2\pi\sigma^2_{W,N}(\underline{x})}} \int_{\mathbb{R}} \exp\Big(t_{\lfloor F(y)/\varepsilon_l \rfloor}\psi(\xi) - \frac{(y-\mu_W(\underline{x}))^2}{2\sigma^2_{W,N}(\underline{x})}\Big)dy,\ \xi \in \mathbb{R}.$$

Here, $\sigma^2_{W,N}$ is the variance function of the approximation W^N, which is given by

$$\sigma^2_{W,N}(\underline{x}) := \mathrm{Var}(W^N(\underline{x})) = \mathbb{E}\Big(\sum_{i=1}^N \sqrt{\lambda_i} Z_i e_i(\underline{x})\Big)^2 = \sum_{i=1}^N \lambda_i e_i^2(\underline{x}),\ \underline{x} \in \mathcal{D}.$$

The function ψ denotes the characteristic exponent of l defined by

$$\psi(\xi) = i\gamma_l \xi - \frac{b}{2}\xi^2 + \int_{\mathbb{R}\setminus\{0\}} e^{i\xi y} - 1 - i\xi y \mathbb{1}_{\{|y|\le 1\}}(y)\nu(dy),$$

for $\xi \in \mathbb{R}$ and, for any positive real number x, we denote by $\lfloor x \rfloor$ the largest integer smaller or equal than x. ◆

Proof. As in the proof of Corollary 8.4.3, we use Lemma 8.4.1 to calculate

$$\begin{aligned}\phi_{l^{(\varepsilon_l)}(F(W^N(\underline{x})))}(\xi) &= \mathbb{E}\Big(\exp(i\xi l^{(\varepsilon_l)}(F(W^N(\underline{x}))))\Big) \\ &= \mathbb{E}(\rho_{l^{(\varepsilon_l)}}(F(W^N(\underline{x})),\xi)),\ \xi \in \mathbb{R}.\end{aligned}$$

In the next step, we compute the charateristic function of the approximation $l^{(\varepsilon_l)}$ of the Lévy process constructed as described in Remark 8.5.3. We use the independence and stationarity of the increments of the Lévy process to obtain

$$l^{(\varepsilon_l)}(t) = \sum_{i=1}^{N_l} \mathbb{1}_{[t_{i-1},t_i)}(t) l(t_{i-1}) = \sum_{i=1}^{N_l} \mathbb{1}_{[t_{i-1},t_i)}(t) \sum_{j=1}^{i-1} l(t_j) - l(t_{j-1}) \overset{\mathcal{D}}{=} \sum_{k=1}^{\lfloor t/\varepsilon_l \rfloor} l_k^{\varepsilon_l},$$

where $(l_k^{\varepsilon_l},\ k \in \mathbb{N})$ are i.i.d. random variables following the distribution of $l(\varepsilon_l)$ and we denote by $\overset{\mathcal{D}}{=}$ equivalence of the corresponding probability distributions. The convolution theorem (see e.g. [79, Lemma 15.11]) yields the representation

$$\begin{aligned}\phi_{l^{(\varepsilon_l)}(t)}(\xi) &= \prod_{k=1}^{\lfloor t/\varepsilon_l \rfloor} \mathbb{E}(\exp(i\xi l_k^{(\varepsilon_l)})) = \prod_{k=1}^{\lfloor t/\varepsilon_l \rfloor} \exp(\varepsilon_l \psi(\xi)) = \exp(\lfloor t/\varepsilon_l \rfloor \varepsilon_l \psi(\xi)) \\ &= \exp(t_{\lfloor t/\varepsilon_l \rfloor}\psi(\xi)),\end{aligned}$$

for $t \in [0, C_F)$ and $\xi \in \mathbb{R}$. Therefore, we obtain

$$\phi_{l^{(\varepsilon_l)}(F(W^N(\underline{x})))}(\xi) = \mathbb{E}(\exp(t_{\lfloor F(W^N(\underline{x}))/\varepsilon_l \rfloor}\psi(\xi))),\ \xi \in \mathbb{R}.$$

The second formula for the characteristic function of the approximated field now follows from the fact that $W^N(\underline{x}) \sim \mathcal{N}(\mu_W(\underline{x}), \sigma^2_{W,N}(\underline{x}))$. □

8.6 The covariance structure of GSLFs

In many modeling applications one aims to use a random field model that mimics a specific covariance structure which is, for example, obtained from empirical data. In such a situation it is useful to have access to the theoretical covariance function of the random fields used in the model. Therefore, we derive a formula for the covariance function of the GSLF in the following section.

Lemma 8.6.1.
Assume W is a GRF and l is an independent Lévy process with existing first and second moment. We denote by μ_W, σ^2_W and q_W, the mean, variance and covariance function of W and by $\mu_l(t) = \mathbb{E}(l(t))$, $\mu_l^{(2)}(t) := \mathbb{E}(l(t)^2)$ the functions for the first second moment of the Lévy process l. For $\underline{x} \neq \underline{x}' \in \mathcal{D}$, the covariance function of the GSLF L is given by

$$\begin{aligned} q_L(\underline{x}, \underline{x}') = &\int_{\mathbb{R}^2} c_l(F(u), F(v)) f_{(W(\underline{x}), W(\underline{x}'))}(u, v) d(u, v) \\ &- \int_{\mathbb{R}} \mu_l(F(u)) f_{W(\underline{x})}(u) du \int_{\mathbb{R}} \mu_l(F(v)) f_{W(\underline{x}')}(v) dv, \end{aligned}$$

where we define

$$\begin{aligned} f_{W(\underline{x})}(u) &:= \frac{\exp\left(-\frac{(u-\mu_W(\underline{x}))^2}{2\sigma^2_W(\underline{x})}\right)}{\sqrt{2\pi\sigma^2_W(\underline{x})}}, \\ \Sigma_W(\underline{x}, \underline{x}') &:= \begin{bmatrix} \sigma^2_W(\underline{x}) & q_W(\underline{x}, \underline{x}') \\ q_W(\underline{x}, \underline{x}') & \sigma^2_W(\underline{x}') \end{bmatrix}, \end{aligned}$$

$$f_{(W(\underline{x}),W(\underline{x}'))}(u,v) := \frac{\exp\Big(-\frac{1}{2}\begin{pmatrix} u-\mu_W(\underline{x}) \\ v-\mu_W(\underline{x}')\end{pmatrix}^T \Sigma_W(\underline{x},\underline{x}')^{-1}\begin{pmatrix} u-\mu_W(\underline{x}) \\ v-\mu_W(\underline{x}')\end{pmatrix}\Big)}{\sqrt{(2\pi)^2\big(\sigma_W^2(\underline{x})\sigma_W^2(\underline{x}')-q_W^2(\underline{x},\underline{x}')\big)}},$$
$$c_l(u,v) := \mu_l(|u-v|)\mu_l(u\wedge v)+\mu_l^{(2)}(u\wedge v),$$

for $u,v\in\mathbb{R}$ with $u\wedge v := \min(u,v)$. For $\underline{x}=\underline{x}'\in\mathcal{D}$, the pointwise variance is given by

$$\sigma_L^2(\underline{x}) = q_L(\underline{x},\underline{x}) = \int_{\mathbb{R}}\mu_l^{(2)}(F(u))f_{W(\underline{x})}(u)du - \Big(\int_{\mathbb{R}}\mu_l(F(u))f_{W(\underline{x})}(u)du\Big)^2.$$

◆

Proof. We compute using Lemma 8.4.1, for $\underline{x}\in\mathcal{D}$

$$\mu_L(\underline{x}) := \mathbb{E}(L(\underline{x})) = \mathbb{E}\Big(l(F(W(\underline{x})))\Big) = \mathbb{E}\Big(\mu_l(F(W(\underline{x})))\Big).$$

Further, we calculate for $\underline{x},\underline{x}'\in\mathcal{D}$

$$\begin{aligned} q_L(\underline{x},\underline{x}') &= \mathbb{E}\Big((L(\underline{x})-\mu_L(\underline{x}))(L(\underline{x}')-\mu_L(\underline{x}'))\Big) \\ &= \mathbb{E}(L(\underline{x})L(\underline{x}'))-\mu_L(\underline{x})\mu_L(\underline{x}'). \end{aligned}$$

Next, we consider $0\le t_1\le t_2$ and use the fact that l has stationary and independent increments to compute

$$\mathbb{E}(l(t_1)l(t_2)) = \mathbb{E}\big((l(t_2)-l(t_1))l(t_1)\big)+\mathbb{E}(l(t_1)^2) = \mu_l(t_2-t_1)\mu_l(t_1)+\mu_l^{(2)}(t_1).$$

Similarly, we obtain for $0\le t_2\le t_1$

$$\mathbb{E}(l(t_1)l(t_2)) = \mathbb{E}\big((l(t_1)-l(t_2))l(t_2)\big)+\mathbb{E}(l(t_2)^2) = \mu_l(t_1-t_2)\mu_l(t_2)+\mu_l^{(2)}(t_2),$$

and, hence, it holds for general $t_1,t_2\ge 0$:

$$c_l(t_1,t_2) := \mathbb{E}(l(t_1)l(t_2)) = \mu_l(|t_1-t_2|)\mu_l(t_1\wedge t_2)+\mu_l^{(2)}(t_1\wedge t_2).$$

Another application of Lemma 8.4.1 and Remark 8.4.2 yields

$$\mathbb{E}(L(\underline{x})L(\underline{x}')) = \mathbb{E}(l(F(W(\underline{x})))l(F(W(\underline{x}')))) = \mathbb{E}(c_l(F(W(\underline{x})), F(W(\underline{x}')))).$$

Putting these results together, we end up with

$$\begin{aligned} q_L(\underline{x}, \underline{x}') &= \mathbb{E}(L(\underline{x})L(\underline{x}')) - \mu_L(\underline{x})\mu_L(\underline{x}') \\ &= \mathbb{E}(c_l(F(W(\underline{x})), F(W(\underline{x}')))) - \mathbb{E}(\mu_l(F(W(\underline{x}))))\mathbb{E}(\mu_l(F(W(\underline{x}')))), \end{aligned}$$

for $\underline{x},\ \underline{x}' \in \mathcal{D}$. The assertion now follows from the fact that $W(\underline{x}) \sim \mathcal{N}(\mu_W(\underline{x}), \sigma_W^2(\underline{x}))$ and $(W(\underline{x}), W(\underline{x}'))^T \sim \mathcal{N}_2((\mu_W(\underline{x}), \mu_W(\underline{x}'))^T, \Sigma_W(\underline{x}, \underline{x}'))$, for $\underline{x} \neq \underline{x}' \in \mathcal{D}$, together with $c_l(t,t) = \mu_l^{(2)}(t)$ for $t \geq 0$. □

8.7 Numerical examples

In this section, we present numerical experiments on the theoretical results presented in the previous sections. The aim is to investigate the results of existing numerical methods and to illustrate the theoretical properties of the GSLF which have been proven in the previous sections, e.g. the pointwise distribution of the approximated fields or the quality of this approximation (see Theorem 8.5.6). Further, the presented numerical experiments and methods may also be useful for fitting the GSLF to existing data in various applications.

8.7.1 Pointwise characteristic function

Corollary 8.4.3 gives access to the pointwise characteristic function of the GSLF $L(\underline{x}) = l(F(W(\underline{x}))),\ \underline{x} \in \mathcal{D}$, with a Lévy process l and a GRF W, which is independent of l. Using the characteristic function and the Fourier inversion (FI) method (see [56]) we may compute the pointwise density function of the GSLF. Note that in both of these steps, the application of Corollary 8.4.3 and of the Fourier inversion theorem, numerical integration is necessary which may be inaccurate or computationally expensive. In this subsection, we choose specific Lévy processes together with a GRF and compare the computed density function of the corresponding GSLF with the histogram of samples of the simulated field. To be precise, we choose a Matérn-1.5-GRF, a Gamma process, set $F = |\cdot| + 1$ and consider the GSLF $L(\underline{x}) = l(F(W(\underline{x}))$ on $\mathcal{D} = [0,1]^2$. The distributions and the corresponding density functions are presented in Figure 8.3. In line with our expectations, the FI approach perfectly matches the true distribution of

the field at $(1, 1)$.

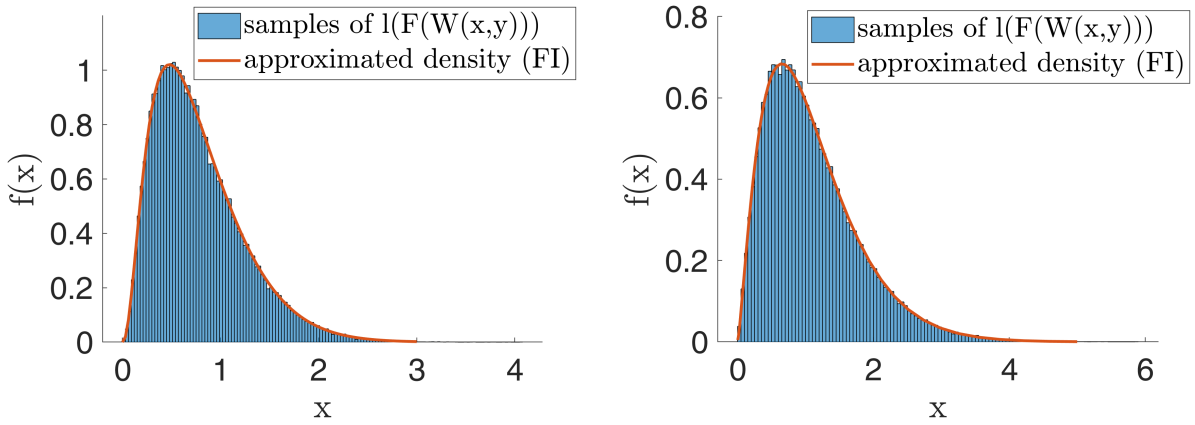

Figure 8.3: 10^5 samples of the GSLF evaluated at $(1, 1)$ and the corresponding density functions approximated via FI. Left: Gamma(3,10) process and a Matérn GRF with $\sigma = 2$. Right: Gamma(2,4) process with Matérn GRF with $\sigma = 1.5$.

8.7.2 Pointwise distribution of approximated fields

In Subsection 8.7.1 we presented a numerical example regarding the pointwise distribution of the GSLF. In applications, it is not possible to draw samples from the exact GSLF and, hence, one has to use approximations instead. The effect of such an approximation on the pointwise distribution of the random field has been investigated theoretically in Subsection 8.5.3. In this section, we aim to provide a numerical example in order to visualize the distributional effect of sampling from an approximation of the GSLF. For a specific choice of the Lévy process l, the transformation function F and the GRF W, we use Corollary 8.5.7 and the FI method to compute the pointwise distribution of the approximated field $l^{(\varepsilon_l)}(F(W^N(\underline{x}))) \approx l(F(W(\underline{x})))$ for different approximation parameters ε_l (resp. N) of the Lévy process (resp. the GRF). The computed densities are then compared with samples of the approximated field. We set $\mathcal{D} = [0, 1]^2$ and consider the evaluation point $\underline{x} = (0.4, 0.6)$. The GRF W is given by the KLE

$$W = \sum_{k=1}^{\infty} \sqrt{\lambda_k} e_k(x, y) Z_k,$$

where the eigenbasis is defined by

$$e_k(x, y) = 2 \sin(\pi k x) \sin(\pi k y), \ \lambda_k = 10(k^2\pi^2 + 0.1^2)^{-\nu},$$

level	1	2	3	4	5	6
ε_l	1	0.5	0.01	0.001	0.0001	1e-7
N	3	5	250	2500	25000	1e7

Table 8.1: Discretization parameters for the approximation of the GSLF.

with $\nu = 0.6$ (see [51, Appendix A]). Further, we set $F(x) = 1 + \min(|x|, 30)$ and choose l to be a Gamma(3,10) process. The threshold 30 in the definition of F is large enough to have no effect in our numerical example since the absolute value of W does not exceed 30 in all considered samples. We use piecewise constant approximations $l^{(\varepsilon_l)}$ of the Lévy process l on an equidistant grid with stepsize $\varepsilon_l > 0$ (see Remark 8.5.3) and approximate the GRF W by the truncated KLE with varying truncation indices N. To be more precise, we choose 6 different approximation levels for these two approximation parameters, as described in Table 8.1. For each discretization level, we compute the characteristic function using Corollary 8.5.7, approximate the density function via FI and compare it with 10^5 samples of the approximated field evaluated at the point $(0.4, 0.6)$. The results are given in Figure 8.4. As expected from

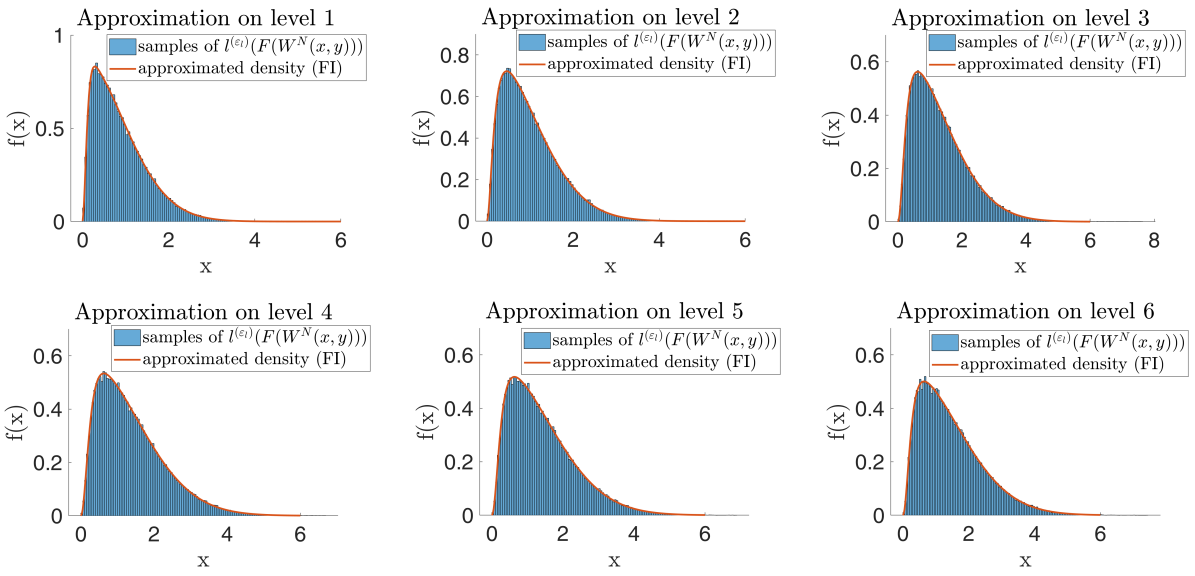

Figure 8.4: Approximated pointwise densities (FI) of the GSLF on the different discretization levels together with samples of the corresponding approximated GSLF.

Subsection 8.7.1, we see that the densities of the pointwise distribution of the approximated GSLF, which are approximated by FI, fit the actual samples of the approximated field accurately. In order to get a better impression of the influence of the approximation on the different levels, Figure 8.5 shows the densities of the evaluated approximated GSLF on the different levels,

together with the density of the exact field. We see how the densities of the approximted GSLF converge to the density of the exact field for $\varepsilon_l \to 0$ and $N \to \infty$. The results also show that the effect of the approximation of the GSLF should not be unterestimated: on the lower levels, we obtain comparatively large deviations of the pointwise densities from the density of the exact field, which should be taken into account in applications. Obviously, the effect of the approximation depends heavily on the specific choice of the Lévy process and the underlying GRF.

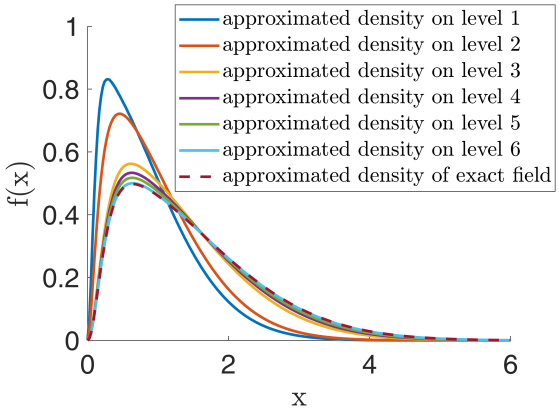

Figure 8.5: Approximated pointwise densities (FI) of the GSLF on the different discretization levels together with the pointwise density of the actual GSLF.

8.7.3 Numerical approximation of the GSLF

In Section 8.5, we considered approximations $l^{(\varepsilon_l)} \approx l$ of the Lévy process and $W^N \approx W$ of the GRF and derived an error bound on the corresponding approximation $l^{(\varepsilon_l)}(F(W^N(\underline{x}))) \approx l(F(W(\underline{x})))$ (see Theorem 8.5.6). In fact, under Assumption 8.5.1, if we choose the approximation parameter N of the GRF W such that $R(N) \sim \varepsilon_l^{1/\delta}$ with $R(N)$ from Equation (8.4), we obtain an overall approximation error which is dominated by $\varepsilon_l^{1/p}$:

$$\|l^{(\varepsilon_l)}(F(W^N)) - l(F(W))\|_{L^p(\Omega;L^p(\mathcal{D}))} = \mathcal{O}(\varepsilon_l^{1/p}),\ \varepsilon_l \to 0.$$

In this section, we present numerical experiments to showcase this approximation result.

We set $F(x) = \min(|x|, 30)$ and consider the domain $\mathcal{D} = [0,1]^2$. Let

$$W(x,y) = \sum_{k=1}^{\infty} \sqrt{\lambda_k} e_k(x,y) Z_k,$$

be a GRF with corresponding eigenbasis

$$e_k(x,y) = 2\sin(\pi kx)\sin(\pi ky)\,,\ \lambda_k = 100\,(k^2\pi^2 + 0.2^2)^{-\nu},\ \nu > 0.5. \tag{8.5}$$

With this choice, Assumption 8.5.1 *i* is satisfied with $\alpha = 1$ and $0 < \beta < 2\nu - 1$, since

$$\sum_{k=1}^{\infty} \lambda_k k^{\beta} \leq C \sum_{k=1}^{\infty} k^{\beta - 2\nu} < \infty,$$

where we used that $\lambda_k \leq Ck^{-2\nu}$ for $k \in \mathbb{N}$. Hence, we obtain by Lemma 8.5.5

$$\|W - W^N\|_{L^n(\Omega; L^\infty(\mathcal{D}))} \leq C(D,n) N^{-\frac{\beta}{2}},$$

for $0 < \beta < 2\nu - 1$, i.e. $R(N) = N^{-\frac{\beta}{2}}$ in Equation (8.4) and Theorem 8.5.6. In our experiments, we choose the Lévy subordinator l to be a Poisson or Gamma process. Approximations $l^{(\varepsilon_l)} \approx l$ of these processes satisfying Assumption 8.5.1 *iii* may be obtained by piecewise constant extensions of values of the process on a grid with stepsize ε_l (see Remark 8.5.3). For these processes, we obtain $\delta = 1$ in (8.2) (see Remark 8.5.2 and [96, Section 7]). Overall, Theorem 8.5.6 yields the error bound

$$\|l^{(\varepsilon_l)}(F(W^N)) - l(F(W))\|_{L^p(\Omega; L^p(\mathcal{D}))} = C(\varepsilon_l^{\frac{1}{p}} + N^{-\frac{\beta}{2p}}),$$

for $0 < \beta < 2\nu - 1$. Hence, in order to equilibrate the error contributions from the GRF approximation and the approximation of the Lévy process, one should choose the cut-off index N of the KLE approximation of the GRF W according to

$$N \simeq \varepsilon_l^{-\frac{2}{2\nu - 1}}, \tag{8.6}$$

which then implies

$$\|l^{(\varepsilon_l)}(F(W^N)) - l(F(W))\|_{L^p(\Omega; L^p(\mathcal{D}))} \leq C\varepsilon_l^{\frac{1}{p}}. \tag{8.7}$$

In our experiments, we set the approximation parameters of the Lévy process to be $\varepsilon_l = 2^{-\ell}$, for $\ell = 2, \ldots, 10$ and the cut-off indices of the GRF are choosen according to (8.6). In order to verify (8.7), we draw 150 samples of the random variable

$$l^{(\varepsilon_l)}(F(W^N)) - l(F(W)),$$

for the described approximation parameters to estimate the corresponding L^p norm of the approximation error for $p \in \{1, 2, 2.5, 3, 3.3\}$ which is expected to behave as $\mathcal{O}(\varepsilon_l^{1/p})$.

In our first example, we set l to be a Poisson(8) process and $\nu = 2.5$ in Equation (8.5). In order to obtain a sufficiently accurate reference field in each sample, we take 150 summands in the KLE of the GRF W and use an exact sample of a Poisson process computed by the Uniform Method (see [109, Section 8.1.2]). The resulting estimates for the L^p approximation error are plotted against ε_l for $p \in \{1, 2, 2.5, 3.3\}$, which is illustrated in the Figure 8.6. As expected,

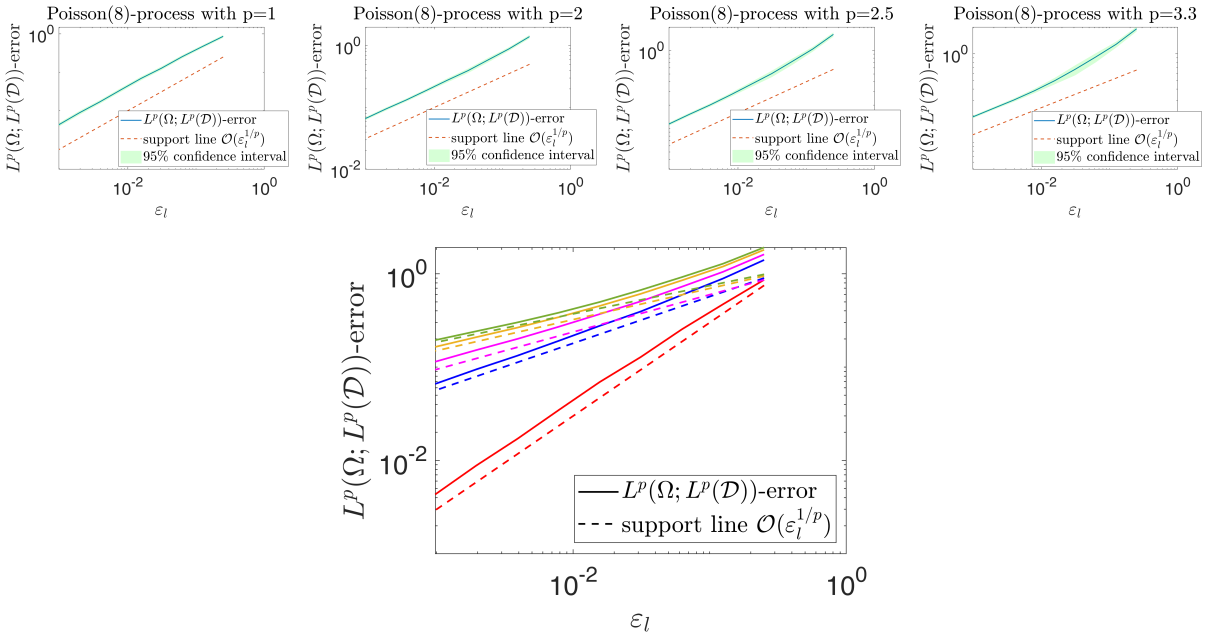

Figure 8.6: Estimated L^p approximation errors against the discretization parameter ε_l for different values of p using a Poisson(8) process (top) and overview for $p = 1, 2, 2.5, 3, 3.3$ (bottom).

the approximated L^p errors converge asymptotically with rate $\varepsilon_l^{1/p}$ for the considered moments p. The bottom plot of Figure 8.6 shows an overview of the L^p approximation errors for different values of p and illustrates that the L^p-errors indeed converge with different rates.

In our second numerical example, we set l to be a Gamma(2,4) process. Further, we set $\nu = 2$ in Equation (8.5). The approximations $l^{(\varepsilon_l)} \approx l$ of the Lévy process on the different levels are again computed by piecewise constant extensions of values of the process on an equidistant grid with stepsize ε_l. Aiming to verify Equation (8.7), we use 150 samples to estimate the L^p approximation error, for $p \in \{1, 2, 2.5, 3, 3.3\}$. In order to compute a sufficiently accurate reference field in each sample, we use 500 summands in the KLE approximation of the GRF W and the Gamma process is computed on a reference grid with stepsize $\varepsilon_l = 2^{-13}$.

The convergence of the estimated L^p error plotted against the discretization parameter ε_l is visualized in Figure 8.7, which shows the expected behaviour of the estimated L^p error for the considered moments p. As in the previous experiment, we provide a plot with all estimated L^p errors in one figure (see bottom plot in Figure 8.7), which again confirms that the L^p-error of the approximation converge in ε_l with rate $1/p$ for the considered values of p.

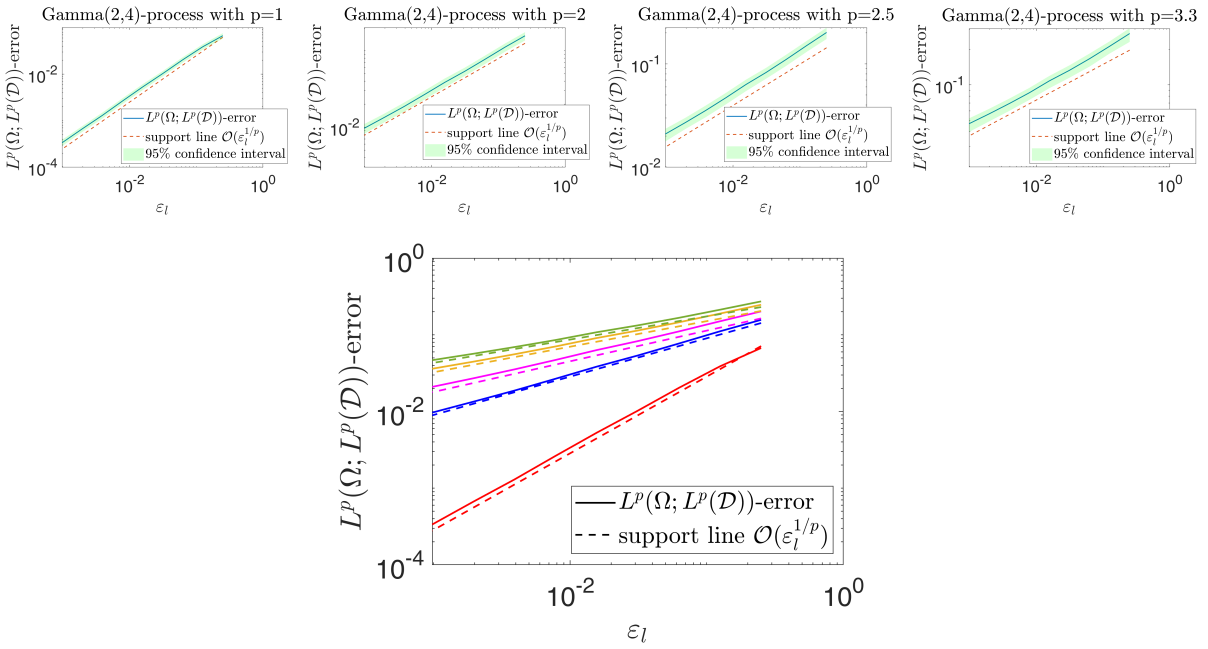

Figure 8.7: Estimated L^p approximation errors against the discretization parameter ε_l for different values of p using a Gamma(2,4) process (top) and overview for $p = 1,\ 2,\ 2.5,\ 3,\ 3.3$ (bottom).

8.7.4 Empirical estimation of the covariance of the GSLF

Lemma 8.6.1 gives access to the covariance function of the GSLF. This is of interest in applications, since it is often required that a random field mimics a specific covariance structure which is determined by (real-world) data. In this example, we choose specific GSLFs and spatial points to compute the corresponding covariance using Lemma 8.6.1 and compare it with empirically estimated covariances using samples of the GSLF. We choose $\mathcal{D} = [0, 2]^2$ and estimate the covariance with a single level Monte Carlo estimator using a growing number of samples of the field L evaluated at the two considered points $\underline{x},\ \underline{x}' \in \mathcal{D}$. If M denotes the number of samples used in this estimation and $E_M(\underline{x}, \underline{x}')$ denotes the Monte Carlo estimation of the covariance,

the convergence rate of the corresponding RMSE for a growing number of samples is $-1/2$, i.e.

$$\text{RMSE} := \|q_L(\underline{x}, \underline{x}') - E_M(\underline{x}, \underline{x}')\|_{L^2(\Omega)} = \mathcal{O}(1/\sqrt{M}),\ M \to \infty.$$

In our experiments, we use Poisson and Gamma processes and W is set to be a centered GRF with squared exponential covariance function, i.e.

$$q_W(\underline{x}, \underline{x}') = \sigma^2 \exp(-|\underline{x} - \underline{x}'|_2^2/r^2),\ \underline{x},\ \underline{x}' \in \mathcal{D},$$

with pointwise variance $\sigma^2 > 0$, correlation length $r > 0$ and $F = |\cdot|$. In our first experiment we choose l to be a Gamma process with varying parameters. The RMSE is estimated for a growing number of samples M and 100 independent MC runs. The results are shown in Figure 8.8. As expected, the approximated RMSE convergences with order $\mathcal{O}(1/\sqrt{M})$ for both experiments. In our second example we set l to be a Poisson process (see Figure 8.9). As in the

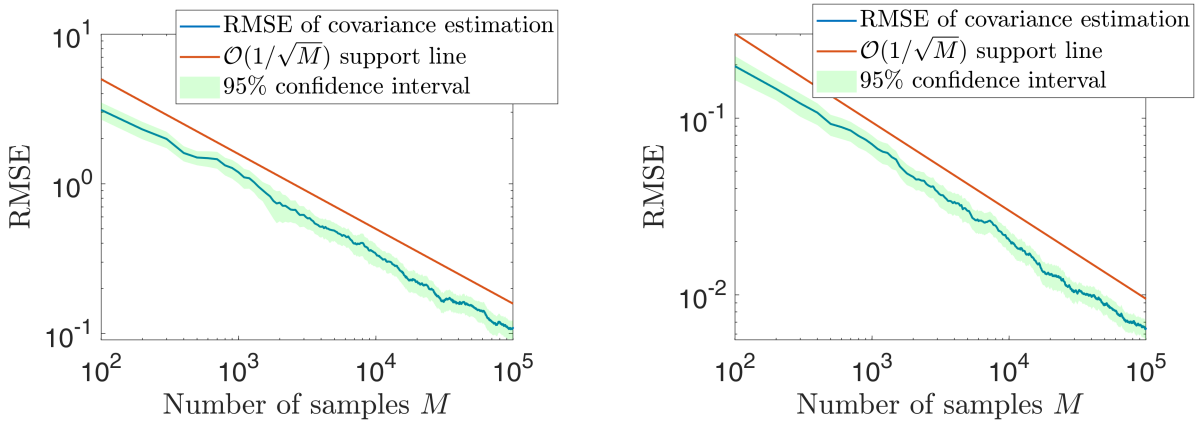

Figure 8.8: Convergence of RMSE of empirical covariance $q_L(\underline{x}, \underline{x}')$; left: l is a Gamma(4,1.5) process, $r = 1$, $\sigma^2 = 4$, $\underline{x} = (0.2, 1.5)$, $\underline{x}' = (0.9, 0.8)$, $q_L(\underline{x}, \underline{x}') \approx 3.0265$; right: l is a Gamma(5,6) process, $r = 1.2$, $\sigma^2 = 1.5^2$, $\underline{x} = (0.9, 1.2)$, $\underline{x}' = (1.6, 0.5)$, $q_L(\underline{x}, \underline{x}') \approx 0.236$.

previous example, we see a convergence rate of order $\mathcal{O}(1/\sqrt{M})$ of the MC estimator for the covariance in each experiment. For small sample numbers, the error values for the estimation of the covariances might seem quite high: for example, in the left plot of Figure 8.9, using $M = 100$ samples, we obtain an approximated RMSE which is approximately two times the exact value of the covariance. This seems to large at first glance. However, one has to keep in mind that the RMSE is bounded by $\sqrt{\text{Var}(L(\underline{x}) \cdot L(\underline{x}'))}/\sqrt{M}$ and the standard deviation of the product of the evaluated field may become quite large. In fact, in the left hand side of

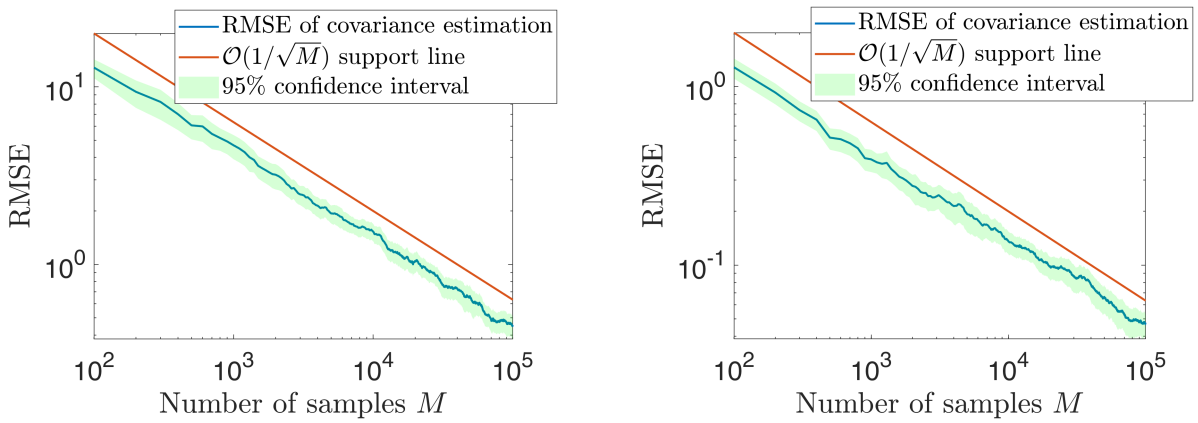

Figure 8.9: Convergence of RMSE of empirical covariance $q_L(\underline{x}, \underline{x}')$; left: l is a Poisson(8) process, $r = 0.5, \sigma^2 = 1.5^2, \underline{x} = (0.5, 0.8), \underline{x}' = (0.6, 1.5), q_L(\underline{x}, \underline{x}') \approx 6.4807$; right: l is a Poisson(3) process, $r = 1, \sigma^2 = 1, \underline{x} = (1.2, 0.6), \underline{x}' = (0.9, 1.7), q_L(\underline{x}, \underline{x}') \approx 1.6485$.

Figure 8.9 we obtain $\sqrt{\mathrm{Var}(L(\underline{x}) \cdot L(\underline{x}'))} \approx 138,46$ which fits well to the observed results, being approximately $10 = \sqrt{100}$ times the approximated RMSE for $M = 100$ samples. In practice, it is therefore important to keep in mind that the estimation of the covariance based on existing data might require a large number of observations.

8.8 GSLFs in elliptic PDEs

In the previous sections, we considered theoretical properties of the GSLF and presented numerical examples to validate and visualize these results. In the last section of this paper we present an application of the GSLF in the context of PDEs. This might be interesting, for example, to model subsurface/groundwater flow in uncertain heterogeneous or fractured media. In such a modeling situation the media is often modeled by a random field, which should therefore be distributionally flexible and allow for spatial discontinuities, both of which are fulfilled in the case of the GSLF. This motivates the investigation of a general elliptic PDE where the GSLF occurs in the diffusion coefficient. We introduce the considered elliptic PDE in Subsection 8.8.1 following [93], [96] and [16]. Spatial discretization methods are discussed in Subsection 8.8.2 and we conclude this section with numerical experiments in Subsection 8.8.3.

8.8.1 Problem formulation and existence of solutions

Let $\mathcal{D} \subset \mathbb{R}^2$ be a bounded, connected Lipschitz domain[2]. Define $H := L^2(\mathcal{D})$ and consider the elliptic PDE

$$-\nabla \cdot (a(\omega, \underline{x}) \nabla u(\omega, \underline{x})) = f(\omega, \underline{x}) \text{ in } \Omega \times \mathcal{D}, \tag{8.8}$$

where we impose the boundary conditions

$$u(\omega, \underline{x}) = 0 \text{ on } \Omega \times \Gamma_1, \tag{8.9}$$

$$a(\omega, \underline{x}) \overrightarrow{n} \cdot \nabla u(\omega, \underline{x}) = g(\omega, \underline{x}) \text{ on } \Omega \times \Gamma_2. \tag{8.10}$$

Here, we split the boundary $\partial\mathcal{D} = \Gamma_1 \dot{\cup} \Gamma_2$ in two one-dimensional manifolds $\Gamma_1,\ \Gamma_2$ and assume that Γ_1 is of positive measure and that the exterior normal derivative $\overrightarrow{n} \cdot \nabla v$ on Γ_2 is well-defined for every $v \in C^1(\overline{\mathcal{D}})$, where $\overrightarrow{n}$ is the outward unit normal vector to Γ_2. The mappings $f : \Omega \times \mathcal{D} \to \mathbb{R}$ and $g : \Omega \times \Gamma_2 \to \mathbb{R}$ a measurable functions and $a : \Omega \times \mathcal{D} \to \mathbb{R}$ is defined by

$$\begin{aligned} &a : \Omega \times \mathcal{D} \to (0, +\infty), \\ &(\omega, x, y) \mapsto \overline{a}(x, y) + \Phi_1(W_1(x, y)) + \Phi_2(l(F(W_2(x, y)))), \end{aligned} \tag{8.11}$$

where

- $\overline{a} : \mathcal{D} \to (0, +\infty)$ is deterministic, continuous and there exist finite constants $\overline{a}_+, \overline{a}_- > 0$ with $\overline{a}_- \leq \overline{a}(x, y) \leq \overline{a}_+$ for $(x, y) \in \mathcal{D}$.
- $\Phi_1,\ \Phi_2 : \mathbb{R} \to [0, +\infty)$ are continuous.
- $F : \mathbb{R} \to \mathbb{R}_+$ is Lipschitz continuous and globally bounded by $C_F > 0$, i.e. $F(x) < C_F,\ x \in \mathbb{R}$.
- W_1 and W_2 are zero-mean GRFs on $\overline{\mathcal{D}}$ with $\mathbb{P}$-a.s. continuous paths.
- l is a Lévy process on $[0, C_F]$.

Note that we consider the case of a homogeneous Dirichlet boundary condition on Γ_1 in the theoretical analysis to simplify notation. Non-homogeneous Dirichlet boundary conditions could also be considered, since such a problem can always be formulated as a version of (8.8) -

[2]Note that the extension to dimensions $d > 2$ is straightforward.

(8.10) with modified source term and Neumann data (see also [16, Remark 2.1]).

Next, we shortly introduce the pathwise weak solution of problem (8.8) - (8.10) following [96] and [93]. We denote by $H^1(\mathcal{D})$ the Sobolev space and by T the trace operator $T : H^1(\mathcal{D}) \to H^{\frac{1}{2}}(\partial\mathcal{D})$ where $Tv = v|_{\partial\mathcal{D}}$ for $v \in C^\infty(\overline{\mathcal{D}})$ (see [41]). Further, we introduce the solution space $V \subset H^1(\mathcal{D})$ by

$$V := \{v \in H^1(\mathcal{D}) \mid Tv|_{\Gamma_1} = 0\},$$

where we take over the standard Sobolev norm, i.e. $\|\cdot\|_V := \|\cdot\|_{H^1(\mathcal{D})}$. We identify H with its dual space H' and work on the Gelfand triplet $V \subset H \simeq H' \subset V'$. Multiplying the left hand side of Equation (8.8) by a test function $v \in V$ and integrating by parts (see e.g. [113, Section 6.3]) we obtain the following pathwise weak formulation of the problem: For fixed $\omega \in \Omega$ and given mappings $f(\omega, \cdot) \in V'$ and $g(\omega, \cdot) \in H^{-\frac{1}{2}}(\Gamma_2)$, find $u(\omega, \cdot) \in V$ such that

$$B_{a(\omega)}(u(\omega, \cdot), v) = F_\omega(v) \tag{8.12}$$

for all $v \in V$. The function $u(\omega, \cdot)$ is then called pathwise weak solution to problem (8.8) - (8.10) and the bilinear form $B_{a(\omega)}$ and the linear operator F_ω are defined by

$$B_{a(\omega)} : V \times V \to \mathbb{R},\ (u, v) \mapsto \int_{\mathcal{D}} a(\omega, \underline{x})\nabla u(\underline{x}) \cdot \nabla v(\underline{x}) d\underline{x},$$

and

$$F_\omega : V \to \mathbb{R},\ v \mapsto \int_{\mathcal{D}} f(\omega, \underline{x})v(\underline{x})d\underline{x} + \int_{\Gamma_2} g(\omega, \underline{x})[Tv](\underline{x})d\underline{x},$$

where the integrals in F_ω are understood as the duality pairings:

$$\int_{\mathcal{D}} f(\omega, \underline{x})v(\underline{x})d\underline{x} = {}_{V'}\langle f(\omega, \cdot), v\rangle_V \text{ and}$$
$$\int_{\Gamma_2} g(\omega, \underline{x})[Tv](\underline{x})d\underline{x} = {}_{H^{-\frac{1}{2}}(\Gamma_2)}\langle g(\omega, \cdot), Tv\rangle_{H^{\frac{1}{2}}(\Gamma_2)},$$

for $v \in V$.

Remark 8.8.1. *Note that any real-valued, càdlàg function $f : [a, b] \to \mathbb{R}$ on a compact interval $[a, b]$, with $a < b$, is bounded. Otherwise, one could find a sequence $(x_n,\ n \in \mathbb{N}) \subset [a, b]$ such that $|f(x_n)| > n$ for all $n \in \mathbb{N}$. In this case, since $[a, b]$ is compact, there exists a subsequence $(x_{n_k},\ k \in \mathbb{N}) \subset [a, b]$ with a limit in $[a, b]$, i.e. $x_{n_k} \to x^* \in [a, b]$ for $k \to \infty$. Since f is*

right-continuous in x^* and $\lim_{x \nearrow x^*} f(x)$ exists, f is bounded in a neighborhood of x^*, i.e. there exists $\delta, C > 0$ such that $|f(x)| \leq C$ for $x \in [a,b]$ with $|x - x^*| < \delta$, which contradicts the fact that $|f(x_{n_k})| > n_k$ since $|x_{n_k} - x^*| < \delta$ and $n_k > C$ both hold for k large enough. ◆

The diffusion coefficient a is jointly measurable by construction (see Remark 8.3.2) and, for any fixed $\omega \in \Omega$, it holds $a(\omega, x, y) \geq \overline{a}_- > 0$ for all $(x, y) \in \mathcal{D}$ and

$$a(\omega, x, y) \leq \overline{a}_+ + \sup_{(x,y)\in\overline{\mathcal{D}}} \Phi_1(W_1(\omega, x, y)) + \sup_{z\in[0,C_F]} \Phi_2(l(\omega, z)) < +\infty,$$

for all $(x, y) \in \mathcal{D}$, where the finiteness follows by the continuity of $\Phi_1,\ \Phi_2,\ W_1$ and Remark 8.8.1.

It follows by a pathwise application of the Lax-Milgram lemma that the elliptic model problem (8.8) - (8.10) with the diffusion coefficient a has a unique, measurable pathwise weak solution (see [96, Theorem 3.7, Remark 2.4] and [16, Theorem 2.5]):

Theorem 8.8.2.
Let $f \in L^q(\Omega; H)$, $g \in L^q(\Omega; L^2(\Gamma_2))$ for some $q \in [1, +\infty)$. There exists a unique pathwise weak solution $u(\omega, \cdot) \in V$ to problem (8.8) - (8.10) with diffusion coefficient (8.11) for $\mathbb{P}$-almost every $\omega \in \Omega$. Furthermore, $u \in L^r(\Omega; V)$ for all $r \in [1, q)$ and

$$\|u\|_{L^r(\Omega;V)} \leq C(\overline{a}_-, \mathcal{D})(\|f\|_{L^q(\Omega;H)} + \|g\|_{L^q(\Omega;L^2(\Gamma_2))}),$$

where $C(\overline{a}_-, \mathcal{D}) > 0$ is a constant depending only on the indicated parameters. ◆

8.8.2 Spatial discretization of the elliptic PDE

In the following, we briefly describe numerical methods to approximate the pathwise solution to the random elliptic PDE, partially following [96, Section 6]. Our goal is to approximate the weak solution u to problem (8.8) - (8.10) with diffusion coefficient a given by Equation (8.11). Therefore, for almost all $\omega \in \Omega$, we aim to approximate the function $u(\omega, \cdot) \in V$ such that

$$\begin{aligned} B_{a(\omega)}(u(\omega, \cdot), v) &:= \int_{\mathcal{D}} a(\omega, \underline{x}) \nabla u(\omega, \underline{x}) \cdot \nabla v(\underline{x}) d\underline{x} \\ &= \int_{\mathcal{D}} f(\omega, \underline{x}) v(\underline{x}) d\underline{x} + \int_{\Gamma_2} g(\omega, \underline{x})[Tv](\underline{x}) d\underline{x} =: F_\omega(v), \end{aligned} \tag{8.13}$$

for every $v \in V$. We compute an approximation of the solution using a standard Galerkin approach with linear basis functions. Therefore, assume a sequence of finite-element subspaces is given, which is denoted by $\mathcal{V} = (V_\ell,\ \ell \in \mathbb{N}_0)$, where $V_\ell \subset V$ are subspaces with growing dimension $\dim(V_\ell) = d_\ell$. We denote by $(h_\ell,\ \ell \in \mathbb{N}_0)$ the corresponding refinement sizes with $h_\ell \to 0$, for $\ell \to \infty$. Let $\ell \in \mathbb{N}_0$ be fixed and denote by $\{v_1^{(\ell)}, \dots, v_{d_\ell}^{(\ell)}\}$ a basis of V_ℓ. The (pathwise) discrete version of problem (8.13) reads: Find $u_\ell(\omega, \cdot) \in V_\ell$ such that

$$B_{a(\omega)}(u_\ell(\omega, \cdot), v_i^{(\ell)}) = F_\omega(v_i^{(\ell)}) \text{ for all } i = 1, \dots, d_\ell.$$

If we expand the solution $u_\ell(\omega, \cdot)$ with respect to the basis $\{v_1^{(\ell)}, \dots, v_{d_\ell}^{(\ell)}\}$, we end up with the representation

$$u_\ell(\omega, \cdot) = \sum_{i=1}^{d_\ell} c_i v_i^{(\ell)},$$

where the coefficient vector $\mathbf{c} = (c_1, \dots, c_{d_\ell})^T \in \mathbb{R}^{d_\ell}$ is determined by the linear system of equations

$$\mathbf{B}(\omega)\mathbf{c} = \mathbf{F}(\omega),$$

with stochastic stiffness matrix $\mathbf{B}(\omega)_{i,j} = B_{a(\omega)}(v_i^{(\ell)}, v_j^{(\ell)})$ and load vector $\mathbf{F}(\omega)_i = F_\omega(v_i^{(\ell)})$ for $i, j = 1, \dots, d_\ell$.

8.8.2.1 Standard linear finite elements

Let $(\mathcal{K}_\ell,\ \ell \in \mathbb{N}_0)$ be a sequence of admissible triangulations of the domain $\mathcal{D}$ (cf. [67, Definition 8.36]) and denote by $\theta_\ell > 0$ the minimum interior angle of all triangles in $\mathcal{K}_\ell$, where we assume $\theta_\ell \geq \theta > 0$ for a positive constant θ. For $\ell \in \mathbb{N}_0$, we denote by $h_\ell := \max_{K \in \mathcal{K}_\ell} \operatorname{diam}(K)$ the maximum diameter of the triangulation $\mathcal{K}_\ell$ and define the finite dimensional subspaces by $V_\ell := \{v \in V \mid v|_K \in \mathcal{P}_1,\ K \in \mathcal{K}_\ell\}$, where $\mathcal{P}_1$ denotes the space of all polynomials up to degree one. If we assume that there exists a positive regularity parameter $\kappa_a > 0$ such that for $\mathbb{P}$-almost all $\omega \in \Omega$ it holds $u(\omega, \cdot) \in H^{1+\kappa_a}(\mathcal{D})$ and $\|u\|_{L^2(\Omega; H^{1+\kappa_a}(\mathcal{D}))} \leq C_u$ for some constant $C_u > \infty$, we immediately obtain the following bound by Céa's lemma (see [16, Section 4], [96, Section 6], [67, Chapter 8])

$$\|u - u_\ell\|_{L^2(\Omega; V)} \leq C\, h_\ell^{\min(\kappa_a, 1)}, \tag{8.14}$$

for some constant C which does not depend on h_ℓ. For general deterministic elliptic interface problems, one obtains a discretization error of order $\kappa_a < 1$ and, hence, one cannot expect the full order of convergence $\kappa_a = 1$ in general for standard triangulations of the domain (see [10] and [16]). Therefore, we present one possible approach to enhance the performance of the FE method for the considered elliptic PDE in Subsection 8.8.2.2. We point out that it is not possible to derive optimal rates $\kappa_a > 0$ such that (8.14) holds for our general random diffusion coefficient (see also [96], [16]). However, we investigate the existence of such a constant numerically in Section 8.8.3. We close this subsection with a remark on the practical simulation of the GRFs $W_1,\ W_2$ and the Lévy process l in the diffusion coefficient (8.11).

Remark 8.8.3. *It is in general not possible to draw exact samples of the Lévy process and the GRFs in the diffusion coefficient* (8.11)*. In practice, one has to use appropriate approximations $l^{(\varepsilon_l)} \approx l$ of the Lévy process and $W_1^N \approx W_1,\ W_2^N \approx W_2$ of the GRFs with approximation parameters $\varepsilon_l > 0$ and $N \in \mathbb{N}$, as introduced in Section 8.5. In the context of FE approximations of the PDE* (8.8) - (8.10) *with diffusion coefficient* (8.11)*, the question arises, how to choose these approximation parameters in practice, given a specific choice of the FE approximation parameter h_ℓ in* (8.14)*. Obviously, the choice of ε_l and N should depend on the FE parameter h_ℓ, since a higher resolution of the FE approximation will be worthless if the approximation of the diffusion coefficient is poor.*

In [96], the authors considered the PDE (8.8) - (8.10) *with a different diffusion coefficient a. The coefficient considered in the mentioned paper also incorporates GRFs and Lévy processes, which in turn have to be approximated in practice, leading to an approximation $\tilde{a} \approx a$. The authors derived a rule on the choice of the approximation parameters, such that the error contributions from the approximation of the diffusion coefficient and the FE discretization are equilibrated (see [96, Section 7]). We want to emphasize that this result is essentially based on the quantification of the approximation error $\tilde{a} - a$ of the corresponding diffusion coefficient in an $L^p(\Omega, L^p(\mathcal{D}))$-norm, for some $p \geq 1$ (see [96, Theorem 4.8 and Theorem 5.11]).*

In Theorem 8.5.6, we derived an error bound on the approximation error of the GSLF in the $L^p(\Omega, L^p(\mathcal{D}))$-norm under Assumption 8.5.1. A corresponding error bound on the approximation of the diffusion coefficient defined in (8.11) *immediately follows under mild assumptions on Φ_1 and Φ_2. Therefore, following exactly the same arguments as in [96] together with Theorem 8.5.6, we obtain the following rule for the practical choice of the approximation parameters ε_l and N such that the overall error contributions from the approximation of the GRFs, the Lévy process and the FE discretization are equilibrated and the error is dominated by the FE refinement parameter*

h_ℓ: For $\ell \in \mathbb{N}$, choose ε_l and N such that

$$\varepsilon_l \simeq h_\ell^{2\kappa_a} \text{ and } R(N) \simeq h_\ell^{\frac{2\kappa_a}{\delta}}.$$

For example, if we approximate the GRF by the KLE approach (see Subsection 8.5.1), one should choose the cut-off index such that $N \simeq h_\ell^{-\frac{4\kappa_a}{\beta\delta}}$ with β from Assumption 8.5.1 i. ◆

8.8.2.2 Adaptive finite elements

As we pointed out in the last section, one cannot expect full order convergence ($\kappa_a = 1$) for the FE method with linear elements in the considered elliptic problem due to the discontinuities in the diffusion coefficient. One common way to improve the FE method is to use triangulations which are adapted to the jump discontinuities in the sense that the spatial jumps lie on edges of elements of the triangulation. This approach leads to sample-dependent triangulations which has been proven to enhance the performance of the FE method significantly compared to the use of standard triangulations, which are not adjusted to the jumps (see for example [16] and [96] and the references therein). In the cited papers, the jump locations are known and the jump geometries allow for an (almost) exact alignment of the triangulation to the interfaces due to their specific geometrical properties. This is, however, not the case for the diffusion coefficient considered in the current paper, where the spatial jump positions are not known explicitly, nor is it possible to align the triangulation exactly in the described sense due to the complex jump geometries.

Another possible approach to improve the FE method are adaptive finite elements (see e.g. [5] and [66] and the references therein). The idea is to identify triangles with a high contribution to the overall error of the FE approximation, which are then refined. For a given FE approximation $u_\ell \in V_\ell \subset V$ of the solution $u \in V$, the discretization error $u - u_\ell$ is estimated in terms of the approximated solution u_ℓ and no information about the true solution u is needed. This may be achieved by the use of the Galerkin orthogonality and partial integration. For a given triangulation $\mathcal{T} = \{K,\ K \subset \mathcal{D}\}$ with corresponding FE approximation u_ℓ, the approximation error of the FE approximation to the considered elliptic problem (8.8) - (8.10) may be estimated by

$$\mathrm{err}_{\mathcal{T}}(u_\ell, a, f, g) = \left(\sum_{K \in \mathcal{T}} \mathrm{err}_{\mathcal{T}}(u_\ell, a, f, g, K) \right)^{\frac{1}{2}}.$$

Here, $\mathrm{err}_{\mathcal{T}}(u_\ell, a, f, g, K)$ corresponds the error contribution of the approximation on the element $K \in \mathcal{T}$, which may be approximated by

$$\begin{aligned}\mathrm{err}_{\mathcal{T}}(u_\ell, a, f, g, K) = h_K^2 \|f\|_{L^2(K)}^2 + \sum_{e \in \partial K \cap \Gamma_2} h_e \|g - \overrightarrow{n}_K \cdot a \, \nabla u_\ell\big|_K\|_{L^2(e)}^2 \\ + \sum_{e \in \partial K \setminus (\Gamma_2 \cup \Gamma_1)} h_e \|\overrightarrow{n}_K \cdot a \, \nabla u_\ell\big|_K + \overrightarrow{n}_{J(K,e)} \cdot a \, \nabla u_\ell\big|_{J(K,e)}\|_{L^2(e)}^2, \quad (8.15)\end{aligned}$$

where we denote by $e \in \partial K$ an edge of the triangle $K \in \mathcal{T}$ and $J(K, e) \in \mathcal{T}$ is the unique triangle which is the direct neighbor of the triangle K along the edge e. Further, h_K is the diameter of the triangle K and h_e is the length of the edge e (see [66] and [19]). The triangle-based estimated error obtained by Equation (8.15) allows for an identification of the triangles with the largest contribution to the overall error. This may then be used to perform a local mesh refinement, which usually consists in the refinement of triangles with high error contribution. One common strategy is to start with an initial triangulation, compute the error contribution of each triangle according to Equation (8.15) and refine all triangles which have an approximated error contribution which is at least 50% of the error contribution with the largest approximated error (see e.g. [114, Section 5]).

Example 8.8.4. *Consider the PDE problem* (8.8) - (8.10) *with homogeneous Dirichlet boundary conditions on* $\mathcal{D} = (0, 1)^2$ *and* $f \equiv 10$. *The diffusion coefficient* a *as defined in Equation* (8.11) *is given by*

$$a(x, y) = 0.1 + l(\min\{|W_1(x, y)|, 30\}),$$

where l *is a Poisson(2) process and* W_1 *is a centered GRF with squared exponential covariance function. In order to illustrate the adaptive mesh generation decribed above, we consider 3 samples of the diffusion coefficient and compute the adaptive meshes, where we use an initial mesh with FE refinement parameter* $h = 0.025$ *and refine all triangles which have an estimated error contribution exceeding* 50% *of the largest estimated error. Figure 8.10 shows the three samples of the diffusion coefficient and the corresponding adaptive triangulations. It is nicely illustrated, how the element-wise a-posteriori estimation of the error according to Equation* (8.15) *enables an identification of the triangles which lie near the discontinuities of the diffusion coefficient and, hence, have a comparatively high error contribution. This results in a local refinement leading to a higher mesh resolution near the discontinuity.* ◆

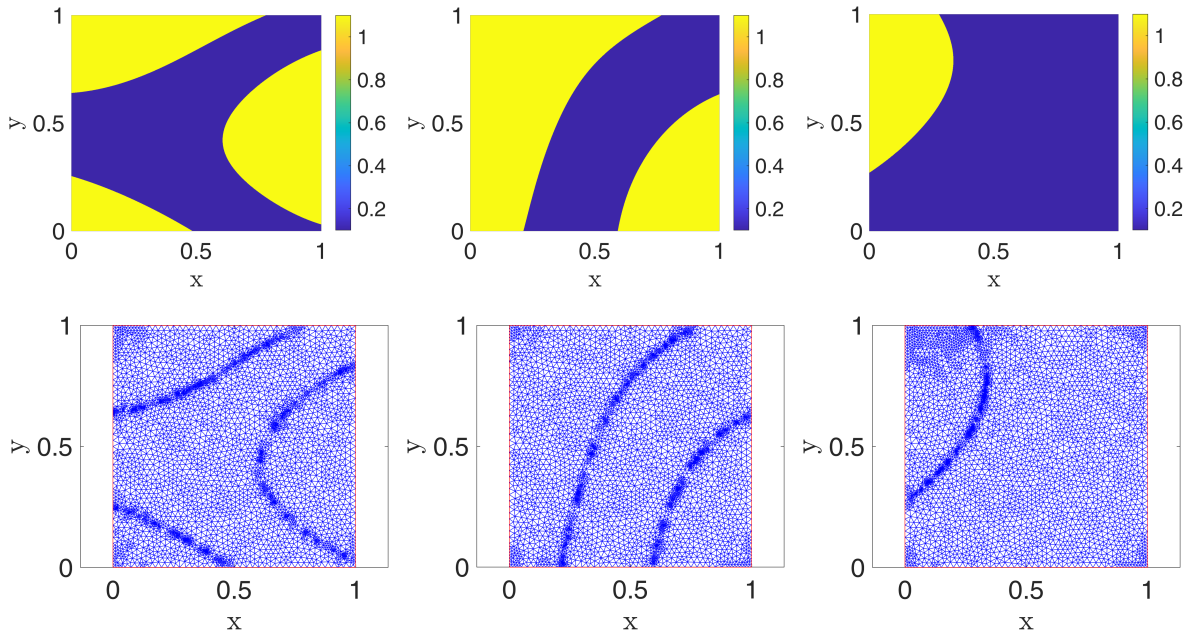

Figure 8.10: Samples of the diffusion coefficient a (top) and adaptive triangulations (bottom).

8.8.3 Numerical experiments for the random elliptic PDE

In this section, we present numerical examples for the experimental investigation of the existence of a positive parameter $\kappa_a > 0$ such that Equation (8.14) holds. Further, in the presented examples, we compare the performance of a standard FE discretization with the FE approach using the local refinement strategy described in Subsection 8.8.2.2. We consider the domain $\mathcal{D} = (0,1)^2$ and set $f \equiv 10$, $\overline{a} \equiv 0.1$, $\Phi_1 = 0.1 \exp(\cdot)$, $\Phi_2 = |\cdot|$, $F = \min(|\cdot|, 30)$ in Equation (8.11). W_1 and W_2 are centered GRFs with squared exponential covariance function (see Subsection 8.7.4), where we set $\sigma = 0.5$ and $r = 1$. We use the circulant embedding method (see cf. [64] and [65]) to draw samples of the GRFs $W_1,\ W_2$ on an equidistant grid with stepsize $h_W = 1/200 = 0.005$ and obtain evaluations everywhere on the domain by multilinear interpolation. Due to the high spatial regularity of W_1 and W_2 and the high correlation length, this stepsize is fine enough to ensure that the approximation error of the GRFs $W_1,\ W_2$ is negligible. The Lévy process l is set to be a Poisson process with intensity parameter $\lambda > 0$, which will be specified later. It follows that $l(t) - l(s) \sim \text{Poiss}((\lambda(t-s))$ for $0 \leq s \leq t$ and we draw samples from the Poisson process by the Uniform Method (see [109, Section 8.1.2]).

The goal of our numerical experiments is to approximate the strong error: We set $h_\ell =$

$0.25 \cdot 2^{-(\ell-1)}$, for $\ell = 1, \dots, 8$ and approximate the left hand side of Equation (8.14) by

$$\mathrm{RMSE}^2 := \|u - u_\ell\|^2_{L^2(\Omega;V)} \approx \frac{1}{M} \sum_{i=1}^{M} \|u^{(i)}_{ref} - u^{(i)}_\ell\|^2_V, \tag{8.16}$$

for $\ell = 1, \dots, 5$, where $(u^{(i)}_{ref} - u^{(i)}_\ell,\ i = 1, \dots, M)$ are i.i.d. copies of the random variable $u_{ref} - u_\ell$ and $M \in \mathbb{N}$. We use a reference grid on $\mathcal{D}$ with 801×801 grid points for interpolation and prolongation and take $u_{ref} := u_8$ as the pathwise reference solution. The RMSE is estimated for the standard FE method and for the FE method with adaptive refinement as described in Subsection 8.8.2.2. In order to obtain comparable approximations on each FE level, we compute the adaptive meshes as follows: for $\ell \in \{1, \dots, 5\}$, we denote by n_ℓ the number of triangles in the non-adaptive triangulation with FE mesh refinement parameter h_ℓ. The (sample-dependent) adaptive mesh on level ℓ is obtained by performing the local refinement procedure described in Subsection 8.8.2.2 until the number of triangles in the adaptive mesh exceeds n_ℓ. The resulting mesh is then used to compute the adaptive FE approximation on level ℓ.

8.8.3.1 Homogeneous Dirichlet boundary conditions

In our first experiment, we choose homogeneous Dirichlet boundary contitions on $\partial\mathcal{D}$ and set $\lambda = 2$. Figure 8.11 shows samples of the diffusion coefficient and the corresponding PDE solutions approximated by the FE method. We use $M = 150$ samples so approximate the

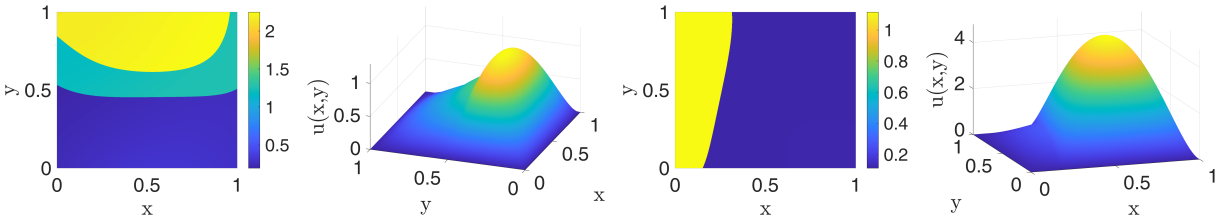

Figure 8.11: Samples of the diffusion coefficient with $\lambda = 2$ and corresponding FE solution to the elliptic PDE with homogeneous Dirichlet boundary conditions.

RMSE according to Equation (8.16) with the non-adaptive and the adaptive FE approach. Figure 8.12 shows the approximated RMSE plotted against the inverse FE refinement parameter. For the adaptive FE approximations, the sample-dependent mesh refinement parameters on each discretization level are averaged over all 150 samples. We see a convergence with rate ≈ 0.65 for the standard FE method, which is in line with our expectations (see Section 8.8.2). Further,

we observe that the adaptive refinement strategy yields an improved convergence rate of ≈ 0.85 and a smaller estimated RMSE on the considered levels. The right hand side of Figure

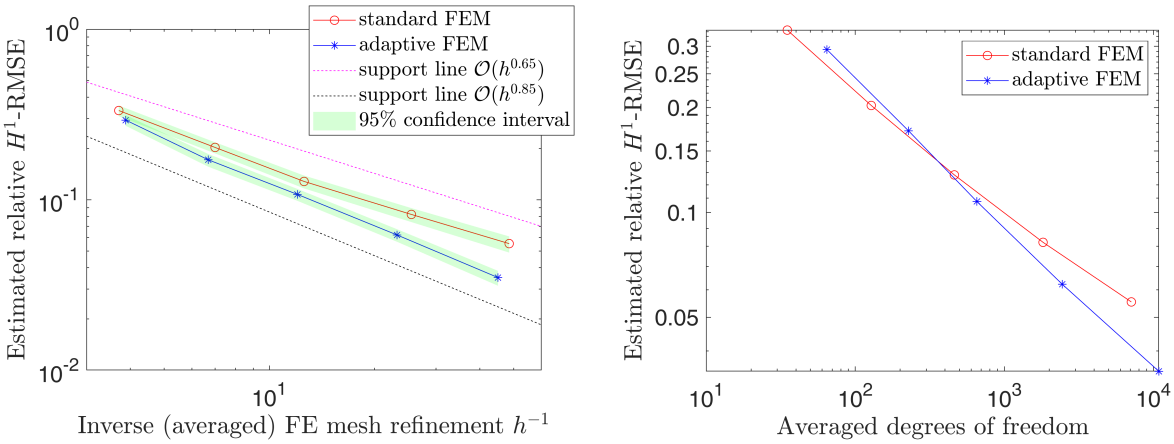

Figure 8.12: Convergence of the (standard and adaptive) FE method (left) and degrees-of-freedom to error plot (right) where l is a Poisson(2) process and we impose homogeneous Dirichlet boundary conditions.

8.12 shows the estimated RMSE plotted against the degrees of freedom of the linear FE-system on each discretization level. For the adaptive FE method, the degrees of freedom are averaged over all samples. After a pre-asymptotic behaviour on the first and second level, we see that the adaptive FE method performs more efficient in terms of the degrees of freedom: the adaptive FE method achieves a certain RMSE with less degrees of freedom compared to the standard FE method.

8.8.3.2 Mixed Dirichlet-Neumann boundary conditions

In the second numerical example, we use mixed Dirichlet-Neumann boundary conditions: we split the domain boundary $\partial\mathcal{D}$ by $\Gamma_1 = \{0,1\} \times [0,1]$ and $\Gamma_2 = (0,1) \times \{0,1\}$ and impose the following pathwise boundary conditions

$$u = \begin{cases} 0.1 & \text{on } \{0\} \times [0,1] \\ 0.3 & \text{on } \{1\} \times [0,1] \end{cases} \text{ and } a\overrightarrow{n} \cdot \nabla u = 0 \text{ on } \Gamma_2,$$

for $\omega \in \Omega$. Further, we set $\lambda = 3$, which results in a higher number of jumps in the diffusion coefficient. Figure 8.13 shows samples of the diffusion coefficient and the corresponding PDE solutions approximated by the FE method. As in the first experiment, we use $M = 150$ samples to approximate the RMSE according to (8.14) with the standard FE approach and the

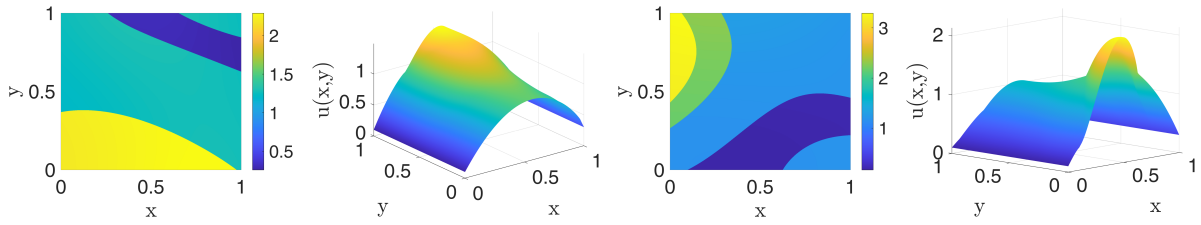

Figure 8.13: Samples of the diffusion coefficient with $\lambda = 3$ and corresponding FE solution to the elliptic PDE with mixed Dirichlet-Neumann boundary conditions.

adaptive approach. The approximated values are plotted against the inverse FE refinement parameter. The results are presented in Figure 8.14, which shows a convergence rate of ≈ 0.6 for the standard FE approach, which is slightly smaller than the observed convergence rate of ≈ 0.65 in the first numerical example, where we imposed homogeneous Dirichlet boundary conditions and considered a Poisson process with intensity parameter $\lambda = 2$, leading to a smaller expected number of jumps in the diffusion coefficient. Further, Figure 8.14 shows a convergence rate of ≈ 0.85 for the adaptive FE approach and smaller magnitudes of the RMSE compared to the standard FE method. The right plot of Figure 8.14 reveals the higher efficiency of the adaptive FE method compared to the standard approach in the sense that the number of degrees of freedom, which are necessary to achieve a certain error, is significantly smaller compared to the standard FE approach. Further, we see that the performance difference of the standard and the adaptive FE method is larger compared to the first example due to the higher number of expected jumps in the diffusion coefficient, which renders the adaptive local refinement strategy even more suitable for this problem. Overall, the results are in line with our expectations.

8.8.3.3 Mixed Dirichlet-Neumann boundary conditions and jump-accentuated coefficients

In our last experiment we consider mixed Dirichlet-Neumann boundary conditions as in the previous section. The diffusion coefficient is set to be

$$a(x, y) = 0.01 + 0.01 \, \exp(W_1(x, y)) + 30 \, l(F(W_2(x, y)),$$

for $(x, y) \in \mathcal{D}$, where l is a Poisson(4) process. This leads to a jump-accentuated coefficient with high contrast. We take $M = 500$ samples to estimate the RMSE for the standard FE method and the adaptive approach according to (8.16). The results are presented in Figure 8.15.

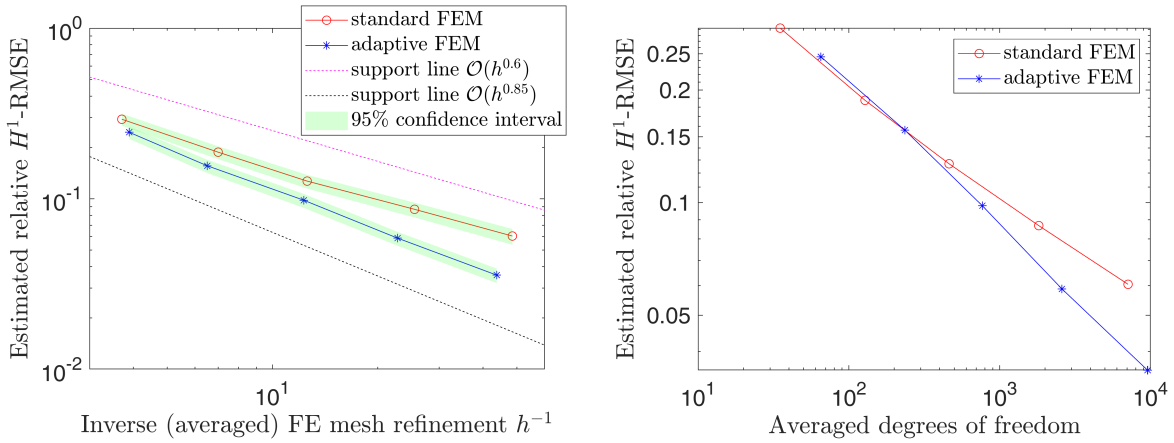

Figure 8.14: Convergence of the (standard and adaptive) FE method (left) and degrees-of-freedom to error plot (right) where l is a Poisson(3) process and we impose mixed Dirichlet-Neumann boundary conditions.

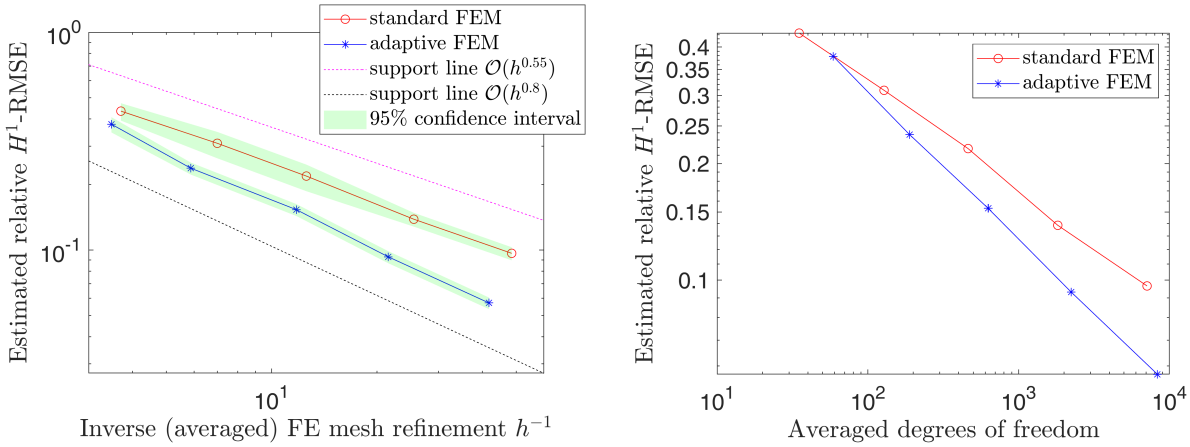

Figure 8.15: Convergence of the (standard and adaptive) FE method (left) and degrees-of-freedom to error plot (right) where l is a Poisson(4) process, we impose mixed Dirichlet-Neumann boundary conditions and use a high-contrast diffusion coefficient.

We obtain a convergence rate of ≈ 0.55 for the standard FE approach and ≈ 0.8 for the adaptive FE method, which is slightly slower than the observed rates in the previous experiment. This is in line with our expectations since we have an increased jump intensity in the underlying Poisson process and larger jump heights in the diffusion coefficient, both having a negative influence on the convergence rate of the FE method (see also [96, 16, 105]). Figure 8.15 also reveals, as expected, that the magnitude of the RMSE is significantly smaller in the adaptive FE approach. The right plot of Figure 8.15 demonstrates that the adaptive refinement strategy is

able to achieve a certain error with significantly less degrees of freedom in the corresponding linear FE system, than the standard FE approach.

Acknowledgements

Funded by Deutsche Forschungsgemeinschaft (DFG, German Research Foundation) under Germany's Excellence Strategy - EXC 2075 - 390740016.

Bibliography

[1] A. Abdulle, A. Barth, and C. Schwab. Multilevel Monte Carlo methods for stochastic elliptic multiscale PDEs. *Multiscale Model. Simul.*, 11(4):1033–1070, 2013.

[2] R. A. Adams and J. J. F. Fournier. *Sobolev Spaces*, volume 140 of *Pure and Applied Mathematics (Amsterdam)*. Elsevier/Academic Press, Amsterdam, second edition, 2003.

[3] R. J. Adler and J. E. Taylor. *Random Fields and Geometry*. Springer Monographs in Mathematics. Springer, New York, 2007.

[4] R. J. Adler, J. E. Taylor, and K. J. Worsley. Applications of random fields and geometry: foundations and case studies. 2015. Available on `https://robert.net.technion.ac.il/publications`.

[5] M. Ainsworth and J. T. Oden. A posteriori error estimation in finite element analysis. *Comput. Methods Appl. Mech. Engrg.*, 142(1-2):1–88, 1997.

[6] C. D. Aliprantis and K. C. Border. *Infinite Dimensional Analysis. A hitchhiker's guide*. Springer, Berlin, third edition, 2006.

[7] M. Altmayer and A. Neuenkirch. Multilevel Monte Carlo quadrature of discontinuous payoffs in the generalized Heston model using Malliavin integration by parts. *SIAM J. Financial Math.*, 6(1):22–52, 2015.

[8] D. Applebaum. *Lévy Processes and Stochastic Calculus*, volume 116 of *Cambridge Studies in Advanced Mathematics*. Cambridge University Press, Cambridge, second edition, 2009.

[9] E. Artin. *Einführung in die Theorie der Gamma-funktion*. Hamburger mathematische

Einzelschriften. B.G. Teubner, 1931.

[10] I. Babuška. The finite element method for elliptic equations with discontinuous coefficients. *Computing (Arch. Elektron. Rechnen)*, 5:207–213, 1970.

[11] I. Babuška, F. Nobile, and R. Tempone. A stochastic collocation method for elliptic partial differential equations with random input data. *SIAM J. Numer. Anal.*, 45(3):1005–1034, 2007.

[12] I. Babuška, R. Tempone, and G. E. Zouraris. Galerkin finite element approximations of stochastic elliptic partial differential equations. *SIAM J. Numer. Anal.*, 42(2):800–825, 2004.

[13] O. E. Barndorff-Nielsen, J. Pedersen, and K.-i. Sato. Multivariate subordination, self-decomposability and stability. *Adv. in Appl. Probab.*, 33(1):160–187, 2001.

[14] A. Barth, C. Schwab, and N. Zollinger. Multi-level Monte Carlo finite element method for elliptic PDEs with stochastic coefficients. *Numer. Math.*, 119(1):123–161, 2011.

[15] A. Barth and A. Stein. Approximation and simulation of infinite-dimensional Lévy processes. *Stoch. Partial Differ. Equ. Anal. Comput.*, 6(2):286–334, 2018.

[16] A. Barth and A. Stein. A study of elliptic partial differential equations with jump diffusion coefficients. *SIAM/ASA J. Uncertain. Quantif.*, 6(4):1707–1743, 2018.

[17] A. Barth and A. Stein. Numerical analysis for time-dependent advection-diffusion problems with random discontinuous coefficients. *ESAIM Math. Model. Numer. Anal.*, 56(5):1545–1578, 2022.

[18] P. Bastian. A fully-coupled discontinuous Galerkin method for two-phase flow in porous media with discontinuous capillary pressure. *Comput. Geosci.*, 18(5):779–796, 2014.

[19] C. Bernardi and R. Verfürth. Adaptive finite element methods for elliptic equations with non-smooth coefficients. *Numer. Math.*, 85(4):579–608, 2000.

[20] P. J. Bickel, F. Götze, and W. R. van Zwet. Resampling fewer than n observations: gains, losses, and remedies for losses. *Statist. Sinica*, 7(1):1–31, 1997.

[21] S. C. Brenner and L. R. Scott. *The Mathematical Theory of Finite Element Methods*, volume 15 of *Texts in Applied Mathematics*. Springer, New York, third edition, 2008.

[22] H. Brezis. *Functional Analysis, Sobolev Spaces and Partial Differential Equations*. Universi-

text. Springer, New York, 2011.

[23] P. J. Brockwell and E. Schlemm. Parametric estimation of the driving Lévy process of multivariate CARMA processes from discrete observations. *J. Multivariate Anal.*, 115:217–251, 2013.

[24] B. Buchmann, B. Kaehler, R. Maller, and A. Szimayer. Multivariate subordination using generalised Gamma convolutions with applications to Variance Gamma processes and option pricing. *Stochastic Process. Appl.*, 127(7):2208–2242, 2017.

[25] B. Buchmann, K. W. Lu, and D. B. Madan. Weak subordination of multivariate Lévy processes and variance generalised gamma convolutions. *Bernoulli*, 25(1):742–770, 2019.

[26] B. Buchmann, K. W. Lu, and D. B. Madan. Self-decomposability of weak variance generalised gamma convolutions. *Stochastic Process. Appl.*, 130(2):630–655, 2020.

[27] S. Burgos and M. B. Giles. Computing Greeks using multilevel path simulation. In *Monte Carlo and quasi-Monte Carlo methods 2010*, volume 23 of *Springer Proc. Math. Stat.*, pages 281–296. Springer, Heidelberg, 2012.

[28] E. Çınlar. *Probability and Stochastics*, volume 261 of *Graduate Texts in Mathematics*. Springer, New York, 2011.

[29] J. Charrier. Strong and weak error estimates for the solutions of elliptic partial differential equations with random coefficients. *[Research Report] RR-7300, INRIA. 2010. inria-00490045v3*, 2011.

[30] J. Charrier, R. Scheichl, and A. L. Teckentrup. Finite element error analysis of elliptic PDEs with random coefficients and its application to multilevel Monte Carlo methods. *SIAM J. Numer. Anal.*, 51(1):322–352, 2013.

[31] Z. Chen and J. Zou. Finite element methods and their convergence for elliptic and parabolic interface problems. *Numer. Math.*, 79(2):175–202, 1998.

[32] K. A. Cliffe, M. B. Giles, R. Scheichl, and A. L. Teckentrup. Multilevel Monte Carlo methods and applications to elliptic PDEs with random coefficients. *Comput. Vis. Sci.*, 14(1):3–15, 2011.

[33] A. Cohen, R. DeVore, and C. Schwab. Analytic regularity and polynomial approximation of parametric and stochastic elliptic PDE's. *Anal. Appl.*, 9(1):11–47, 2011.

[34] R. Cont. Empirical properties of asset returns: stylized facts and statistical issues.

Quantitative Finance, 1:223–236, 2001.

[35] G. Da Prato and J. Zabczyk. *Stochastic Equations in Infinite Dimensions*, volume 152 of *Encyclopedia of Mathematics and its Applications*. Cambridge University Press, Cambridge, second edition, 2014.

[36] G. Dagan, U. Hornung, and P. Knabner, editors. *Mathematical Modeling for Flow and Transport Through Porous Media*. Springer Netherlands, 1991.

[37] C.-S. Deng and R. L. Schilling. On shift Harnack inequalities for subordinate semigroups and moment estimates for Lévy processes. *Stochastic Process. Appl.*, 125(10):3851–3878, 2015.

[38] G. Detommaso, T. Dodwell, and R. Scheichl. Continuous level Monte Carlo and sample-adaptive model hierarchies. *SIAM/ASA J. Uncertain. Quantif.*, 7(1):93–116, 2019.

[39] E. Di Nezza, G. Palatucci, and E. Valdinoci. Hitchhiker's guide to the fractional Sobolev spaces. *Bull. Sci. Math.*, 136(5):521–573, 2012.

[40] J. Dick, F. Y. Kuo, and I. H. Sloan. High-dimensional integration: the quasi-Monte Carlo way. *Acta Numer.*, 22:133–288, 2013.

[41] Z. Ding. A proof of the trace theorem of Sobolev spaces on Lipschitz domains. *Proc. Amer. Math. Soc.*, 124(2):591–600, 1996.

[42] R. L. Dobrushin. Gaussian and their subordinated self-similar random generalized fields. *Ann. Probab.*, 7(1):1–28, 1979.

[43] P. Dreyfuss. Higher integrability of the gradient in degenerate elliptic equations. *Potential Anal.*, 26(2):101–119, 2007.

[44] R. M. Dudley. *Real Analysis and Probability*, volume 74 of *Cambridge Studies in Advanced Mathematics*. Cambridge University Press, Cambridge, 2002. Revised reprint of the 1989 original.

[45] O. R. A. Dunbar, M. M. Dunlop, C. M. Elliott, V. H. Hoang, and A. M. Stuart. Reconciling Bayesian and perimeter regularization for binary inversion. *SIAM J. Sci. Comput.*, 42(4):A1984–A2013, 2020.

[46] M. M. Dunlop, M. A. Iglesias, and A. M. Stuart. Hierarchical Bayesian level set inversion. *Stat. Comput.*, 27(6):1555–1584, 2017.

[47] A. Ebert, P. Kritzer, and D. Nuyens. Constructing QMC finite element methods for elliptic PDEs with random coefficients by a reduced CBC construction. In *Monte Carlo and quasi-Monte Carlo methods*, volume 324 of *Springer Proc. Math. Stat.*, pages 183–205. Springer, Cham, [2020] © 2020.

[48] M. Eigel, C. J. Gittelson, C. Schwab, and E. Zander. Adaptive stochastic Galerkin FEM. *Comput. Methods Appl. Mech. Engrg.*, 270:247–269, 2014.

[49] O. G. Ernst, H. Gottschalk, T. Kalmes, T. Kowalewitz, and M. Reese. Integrability and approximability of solutions to the stationary diffusion equation with Lévy coefficient. *ArXiv e-prints, arXiv:2010.14912 [math.AP]*, 2021.

[50] L. C. Evans. *Partial Differential Equations*, volume 19 of *Graduate Studies in Mathematics*. American Mathematical Society, Providence, RI, second edition, 2010.

[51] G. Fasshauer and M. McCourt. *Kernel-based Approximation Methods Using Matlab*. Interdisciplinary Mathematical Sciences. World Scientific Publishing Company, 2015.

[52] I. Fedotenkov. A bootstrap method to test for the existence of finite moments. *J. Nonparametr. Stat.*, 25(2):315–322, 2013.

[53] I. Fedotenkov. A note on the bootstrap method for testing the existence of finite moments. *Statistica*, 74(4):447–453, 2014.

[54] I. Fedotenkov. A simple nonparametric test for the existence of finite moments. MPRA Paper 66089, University Library of Munich, Germany, Aug. 2015.

[55] P. Frauenfelder, C. Schwab, and R. A. Todor. Finite elements for elliptic problems with stochastic coefficients. *Comput. Methods Appl. Mech. Engrg.*, 194(2-5):205–228, 2005.

[56] J. Gil-Pelaez. Note on the inversion theorem. *Biometrika*, 38:481–482, 1951.

[57] M. B. Giles. Multilevel Monte Carlo path simulation. *Oper. Res.*, 56(3):607–617, 2008.

[58] M. B. Giles. Multilevel Monte Carlo for basket options. In *Proceedings of the 2009 Winter Simulation Conference*, pages 1283–1290. IEEE, 2009.

[59] M. B. Giles. Multilevel Monte Carlo methods. *Acta Numer.*, 24:259–328, 2015.

[60] M. B. Giles and B. J. Waterhouse. Multilevel quasi-Monte Carlo path simulation. In *Advanced financial modelling*, volume 8 of *Radon Ser. Comput. Appl. Math.*, pages 165–181. Walter de Gruyter, Berlin, 2009.

[61] M. B. Giles and Y. Xia. Multilevel Monte Carlo for exponential Lévy models. *Finance Stoch.*, 21(4):995–1026, 2017.

[62] P. Glasserman. *Monte Carlo Methods in Financial Engineering*, volume 53 of *Applications of Mathematics (New York)*. Springer-Verlag, New York, 2004.

[63] I. G. Graham, F. Y. Kuo, J. A. Nichols, R. Scheichl, C. Schwab, and I. H. Sloan. Quasi-Monte Carlo finite element methods for elliptic PDEs with lognormal random coefficients. *Numer. Math.*, 131(2):329–368, 2015.

[64] I. G. Graham, F. Y. Kuo, D. Nuyens, R. Scheichl, and I. H. Sloan. Analysis of circulant embedding methods for sampling stationary random fields. *SIAM J. Numer. Anal.*, 56(3):1871–1895, 2018.

[65] I. G. Graham, F. Y. Kuo, D. Nuyens, R. Scheichl, and I. H. Sloan. Circulant embedding with QMC: analysis for elliptic PDE with lognormal coefficients. *Numer. Math.*, 140(2):479–511, 2018.

[66] T. Grätsch and K.-J. Bathe. A posteriori error estimation techniques in practical finite element analysis. *Comput. & Structures*, 83(4-5):235–265, 2005.

[67] W. Hackbusch. *Elliptic Differential Equations. Theory and Numerical Treatment.*, volume 18 of *Springer Series in Computational Mathematics*. Springer-Verlag, Berlin, second edition, 2017.

[68] A.-L. Haji-Ali, F. Nobile, and R. Tempone. Multi-index Monte Carlo: when sparsity meets sampling. *Numer. Math.*, 132(4):767–806, 2016.

[69] S. Heinrich. Monte Carlo complexity of global solution of integral equations. *J. Complexity*, 14(2):151–175, 1998.

[70] S. Heinrich. Multilevel Monte Carlo methods. In S. Margenov, J. Waśniewski, and P. Yalamov, editors, *Large-Scale Scientific Computing*, pages 58–67, Berlin, Heidelberg, 2001. Springer Berlin Heidelberg.

[71] B. M. Hill. A simple general approach to inference about the tail of a distribution. *Ann. Statist.*, 3(5):1163–1174, 1975.

[72] B. Hosseini. Well-posed Bayesian inverse problems with infinitely divisible and heavy-tailed prior measures. *SIAM/ASA J. Uncertain. Quantif.*, 5(1):1024–1060, 2017.

[73] P. Hughett. Error bounds for numerical inversion of a probability characteristic function.

SIAM J. Numer. Anal., 35(4):1368–1392, 1998.

[74] T. Hytönen, J. van Neerven, M. Veraar, and L. Weis. *Analysis in Banach Spaces. Vol. I. Martingales and Littlewood-Paley theory*, volume 63 of *Ergebnisse der Mathematik und ihrer Grenzgebiete. 3. Folge. A Series of Modern Surveys in Mathematics [Results in Mathematics and Related Areas. 3rd Series. A Series of Modern Surveys in Mathematics]*. Springer, Cham, 2016.

[75] M. A. Iglesias, K. Lin, and A. M. Stuart. Well-posed Bayesian geometric inverse problems arising in subsurface flow. *Inverse Problems*, 30(11):114001, 39, 2014.

[76] M. A. Iglesias, Y. Lu, and A. Stuart. A Bayesian level set method for geometric inverse problems. *Interfaces Free Bound.*, 18(2):181–217, 2016.

[77] O. Kallenberg. *Foundations of Modern Probability*, volume 99 of *Probability Theory and Stochastic Modelling*. Springer, Cham, third edition, [2021] © 2021.

[78] D. Kelker. Infinite divisibility and variance mixtures of the normal distribution. *Ann. Math. Statist.*, 42:802–808, 1971.

[79] A. Klenke. *Wahrscheinlichkeitstheorie*. Springer Berlin Heidelberg, 2013. 3. Auflage.

[80] N. B. Kovachki, Z. Li, B. Liu, K. Azizzadenesheli, K. Bhattacharya, A. M. Stuart, and A. Anandkumar. Neural operator: Learning maps between function spaces. *CoRR*, abs/2108.08481, 2021. URL: https://arxiv.org/abs/2108.08481.

[81] F. Y. Kuo, R. Scheichl, C. Schwab, I. H. Sloan, and E. Ullmann. Multilevel quasi-Monte Carlo methods for lognormal diffusion problems. *Math. Comp.*, 86(308):2827–2860, 2017.

[82] F. Y. Kuo, C. Schwab, and I. H. Sloan. Quasi-Monte Carlo finite element methods for a class of elliptic partial differential equations with random coefficients. *SIAM J. Numer. Anal.*, 50(6):3351–3374, 2012.

[83] F. Y. Kuo, C. Schwab, and I. H. Sloan. Multi-level quasi-Monte Carlo finite element methods for a class of elliptic PDEs with random coefficients. *Found. Comput. Math.*, 15(2):411–449, 2015.

[84] S. Larsson and V. Thomée. *Partial Differential Equations with Numerical Methods*, volume 45 of *Texts in Applied Mathematics*. Springer-Verlag, Berlin, 2003.

[85] N. N. Leonenko, M. D. Ruiz-Medina, and M. S. Taqqu. Rosenblatt distribution subordinated to Gaussian random fields with long-range dependence. *Stoch. Anal. Appl.*,

35(1):144–177, 2017.

[86] R. J. LeVeque. *Finite Difference Methods for Ordinary and Partial Differential Equations. Steady-State and Time-Dependent Problems.* Society for Industrial and Applied Mathematics (SIAM), Philadelphia, PA, 2007.

[87] J. Li, X. Wang, and K. Zhang. Multi-level Monte Carlo weak Galerkin method for elliptic equations with stochastic jump coefficients. *Appl. Math. Comput.*, 275:181–194, 2016.

[88] Z. Li. The immersed interface method using a finite element formulation. *Appl. Numer. Math.*, 27(3):253–267, 1998.

[89] L. Lu, P. Jin, G. Pang, H. Zang, and G. Karniadakis. Learning nonlinear operators via DeepONet based on the universal approximation theorem of operators. *Nature Machine Intelligence*, 3:218–229, 03 2021.

[90] H. Luschgy and G. Pagès. Moment estimates for Lévy processes. *Electron. Commun. Probab.*, 13:422–434, 2008.

[91] V. Makogin and E. Spodarev. Limit theorems for excursion sets of subordinated Gaussian random fields with long-range dependence. *Stochastics*, 94(1):111–142, 2022.

[92] B. B. Mandelbrot. The variation of certain speculative prices. *Journal of Business*, 36(4):394–419, 1963.

[93] R. Merkle and A. Barth. Multilevel Monte Carlo estimators for elliptic PDEs with Lévy-type diffusion coefficient. *Bit Numer Math 62, 1279–1317*, 2022. https://doi.org/10.1007/s10543-022-00912-4.

[94] R. Merkle and A. Barth. On properties and applications of Gaussian subordinated Lévy fields. *ArXiv e-prints, arXiv:2208.01278 [math.PR]*, 2022. submitted to Methodology and Computing in Applied Probability.

[95] R. Merkle and A. Barth. On some distributional properties of subordinated Gaussian random fields. *Methodol Comput Appl Probab*, 2022. https://doi.org/10.1007/s11009-022-09958-x.

[96] R. Merkle and A. Barth. Subordinated Gaussian random fields in elliptic partial differential equations. *Stoch PDE: Anal Comp*, 2022. https://doi.org/10.1007/s40072-022-00246-w.

[97] A. Mugler and H.-J. Starkloff. On the convergence of the stochastic Galerkin method for random elliptic partial differential equations. *ESAIM Math. Model. Numer. Anal.*,

47(5):1237–1263, 2013.

[98] R. L. Naff, D. F. Haley, and E. A. Sudicky. High-resolution Monte Carlo simulation of flow and conservative transport in heterogeneous porous media: 1. Methodology and flow results. *Water Resources Research*, 34(4):663–677, Apr. 1998.

[99] W. L. Ng and C. Y. Yau. Test for the existence of finite moments via bootstrap. *J. Nonparametr. Stat.*, 30(1):28–48, 2018.

[100] F. Nobile, R. Tempone, and C. G. Webster. A sparse grid stochastic collocation method for partial differential equations with random input data. *SIAM J. Numer. Anal.*, 46(5):2309–2345, 2008.

[101] F. Nobile and F. Tesei. A multi level Monte Carlo method with control variate for elliptic PDEs with log-normal coefficients. *Stoch. Partial Differ. Equ. Anal. Comput.*, 3(3):398–444, 2015.

[102] P. Percell and M. F. Wheeler. A C^1 finite element collocation method for elliptic equations. *SIAM J. Numer. Anal.*, 17(5):605–622, 1980.

[103] W. R. Pestman. *Mathematical Statistics*. De Gruyter Textbook. Walter de Gruyter & Co., Berlin, second edition, 2009.

[104] S. Peszat and J. Zabczyk. *Stochastic Partial Differential Equations with Lévy Noise. An Evolution Equation Approach*, volume 113 of *Encyclopedia of Mathematics and its Applications*. Cambridge University Press, Cambridge, 2007.

[105] M. Petzoldt. Regularity results for Laplace interface problems in two dimensions. *Zeitschrift für Analysis und ihre Anwendungen*, 20(2):431–455, 2001.

[106] P. E. Protter. *Stochastic Integration and Differential Equations*, volume 21 of *Applications of Mathematics (New York)*. Springer-Verlag, Berlin, second edition, 2004.

[107] A. Quarteroni and A. Valli. *Numerical Approximation of Partial Differential Equations*, volume 23 of *Springer Series in Computational Mathematics*. Springer-Verlag, Berlin, 1994.

[108] K.-I. Sato. *Lévy Processes and Infinitely Divisible Distributions*, volume 68 of *Cambridge Studies in Advanced Mathematics*. Cambridge University Press, Cambridge, 2013.

[109] W. Schoutens. *Lévy Processes in Finance: Pricing Financial Derivatives*. Wiley Series in Probability and Statistics. Wiley, 2003.

[110] A. Stein and A. Barth. A multilevel Monte Carlo algorithm for parabolic advection-diffusion problems with discontinuous coefficients. In *Monte Carlo and quasi-Monte Carlo methods*, volume 324 of *Springer Proc. Math. Stat.*, pages 445–466. Springer, Cham, [2020] © 2020.

[111] A. L. Teckentrup. Multilevel Monte Carlo methods for highly heterogeneous media. In *Proceedings of the 2012 Winter Simulation Conference (WSC)*, pages 1–12, 2012.

[112] A. L. Teckentrup, R. Scheichl, M. B. Giles, and E. Ullmann. Further analysis of multilevel Monte Carlo methods for elliptic PDEs with random coefficients. *Numer. Math.*, 125(3):569–600, 2013.

[113] A. Valli. *A Compact Course on Linear PDEs*, volume 126 of *Unitext - La Matematica per il 3+2*. Springer, Cham, [2020] © 2020.

[114] R. Verfürth. A posteriori error estimation and adaptive mesh-refinement techniques. *Journal of Computational and Applied Mathematics*, 50(1-3):67–83, 1994.

[115] D. Werner. *Funktionalanalysis*. Springer-Lehrbuch. Springer Berlin Heidelberg, 2011.

[116] A. Winkelbauer. Moments and absolute moments of the normal distribution. *ArXiv e-prints, arXiv:1209.4340v2 [math.ST]*, 2012.

[117] Y. Xia and M. B. Giles. Multilevel path simulation for jump-diffusion SDEs. In *Monte Carlo and quasi-Monte Carlo methods 2010*, volume 23 of *Springer Proc. Math. Stat.*, pages 695–708. Springer, Heidelberg, 2012.

[118] D. Zhang and Q. Kang. Pore scale simulation of solute transport in fractured porous media. *Geophys. Res. Lett.*, 31(12), June 2004.

[119] T. Zhou. Stochastic Galerkin methods for elliptic interface problems with random input. *J. Comput. Appl. Math.*, 236(5):782–792, 2011.